

FROM FIRST PRINCIPLES: THE APPLICATION OF QUANTUM MECHANICS TO
COMPLEX MOLECULES AND SOLVATED SYSTEMS

by

MARK ALAN FREITAG

A dissertation submitted to the graduate faculty
in partial fulfillment of the requirements for the degree of
DOCTOR OF PHILOSOPHY

MAJOR: PHYSICAL CHEMISTRY

Program of Study Committee:
Mark Gordon (Major Professor)
James W. Evans
David K. Hoffman
Gordon J. Miller
Gerald J. Small

Iowa State University

Ames, Iowa

2002

Graduate College
Iowa State University

This is to certify that the doctoral dissertation of

MARK ALAN FREITAG

has met the dissertation requirements of Iowa State University

Geoff Small
Committee Member

Guy J. McL
Committee Member

David K. Johnson
Committee Member

J. D. Green
Committee Member

Mark C
Major Professor

Mark C
For the Major Program

To Professor James B. Togeas: for inspiration.

To Mary Bernadette Freitag: for patience.

CONTENTS

CHAPTER 1. GENERAL INTRODUCTION	
I. Historical Background	1
II. Theoretical Methods	11
III. Dissertation Organization	19
CHAPTER 2. EVALUATION OF CHARGE PENETRATION BETWEEN DISTRIBUTED MULTIPOLAR EXPANSIONS	
I. Introduction	21
II. Theory	25
III. Results and Discussion	33
IV. Summary and Conclusions	39
V. Acknowledgements	40
CHAPTER 3. MODELING SOLVENT EFFECTS IN NUCLEAR MAGNETIC RESONANCE SPECTRA	
I. Introduction	41
II. Chemical Shifts and Gauge Invariant Atomic Orbitals	42
III. Self-Consistent Antisymmetric Perturbation Theory for Perturbation Dependent, Non-Orthogonal Basis Sets	52
IV. McMurchie-Davidson Integrals	61
V. Strategies for Incorporating Solvent Effects	74
VI. Summary and Conclusions	76
CHAPTER 4. THE SOLVATION OF FORMIC AND ACETIC ACIDS	
I. Introduction	77
II. Theoretical Methods	77
III. Preliminary Results	81
CHAPTER 5. TOWARDS MULTI-REFERENCE EQUIVALENTS OF THE G2 AND G3 METHODS	
I. Introduction	83
II. Methods	85
III. Results and Discussion	90
IV. Conclusions	97
V. Acknowledgements	98
CHAPTER 6. ON THE ELECTRONIC STRUCTURE OF BIS(η^5- CYCLOPENTADIENYL) TITANIUM	
I. Introduction	114
II. Methods	119
III. Results and Discussion	120
IV. Conclusions	127
CHAPTER 7. GENERAL CONCLUSIONS	129

APPENDIX A. CARTESIAN VS. SPHERICAL HARMONIC FUNCTIONS	133
APPENDIX B. GRADIENTS(∇), DIVERGENCE($\nabla \cdot$) AND CURLS($\nabla \times$)	140
APPENDIX C. GAUGE INVARIANT ATOMIC ORBITAL DERIVATIONS	143
APPENDIX D. ANTSYMMETRIC PERTURBATION THEORY FOR FIELD-DEPENDENT NON-ORTHOGONAL BASES	161
APPENDIX E. McMURCHIE-DAVIDSON ONE- AND TWO-ELECTRON INTEGRALS	165
APPENDIX F. SUPPLEMENTAL TABLES FOR MRG n THEORY	175
ACKNOWLEDGEMENTS	195
REFERENCES	194

CHAPTER 1: GENERAL INTRODUCTION

I. Historical Background

The major title of this dissertation, 'From first principles,' is a phrase often heard in the study of thermodynamics and quantum mechanics. These words embody a powerful idea in the physical sciences; namely, that it is possible to distill the complexities of nature into a set of simple, well defined mathematical laws, from which specific relations can then be derived. In thermodynamics, these fundamental laws are immediately familiar to the physical scientist by their numerical order: the First, Second and Third Laws. However, the subject of the present volume is quantum mechanics - specifically, non-relativistic quantum mechanics, which is appropriate for most systems of chemical interest. The first principles of this field are commonly expressed by an equation first written by Schrödinger in 1926:¹

$$i\hbar \frac{\partial \Psi(\mathbf{q},t)}{\partial t} = -\frac{\hbar^2}{2m} \nabla^2 \Psi(\mathbf{q},t) + V(\mathbf{q})\Psi(\mathbf{q},t) \quad (1.1)$$

where i is the square root of negative one, \hbar is Planck's constant divided by 2π , $\Psi(\mathbf{q},t)$ represents the system's so-called wavefunction, which is a function of space and time, respectively, m is the system's mass, and V is the potential energy of the system. There are various ways that one could 'derive' this equation or justify its form based on the matter-wave theories of de Broglie,² or perhaps by using Heisenberg's³ famous commutation relation, $[\mathbf{q}, \mathbf{p}] = i\hbar\mathbf{1}$, which first appeared in the paper 'Zur Quantenmechanik' by Born and Jordan,⁴ and independently a few months later in Dirac's first paper on quantum mechanics.⁵ For our purposes here, it is entirely reasonable to consider Eq. (1.1) as a fundamental quantum postulate, and then derive our relations from it; i.e. from first principles.

In the study of electronic structure, one usually begins from the time independent form of Schrödinger's equation, since, in the absence of a time-varying field, the time dependence of the wavefunction is easily integrated out by separation of variables. Let $\Psi(\mathbf{q},t) = \psi(\mathbf{q})f(t)$; then

$$i\hbar \frac{1}{f(t)} \frac{\partial f(t)}{\partial t} = -\frac{\hbar^2}{2m} \frac{1}{\psi(\mathbf{q})} \nabla^2 \psi(\mathbf{q}) + V(\mathbf{q}) \quad (1.2)$$

Since both sides of Eq. (1.2) are functions of independent variables (space and time), each side must therefore be equal to the same constant, E . Consider the solution of the left-hand side (LHS):

$$\frac{df(t)}{f(t)} = -\frac{iE}{\hbar} dt \Rightarrow \int \frac{df(t)}{f(t)} = -\frac{iE}{\hbar} \int dt \Rightarrow \ln f(t) = -\frac{iEt}{\hbar} \Rightarrow f(t) = e^{-\frac{iEt}{\hbar}} \quad (1.3)$$

such that evolution of the wavefunction is now known for all times, and is given by the phase factor in Eq. (1.3). The right-hand side (RHS) of Eq. (1.2) is then:

$$\begin{aligned} -\frac{\hbar^2}{2m} \nabla^2 \psi(\mathbf{q}) + V(\mathbf{q}) \psi(\mathbf{q}) &= E \psi(\mathbf{q}) \Rightarrow \left[-\frac{\hbar^2}{2m} \nabla^2 + V(\mathbf{q}) \right] \psi(\mathbf{q}) = E \psi(\mathbf{q}) \\ &\Rightarrow H \psi(\mathbf{q}) = E \psi(\mathbf{q}) \end{aligned} \quad (1.4)$$

where the Hamiltonian operator, H , has been defined as the sum of the kinetic and potential energies of the system. In Dirac notation, the time-independent Schrödinger equation is written as

$$H|\psi\rangle = E|\psi\rangle \quad (1.5)$$

In this form, it is easy to demonstrate that the expectation value of the energy operator, H , gives the energy, E , of the system since the wavefunction itself is normalizable.

For a system of interacting electrons and nuclei, we have the following Hamiltonian in atomic units.⁶

$$H = -\frac{1}{2} \sum_i \nabla_i^2 - \frac{1}{2} \sum_A \frac{1}{M_A} \nabla_A^2 - \sum_i \sum_A \frac{Z_A}{r_{iA}} + \sum_i \sum_{j>i} \frac{1}{r_{ij}} + \sum_A \sum_{B>A} \frac{Z_A Z_B}{R_{AB}} \quad (1.6)$$

where i indexes the electrons, A indexes the nuclei, M_A is the mass of nucleus A , and Z_A is the charge on nucleus A . This Hamiltonian can be simplified upon application of the Born-Oppenheimer approximation,⁷ which states that since the nuclei are approximately 1800 times as massive as the electrons, they can be considered as stationary points, and the electrons move in their constant potential field. In this case, the second term in Eq. (1.6) is zero, since the nuclei have no kinetic energy, and the last term is a constant, since the distance between the nuclei will not change. Eq. (1.6) becomes

$$H = -\frac{1}{2} \sum_i \nabla_i^2 - \sum_i \sum_A \frac{Z_A}{r_{iA}} + \sum_i \sum_{j>i} \frac{1}{r_{ij}} \quad (1.7)$$

Another technique used to simplify Schrödinger's equation is called the orbital approximation. Here, the many-electron wavefunction is written as the product of one-electron wavefunctions:

$$\psi_{total} = \psi_1(1)\psi_2(2)\cdots\psi_N(N) \quad (1.8)$$

where there are N electrons in the system. The RHS is called a Hartree product,⁸ and each individual function ψ_i is called a spatial orbital. According to the Born interpretation of the wavefunction,⁹ a part of the full Copenhagen interpretation of quantum mechanics, named after the place where Niels Bohr worked as its principal creator,¹⁰ the spatial probability density is given by $|\psi|^2 d\tau$, where $d\tau$ is an element of volume. If the wavefunction is written as a Hartree product, then this probability density must be the product of the squares of the individual orbitals. According to probability theory, this can only be true if the probability represented by the individual orbitals are independent of one another. This approach is therefore called the independent electron model.¹¹ If it was possible to write the Hamiltonian,

Eq. (1.7), as the sum of one-electron terms, then the solution of Schrödinger's equation would be a simple task by separation of variables. As it is, the Hamiltonian depends on r_{ij}^{-1} , which means that we must know the instantaneous relative positions of two electrons. Therefore, the full Hamiltonian cannot be written as the sum of one-electron Hamiltonians; but since the utility of such a representation is clear, there has been considerable effort to generate *approximate* one-electron Hamiltonians. Consider the following expression:

$$H_{\text{approx}} = \sum_i h(i) = \sum_i \left[-\frac{1}{2} \nabla_i^2 + V(i) \right] \quad (1.9)$$

where $V(i)$ is some *average* potential resulting from the field of the other electrons in the system. As written, this approximate Hamiltonian does not explicitly include electron correlation, which is the instantaneous interaction of pairs of electrons.

According to Pauli's Exclusion Principle,¹² no two electrons in the same atom can have the same set of quantum numbers. Since electrons have spin quantum numbers of $\pm 1/2$, this means that each orbital can at most contain two electrons, one 'spin up' and the other 'spin down'. This condition arises naturally if we assume that the system's wavefunction is antisymmetric - i.e. the wavefunction changes sign when two electronic coordinates are interchanged.¹³ The first use of the antisymmetry property was by Heisenberg in his 1926 study of the spectrum of helium.¹⁴ Pauli's exclusion principle had been developed in the context of the old quantum theory, and so to incorporate this into Schrödinger's wavefunction terminology, Heisenberg reasoned as follows: Let $\psi(1,2)$ represent the wavefunction of a two-electron system, where the "1" represents the four coordinates of electron 1 (three spatial and one spin). Pauli said that no two electrons can have identical coordinates, so the most natural way to represent this was to write $\psi(1,2) = -\psi(2,1)$; therefore if the two sets of coordinates *are* the same, we have $\psi(1,1) = -\psi(1,1)$, which must be zero.¹⁵ Note that since physical properties depend on the square of the wavefunction, the antisymmetry property does not

directly affect them. Mathematically, we can write antisymmetry in terms of an operator, A_{ij} , which interchanges the coordinates of electron i and j :

$$\begin{aligned} A_{ij}\psi(1,2,\dots,i,j,\dots,N) &= \psi(1,2,\dots,j,i,\dots,N) \\ &= -\psi(1,2,\dots,i,j,\dots,N) \end{aligned} \quad (1.10)$$

It is apparent from the form of the Hartree product formulation of the wavefunction (Eq. 1.8) that it is *not* antisymmetric. If, on the other hand, Eq. (1.8) is formulated as a determinant,¹⁶ it will be antisymmetric:

$$\psi_{total} = \mathcal{N} \sum_{i,j,k,\dots}^N \epsilon_{ijk\dots} \psi_1(i)\psi_2(j)\psi_3(k)\dots \quad (1.11)$$

where $\epsilon_{ijk\dots}$ is analogous to the three-dimensional Levi-Civita symbol:¹⁷ it is +1 for even permutations of $ijk\dots$, -1 for odd permutations, and zero if any index is repeated. (In a linear sequence $abcd$, any single (or other odd number of) interchange(s) of two adjacent elements is an *odd* permutation. An even number of such interchanges results in a *even* permutation.) \mathcal{N} is a normalization factor.

In keeping with the theme of ‘from first principles,’ and in order to lead into the treatment of NMR chemical shifts for closed-shell molecules in Chapter 3, let us consider the restricted Hartree-Fock formalism in some detail. A closed shell molecule is one in which all N electrons are paired spin-up and spin-down in $N/2$ orbitals. The wavefunction for such a system is a simple modification of Eq. (1.11):

$$\begin{aligned} \psi &= \mathcal{N} \sum_{i,j,k,\dots}^N \epsilon_{ijk\dots} \psi_1(i)\alpha(i)\psi_1(j)\beta(j)\dots\psi_{N/2}(N)\beta(N) \\ &= \mathcal{N} \sum_{i,j,k,\dots}^N \epsilon_{ijk\dots} \chi_1(i)\chi_2(j)\dots\chi_N(N) \end{aligned} \quad (1.12)$$

where α represents spin-up, and β spin-down. The spin and spatial orbitals are orthonormal:

$$\begin{aligned}
S_{ij} &= \int d\tau(1) \psi_i^*(1) \psi_j(1) = \delta_{ij} \\
\int d\omega(1) \alpha^*(1) \beta(1) &= \delta_{\alpha\beta} \\
\int d\omega d\tau(1) \chi_i^*(1) \chi_j(1) &= \delta_{ij}
\end{aligned} \tag{1.13}$$

The normalization constant can be derived by considering the normalization of the total probability density:

$$\begin{aligned}
1 &= \int \psi^* \psi d\tau(1) \cdots d\tau(N) \\
&= \mathcal{N}^2 \left\langle \sum_{i,j,k,\dots}^N \varepsilon_{ijk\dots} \chi_1(i) \chi_2(j) \cdots \chi_N(N) \middle| \sum_{l,m,n,\dots}^N \varepsilon_{lmn\dots} \chi_1(l) \chi_2(m) \cdots \chi_N(N) \right\rangle \\
&= \mathcal{N}^2 \sum_{i,j,k,\dots}^N \sum_{l,m,n,\dots}^N \varepsilon_{ijk\dots} \varepsilon_{lmn\dots} \langle \chi_1(i) \chi_2(j) \cdots \chi_N(N) | \chi_1(l) \chi_2(m) \cdots \chi_N(N) \rangle
\end{aligned} \tag{1.14}$$

then since the integration is over the coordinates of all N electrons,

$$\begin{aligned}
1 &= \mathcal{N}^2 \sum_{i,j,k,\dots}^N \sum_{l,m,n,\dots}^N \varepsilon_{ijk\dots} \varepsilon_{lmn\dots} \delta_{il} \delta_{jm} \delta_{kn} \cdots \\
&= \mathcal{N}^2 \sum_{i,j,k,\dots}^N \varepsilon_{ijk\dots}^2 = \mathcal{N}^2 (N)!
\end{aligned} \tag{1.15}$$

to leave a normalization factor of $\mathcal{N} = (N!)^{-1/2}$.

With a full form of the wavefunction, Eq. (1.12), we can now evaluate the energy expectation value

$$E = \langle \psi | H | \psi \rangle \tag{1.16}$$

for a closed-shell molecule. Let the Hamiltonian, Eq. (1.7) be written as

$$H = \sum_i \left(-\frac{1}{2} \nabla_i^2 - \sum_A \frac{Z_A}{r_{iA}} \right) + \sum_i \sum_{j>i} \frac{1}{r_{ij}} = \sum_i H^{\text{core}}(i) + H_2 = H_1 + H_2 \quad (1.17)$$

This allows Eq. (1.16) to be written as

$$E = \langle \psi | H_1 | \psi \rangle + \langle \psi | H_2 | \psi \rangle \quad (1.18)$$

Consider the one-electron term first:

$$\langle \psi | H_1 | \psi \rangle = \sum_i^N \left\langle \psi \left(-\frac{1}{2} \nabla_i^2 - \sum_A \frac{Z_A}{r_{iA}} \right) \psi \right\rangle = N \langle \psi | H^{\text{core}}(1) | \psi \rangle \quad (1.19)$$

since the electrons are equivalent and indistinguishable in both the Hamiltonian and the wavefunction. Using the full form of Eq. (1.12), Eq. (1.19) becomes

$$\frac{N}{N!} \sum_{i,j,k,\dots}^N \sum_{l,m,n,\dots}^N \epsilon_{ijk\dots} \epsilon_{lmn\dots} \langle \chi_1(i) \chi_2(j) \dots \chi_N(N) | H^{\text{core}}(1) | \chi_1(l) \chi_2(m) \dots \chi_N(N) \rangle \quad (1.20)$$

Now, since the core Hamiltonian is a function of the coordinates electron 1 only, and the Levi-Civita symbol ensures that no index will be repeated, choose $i = l = 1$ and integrate over the other electronic coordinates:

$$\begin{aligned} &= [(N-1)!]^{-1} \sum_{i,j,k,\dots}^N \epsilon_{1jk\dots} \epsilon_{1mn\dots} \langle \chi_1(1) | H^{\text{core}}(1) | \chi_1(l) \rangle \delta_{jm} \delta_{kn} \dots \\ &= [(N-1)!]^{-1} \sum_{j,k,\dots}^{N-1} \epsilon_{1jk\dots}^2 \langle \chi_1(1) | H^{\text{core}}(1) | \chi_1(1) \rangle \\ &= [(N-1)!]^{-1} \langle \chi_1(1) | H^{\text{core}}(1) | \chi_1(1) \rangle \sum_{j,k,\dots}^{N-1} \epsilon_{1jk\dots}^2 \end{aligned} \quad (1.21)$$

The sum over the squares of the Levi-Civita symbol will give a factor of $(N-1)!$, which leaves

$$\langle \psi_1(1) | H^{core}(1) | \psi_1(1) \rangle \quad (1.22)$$

Note that we could have picked any of the i, j, k, \dots electrons to be electron 1 in the derivation, so the full form of the expectation value is the sum of Eq. (1.22) over all N spin orbitals:

$$\langle \psi | H_1 | \psi \rangle = \sum_i^N \langle \chi_i(1) | H^{core}(1) | \chi_i(1) \rangle = \sum_i^N H_{ii} \quad (1.23)$$

This formulation makes the integration over the coordinates of electron 1 more transparent.

Now consider the expectation value of the two-electron Hamiltonian:

$$\langle \psi | H_2 | \psi \rangle = \langle \psi | \sum_i^N \sum_{j>i}^N \frac{1}{r_{ij}} | \psi \rangle = \frac{N(N-1)}{2} \langle \psi | \frac{1}{r_{12}} | \psi \rangle \quad (1.24)$$

since electrons are again indistinguishable. We can then apply similar techniques as for the one-electron term by substituting in Eq. (1.12):

$$\frac{1}{2} [(N-2)!]^{-1} \sum_{i,j,\dots,l,m,\dots}^{2N} \epsilon_{ijk\dots} \epsilon_{lmn\dots} \langle \chi_1(i) \chi_2(j) \dots \chi_N(N) | \frac{1}{r_{12}} | \chi_1(l) \chi_2(m) \dots \chi_N(N) \rangle \quad (1.25)$$

One is now left with a case slightly different than before; the two-electron operator is a function of two electronic coordinates, so the permutations of electrons can either be identical, or they can differ by the interchange of one pair. This can be represented in the following way, where i, j, l , and m have been chosen to represent electrons 1 and 2:

$$= \frac{1}{2} [(N-2)!]^{-1} \sum_{i,j,\dots,l,m,\dots}^{2N} \epsilon_{ijk\dots} \epsilon_{lmn\dots} \langle \chi_1(i) \chi_2(j) \dots \chi_N(N) | \frac{1}{r_{12}} | \chi_1(l) \chi_2(m) \dots \chi_N(N) \rangle \times (\delta_{i1} \delta_{j2} \delta_{l1} \delta_{m2}) - (\delta_{i1} \delta_{j2} \delta_{l2} \delta_{m1}) \quad (1.26)$$

where the negative sign arises because of the interchange of l and m . One can then integrate over the coordinates of the other $2N-2$ electrons:

$$= \frac{1}{2} [(N-2)!]^{-1} \sum_{i,j,k,\dots}^N \sum_{l,m}^N \epsilon_{ijk\dots} \epsilon_{lmk\dots} \langle \chi_1(i) \chi_2(j) | \frac{1}{r_{12}} | \chi_1(l) \chi_2(m) \rangle \times (\delta_{i1} \delta_{j2} \delta_{l1} \delta_{m2}) - (\delta_{i1} \delta_{j2} \delta_{l2} \delta_{m1}) \quad (1.27)$$

Then by application of the remaining Kronecker delta functions:

$$\begin{aligned} &= \frac{1}{2} [(N-2)!]^{-1} \left[\sum_{k,\dots}^{N-2} \epsilon_{12k\dots}^2 \langle \chi_1(1) \chi_2(2) | \frac{1}{r_{12}} | \chi_1(1) \chi_2(2) \rangle - \sum_{k,\dots}^{N-2} \epsilon_{21k\dots}^2 \langle \chi_1(1) \chi_2(2) | \frac{1}{r_{12}} | \chi_1(2) \chi_2(1) \rangle \right] \\ &= \frac{1}{2} \left[\langle \chi_1(1) \chi_2(2) | \frac{1}{r_{12}} | \chi_1(1) \chi_2(2) \rangle - \langle \chi_1(1) \chi_2(2) | \frac{1}{r_{12}} | \chi_1(2) \chi_2(1) \rangle \right] \end{aligned} \quad (1.28)$$

As before, we need not have chosen i, j, l , and m to designate electrons 1 and 2. To find the whole expectation value, we again sum over spin orbitals:

$$\begin{aligned} \langle \psi | H_2 | \psi \rangle &= \frac{1}{2} \left[\sum_{i,j}^N \left(\langle \chi_i(1) \chi_j(2) | \frac{1}{r_{12}} | \chi_i(1) \chi_j(2) \rangle - \langle \chi_i(1) \chi_j(2) | \frac{1}{r_{12}} | \chi_i(2) \chi_j(1) \rangle \right) \right] \\ &= \frac{1}{2} \left[\sum_{i,j}^N \left(\langle \chi_i(1) | \mathcal{J}_j(1) | \chi_i(1) \rangle - \langle \chi_i(1) | \mathcal{K}_j(1) | \chi_i(1) \rangle \right) \right] \end{aligned} \quad (1.29)$$

where the coulomb (\mathcal{J}) and exchange (\mathcal{K}) operators have been defined. Or, by introducing a simplified notation,

$$\langle \psi | H_2 | \psi \rangle = \frac{1}{2} \sum_{i,j}^N (J_{ij} - K_{ij}) \quad (1.30)$$

And finally, substitution of Eq. (1.23) and Eq. (1.30) into Eq. (1.18), the total energy expectation value is given by

$$E = \sum_i^N H_{ii} + \frac{1}{2} \sum_{i,j}^N (J_{ij} - K_{ij}) \quad (1.31)$$

in terms of spin orbitals.

The energy given in Eq. (1.31) can be minimized with respect to the spin orbitals, subject to the restraint that the spin orbitals remain orthonormal, by standard methods.⁶ The result is a set of integro-differential equations, known as the Hartree-Fock equations:

$$f|\chi_i\rangle = \gamma_i |\chi_i\rangle \quad (1.32)$$

Hartree-Fock theory is a common starting point for many more advanced theoretical methods, some of which are outlined in the next section.

To finish this historical background, it should be noted that the practical method for solving Eqs. (1.32) is by expanding the spatial molecular orbitals as a linear combination of atomic orbitals, commonly called the LCAO approximation:

$$\psi_i = \sum_{\mu} C_{\mu i} \phi_{\mu} \quad (1.33)$$

where the ϕ_{μ} are typically a set of well-defined standard Gaussian functions, which are in turn often constructed from a linear combination of *primitive* Gaussian functions. [See Eq. (3.112).]

$$\phi_{\mu} = x_{\mu}^n y_{\mu}^l z_{\mu}^m e^{-\alpha_{\mu} r_{\mu}^2} \quad (1.34)$$

Eq. (1.34) is an example of a Cartesian Gaussian function centered at a point μ , where the angular momentum of the function is represented by the x , y , and z components as shown. This leads to a physically odd situation where a d shell is represented by six functions rather than the familiar five. This is due to a linear dependence in the Cartesian space. Appendix A demonstrates the nature of this linear dependence and shows how to remove it in practice.

A note on terminology: if a single atomic orbital is represented by a single function, this is termed a *minimal basis set*; if two functions are used per atomic orbital, this is called a *double-zeta* basis. Triple-zeta and higher basis sets have analogous meanings.

Frequently, basis sets are modified by the addition of polarization functions of a higher angular momentum. For the case of hydrogen, which in a standard basis is represented by functions of s character, this would mean adding a function of p character, and this would allow for a distortion away from spherical symmetry, in the direction of any applied or environmental field. Basis sets are also augmented by the use of diffuse functions. Interactions like hydrogen bonding are by their nature weaker, and take place over larger distances. Therefore to account for these kinds of interactions, functions that are more “diffuse,” i.e., are spread over a greater physical space, are required.

II. Theoretical Methods

This section contains brief overviews of the theoretical methods that will be employed or considered in later chapters.

A. Restricted Open-Shell Hartree Fock

In the above formulation of closed shell Hartree-Fock theory, we have restricted each of the occupied orbitals to contain exactly two electrons; one spin-up, the other spin-down. One need not impose this condition. If the spatial part of the

doubly occupied orbitals are restricted to the same form, but some orbitals are allowed to be singly occupied, i.e. open shell, this method is referred to as Restricted Open Shell Hartree Fock (ROHF).

B. Unrestricted Hartree-Fock

In unrestricted Hartree-Fock (UHF) theory, the orbitals containing individual electrons are allowed to vary such that the spin-up (alpha) orbitals are not identical to the spin-down (beta) orbitals. This allows for the representation of open-shell molecules, where the electrons are not necessarily paired evenly. The major drawback to this theory is that the resulting wavefunction is not normally an eigenfunction of the total spin operator, S^2 , which generates the value of the total spin squared.¹⁸ Therefore one does not obtain pure spin states from UHF theory; a singlet state will contain contributions from higher triplet, quintet, etc. states; this phenomenon is known as spin contamination.

C. Perturbation Theory

A common technique for approximating the electron correlation energy not accounted for in Hartree-Fock methods is called perturbation theory. Since the correlation energy can be considered a small perturbation on the Hartree-Fock energy, the full Hamiltonian can be written in the following way:

$$H = H^{HF} + \lambda H^1 \quad (1.35)$$

where H^{HF} is the Hartree-Fock Hamiltonian, λ is called an ordering parameter which varies between zero and unity, and H^1 is the perturbation. By using Eq. (1.35) as the Hamiltonian of the system and expanding the resulting equations as a Taylor expansion in λ , one can set like terms equal to one another and thus obtain zeroth order, first order, second order, etc. corrections to the energy and wavefunction. This general scheme is known as many-body perturbation theory (MBPT),¹⁹ but when the zeroth order Hamiltonian is chosen to be the sum over Fock operators, the

method is known as Møller-Plesset²⁰ (MP) perturbation theory. At second order, the MP and MBPT methods are equivalent.²¹

D. Configuration Interaction

The solution of the Hartree-Fock (HF) equations leads to a 'ground state' wavefunction, where in the closed-shell case outlined above, all the electrons are paired. In addition to this state, one can also form wavefunctions (determinants) that differ from the ground state by various excitations of electrons from occupied orbitals to vacant ones. In considering these excitations, one automatically incorporates electron correlation into the model. In other words, to account for correlation, the mental image of electrons neatly occupying specific orbitals must be abandoned. Let Φ be the exact many-electron wavefunction. It is then expanded in terms of excited-state wavefunctions:

$$\Phi = c_0 \psi_{HF} + \underbrace{\left(\frac{1}{1!}\right)^2 \sum_{ar} c_a^r \psi_a^r}_{\text{single excitations}} + \underbrace{\left(\frac{1}{2!}\right)^2 \sum_{abrs} c_{ab}^{rs} \psi_{ab}^{rs}}_{\text{double excitations}} + \underbrace{\left(\frac{1}{3!}\right)^2 \sum_{abcrst} c_{abc}^{rst} \psi_{abc}^{rst}}_{\text{triple excitations}} + \dots \quad (1.36)$$

where ψ_{HF} is the Hartree-Fock wavefunction, and the electronic excitations are from occupied a, b, c , etc. HF orbitals to unoccupied r, s, t , etc. HF orbitals, which are *not* re-optimized during any variation of the CI procedure. If this expansion is carried out to all possible excitations, 'full CI' leads to an exact solution of Schrödinger's equation *in the space spanned by the basis set*. The most common applications of CI are single excitations (CIS) and single and double excitations (CISD).

E. Multi-Configurational Self-Consistent Field

An approximation to full CI is to truncate the CI expansion at a given order, and to optimize the CI coefficients *and* the HF orbitals. This is known as Multi-Configurational Self-Consistent Field (MCSCF) theory. (For a full CI expansion, there is no need to vary the HF orbitals.) Further, one allows the excitations to take

place only in a well-defined *active space*, which is composed of a given number of electrons in chemically important orbitals. This is a powerful and essential method when the system of interest is not well represented by a single electronic configuration; i.e. a single Lewis structure. Radicals, transition states, and compounds containing transition metals quite often require a multi-configurational wavefunction.

F. Coupled Cluster Theory

Another approximation to full CI is called coupled cluster theory, which is similar in some respects to perturbation theory, discussed above. Perturbation theory can be thought of as all types of excitations (singles, doubles, triples, etc.) applied to the reference wave function to a given order.¹⁸ Conversely, coupled cluster theory seeks to include to infinite order all excitations of a given type. Let the coupled cluster wavefunction be written as

$$\psi_{CC} = e^T \psi_{HF} \quad (1.37)$$

where the cluster operator is given by

$$T = T_1 + T_2 + \dots + T_N \quad (1.38)$$

Here, the T_i operator acts on the HF wavefunction to give all the i th excitations. Therefore, if Eq. (1.38) is truncated at two terms, the method is referred to as CCSD for coupled cluster singles and doubles. If Eq. (1.38) is truncated at the triples term, the method is CCSDT, etc.

G. Density Functional Theory

The electron correlation can also be approximately calculated by replacing parts of the HF Hamiltonian with terms that are functions of the electron density.²²

This density functional theory (DFT) is based on the fact that the ground state electronic energy is completely determined by the electron density, given the appropriate functional which extracts the energy from the density function.²³ The exact functional is not known, and so the approximate nature of this method arises because of the use of inexact or semi-empirical functionals.

H. The Effective Fragment Potential Method

This method is a major player in Chapters 2, 3, and 4, and so its general features will be introduced here. The version of the EFP described²⁴ is what is presently implemented in the quantum chemistry package GAMESS, and will be referred to as EFP1; EFP2 is currently in development. The EFP1 model has been developed at the Hartree-Fock (HF) level of theory; that is, the three terms included in the model represent the type of interactions that one would expect to be represented at the HF level: electrostatics, polarization (dipole - induced dipole interactions), and exchange repulsion/charge transfer. EFP2 is a more general method applicable to any solvent. The general structure of each of the three terms in EFP1 (hereafter simply EFP) will be described in turn, after a short overview of the entire method is given.

The EFP method for treating discrete solvent effects begins with the *ab initio* Hamiltonian of the “solute,” which may include a small number of solvent molecules. The remaining solvent molecules are then treated by adding their effect on the system as one-electron terms in the *ab initio* Hamiltonian:

$$H = H_{AR} + V \quad (1.39)$$

Where H is the Hamiltonian for the entire system, H_{AR} is the *ab initio* Hamiltonian of the “solute,” or active region, and V represents the one-electron terms that describe the potential due to the fragment molecules.

This potential includes *ab initio* - fragment, *ab initio*(nuclei) - fragment, and fragment - fragment interactions, each including the three terms mentioned above (except for the *ab initio*(nuclei) - fragment interaction; there are no exchange

repulsion/charge transfer terms there.) Note that Eq. (4.2) deals ONLY with the *ab initio* - fragment interactions.

$$V_{el}(\mu, s) = \sum_{k=1}^K V_k^{elec}(\mu, s) + \sum_{l=1}^L V_l^{pol}(\mu, s) + \sum_{m=1}^M V_m^{rep}(\mu, s) \quad (1.40)$$

Where μ labels the fragments, s the *ab initio* electronic coordinates, V^{elec} is the electrostatic potential, V^{pol} is the polarization, and V^{rep} is the exchange repulsion/charge transfer. k , l , and m will be discussed with each term below.

1. The Electrostatic Term

The electrostatic potential is represented using a distributed multipolar analysis (DMA) of the fragment charge densities. The total potential is given by

$$\sum_{k=1}^K V_k^{elec}(\mu, s) \quad (1.41)$$

where k labels the expansion points, which are defined as the atom (nuclear) centers, and the bond midpoints in the fragment. [e.g. for water, $K=5$; see Fig. (1.1)]

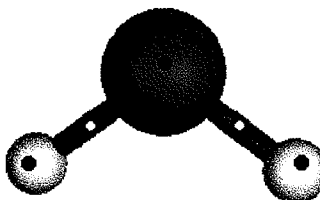


Fig. (1.1) The dots indicate the location of the DMA expansion points, k .

The above expansion, Eq. (1.41), is a point-charge model, and thus knows nothing of continuous three dimensional charge densities. This model works fine as long as the two charge densities are far apart, but as they approach one another, the

charge densities overlap and the nuclei become unshielded with respect to interactions with electrons. Therefore the actual interaction at short distances is always more attractive than a DMA analysis would predict. This shortfall is accounted for by a screening function that diminishes the magnitude of the electrostatic potential for small distances: (See Chapter 2 for a derivation of fragment-fragment charge penetration.)

$$V_k^{elec}(\mu, s) \rightarrow [1 - \beta_k(\mu) e^{-\alpha_k(\mu) r_{sk}^2}] V_k^{elec}(\mu, s) \quad (1.42)$$

where α and β represent adjustable parameters for the given fragment species (e.g. water).

Again, the above discussion is for *ab initio* - fragment interactions; for inter-fragment electrostatic interactions, simple classical expressions are used (dipole-dipole, quadrupole-quadrupole, etc.)

2. The Polarization Term

The fragment molecules are polarized by the electric field of the *ab initio* molecules. This is represented by an iterative perturbation model which uses bonding and lone-pair localized orbital dipole polarizabilities, $\alpha_{\alpha\beta}$ [centered at points l in Eq. (1.40), see Fig. (1.2)]. These polarizabilities are extracted from finite-field perturbed HF calculations on isolated fragment molecules. The iterations are needed because a single fragment surrounded by other fragments and the *ab initio* molecule(s) will 'feel' the electric field, and an induced dipole will result in the fragment.

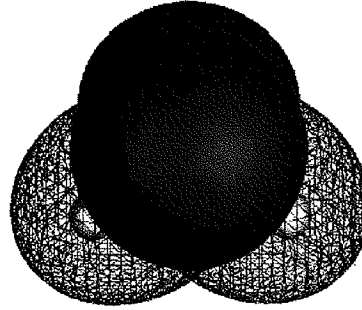


Fig. (1.2) The points l are located at the centroids of the localized orbitals of the fragment, shown here for water. The core orbital associated with the oxygen is hidden.

The presence of this induced dipole has now affected the total field, which will in turn affect the original induced dipole. This process must be iterated mathematically until the entire system converges to a self-consistent polarization energy.

3. The Exchange Repulsion/Charge Transfer Term

The exchange repulsion between two entities with like or dislike charges is purely a quantum mechanical effect. This interaction between the *ab initio* part and the fragments is modeled by a one-electron term in the *ab initio* Hamiltonian.

$$V_m^{rep}(\mu, s) = \sum_j^J \beta_{m,j}(\mu) e^{-\alpha_{m,j}(\mu) r_{m,s}^2} \quad (1.43)$$

Here, m counts the number of repulsive points in the fragment [$M=4$ for water, see Fig. (1.3)], and α and β are fitted parameters; $J=2$ such that the function is a linear combination of two Gaussians.

The Gaussian functions are centered on the fragment atom centers and center of mass and are fitted using the following method.

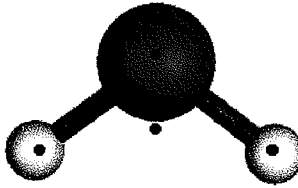


Fig. (1.3) The centers of the Gaussian functions, m in Eq. (1.43).

Ab initio calculations are performed on a number of points (192 for water dimer). Using these, the *ab initio* exchange repulsion/charge transfer is found by

$$E_{\text{remainder}} = E_{\text{total}} - E_{\text{electrostatic}} - E_{\text{polarization}} \quad (1.44)$$

Then, the exchange repulsion/charge transfer term is fitted to Eq. (1.45) (i.e. $\Delta \rightarrow 0$)

$$\Delta = \sum_p \omega_p \left[\langle \psi | \sum_m^M V_m^{\text{rep}} | \psi \rangle - E_{\text{rem}}^p \right]^2 \quad (1.45)$$

Where ω_p is a weighting factor (set to unity for water) and p counts a number of grid points. ψ is the *ab initio* wavefunction.

For fragment-fragment interactions, we use exponential rather than Gaussian functions, and a smaller number of points for the fit.

III. Dissertation Organization

The present work contains seven chapters and six appendices: chapters 2 through 6 are papers accepted, submitted to, or in preparation for submission to appropriate peer reviewed journals with the present author as the primary (chapters 2, 3, 4, and 6) or secondary (chapter 5) contributor.

Chapter 2 details the derivation and implementation of an expression for intermolecular charge penetration, an effect which is not accounted for when one

represents a three-dimensional charge density using a distributed multipolar expansion.

Chapter 3 introduces a modified derivation of Ditchfield's gauge invariant atomic orbital method for calculating chemical shifts. This method is coupled with a modified implementation of McMurchie-Davidson one- and two-electron integrals. The ultimate goal is to couple these methods with the Effective Fragment Potential (EFP) method for solvation to allow for the prediction of chemical shifts in solution.

Chapter 4 describes an application of the EFP method to study the solvation of formic and acetic acids. As many as five water fragments model solvation of the weak acids, and physical properties such as dissociated bond length, Mullikan charges, and energy are monitored as a function of the number of added waters.

Chapter 5 describes the implementation and reports results for the generalization of the Gaussian-2 and Gaussian-3 methods for multi-configurational wavefunctions. The purpose of these methods is to theoretically predict thermodynamic values to chemical accuracy.

Chapter 6 is a study of the electronic structure of titanocene, the titanium analog of ferrocene. A variety of theoretical methods are used, including HF, second-order Møller-Plesset (MP2) theory, DFT, MCSCF, and coupled cluster theories.

CHAPTER 2: EVALUATION OF CHARGE PENETRATION BETWEEN DISTRIBUTED MULTIPOLAR EXPANSIONS

Taken from a paper that has been published in the *Journal of Chemical Physics*.
Reprinted with permission from the *Journal of Chemical Physics* 112(17),
May 1, 2000, pp 7300-7306.
Copyright 2000 American Institute of Physics

Mark A. Freitag, Mark S. Gordon, Jan H. Jensen, and Walter J. Stevens

Abstract

A formula to calculate the charge penetration energy that results when two charge densities overlap has been derived for molecules described by an effective fragment potential (EFP). The method has been compared with the *ab initio* charge penetration, taken to be the difference between the electrostatic energy from a Morokuma analysis and Stone's Distributed Multipole Analysis. The average absolute difference between the EFP method and the *ab initio* charge penetration for dimers of methanol, acetonitrile, acetone, DMSO, and dichloromethane at their respective equilibrium geometries is 0.32 kcal mol⁻¹.

I. Introduction

There are several fundamental long and short-range intermolecular interactions that occur between closed shell molecules in their ground states: Long range interactions ($U \propto r^{-n}$) are due to electrostatics, polarization and dispersion; while exchange repulsion, charge transfer, and charge penetration are considered to be short-range ($U \propto e^{-\alpha r}$).²⁵ In principle, one can calculate all these interactions to a desired level of accuracy from the system's approximate wavefunction using *ab initio* techniques. In practice, the computational demands of such calculations quickly become insurmountable as the size of the system increases. This is a particularly difficult problem when one wishes to study solvated species, and so in recent years there has been considerable work in developing discrete potentials, given in terms of the above intermolecular interactions, for common solvents, particularly water.²⁶

The goal in these studies is to develop a pseudo-quantum potential that can recover *ab initio* results while requiring minimal CPU time.

One such effort has been the development of the Effective Fragment Potential (EFP) method.²⁷ In this method, one typically divides the total system into two parts, an *ab initio*, or active region, and a fragment region (although there is no explicit need for an *ab initio* region). Then the fragment-fragment and/or fragment-*ab initio* interactions are calculated within the framework of the EFP methodology. Since the EFP model to date has been based on Hartree-Fock theory, EFPs allow for the calculation of those intermolecular interactions that one would expect to find at the Hartree-Fock level of theory: Electrostatics, polarization, exchange repulsion/charge transfer, and charge penetration. (See Chapter 4 for a detailed discussion of the EFP method.)

In several recent papers a modification of the original EFP method has been discussed,²⁸ the key feature of which is the method's generalization to *any* solvent. This discussion is continued in the present work with a focus on the calculation of fragment-fragment charge penetration.

Conceptually, charge penetration can be understood in the following way: Consider two molecules separated by a large distance from one another in space. The electrostatic interaction between these two species is then very well represented by Stone's distributed multipolar analysis (DMA),²⁹ in which the electrostatic potential of each molecule is expanded about several points, typically the atom centers and bond midpoints, into monopoles, dipoles, quadrupoles, octopoles, etc.³⁰ The interaction energy is then calculated using the expressions for classical multipolar interactions. However, if the two molecules are brought close enough, such that their charge densities overlap, the nuclei on one molecule will no longer be shielded by its own electron density, and will experience a greater attraction for the electron density associated with the other species. The energy difference resulting from this increased attraction is referred to as charge penetration.

Mathematically, Stone demonstrated the origin of charge penetration through the following simple example:²⁵ Consider the interaction of a hydrogen-like atom with nuclear charge Z and a proton. The wavefunction of the former is given by

$$\psi(r) = \left(\frac{Z^3}{\pi} \right)^{\frac{1}{2}} e^{-Zr} \quad (2.1)$$

and the electron charge density is given by

$$\rho(r) = -\frac{Z^3}{\pi} e^{-2Zr}. \quad (2.2)$$

One can then use Poisson's equation $\nabla^2 V = -\frac{\rho}{\epsilon_0}$, where ϵ_0 is the permittivity of free space, to find the potential due to that density. This results in

$$V(r) = -\frac{1}{r} + e^{-2Zr} \left(Z + \frac{1}{r} \right). \quad (2.3)$$

Since a multipolar expansion is in essence a Taylor expansion of the potential, which is a simple function of $1/r$, the second term in Eq. (2.3) is identified as the charge penetration. At moderate distances, the charge penetration falls off as a simple exponential.

It is well known that the exchange repulsion decays exponentially with distance. Murrell and Teixeira-Dias³¹ have shown that charge penetration (E^{pen}) and exchange repulsion energies (E^{XR}) behave similarly, and have suggested the following relation between the two:

$$E^{XR} = -E^{pen}(a + bR) \quad (2.4)$$

where a and b are empirical parameters, and R is the intermolecular separation. Conceptually, charge penetration should also be related to the intermolecular overlap. Murrell had earlier observed that

$$E^{XR} = \frac{kS^2}{R} \quad (2.5)$$

where k is an empirical parameter and S is the overlap integral between two molecular wavefunctions. Taken together, Eqs. (2.4) and (2.5) suggest that E^{pen} roughly scales as the square of the intermolecular overlap. This suggestion is supported by a recently published equation³² for E^{pen} between two non-orthogonal MO's i and j ,

$$E_{ij}^{pen} = -2 \left(\frac{1}{-2 \ln S_{ij}} \right)^{\frac{1}{2}} \frac{S_{ij}^2}{R_{ij}} \quad (2.6)$$

where R_{ij} is the distance between Gaussian centers. Eq. (2.6) is derived within the Spherical Gaussian Overlap³³ approximation, and yields charge penetration energies that are, on average, within 0.25 kcal mol⁻¹³⁴ of the exact result for six different homomolecular dimers of common solvents.³²

An alternative, presumably less computationally demanding, way to calculate charge penetration between fragments is to introduce a damping function that multiplies the electrostatic potential. Consider Eq. (2.3), when rewritten as²⁵

$$V(r) = \left[1 - e^{-2Zr} (1 + rZ) \right] \left[-\frac{1}{r} \right] = f^{damp}(r) V^{mult}(r) . \quad (2.7)$$

This suggests that a multipole expansion of the electrostatic potential (V^{mult}) can be corrected for charge penetration effects by using a damping function, f^{damp} . Indeed, as part of the original EFP method, Day *et. al.* have used a damping function to model the electrostatic charge penetration between a distributed multipole expansion and an *ab initio* charge density²⁷. Damping functions have also been used to correct multipolar expansion models of the induction energy,³⁵ and dispersion energy.³⁶

The present paper describes the use of damping functions to model charge penetration effects between two or more multipole expansions, i.e. to correct the DMA electrostatic interactions between EFPs. The basic procedure is as follows: One must choose the parameter in the damping function such that the function fits the molecular *ab initio* electrostatic potential well in the region of interest. Then the difference between the damped and undamped electrostatic interactions, within the framework of the DMA, will be a good approximation to the charge penetration. A derivation of this EFP/EFP charge penetration energy, along with an explanation of how the damping function parameter is found, is given in Section II. The success of this method for several homomolecular dimers is demonstrated in Section III. A summary of our findings is presented in Section IV. The entire procedure described here has been implemented in the electronic structure code GAMESS.³⁷

II. Theory

The notation used in the following equations is defined in Fig. (2.1). The charge densities ρ_A and ρ_B are centered at points A and B, respectively. These points represent the atomic centers and bond midpoints for EFPs. Points 1 and 2 represent electronic positions associated with ρ_A and ρ_B , respectively. All points are referenced from an arbitrary origin, O . Using these definitions, the electrostatic interaction of two charge densities ρ_A and ρ_B is given by

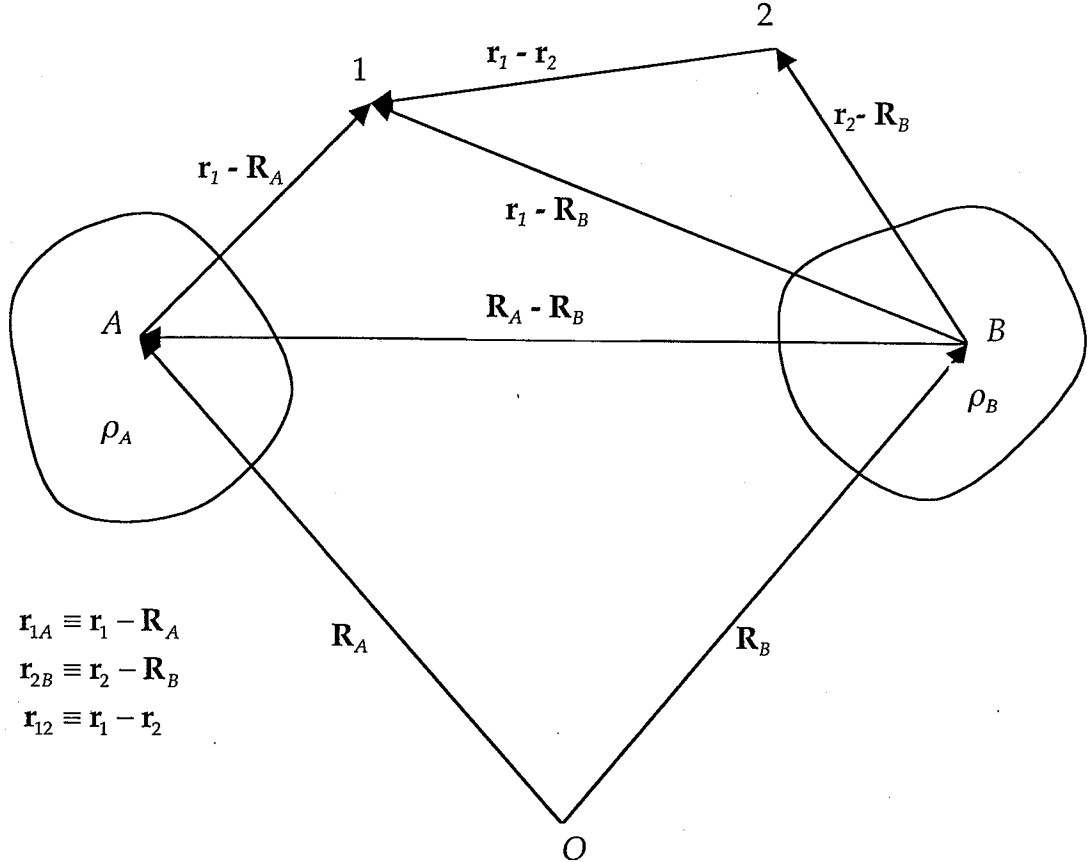


Fig. (2.1) Notation used in Section II. (See text for explanation.)

$$\begin{aligned}
 E^{Elec} &= \iint d\mathbf{r}_1 d\mathbf{r}_2 \rho_A(\mathbf{r}_{1A}) \rho_B(\mathbf{r}_{2B}) |\mathbf{r}_{12}|^{-1} \\
 &= \int d\mathbf{r}_1 \rho_A(\mathbf{r}_{1A}) \int d\mathbf{r}_2 \rho_B(\mathbf{r}_{2B}) |\mathbf{r}_{12}|^{-1}
 \end{aligned} \tag{2.8}$$

where $\mathbf{r}_{1A} = \mathbf{r}_1 - \mathbf{R}_A$. In the EFP method the electrostatic potential due to the charge density is expanded in terms of charges, dipoles, quadrupoles, and octupoles at each atomic center and bond midpoint using Stone's distributed multipolar analysis:

$$\begin{aligned}
 E^{Elec} &= \int d\mathbf{r}_1 \rho_A(\mathbf{r}_{1A}) \int d\mathbf{r}_2 \rho_B(\mathbf{r}_{2B}) \left[|\mathbf{r}_{1B}|^{-1} - \frac{(\mathbf{r}_{12} - \mathbf{r}_{1B}) \mathbf{r}_{1B}}{r_{1B}^3} + \dots \right] \\
 &= \int d\mathbf{r}_1 \rho_A(\mathbf{r}_{1A}) V_B^{mult}(\mathbf{r}_{1B})
 \end{aligned} \tag{2.9}$$

where, as suggested by Eq. (2.9), V_B^{mult} is expanded in multipolar terms:

$$V_B^{mult}(\mathbf{r}_{1B}) = V_B^{charge}(\mathbf{r}_{1B}) + V_B^{dipole}(\mathbf{r}_{1B}) + \dots \quad (2.10)$$

Then, as indicated above, the effect of charge penetration is accounted for by multiplying Eq. (2.10) by a damping function. This damping function should have a number of features: a) go to unity for large R_{AB} and fall off towards zero as R_{AB} approaches zero (where R_{AB} is the distance between points A and B); b) fit well to the *ab initio* electrostatic potential of an isolated fragment in a region near its van der Waals radius, and c) give rise to tractable integrals in Eq. (2.9). After numerous tests with many functions that fit one or more of these criteria, it was found that a simple exponential function gave the best balance of the desired qualities:

$$\tilde{V}_A^{mult}(\mathbf{r}_{1A}) = (1 - e^{-\alpha_A r_{1A}}) V_A^{mult}(\mathbf{r}_{1A}). \quad (2.11)$$

The parameter α is determined by minimizing the difference, Δ , between the quantum mechanical electrostatic potential (*ES*) and the multipolar expansion of the potential over a grid of points:

$$\Delta = \sum_{grid\ points} \left[V_{ab\ initio}^{ES} - V_{damped\ multipole}^{ES} \right]^2.$$

To account for the fact that two damped distributed multipolar expansions are interacting, the charge density on A, $\rho_A(\mathbf{r}_{1A})$, is found by applying Poisson's equation to the damped charge potential, Eq. (2.11):

$$\rho_A(\mathbf{r}_{1A}) = -\epsilon_0 \nabla^2 \tilde{V}_A^{mult}(\mathbf{r}_{1A}) = \rho_A^{charge}(\mathbf{r}_{1A}) + \rho_A^{dipole}(\mathbf{r}_{1A}) + \dots \quad (2.12)$$

Since Poisson's equation is applied to each term in the damped charge electrostatic potential, the charge density is also expressed in terms of charge, dipole,

quadrupole, etc. contributions. Then using Eqs. (2.12) and (2.10), the integral in Eq. (2.9) becomes

$$\begin{aligned}\tilde{E}^{Elec} &= \int d\mathbf{r}_1 \rho_A(\mathbf{r}_{1A}) \tilde{V}_B^{mult}(\mathbf{r}_{1B}) \\ &= \int d\mathbf{r}_1 [\rho_A^{charge}(\mathbf{r}_{1A}) + \rho_A^{dipole}(\mathbf{r}_{1A}) + \dots] [\tilde{V}_B^{charge}(\mathbf{r}_{1B}) + \tilde{V}_B^{dipole}(\mathbf{r}_{1B}) + \dots].\end{aligned}\quad (2.13)$$

Consider the first integral in Eq. (2.13):

$$\tilde{E}_{chg-chg}^{Elec} \approx \int d\mathbf{r}_1 \rho_A^{charge}(\mathbf{r}_{1A}) \tilde{V}_B^{charge}(\mathbf{r}_{1B}). \quad (2.14)$$

The approximate equality in Eq. (2.14) is due to the fact that it is not symmetric with respect to interchange of points A and B. In Eq. (2.14), the charge density on A interacts with the damped charge potential on B. If the points are interchanged, the charge density on B interacts with the damped charge potential on A. Since we wish to calculate, e.g. charge-charge, charge-dipole, dipole-charge, etc. interactions separately, the integrals must be symmetrized with respect to interchange of points. This is done by adding the interchanged integral and taking a simple average of the resulting energies; for example,

$$\tilde{E}_{chg-chg}^{Elec} = \frac{1}{2} \left[\int d\mathbf{r}_1 \rho_A^{charge}(\mathbf{r}_{1A}) \tilde{V}_B^{charge}(\mathbf{r}_{1B}) + \int d\mathbf{r}_1 \rho_B^{charge}(\mathbf{r}_{1B}) \tilde{V}_A^{charge}(\mathbf{r}_{1A}) \right]. \quad (2.15)$$

For clarity, only the integral Eq. (2.14) will be explicitly discussed; the second term in Eq. (2.15) can be found trivially at the end of the derivation by exchanging points A and B.

From Eqs. (2.10), (2.11), and (2.12) one finds

$$\rho_A^{charge}(\mathbf{r}_{1A}) = \frac{q_A \alpha_A^2 \epsilon_0}{r_{1A}} e^{-\alpha_A r_{1A}} \quad (2.16)$$

$$\tilde{V}_B^{charge}(\mathbf{r}_{1B}) = [1 - e^{-\alpha_B r_{1B}}] q_B r_{1B}^{-1} \quad (2.17)$$

where the charge at point A, q_A , is found using Stone's method,²⁹ and ϵ_0 is the permittivity of free space.²⁵ Then Eq. (2.14) becomes

$$\tilde{E}_{chg-chg}^{Elec} \approx q_A q_B \alpha_A^2 \epsilon_0 \left[\int d\mathbf{r}_1 \frac{e^{-\alpha_A r_{1A}}}{r_{1A} r_{1B}} - \int d\mathbf{r}_1 \frac{e^{-\alpha_A r_{1A}} e^{-\alpha_B r_{1B}}}{r_{1A} r_{1B}} \right], \quad (2.18)$$

which can be evaluated using the following integrals:³⁸

$$\begin{aligned} \int d\mathbf{r}_1 e^{-2\alpha_A r_{1A}} r_{1B}^{-1} &= \frac{\pi}{R_{AB} \alpha_A^3} \left[1 - e^{-2\alpha_A R_{AB}} (1 + \alpha_A R_{AB}) \right] \\ \int d\mathbf{r}_1 e^{-2\alpha_A r_{1A}} e^{-2\alpha_B r_{1B}} r_{1B}^{-1} &= \frac{\pi}{R_{AB} (\alpha_A^2 - \alpha_B^2)^2} \left\{ \alpha_A e^{-2\alpha_B R_{AB}} - e^{-2\alpha_A R_{AB}} [\alpha_A + R_{AB} (\alpha_A^2 - \alpha_B^2)] \right\} \\ \int d\mathbf{r}_1 e^{-2\alpha_A r_{1A}} e^{-2\alpha_B r_{1B}} &= \frac{8\pi}{R_{AB} (\alpha_A^2 - \alpha_B^2)^3} \left\{ \begin{aligned} &\alpha_B e^{-2\alpha_A R_{AB}} [R_{AB} (\alpha_A^2 - \alpha_B^2) + 2\alpha_A] \\ &+ \alpha_A e^{-2\alpha_B R_{AB}} [R_{AB} (\alpha_A^2 - \alpha_B^2) - 2\alpha_B] \end{aligned} \right\} \end{aligned}$$

The second two are given by Coulson; the first has been evaluated using his method: First, transform to spheroidal coordinates,³⁹ where

$$\begin{aligned} r_{1A} &= \frac{R_{AB}}{2} (\lambda - \mu) & r_{1B} &= \frac{R_{AB}}{2} (\lambda + \mu) \\ d\mathbf{r}_1 &= d\tau = \frac{1}{8} R_{AB}^3 (\lambda^2 - \mu^2) d\lambda d\mu d\phi \\ 1 \leq \lambda < \infty & \quad -1 \leq \mu \leq +1 & 0 \leq \phi \leq 2\pi \end{aligned}$$

such that

$$\begin{aligned} \int d\mathbf{r}_1 e^{-2\alpha_A r_{1A}} r_{1B}^{-1} &= \frac{1}{4} R_{AB}^2 \int_1^\infty \int_{-1}^1 \int_0^{2\pi} d\lambda d\mu d\phi (\lambda - \mu) e^{-\alpha_A R_{AB}(\lambda - \mu)} \\ &= \frac{\pi}{2} R_{AB}^2 \int_1^\infty \int_{-1}^1 d\lambda d\mu (\lambda - \mu) e^{-\alpha_A R_{AB}(\lambda - \mu)} \end{aligned}$$

substitute $x = \lambda - \mu$:

$$\begin{aligned}
 \int d\mathbf{r}_1 e^{-2\alpha_A r_{1A}} r_{1B}^{-1} &= \frac{\pi}{2} R_{AB}^2 \int_{1-\mu}^{\infty} \int_{-1}^1 d\mu dx x e^{-\alpha_A R_{AB} x} \\
 &= \frac{\pi}{2} R_{AB}^2 \int_{-1}^1 d\mu \left(-\frac{1}{\alpha_A R_{AB}} e^{-\alpha_A R_{AB} x} x + \frac{1}{\alpha_A R_{AB}} \int dx e^{-\alpha_A R_{AB} x} \right) \\
 &= \frac{\pi}{2} R_{AB}^2 \int_{-1}^1 d\mu \left[e^{-\alpha_A R_{AB}(1-\mu)} \left(\frac{(1-\mu)}{\alpha_A R_{AB}} + \frac{1}{\alpha_A^2 R_{AB}^2} \right) \right] \\
 &= \frac{\pi}{2} R_{AB}^2 \left(\frac{1}{\alpha_A R_{AB}} \int_{-1}^1 d\mu e^{-\alpha_A R_{AB}(1-\mu)} (1-\mu) + \frac{1}{\alpha_A^2 R_{AB}^2} \int_{-1}^1 d\mu e^{-\alpha_A R_{AB}(1-\mu)} \right)
 \end{aligned}$$

substitute $x = 1 - \mu$:

$$\begin{aligned}
 \int d\mathbf{r}_1 e^{-2\alpha_A r_{1A}} r_{1B}^{-1} &= \frac{\pi}{2} R_{AB}^2 \left(\frac{1}{\alpha_A R_{AB}} \int_0^2 dx e^{-\alpha_A R_{AB} x} x + \frac{1}{\alpha_A^2 R_{AB}^2} \int_0^2 dx e^{-\alpha_A R_{AB} x} \right) \\
 &= \frac{\pi}{2} R_{AB}^2 \left(\frac{1}{\alpha_A R_{AB}} \left[-e^{-2\alpha_A R_{AB}} \left(\frac{1}{\alpha_A^2 R_{AB}^2} + \frac{2}{\alpha_A R_{AB}} \right) + \frac{1}{\alpha_A^2 R_{AB}^2} \right] \right. \\
 &\quad \left. + \frac{1}{\alpha_A^2 R_{AB}^2} \left[-\frac{1}{\alpha_A R_{AB}} e^{-2\alpha_A R_{AB}} + \frac{1}{\alpha_A R_{AB}} \right] \right) \\
 &= \frac{\pi}{2} R_{AB}^2 \left(\frac{1}{\alpha_A^3 R_{AB}^3} \left[1 - e^{-2\alpha_A R_{AB}} (1 + 2\alpha_A R_{AB}) \right] + \frac{1}{\alpha_A^3 R_{AB}^3} \left[1 - e^{-2\alpha_A R_{AB}} \right] \right) \\
 &= \frac{\pi}{2\alpha_A^3 R_{AB}} \left(1 - e^{-2\alpha_A R_{AB}} - 2\alpha_A R_{AB} e^{-2\alpha_A R_{AB}} + 1 - e^{-2\alpha_A R_{AB}} \right) \\
 &= \frac{\pi}{2\alpha_A^3 R_{AB}} \left[2 - 2e^{-2\alpha_A R_{AB}} (1 + \alpha_A R_{AB}) \right] \\
 &= \frac{\pi}{\alpha_A^3 R_{AB}} \left[1 - e^{-2\alpha_A R_{AB}} (1 + \alpha_A R_{AB}) \right]
 \end{aligned}$$

which was to be demonstrated (Q.E.D.). The use of these integrals yields

$$\tilde{E}_{chg-chg}^{Elec} \approx \frac{q_A q_B}{R_{AB}} \left[1 - e^{-\alpha_A R_{AB}} - \frac{\alpha_A^2}{(\alpha_A^2 - \alpha_B^2)} \left[e^{-\alpha_B R_{AB}} - e^{-\alpha_A R_{AB}} \right] \right] \quad (2.19)$$

where the charge at point A, q_A , is found using Stone's method,²⁹ and ϵ_0 is the permittivity of free space.²⁵ Then Eq. (2.14) becomes

$$\tilde{E}_{chg-chg}^{Elec} \approx q_A q_B \alpha_A^2 \epsilon_0 \left[\int d\mathbf{r}_1 \frac{e^{-\alpha_A r_{1A}}}{r_{1A} r_{1B}} - \int d\mathbf{r}_1 \frac{e^{-\alpha_A r_{1A}} e^{-\alpha_B r_{1B}}}{r_{1A} r_{1B}} \right], \quad (2.18)$$

which can be evaluated using the following integrals.³⁸

$$\begin{aligned} \int d\mathbf{r}_1 e^{-2\alpha_A r_{1A}} r_{1B}^{-1} &= \frac{\pi}{R_{AB} \alpha_A^3} \left[1 - e^{-2\alpha_A R_{AB}} (1 + \alpha_A R_{AB}) \right] \\ \int d\mathbf{r}_1 e^{-2\alpha_A r_{1A}} e^{-2\alpha_B r_{1B}} r_{1B}^{-1} &= \frac{\pi}{R_{AB} (\alpha_A^2 - \alpha_B^2)^2} \left\{ \alpha_A e^{-2\alpha_B R_{AB}} - e^{-2\alpha_A R_{AB}} [\alpha_A + R_{AB} (\alpha_A^2 - \alpha_B^2)] \right\} \\ \int d\mathbf{r}_1 e^{-2\alpha_A r_{1A}} e^{-2\alpha_B r_{1B}} &= \frac{8\pi}{R_{AB} (\alpha_A^2 - \alpha_B^2)^3} \left\{ \begin{aligned} &\alpha_B e^{-2\alpha_A R_{AB}} [R_{AB} (\alpha_A^2 - \alpha_B^2) + 2\alpha_A] \\ &+ \alpha_A e^{-2\alpha_B R_{AB}} [R_{AB} (\alpha_A^2 - \alpha_B^2) - 2\alpha_B] \end{aligned} \right\} \end{aligned}$$

The second two are given by Coulson; the first has been evaluated using his method: First, transform to spheroidal coordinates,³⁹ where

$$\begin{aligned} r_{1A} &= \frac{R_{AB}}{2} (\lambda - \mu) & r_{1B} &= \frac{R_{AB}}{2} (\lambda + \mu) \\ d\mathbf{r}_1 &= d\tau = \frac{1}{8} R_{AB}^3 (\lambda^2 - \mu^2) d\lambda d\mu d\phi \\ 1 \leq \lambda < \infty & \quad -1 \leq \mu \leq +1 & 0 \leq \phi \leq 2\pi \end{aligned}$$

such that

$$\begin{aligned} \int d\mathbf{r}_1 e^{-2\alpha_A r_{1A}} r_{1B}^{-1} &= \frac{1}{4} R_{AB}^2 \int_1^\infty \int_{-1}^1 \int_0^{2\pi} d\lambda d\mu d\phi (\lambda - \mu) e^{-\alpha_A R_{AB}(\lambda - \mu)} \\ &= \frac{\pi}{2} R_{AB}^2 \int_1^\infty \int_{-1}^1 d\lambda d\mu (\lambda - \mu) e^{-\alpha_A R_{AB}(\lambda - \mu)} \end{aligned}$$

substitute $x = \lambda - \mu$:

$$\begin{aligned}
 \int d\mathbf{r}_1 e^{-2\alpha_A r_{1A}} r_{1B}^{-1} &= \frac{\pi}{2} R_{AB}^2 \int_{1-\mu}^{\infty} \int_{-1}^1 d\mu dx \ x e^{-\alpha_A R_{AB} x} \\
 &= \frac{\pi}{2} R_{AB}^2 \int_{-1}^1 d\mu \left(-\frac{1}{\alpha_A R_{AB}} e^{-\alpha_A R_{AB} x} x + \frac{1}{\alpha_A R_{AB}} \int dx e^{-\alpha_A R_{AB} x} \right) \\
 &= \frac{\pi}{2} R_{AB}^2 \int_{-1}^1 d\mu \left[e^{-\alpha_A R_{AB} (1-\mu)} \left(\frac{(1-\mu)}{\alpha_A R_{AB}} + \frac{1}{\alpha_A^2 R_{AB}^2} \right) \right] \\
 &= \frac{\pi}{2} R_{AB}^2 \left(\frac{1}{\alpha_A R_{AB}} \int_{-1}^1 d\mu e^{-\alpha_A R_{AB} (1-\mu)} (1-\mu) + \frac{1}{\alpha_A^2 R_{AB}^2} \int_{-1}^1 d\mu e^{-\alpha_A R_{AB} (1-\mu)} \right)
 \end{aligned}$$

substitute $x = 1 - \mu$:

$$\begin{aligned}
 \int d\mathbf{r}_1 e^{-2\alpha_A r_{1A}} r_{1B}^{-1} &= \frac{\pi}{2} R_{AB}^2 \left(\frac{1}{\alpha_A R_{AB}} \int_0^2 dx e^{-\alpha_A R_{AB} x} x + \frac{1}{\alpha_A^2 R_{AB}^2} \int_0^2 dx e^{-\alpha_A R_{AB} x} \right) \\
 &= \frac{\pi}{2} R_{AB}^2 \left(\frac{1}{\alpha_A R_{AB}} \left[-e^{-2\alpha_A R_{AB}} \left(\frac{1}{\alpha_A^2 R_{AB}^2} + \frac{2}{\alpha_A R_{AB}} \right) + \frac{1}{\alpha_A^2 R_{AB}^2} \right] \right. \\
 &\quad \left. + \frac{1}{\alpha_A^2 R_{AB}^2} \left[-\frac{1}{\alpha_A R_{AB}} e^{-2\alpha_A R_{AB}} + \frac{1}{\alpha_A R_{AB}} \right] \right) \\
 &= \frac{\pi}{2} R_{AB}^2 \left(\frac{1}{\alpha_A^3 R_{AB}^3} \left[1 - e^{-2\alpha_A R_{AB}} (1 + 2\alpha_A R_{AB}) \right] + \frac{1}{\alpha_A^3 R_{AB}^3} \left[1 - e^{-2\alpha_A R_{AB}} \right] \right) \\
 &= \frac{\pi}{2\alpha_A^3 R_{AB}} \left(1 - e^{-2\alpha_A R_{AB}} - 2\alpha_A R_{AB} e^{-2\alpha_A R_{AB}} + 1 - e^{-2\alpha_A R_{AB}} \right) \\
 &= \frac{\pi}{2\alpha_A^3 R_{AB}} \left[2 - 2e^{-2\alpha_A R_{AB}} (1 + \alpha_A R_{AB}) \right] \\
 &= \frac{\pi}{\alpha_A^3 R_{AB}} \left[1 - e^{-2\alpha_A R_{AB}} (1 + \alpha_A R_{AB}) \right]
 \end{aligned}$$

which was to be demonstrated (Q.E.D.). The use of these integrals yields

$$\tilde{E}_{chg-chg}^{Elec} \approx \frac{q_A q_B}{R_{AB}} \left[1 - e^{-\alpha_A R_{AB}} - \frac{\alpha_A^2}{(\alpha_A^2 - \alpha_B^2)} \left[e^{-\alpha_B R_{AB}} - e^{-\alpha_A R_{AB}} \right] \right] \quad (2.19)$$

when $\alpha_A \neq \alpha_B$, and

$$\tilde{E}_{chg-chg}^{Elec} \approx \frac{q_A q_B}{R_{AB}} \left[1 - e^{-\alpha R_{AB}} \left(1 + \frac{\alpha R_{AB}}{2} \right) \right] \quad (2.20)$$

when $\alpha_A = \alpha_B = \alpha$. In deriving Eqs. (2.19) and (2.20), we have used the fact that $4\pi\epsilon_0 = 1$ in atomic units, and R_{AB} represents the distance between expansion points A and B .

A similar procedure is used to calculate electron-nuclear interactions; here the damped monopole contribution to the density is allowed to interact with the unscreened nuclear charge. Again, starting from Eq. (2.9), the interaction is given by

$$\begin{aligned} E_{chg}^{Elec-Nuc} &= \int d\mathbf{r}_1 \rho_A^{charge}(\mathbf{r}_{1A}) Z_B r_{1B}^{-1} + \int d\mathbf{r}_1 \rho_B^{charge}(\mathbf{r}_{1B}) Z_A r_{1A}^{-1} \\ &= q_A Z_B \alpha_A^2 \int d\mathbf{r}_1 \frac{e^{-\alpha_A r_{1A}}}{r_{1A} r_{1B}} + q_B Z_A \alpha_B^2 \int d\mathbf{r}_1 \frac{e^{-\alpha_B r_{1B}}}{r_{1A} r_{1B}} \\ &= \frac{q_A Z_B}{R_{AB}} [1 - e^{-\alpha_A R_{AB}}] + \frac{q_B Z_A}{R_{AB}} [1 - e^{-\alpha_B R_{AB}}] \end{aligned} \quad (2.21)$$

Note that Eq. (2.21) is already symmetric with respect to interchange of A and B . Finally, summing Eqs. (2.19) and (2.21), including the symmetrization, and subtracting out the undamped interactions, the charge penetration energy for charge-charge interactions only becomes

$$E_{chg-chg}^{Pen} = -\frac{1}{2R_{AB}} \left[q_A (q_B + 2Z_B) e^{-\alpha_A R_{AB}} + q_B (q_A + 2Z_A) e^{-\alpha_B R_{AB}} + \frac{q_A q_B (\alpha_A^2 + \alpha_B^2)}{\alpha_A^2 - \alpha_B^2} (e^{-\alpha_B R_{AB}} - e^{-\alpha_A R_{AB}}) \right] \quad (2.22)$$

where $\alpha_A \neq \alpha_B$ and $Z_{A,B} = 0$ for bond midpoints. For the $\alpha_A = \alpha_B = \alpha$ case,

$$E_{chg-chg}^{Pen} = -\frac{1}{R_{AB}} \left[q_A q_B \left(1 + \frac{\alpha R_{AB}}{2} \right) + q_A Z_B + q_B Z_A \right] e^{-\alpha R_{AB}} \quad (2.23)$$

Note in Eqs. (2.22) and (2.23) the total charge penetration is the sum of all charge penetration energies between unique pairs of intermolecular DMA points A and B.

If one follows the above procedures for charge-dipole interactions, an equation analogous to Eq. (2.13) is found:

$$\int d\mathbf{r}_1 \rho_A^{charge}(\mathbf{r}_{1A}) \tilde{V}_B^{dipole}(\mathbf{r}_{1B}) = q_A \mu_B \alpha_A^2 \epsilon_o \left[\int d\mathbf{r}_1 \frac{e^{-\alpha_A r_{1A}}}{r_{1A} r_{1B}^2} \cos \theta_B + \int d\mathbf{r}_1 \frac{e^{-\alpha_A r_{1A}} e^{-\alpha_B r_{1B}}}{r_{1A} r_{1B}^2} \cos \theta_B \right] \quad (2.24)$$

The integrals in Eq. (2.24) can also be evaluated analytically using Coulson's method, however, the first two dipole-charge integrals,

$$\int d\mathbf{r}_1 \rho_A^{dipole}(\mathbf{r}_{1A}) \tilde{V}_B^{charge}(\mathbf{r}_{1B}) = q_B \mu_A \alpha_A \epsilon_o \left[2 \int d\mathbf{r}_1 \frac{e^{-\alpha_A r_{1A}} \cos \theta_A}{r_{1A}^3 r_{1B}} - 2 \int d\mathbf{r}_1 \frac{e^{-\alpha_A r_{1A}} e^{-\alpha_B r_{1B}} \cos \theta_A}{r_{1A}^3 r_{1B}} \right. \\ \left. + \alpha_A \int d\mathbf{r}_1 \frac{e^{-\alpha_A r_{1A}} \cos \theta_A}{r_{1A}^2 r_{1B}} - \alpha_A \int d\mathbf{r}_1 \frac{e^{-\alpha_A r_{1A}} e^{-\alpha_B r_{1B}} \cos \theta_A}{r_{1A}^2 r_{1B}} \right] \quad (2.25)$$

do not converge analytically. The resulting increase in CPU time rules out a numerical analysis of these integrals, and evaluating charge-dipole interactions without dipole-charge means not including all terms of a given order. Since this is undesirable as well, the following analysis includes only charge-charge interactions. It will be shown that even with such a seemingly severe truncation, a major percentage of the total charge penetration is still recovered.

Before the results of the above analysis are given, the procedure for determining the alpha parameter in the damping function will be briefly described. Consider the error function

$$\Delta = \sum_{\text{grid points}} \left[V_{\text{ab initio}}^{\text{ES}} - V_{\text{damped multipole}}^{\text{ES}} \right]^2 \quad (2.26)$$

based on the difference between the *ab initio* and multipolar electrostatic potentials. A grid is defined about an isolated fragment molecule in the following manner: Concentric spheres are placed about each of the atom centers at 67% and 300% of the van der Waals radius of the corresponding atom. As will be shown in the next section, these values were chosen because they result in the best fit of the damping function to the *ab initio* density, and they were found to describe the physically most important regions in terms of charge penetration. The fragment is then placed within a three-dimensional Cartesian grid with a spacing of 0.50 Bohr in each direction, and any point not within the two spheres is discarded. It was found that the spacing has little effect on the fit unless the distance between grid points becomes too large; 0.50 Bohr balances run time and accuracy well. The *ab initio* density is calculated on the fragment during a GAMESS run, and the electrostatic potential is computed at each grid point. Finally, the parameter α is optimized in the exponential damping function such that Δ in Eq. (2.26) is minimized. Note that α is a property of the isolated monomer molecule.

III. Results and Discussion

Several tests were run to determine the optimal values of (r_{\min}/r_{\max}) for the radii of the concentric spheres about each atom to determine the set grid of points used in (19). Fig. (2.2) shows the results on the water dimer using charge-charge interactions only. The dimer geometry used here was obtained by first finding the *ab initio* geometry at the RHF/6-31+G(d,p) level of theory, and then superimposing the individual fragment monomer geometries on the dimer structure.³² The abscissa is the relative distance between the water molecules; 0 Å represents the equilibrium distance between the oxygen atoms, negative values bring the fragments closer together, positive values move them further apart along a line connecting the oxygen atoms.

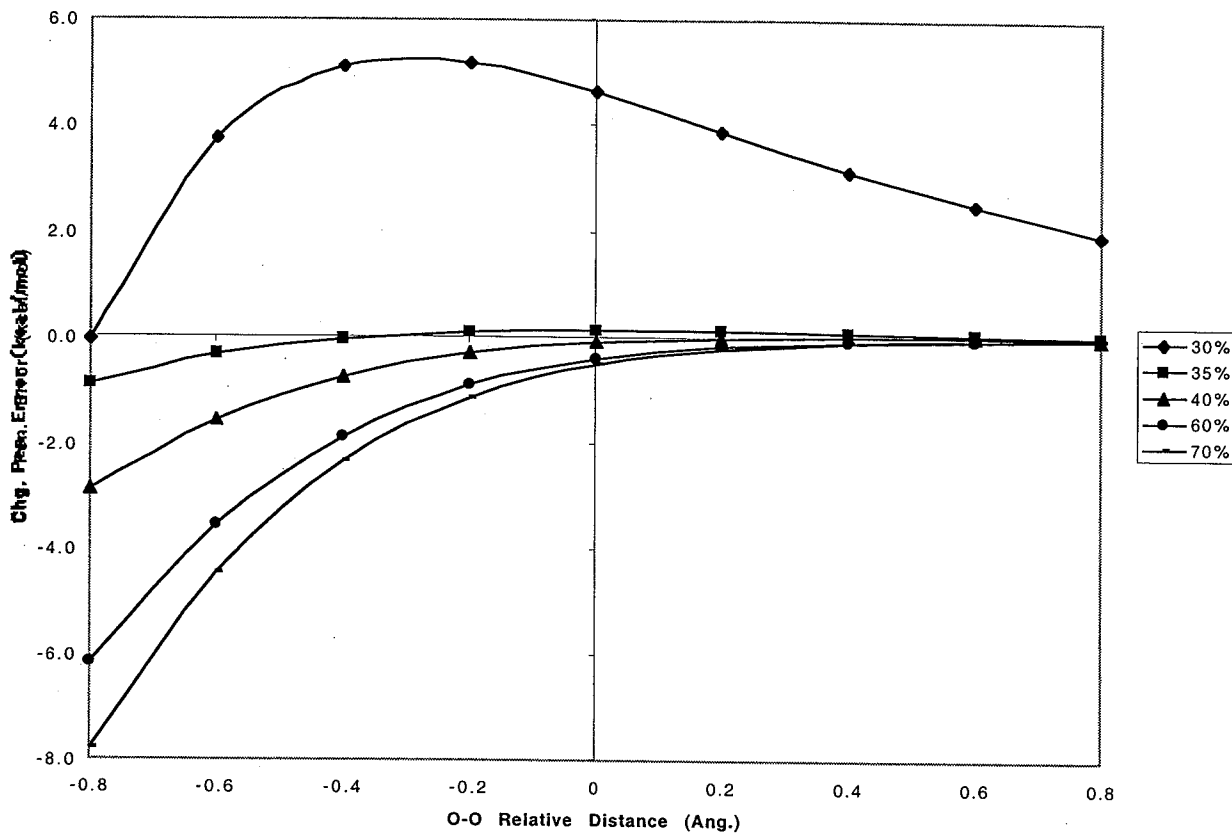


Fig. (2.2) Charge penetration error in kcal mol^{-1} as a function of oxygen-oxygen distance in the water dimer, and as a function of r_{\min} (separate curves). r_{\max} is 300% of the Van der Waals radius of each atom.

The fragment geometries described above are used for the Morokuma analysis [6-31+G(d,p)], and the resulting electrostatic energies are taken to be the exact interactions for *ab initio* electronic densities. The FRAGONLY electrostatic energies are obtained from a fragment-only calculation on the dimer, and do not include any damping in the DMA. The difference between the Morokuma analysis and the FRAGONLY run is then taken to be the charge penetration that the present method is meant to calculate. It has been shown that a simple model of undamped electrostatics and hard spheres leads to a good prediction of equilibrium geometries for Van der Waals complexes,⁴⁰ so only the relevant interaction energies, with and

without charge penetration, are reported here. In Fig. (2.2), r_{\max} is set at 300% of the Van der Waals radius of each atom, and r_{\min} is varied from 30% to 70% of the Van der Waals radius. The ordinate is the difference between our calculated charge penetration and the exact (Morokuma-FRAGONLY) charge penetration.

As r_{\min} approaches the atomic nuclei, the simplistic exponential damping function breaks down as evidenced by the large error for the $r_{\min} = 30\%$ curve. To understand this, consider the functional form of Stone's estimate of charge penetration given by the second term of Eq. (2.3) versus a simple exponential. The single parameter exponential function crosses the ordinate at unity when $r = 0$, whereas Stone's function rises towards infinity. Therefore the exponential function does not contain adequate flexibility to fit the *ab initio* potential in this region close to the nuclear cusp. Depending on the specific monomer potential being fit, a breakdown is expected to occur somewhere in this region. Once this region has been entered, the alpha fitting procedure for the simple exponential quickly deteriorates, the foundation of the method erodes and results in unpredictable error in the calculated charge penetration. This can be seen in Fig. (2.3) for other dimers, where the average breakdown point occurs in the region of $r_{\min} = 55\text{-}60\%$. Referring back to Fig. (2.2): For the higher values of r_{\min} , as the monomers move farther apart the charge penetration, and thus the error, goes to zero. At roughly $r_{\min} = 40\%$, almost all of the charge penetration is recovered at the equilibrium water dimer geometry,

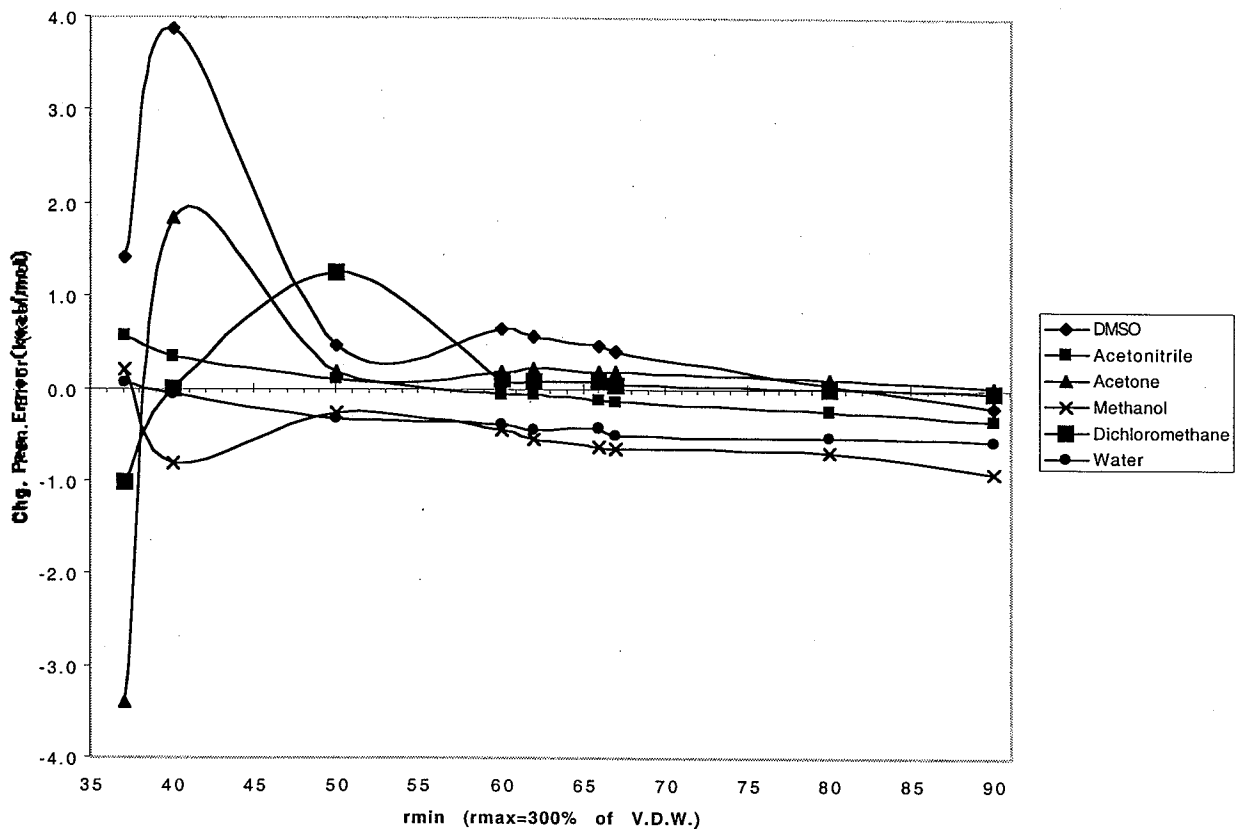


Fig. (2.3) Charge penetration error in kcal mol^{-1} for six homomolecular dimers at their equilibrium geometries, as described in the text. The charge penetration error is given as a function of r_{\min} . $r_{\max} = 300\%$ of the Van der Waals radius on each atom.

although we have seen that this value is most likely too close to the nuclear center to be used in general.

Tests on solvents other than water are shown in Fig. (2.3). It should be noted that although these tests were done on dimers of identical monomers, the method does not require this restriction; the charge penetration between *any* types of fragments can be found this way. The geometries were found using the same method as described above for water dimer. The Morokuma analysis was also performed using the 6-31+G(d,p) basis. Again we note that at smaller values of r_{\min} the absolute error in all of the dimers increases unpredictably. As r_{\min} increases to a

range of 60-80%, the error becomes more stable, and as r_{\min} increases further, outside of the physically meaningful region for charge penetration, the error increases again for most dimers. One could find an optimal value of r_{\min} for each of the dimers shown, but overall the best choice seems to be in the range 60-80%. Fig. (2.4) shows the

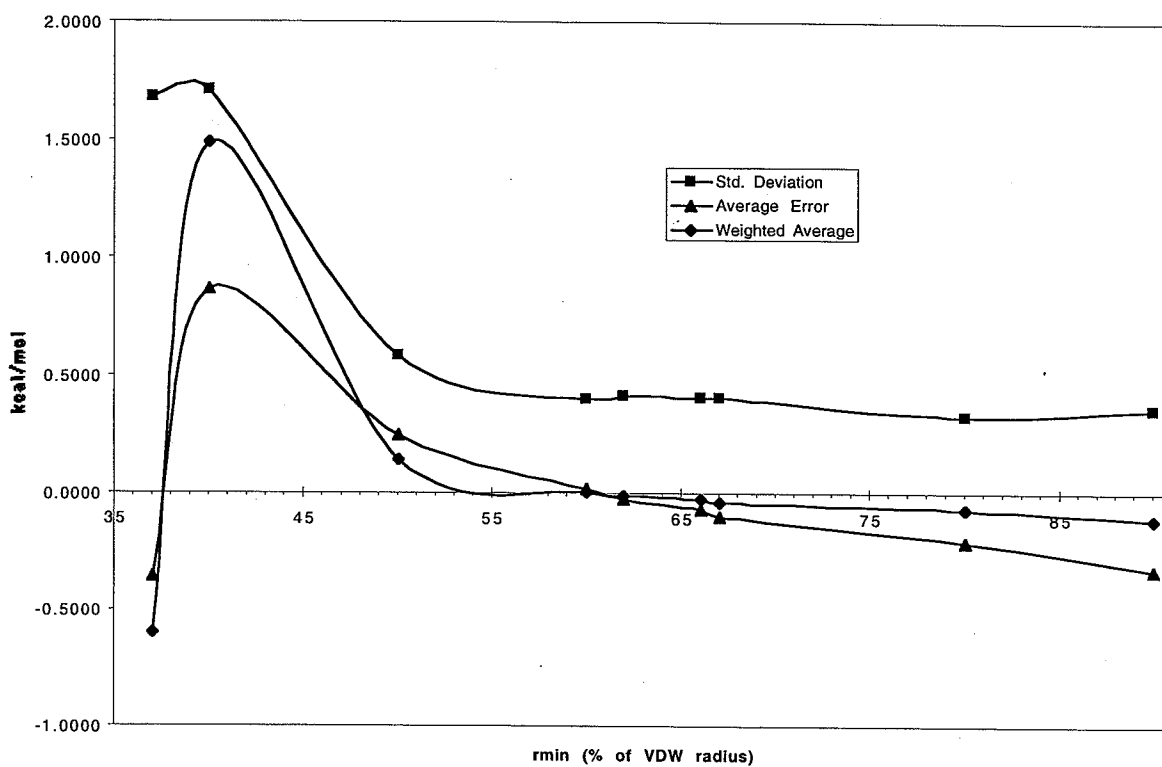


Fig. (2.4) The average error, standard deviation, and weighted average of the six homomolecular dimers in Fig. (2.3), as described in the text. The charge penetration error is given as a function of r_{\min} . $r_{\max} = 300\%$ of the Van der Waals radius on each atom.

average error of the six dimers, the standard deviation, and the average error weighted against the standard deviation. This plot shows where the standard deviation is both small and centered about zero error. Although this plot suggests the optimal value of r_{\min} is 60%, the weighted average difference between $r_{\min}=60\%$ and 67% is only 0.05 kcal mol⁻¹, so very little is lost by choosing the larger, more

conservative value of $r_{\min} = 67\%$. This choice is merely a suggestion based on the six dimers tested, and can be changed in GAMESS by the user. Table (2.1) shows the numerical results when $r_{\min} = 67\%$. The average absolute error is 0.32 kcal mol⁻¹; the largest absolute error is 0.65 kcal mol⁻¹ for methanol. If $r_{\min} = 80\%$, the average absolute error for these six dimers is reduced to 0.27 kcal mol⁻¹; however, this value of r_{\min} seems too high, since it nears the Van der Waals radius and the error is not spread as evenly about zero. Note that only the absolute value of the error is important. The overall charge penetration itself is attractive and thus negative, but there is no assurance that the charge penetration will not be overestimated using this method. This is especially true since only charge-charge interactions are included.

Dimer	Electrostatic energies				
	Morokuma	FRAGONLY	Difference	Charge-charge	Error
(CH ₃) ₂ SO	-10.89	-8.42	-2.47	-2.89	0.42
CH ₃ CN	-5.12	-4.22	-0.90	-0.78	-0.12
(CH ₃) ₂ OO	-3.26	-2.66	-0.59	-0.78	0.19
CH ₃ OH	-8.12	-6.89	-1.23	-0.59	-0.65
CH ₂ Cl ₂	-1.74	-1.47	-0.28	-0.33	0.06
H ₂ O	-8.21	-7.12	-1.09	-0.60	-0.49

Table (2.1) Charge penetration results, 6-31+G(d,p), for dimers of six common solvents; $r_{\min} / r_{\max} = 67\% / 300\%$ of van der Waals radius on each atom. (Grid spacing = 0.50 Bohr. All values are in kcal mol⁻¹. The average absolute error is 0.32 kcal mol⁻¹. See text for discussion.)

The values of alpha for $r_{\min} = 67\%$ are given in Table (2.2). Note that since α is found by fitting the isolated monomer, these values will not change when used in heteromolecular fragment systems.

Monomer	DMA point	Alpha
$(\text{CH}_3)_2\text{SO}$	C	2.91
	H	1.66
	S	1.82
	O	1.94
	S-C bm	1.22
	S-O bm	10.00
	C-H bm	1.49
CH_3CN	C (methyl)	2.17
	C (cyano)	1.96
	N	1.81
	H	1.76
	C-N bm	1.48
	C-C bm	0.56
	C-H	1.54
$(\text{CH}_3)_2\text{CO}$	C (methyl)	1.89
	C (carboxyl)	1.75
	O	1.97
	H	1.75
	C-O bm	1.57
	C-C bm	1.03
	C-H bm	2.08
CH_3OH	C	9.87
	O	1.93
	H (methyl)	1.65
	H (hydroxyl)	3.06
	C-H bm	1.63
	C-O bm	10.00
	O-H bm	10.00
CH_2Cl_2	C	10.00
	Cl	1.78
	H	1.76
	C-H bm	2.00
	C-Cl bm	10.00
H_2O	O	1.88
	H	2.95
	O-H bm	10.00

Table (2.2) Values of the alpha parameter used for the monomers that make up the dimers in Table (2.1). (The abbreviation "bm" refers to bond mid-point.)

IV. Summary and Conclusions

A formula to calculate the charge penetration energy that results when two charge densities overlap has been derived for molecules described by an effective

fragment potential (EFP). The method has been compared with the *ab initio* charge penetration, taken to be the difference between the electrostatic energy from a Morokuma analysis and Stone's Distributed Multipole Analysis. The average absolute difference between the EFP method and the *ab initio* charge penetration for dimers of water, methanol, acetonitrile, acetone, DMSO, and dichloromethane at their equilibrium geometry is 0.32 kcal mol⁻¹.

The EFP method in general has been shown to reproduce *ab initio* results very accurately for water⁴¹, and this work is another step in the continuing development of a general EFP method that will accurately model *any* solvent. The derivation and implementation of dispersion and a parameter-free charge transfer in the EFP will be the subjects of future work.

V. Acknowledgements

This work was supported in part by grants from the National Science Foundation and the Air Force Office of Scientific Research (F49620-98-1-0164 and F49620-97-1-0522).

CHAPTER 3: MODELING SOLVENT EFFECTS IN NUCLEAR MAGNETIC RESONANCE SPECTRA

I. Introduction

Nuclear Magnetic Resonance (NMR) spectroscopy has been an invaluable source of information on molecular structure since its inception during the winter of 1945-46 by Bloch, *et. al.*⁴² and independently by Purcell, *et. al.*⁴³ Since 1974, there has also been significant development in the *ab initio* theory of NMR chemical shifts. In that year, Ditchfield presented a Gauge Invariant Atomic Orbital (GIAO)⁴⁴ method that has proven to be quite popular and accurate, especially when applied in the context of highly correlated *ab initio* methods, such as perturbation theory and coupled cluster theory.⁴⁵ Traditionally, these calculations are carried out in the gas phase, and the lack of consideration for solvent effects is one of the more obvious sources of discrepancy between experimental reality and theoretical models.

Several methods have been developed for treating solvent effects on NMR spectra; these have been reviewed recently by Helgaker, Jaszunski, and Ruud,⁴⁵ and will only be summarized here. Due to the large size of the typical solvated system, the majority of the research has focused on a "supermolecule" SCF description, which at the HF level does not include dispersion effects. This approach has all the well-known advantages and disadvantages of a typical supermolecule calculation; an example of the latter is computational cost. There have also been two attempts to use continuum models of solvation, which describe the electrostatic effects of the solvent without treating a discrete solvent explicitly. (See Chapter 2 for more comments on continuum models.) The first is the GIAO/(Multi-Configurational) Self-Consistent Reaction Field (MCSCRF) method due to Mikkelsen, *et. al.*⁴⁶ and the second is the IGLO/Polarizable Continuum Model (PCM) of Cremer, *et. al.*⁴⁷ In the MCSCRF model, the molecule is placed within a spherical cavity, and the energy of interaction between the molecule and the continuum is written as a multipolar expansion. In the IGLO/PCM model, the molecular cavity is more complex; each atom is surrounded by a sphere, and point charges placed on the cavity surface are used as a tool to model the interaction of the solute with the continuum. With the

popularity of QM/MM methods, such as the EFP method described in some detail in Chapter 1, there have been attempts to use these types of methods to calculate chemical shifts. The main focus has been on molecular dynamic techniques using empirical potentials; see the Helgaker review for details and references.

The purpose of this chapter is to show in detail how the EFP method can be coupled with Ditchfield's GIAO formalism to predict NMR chemical shifts in solution. Section II will give a modified derivation of the GIAO equations, and Section III will derive the relevant antisymmetric perturbation theory equations for field dependent non-orthogonal basis sets that are needed to calculate the first derivative of the density matrix. Section IV will describe how the one- and two-electron integrals derived in Section II are calculated within a hybrid McMurchie-Davidson/Dupuis shell structure scheme, and Section V will describe various strategies for incorporating solvent effects using effective fragments.

II. Chemical Shifts and Gauge-Invariant Atomic Orbitals

The derivation found here is based entirely on that presented by Ditchfield in 1974.⁴⁴ It has been modified slightly into a form which is more consistent and formal than the original. In order to facilitate a smooth presentation without neglecting the details, the reader will be referred repeatedly to Appendices B (vector identities) and C (GIAOs) for explicit derivations. The notation (B.4) will refer, for example, to Appendix B, part 4.

The electronic Hamiltonian describing a closed-shell molecule in the total magnetic field due to a uniform external magnetic field \mathbf{H} and the dipole fields arising from nuclear magnetic moments μ_C, μ_D, \dots situated at fixed nuclear positions $\mathbf{R}_C, \mathbf{R}_D, \dots$ has the form

$$\mathcal{H}(\mathbf{H}, \mu) = \frac{1}{2} \sum_j \left\{ \left(-i\nabla_j + \frac{1}{c} \mathbf{A}'(\mathbf{r}_j) \right)^2 - 2 \sum_C \frac{Z_C}{r_{jC}} \right\} + \sum_{j \neq l} \frac{1}{r_{jl}} + \sum_{C \neq D} \frac{Z_C Z_D}{R_{CD}} \quad (3.1)$$

where \mathbf{r}_j is the distance vector between electron j and an arbitrary origin, and

$$\begin{aligned}\mathbf{r}_{jC} &= \mathbf{r}_j - \mathbf{R}_C \\ \mathbf{R}_{CD} &= \mathbf{R}_C - \mathbf{R}_D\end{aligned}\quad (3.2)$$

as shown in Fig. (3.1).⁴⁸

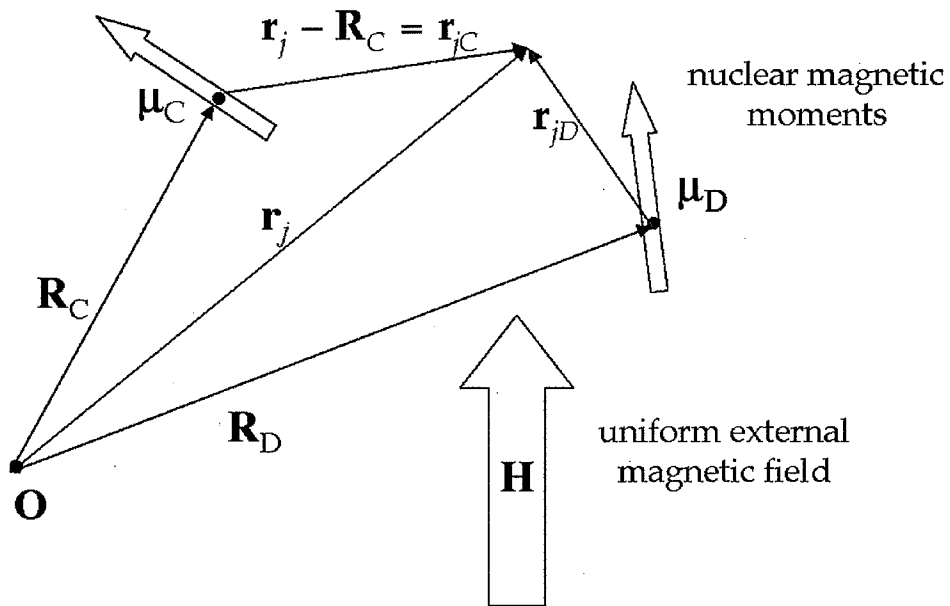


Fig. (3.1) Definitions of vectors and notation in Eq. (3.1).

Note that $\mathbf{A}'(\mathbf{r}_j)$ is the vector potential representing the **total** magnetic field at the position of electron j , and $\mathbf{A}(\mathbf{r}_j)$ is the vector potential without the contribution from the nuclear magnetic moments, μ_B :

$$\begin{aligned}\mathbf{A}'(\mathbf{r}_j) &= \mathbf{A}(\mathbf{r}_j) + \sum_B \frac{\mu_B \times \mathbf{r}_{jB}}{r_{jB}^3} \\ \mathbf{A}(\mathbf{r}_j) &= \frac{1}{2} \mathbf{H} \times \mathbf{r}_j\end{aligned}\quad (3.3a,b)$$

Although the vector potential $\mathbf{A}'(\mathbf{r}_j)$ is completely defined by the above expressions - the first term representing the effect of the external magnetic field at

the electronic coordinates, and the second term representing the magnetic field that results from the nuclear dipole, (C.1) - some discussion of its form and properties is both appropriate and necessary. In 1864, Maxwell introduced his electromagnetic theory, which can be summarized by four equations. One of these states that the divergence of a uniform magnetic field vanishes; i.e. $\nabla \cdot \mathbf{H} = 0$, where \mathbf{H} represents the magnetic field vector. A vector with this property (zero divergence) is said to be solenoidal, and as such, can be represented as the curl of another so-called *vector potential*, in this case represented by \mathbf{A} :

$$\mathbf{H} = \nabla \times \mathbf{A} \quad (3.4)$$

since, for example,

$$\begin{aligned} \nabla \times \mathbf{A} &= \nabla \times \left(\frac{1}{2} \mathbf{H} \times \mathbf{r} \right) = \frac{1}{2} \nabla \times \mathbf{H} \times \mathbf{r} \\ &= \frac{1}{2} [(\mathbf{r} \cdot \nabla) \mathbf{H} - (\mathbf{H} \cdot \nabla) \mathbf{r} - \mathbf{r}(\nabla \cdot \mathbf{H}) + \mathbf{H}(\nabla \cdot \mathbf{r})] \\ &= \frac{1}{2} [-(\mathbf{H} \cdot \nabla) \mathbf{r} + 3\mathbf{H}] = \frac{1}{2} [-\mathbf{H} + 3\mathbf{H}] = \mathbf{H} \end{aligned}$$

using (B.10) and the solenoidal property of \mathbf{H} . The difficulty is that the vector potential, \mathbf{A} , is not uniquely determined by the magnetic field, \mathbf{H} . Consider a vector potential modified by the gradient of a scalar function, f :

$$\mathbf{A}'' = \mathbf{A} + \nabla f(\mathbf{r}) \quad (3.5)$$

The curl of this modified vector potential also gives the original magnetic field:

$$\nabla \times \left(\frac{1}{2} \mathbf{H} \times \mathbf{r} + \nabla f(\mathbf{r}) \right) = \mathbf{H} + \nabla \times \nabla f(\mathbf{r}) = \mathbf{H} \quad (3.6)$$

using (B.5). Consider a specific scalar function, $f(\mathbf{r}) = \frac{1}{2} \mathbf{H} \times \mathbf{r}_0 \cdot \mathbf{r}$, where \mathbf{r}_0 is an arbitrary point in space. The gradient of this function is $\frac{1}{2} \mathbf{H} \times \mathbf{r}_0$, and Eq. (3.5) becomes:

$$\mathbf{A}'' = \frac{1}{2} \mathbf{H} \times (\mathbf{r} + \mathbf{r}_0) \quad (3.7)$$

This modification in effect moves the coordinates of the nucleus in question by a distance \mathbf{r}_0 . The physical implications of the vector potential's mathematical properties are as follows: one can modify the vector potential without changing the external magnetic field, and therefore without changing the physical system. However, the *description* of the physical system, the Hamiltonian, depends on the vector potential, not the resulting magnetic field. Changing the vector potential as, for example, in Eq. (3.7), will change the Hamiltonian and thus the observable energy, but since the physical system has not in fact changed, the observable eigenvalue should also remain unaffected. This means that the wavefunction must change by some complex phase factor to cancel out the change to the Hamiltonian, leaving the observable unchanged. Modern quantum chemical techniques formulate an *approximate* wavefunction expanded in an appropriate basis set, (see Chapter 1) and unless it is unusually large, this basis is not flexible enough to allow for the necessary changes in the wavefunction.

The factor of \mathbf{r}_0 can be referred to as the gauge origin, and the resulting dependence on the choice of this origin is called gauge dependence. For atoms, this origin is easy to choose to give constant results: the nucleus. For molecular systems, the gauge origin cannot be chosen so easily. To compensate for this, Ditchfield, following London,⁴⁹ used gauge invariant atomic orbitals (GIAOs) which act to cancel out the gauge dependence in the wavefunction:

$$\chi_j(\mathbf{H}) = e^{-\frac{i}{2c} \mathbf{H} \times \mathbf{R}_j \cdot \mathbf{r}} \phi_j \quad (3.8)$$

We will return to the use of these GIAOs later, but for now simply note that the phase factor is a function of the external magnetic field and contains the ultimate integration variable \mathbf{r} just as the unperturbed basis function, ϕ_j , does. [See Eqs. (1.34) and (3.66).] First, let us return to the form of the Hamiltonian.

Eq. (3.1) can be expanded (C.2) to give

$$\begin{aligned}
 \mathcal{H}(\mathbf{H}, \boldsymbol{\mu}) = & -\frac{1}{2} \sum_j \left\{ \nabla_j^2 - \sum_B \frac{Z_B}{r_{jB}} \right\} + \sum_l \sum_{j \neq l} \frac{1}{r_{jl}} + \sum_D \sum_{B \neq D} \frac{Z_B Z_D}{R_{BD}} \\
 & - \frac{i}{2c} \sum_{\alpha} H_{\alpha} \sum_j (\mathbf{r}_j \times \nabla_j)_{\alpha} - \frac{i}{c} \sum_{\alpha, B} \mu_{B\alpha} \sum_j \frac{(\mathbf{r}_{jB} \times \nabla_j)_{\alpha}}{r_{jB}^3} \\
 & + \frac{1}{8c^2} \sum_{\alpha, \beta} H_{\alpha} \sum_j (r_j^2 \delta_{\alpha\beta} - r_{j\alpha} r_{j\beta}) H_{\beta} \\
 & + \frac{1}{2c^2} \sum_{B, \alpha, \beta} H_{\alpha} \sum_j \frac{(\mathbf{r}_j \cdot \mathbf{r}_{jB} \delta_{\alpha\beta} - r_{j\alpha} r_{jB\beta})}{r_{jB}^3} \mu_{B\beta}
 \end{aligned} \tag{3.9}$$

Where the subscript greek indices are tensor notation, and refer to any one of the x , y , or z Cartesian directions. One can then use the following definitions to simplify the above expression:

$$\mathcal{H}^{(0)} = -\frac{1}{2} \sum_j \left\{ \nabla_j^2 - \sum_B \frac{Z_B}{r_{jB}} \right\} + \sum_l \sum_{j \neq l} \frac{1}{r_{jl}} + \sum_D \sum_{B \neq D} \frac{Z_B Z_D}{R_{BD}} \tag{3.10}$$

$$\left. \frac{\partial \mathcal{H}(\mathbf{H}, \boldsymbol{\mu})}{\partial H_{\alpha}} \right|_0 = -\frac{i}{2c} \sum_j (\mathbf{r}_j \times \nabla_j)_{\alpha} = -\frac{i}{2c} \sum_j L_{j\alpha} = i \mathcal{H}_{\alpha}^{(1,0)} \tag{3.11}$$

$$\left. \frac{\partial \mathcal{H}(\mathbf{H}, \boldsymbol{\mu})}{\partial H_{\alpha} \partial H_{\beta}} \right|_0 = \frac{1}{8c^2} \sum_j (r_j^2 \delta_{\alpha\beta} - r_{j\alpha} r_{j\beta}) = \frac{1}{2} \mathcal{H}_{\alpha\beta}^{(2,0)} \tag{3.12}$$

$$\left. \frac{\partial \mathcal{H}(\mathbf{H}, \boldsymbol{\mu})}{\partial \mu_{B\alpha}} \right|_0 = -\frac{i}{c} \sum_j \frac{(\mathbf{r}_{jB} \times \nabla_j)_{\alpha}}{r_{jB}^3} = -\frac{i}{c} \sum_j \frac{L_{jB\alpha}}{r_{jB}^3} = i \mathcal{H}_{B\alpha}^{(0,1)} \tag{3.13}$$

$$\left. \frac{\partial \mathcal{H}(\mathbf{H}, \boldsymbol{\mu})}{\partial H_\alpha \partial \mu_{B\beta}} \right|_0 = \frac{1}{2c^2} \sum_j \frac{(\mathbf{r}_j \cdot \mathbf{r}_{jB} \delta_{\alpha\beta} - r_{j\alpha} r_{jB\beta})}{r_{jB}^3} = \mathcal{H}_{B\alpha\beta}^{(1,1)} \quad (3.14)$$

These definitions allow the Hamiltonian in Eq. (3.9) to be written as

$$\begin{aligned} \mathcal{H}(\mathbf{H}, \boldsymbol{\mu}) = & \mathcal{H}^{(0)} + i \sum_\alpha H_\alpha \mathcal{H}_\alpha^{(1,0)} + i \sum_{\alpha, B} \mu_{B\alpha} \mathcal{H}_{B\alpha}^{(0,1)} \\ & + \frac{1}{2} \sum_{\alpha, \beta} H_\alpha \mathcal{H}_{\alpha\beta}^{(2,0)} H_\beta + \sum_{B, \alpha, \beta} H_\alpha \mathcal{H}_{B\alpha\beta}^{(1,1)} \mu_{B\beta} \end{aligned} \quad (3.15)$$

The most critical point here is that the first order terms are pure imaginary, which is a result of expanding the NMR Hamiltonian in an exact Taylor-like series.⁵⁰ (The perturbation is therefore said to be “antisymmetric” to first order.) The energy associated with this Hamiltonian is given by Schrödinger’s equation:

$$\mathcal{H}(\mathbf{H}, \boldsymbol{\mu}_B) \Psi(\mathbf{H}, \boldsymbol{\mu}_B) = E(\mathbf{H}, \boldsymbol{\mu}_B) \Psi(\mathbf{H}, \boldsymbol{\mu}_B) \quad (3.16)$$

For small values of \mathbf{H} and $\boldsymbol{\mu}_B$, we can similarly expand the wavefunction and energy in a Taylor series about their zero-field values. Again, it is critical to note that since the Hamiltonian has pure imaginary terms at first order when expanded, so will the wavefunction and the energy, which allows us to exploit a similar notation: (a superscript “+” denotes adjoint)

$$\begin{aligned} \Psi(\mathbf{H}, \boldsymbol{\mu}_B) &= \Psi^{(0)} + \mathbf{H} \cdot \left. \frac{\partial \Psi}{\partial \mathbf{H}} \right|_0 + \boldsymbol{\mu}_B \cdot \left. \frac{\partial \Psi}{\partial \boldsymbol{\mu}_B} \right|_0 + \dots \\ &= \Psi^{(0)} + i \sum_\alpha H_\alpha \Psi_\alpha^{(1,0)} + i \sum_\alpha \mu_{B\alpha} \Psi_{B\alpha}^{(0,1)} + \dots \end{aligned} \quad (3.17)$$

$$\begin{aligned}
E(\mathbf{H}, \boldsymbol{\mu}_B) &= E^{(0)} + \mathbf{H} \cdot \frac{\partial E}{\partial \mathbf{H}} \Big|_0 + \boldsymbol{\mu}_B \cdot \frac{\partial E}{\partial \boldsymbol{\mu}_B} \Big|_0 + \frac{1}{2} \mathbf{H}^+ \cdot \frac{\partial^2 E}{\partial \mathbf{H}^2} \Big|_0 \cdot \mathbf{H} + \frac{1}{2} \mathbf{H}^+ \cdot \frac{\partial^2 E}{\partial \mathbf{H} \partial \boldsymbol{\mu}_B} \Big|_0 \cdot \boldsymbol{\mu}_B \\
&\quad + \frac{1}{2} \boldsymbol{\mu}_B^+ \cdot \frac{\partial^2 E}{\partial \boldsymbol{\mu}_B \partial \mathbf{H}} \Big|_0 \cdot \mathbf{H} + \frac{1}{2} \boldsymbol{\mu}_B^+ \cdot \frac{\partial^2 E}{\partial \boldsymbol{\mu}_B^2} \Big|_0 \cdot \boldsymbol{\mu}_B + \dots \\
&= E^{(0)} + i \sum_{\alpha} H_{\alpha} E_{\alpha}^{(1,0)} + i \sum_{\alpha} \mu_{B\alpha} E_{B\alpha}^{(0,1)} + \frac{1}{2} \sum_{\alpha\beta} H_{\alpha} E_{\alpha\beta}^{(2,0)} H_{\beta} \\
&\quad + \sum_{\alpha\beta} H_{\alpha} E_{B\alpha\beta}^{(1,1)} \mu_{B\beta} + \frac{1}{2} \sum_{\alpha\beta} \mu_{B\alpha} E_{B\alpha\beta}^{(0,2)} \mu_{B\beta} + \dots
\end{aligned} \tag{3.18}$$

The following is a qualitative, experimental expression for the energy of a molecular system in the presence of a uniform external magnetic field:

$$E(\mathbf{H}, \boldsymbol{\mu}_B) = E^{(0)} - \sum_{\alpha} H_{\alpha} \gamma_{\alpha} - \sum_{\alpha} \mu_{B\alpha} H_{\alpha} - \frac{1}{2} \sum_{\alpha\beta} H_{\alpha} \chi_{\alpha\beta} H_{\beta} + \sum_{\alpha\beta} H_{\alpha} \sigma_{B\alpha\beta} \mu_{B\beta} + \dots \tag{3.19}$$

Where γ_{α} is the permanent magnetic dipole of the molecule, $\chi_{\alpha\beta}$ is the molecular diamagnetic susceptibility tensor, and $\sigma_{B\alpha\beta}$ is the magnetic shielding tensor on nucleus B . Comparison with the expanded expression for the energy, Eq. (3.18), allows for the identification of the shielding tensor with a second derivative of the energy:

$$\therefore \sigma_{B\alpha\beta} = E_{B\alpha\beta}^{(1,1)} \tag{3.20}$$

Therefore, the task of calculating the shielding constants has been reduced to the evaluation of the second derivative of the energy with respect to the external magnetic field and the nuclear magnetic moments at zero total field strength. Note that Eq. (3.20) is ultimately a definition, and the above comparison has been given as a physical justification.

At this point, we return to the use of GIAOs, and construct molecular orbitals from them:

$$\psi_j(\mathbf{H}, \mu_B) = \sum_v c_{vj}(\mathbf{H}, \mu_B) \chi_v(\mathbf{H}) \quad (3.21)$$

$$\chi_v(\mathbf{H}) = e^{-\frac{i}{c} \mathbf{A}_v \cdot \mathbf{r}} \phi_v = f_v \phi_v \quad (3.22)$$

$$\mathbf{A}_v = \frac{1}{2} \mathbf{H} \times \mathbf{R}_v \quad (3.23)$$

Note that the molecular orbitals (MOs) are complex and field-dependent. One can then use these orbitals in standard closed-shell Hartree-Fock theory and arrive at an analogous Roothaan equation:

$$\sum_v (F_{v\lambda} - \epsilon_j S_{v\lambda}) c_{vj} = 0 \quad (3.24)$$

where

$$S_{v\lambda} = \langle \chi_v | \chi_\lambda \rangle \quad (3.25)$$

$$F_{v\lambda} = H_{v\lambda} + G_{v\lambda} \quad (3.26)$$

and further,

$$H_{v\lambda} = \langle \chi_v | \left\{ \frac{1}{2} \left(-i\nabla + \frac{1}{c} \mathbf{A}'(\mathbf{r}) \right)^2 - \sum_B \frac{Z_B}{r_B} \right\} | \chi_\lambda \rangle \quad (3.27)$$

$$G_{v\lambda} = \sum_{\rho\sigma} P_{\rho\sigma} \left[\left(\chi_v^* \chi_\lambda | \chi_\rho^* \chi_\sigma \right) - \frac{1}{2} \left(\chi_v^* \chi_\sigma | \chi_\rho^* \chi_\lambda \right) \right] = \sum_{\rho\sigma} P_{\rho\sigma} G_{v\lambda\rho\sigma} \quad (3.28)$$

Note that in the matrix elements of the core Hamiltonian, Eq. (3.27), we integrate over \mathbf{r} , the coordinates of electron 1. See, for example, the reasoning leading to Eq. (1.23). Following through with HF theory, the energy of the system is given by

$$E = \sum_{v\lambda} P_{v\lambda} \left(H_{v\lambda} + \frac{1}{2} G_{v\lambda} \right) \quad (3.29)$$

which is the result of introducing a basis set into Eq. (1.31).

With the introduction of Eq. (3.29), and recalling the definition of the shielding tensor, our task is well-defined: we must take the second derivative of Eq. (3.29) with respect to the external magnetic field and the nuclear magnetic moments, a dependence which appears in the GIAOs and Hamiltonian. In practice, we will evaluate this derivative to first-order, and in order to do this, we expand the various fundamental quantities in expansions similar to the Hamiltonian, Eq. (3.15), energy, Eq. (3.18), and wavefunction, Eq. (3.17). Just as with these prior expansions, the first order terms will be pure imaginary:

$$\begin{aligned}
 c_{vj}(H_\alpha, \mu_{B\alpha}) &= c_{vj}^{(0)} + iH_\alpha \left(c_{vj}^{(1,0)} \right)_\alpha + i\mu_{B\alpha} \left(c_{Bvj}^{(0,1)} \right)_\alpha + \dots \\
 P_{v\lambda}(H_\alpha, \mu_{B\alpha}) &= P_{v\lambda}^{(0)} + iH_\alpha \left(P_{v\lambda}^{(1,0)} \right)_\alpha + i\mu_{B\alpha} \left(P_{Bv\lambda}^{(0,1)} \right)_\alpha + \dots \\
 G_{v\lambda}(H_\alpha, \mu_{B\alpha}) &= G_{v\lambda}^{(0)} + iH_\alpha \left(G_{v\lambda}^{(1,0)} \right)_\alpha + i\mu_{B\alpha} \left(G_{Bv\lambda}^{(0,1)} \right)_\alpha + \dots \\
 H_{v\lambda}(H_\alpha, \mu_{B\alpha}) &= H_{v\lambda}^{(0)} + iH_\alpha \left(H_{v\lambda}^{(1,0)} \right)_\alpha + i\mu_{B\alpha} \left(H_{Bv\lambda}^{(0,1)} \right)_\alpha + \dots
 \end{aligned} \tag{3.30a,b,c,d}$$

where we note that (C.3)

$$\begin{aligned}
 \left(P_{v\lambda}^{(1,0)} \right)_\alpha &= 2 \sum_j^{occ} \left[\left(c_{vj}^{(1,0)} \right)_\alpha c_{\lambda j}^{(0)} - c_{vj}^{(0)} \left(c_{\lambda j}^{(1,0)} \right)_\alpha \right] \\
 \left(P_{Bv\lambda}^{(0,1)} \right)_\beta &= 2 \sum_j^{occ} \left[\left(c_{Bvj}^{(0,1)} \right)_\beta c_{\lambda j}^{(0)} - c_{vj}^{(0)} \left(c_{B\lambda j}^{(0,1)} \right)_\beta \right]
 \end{aligned} \tag{3.31a,b}$$

and (C.4);

$$\left(G_{Bv\lambda}^{(0,1)} \right)_\beta = \sum_{\rho\sigma} \left(P_{B\rho\sigma}^{(0,1)} \right)_\alpha G_{v\lambda\rho\sigma}^{(0)} \tag{3.32}$$

results which will be handy later in the derivation.

To begin, substitute the expansions, Eqs. (3.30b,c,d) into the energy expression, Eq. (3.29), and differentiate with respect to the nuclear magnetic moments: (C.5)

$$\left. \frac{\partial E}{\partial \mu_{B\beta}} \right|_0 = i \sum_{\nu\lambda} \left\{ \left(P_{B\nu\lambda}^{(0,1)} \right)_\beta F_{\nu\lambda}^{(0)} + P_{\nu\lambda}^{(0)} \left(H_{B\nu\lambda}^{(0,1)} \right)_\beta \right\} \quad (3.33)$$

This can be simplified if we note that (C.6)

$$\frac{\partial}{\partial \mu_{B\beta}} \left(\sum_{\nu\lambda} c_{\nu j}^* c_{\lambda l} S_{\nu\lambda} = \delta_{jl} \right) \Rightarrow i \sum_{\nu\lambda} \left[c_{\nu j}^{(0)} \left(c_{B\lambda l}^{(0,1)} \right)_\beta - \left(c_{B\nu j}^{(0,1)} \right)_\beta c_{\lambda l}^{(0)} \right] S_{\nu\lambda}^{(0)} = 0 \quad (3.34)$$

This, along with the explicit derivative of the density matrix, Eq. (3.31b), and the Roothaan equation, Eq. (3.24), gives: (C.7)

$$\left. \frac{\partial E}{\partial \mu_{B\beta}} \right|_0 = i \sum_{\nu\lambda} P_{\nu\lambda}^{(0)} \left(H_{B\nu\lambda}^{(0,1)} \right)_\beta \quad (3.35)$$

Recall the definition

$$E_{B\beta}^{(0,1)} = -i \left. \frac{\partial E}{\partial \mu_{B\beta}} \right|_0 = \sum_{\nu\lambda} P_{\nu\lambda}^{(0)} \left(H_{B\nu\lambda}^{(0,1)} \right)_\beta \quad (3.36)$$

which allows us to easily take the second derivative and find the expression for the shielding tensor:

$$\begin{aligned}
\sigma_{B\alpha\beta} &= E_{B\alpha\beta}^{(1,1)} = \frac{\partial E_{B\beta}^{(0,1)}}{\partial H_\alpha} \Big|_0 = \frac{\partial}{\partial H_\alpha} \left[\sum_{v\lambda} P_{v\lambda}^{(0)} (H_{Bv\lambda}^{(0,1)})_\beta \right] \\
&= \sum_{v\lambda} \left\{ \frac{\partial P_{v\lambda}^{(0)}}{\partial H_\alpha} (H_{Bv\lambda}^{(0,1)})_\beta + P_{v\lambda}^{(0)} \frac{\partial (H_{Bv\lambda}^{(0,1)})_\beta}{\partial H_\alpha} \right\} \\
&= \sum_{v\lambda} \left\{ (P_{v\lambda}^{(1,0)})_\alpha (H_{Bv\lambda}^{(0,1)})_\beta + P_{v\lambda}^{(0)} (H_{Bv\lambda}^{(1,1)})_{\alpha\beta} \right\}
\end{aligned} \tag{3.37}$$

Note that $\frac{\partial P_{v\lambda}^{(0)}}{\partial H_\alpha} \neq i(P_{v\lambda}^{(1,0)})_\alpha$ since $P_{v\lambda}^{(0)} \neq P_{v\lambda}$, and in the last line, $P_{v\lambda}^{(0)}$ is now *totally* field independent, whereas it still depended on H before the derivative was taken. The specific derivatives in the shielding expression are then given by (C.8)

$$(H_{Bv\lambda}^{(0,1)})_\beta = -\frac{1}{c} \langle \phi_v | \frac{L_\beta^B}{r_B^3} | \phi_\lambda \rangle \tag{3.38}$$

where $L_\beta^B = (\mathbf{r}_B \times \nabla)_\beta$, and (C.9)

$$\begin{aligned}
(H_{Bv\lambda}^{(1,1)})_{\alpha\beta} &= \frac{1}{2c^2} \left\{ \left\langle (\mathbf{T}_{v\lambda})_\alpha \phi_v \left| \frac{L_\beta^B}{r_B^3} \right| \phi_\lambda \right\rangle + (\mathbf{Q}_{v\lambda})_\alpha \left\langle \phi_v \left| \frac{L_\beta^B}{r_B^3} \right| \phi_\lambda \right\rangle \right\} \\
&\quad + \frac{1}{2c^2} \left\langle \phi_v \left| \frac{[\mathbf{r}_\lambda \cdot \mathbf{r}_B \delta_{\alpha\beta} - (\mathbf{r}_\lambda)_\alpha (\mathbf{r}_B)_\beta]}{r_B^3} \right| \phi_\lambda \right\rangle
\end{aligned} \tag{3.39}$$

where $\mathbf{T}_{v\lambda} = \mathbf{R}_{v\lambda} \times \mathbf{r}_v$ and $\mathbf{Q}_{v\lambda} = \mathbf{R}_v \times \mathbf{R}_\lambda$. (Note that these matrices are antisymmetric; i.e. $\mathbf{T}_{v\lambda}^T = -\mathbf{T}_{v\lambda}$, which is to be expected for an antisymmetric perturbation.) The remaining piece of the shielding tensor is the first derivative of the density matrix with respect to the external magnetic field. This is the subject of the next section.

III. Self-Consistent Antisymmetric Perturbation Theory for Perturbation Dependent Non-Orthogonal Basis Sets

The first derivative of the density matrix is given by Eq. (3.31a), and depends on the perturbed coefficients, $(c_{\nu j}^{(1,0)})_{\alpha}$. Rather than calculate these quantities, as Ditchfield does, we instead wish to derive a direct expression for the full matrix $(P_{\nu \lambda}^{(1,0)})_{\alpha}$. In order to do this, we must consider antisymmetric perturbation theory for non-orthogonal, field dependent basis sets, of which GIAOs are an example. The term 'antisymmetric' is used because to first order, perturbations due to the external magnetic field and nuclear moments are pure imaginary, as seen in the previous section. The following will be a summary of two papers; the first is a general work by Dodds, McWeeny and Sadlej⁵¹ which treats the general *symmetric* problem, and the second by Wolinski, Hinton and Pulay,⁵² which deals specifically with GIAO chemical shift calculations. As in the previous section, the reader will be referred to Appendix C and D for detailed derivations.

Consider a closed-shell system with n singly-occupied orbitals $\{\psi_1, \psi_2, \dots, \psi_n\}$ constructed from m basis functions $\{\chi_1, \chi_2, \dots, \chi_m\} = \chi$, where this set is not orthonormal. It is always possible to make the set orthonormal, however, by multiplying by an appropriate unitary matrix:

$$\bar{\chi} = \chi U \quad (3.40)$$

where the bar denotes an orthonormal basis. Since $\langle \bar{\chi} | \bar{\chi} \rangle = 1$, we have

$$1 = \langle \bar{\chi} | \bar{\chi} \rangle = \langle \chi U | \chi U \rangle = U^+ \chi^+ \chi U = U^+ S U \quad (3.41)$$

where we are free to choose $U = S^{-\frac{1}{2}}$, which is known as Löwdin orthonormalization. This has the feature that

$$U^+ = S^+^{-\frac{1}{2}} = S^{-\frac{1}{2}} = U \quad (3.42)$$

since the overlap matrix is always Hermitian.

The SCF Fock equation in matrix form is given by

$$\mathbf{FT} = \mathbf{STe} \quad (3.43)$$

where \mathbf{T} is an $m \times n$ matrix of basis function coefficients, and $\bar{\mathbf{T}} = \mathbf{U}^{-1}\mathbf{T}$, thus

$$\mathbf{FT} = \mathbf{STe} \Rightarrow \mathbf{FUT} = \mathbf{SUTe} \Rightarrow \mathbf{UFUT} = \mathbf{USU}\bar{\mathbf{T}}\mathbf{e} \Rightarrow \bar{\mathbf{FT}} = \bar{\mathbf{T}}\mathbf{e} \quad (3.44)$$

where we have identified $\bar{\mathbf{T}} = \mathbf{U}^{-1}\mathbf{T}$ and $\bar{\mathbf{F}} = \mathbf{U}^{\dagger}\mathbf{F}\mathbf{U}$. The density matrix can thus be defined as

$$\bar{\mathbf{R}} = \bar{\mathbf{T}}\bar{\mathbf{T}}^+ \quad (3.45)$$

Note that we have previously defined the density matrix as $\bar{\mathbf{P}} = 2\bar{\mathbf{T}}\bar{\mathbf{T}}^+$, (see C.3) but these two definitions are simply related by $\bar{\mathbf{R}} = \frac{1}{2}\bar{\mathbf{P}}$. Note that since $\bar{\mathbf{R}} = \bar{\mathbf{T}}\bar{\mathbf{T}}^+$, where $\bar{\mathbf{T}}$ is an $m \times n$ matrix, $\bar{\mathbf{R}}$ is therefore $m \times m$, where only n of the orbitals are singly occupied. It can be written in terms of column vectors of $\bar{\mathbf{T}}$, $\bar{\mathbf{c}}_I$, in the following way: (Note that $\bar{\mathbf{c}}_I$ is a vector of length m .)

$$\bar{\mathbf{R}} = \bar{\mathbf{T}}\bar{\mathbf{T}}^+ = \sum_I^n \bar{\mathbf{c}}_I \bar{\mathbf{c}}_I^+ \quad (3.46)$$

To find the perturbed SCF equations, we assume a solution to the unperturbed problem has been found, and allow for a perturbation to the system:

$$\begin{aligned} \mathbf{S} &= \mathbf{S}^{(0)} + \mathbf{S}^{(1)} + \dots \\ \mathbf{F} &= \mathbf{F}^{(0)} + \mathbf{F}^{(1)} + \dots \\ \mathbf{H} &= \mathbf{H}^{(0)} + \mathbf{H}^{(1)} + \dots \end{aligned} \quad (3.47a,b,c)$$

where the superscript (0) indicates an unperturbed quantity. (Note again that for the specific case of a magnetic field perturbation, the perturbation is pure imaginary, or antisymmetric. *This characteristic will arise naturally in the following derivation.*) The first order terms can be expressed using the same general expansion as in the previous section:

$$\begin{aligned}
 S_{pq} &= \langle \chi_p(\mathbf{H}) | \chi_q(\mathbf{H}) \rangle = \langle f_p^* f_q \phi_p | \phi_q \rangle \\
 S_{pq} &= S_{pq}^{(0)} + H_\alpha \left(S_{pq}^{(1)} \right)_\alpha + \dots \\
 \Rightarrow \left(S_{pq}^{(1)} \right)_\alpha &= \frac{\partial S_{pq}}{\partial H_\alpha} \bigg|_0 = \frac{\partial}{\partial H_\alpha} \langle f_p^* f_q \phi_p | \phi_q \rangle \bigg|_0 = \left\langle \frac{\partial f_p^* f_q}{\partial H_\alpha} \phi_p \bigg| \phi_q \right\rangle \bigg|_0
 \end{aligned}$$

where f_q was defined in Eq. (3.22). Then, using (C.9.3),

$$\begin{aligned}
 \left(S_{pq}^{(1)} \right)_\alpha &= \left\langle \frac{i}{2c} \left[\left(\mathbf{T}_{pq} \right)_\alpha + \left(\mathbf{Q}_{pq} \right)_\alpha \right] \phi_p \bigg| \phi_q \right\rangle = \frac{i}{2c} \left[\left\langle \left(\mathbf{T}_{pq} \right)_\alpha \phi_p \bigg| \phi_q \right\rangle + \left(\mathbf{Q}_{pq} \right)_\alpha \langle \phi_p | \phi_q \rangle \right] \\
 \left(S_{pq}^{(1)} \right)_\alpha &= i \left(S_{pq}^{(1,0)} \right)_\alpha
 \end{aligned} \tag{3.48}$$

Note that since \mathbf{T}_{pq} and \mathbf{Q}_{pq} are antisymmetric, [see Eq. (3.39)] $S_{pq}^{(1)}$ is also antisymmetric.

Similarly, the first order term of Eq. (3.47b) can be evaluated (C.10):

$$\begin{aligned}
 \left(F_{\nu\lambda}^{(1)} \right)_\alpha &= i \left[\left(H_{\nu\lambda}^{(1,0)} \right)_\alpha + \sum_{\rho\sigma} \left\{ \left(P_{\rho\sigma}^{(1,0)} \right)_\alpha G_{\nu\lambda\rho\sigma}^{(0)} + P_{\rho\sigma}^{(0)} \left(G_{\nu\lambda\rho\sigma}^{(1,0)} \right)_\alpha \right\} \right] \\
 &= i \left(F_{\nu\lambda}^{(1,0)} \right)_\alpha
 \end{aligned} \tag{3.49}$$

which includes the first order term of Eq. (3.47c), given by (C.11)

$$\left(H_{\nu\lambda}^{(1,0)} \right)_\alpha = \frac{1}{2c} \left[\left\langle \left(\mathbf{T}_{\nu\lambda} \right)_\alpha \phi_\nu \bigg| H^{core} \bigg| \phi_\lambda \right\rangle + \left(\mathbf{Q}_{\nu\lambda} \right)_\alpha \langle \phi_\nu | H^{core} | \phi_\lambda \rangle - \langle \phi_\nu | L_\alpha^\lambda | \phi_\lambda \rangle \right] \tag{3.50}$$

where we have used the notation [c.f. Eq. (1.17)]

$$H^{core} = -\frac{1}{2} \nabla^2 - \sum_B \frac{Z_B}{r_B} \quad (3.51)$$

The final remaining piece is the first-order derivative of the two-electron integrals, $(G_{\nu\lambda\rho\sigma}^{(1,0)})_\alpha$ in Eq. (3.49), which can be constructed from the individual two-electron derivatives: (C.12)

$$(\chi_p \chi_q | \chi_r \chi_s)^{(1,0)} = \frac{1}{2c} \left\{ \begin{aligned} & [(\mathbf{Q}_{pq})_\alpha + (\mathbf{Q}_{rs})_\alpha] (\phi_p \phi_q | \phi_r \phi_s) \\ & + [(\mathbf{T}_{pq})_\alpha \phi_p \phi_q | \phi_r \phi_s] + (\phi_p \phi_q | (\mathbf{T}_{rs})_\alpha \phi_r \phi_s) \end{aligned} \right\} \quad (3.52)$$

(Ditchfield omits the factor of 1/2 - this is most likely due to a typographical error.)

Note that the expression for the first order Fock matrix contains the first order density matrix, which is the quantity we wish to calculate. Therefore we see that this will be an iterative procedure. We have yet to write down the form of the perturbed SCF equations, so let us do this now, and then write them in an antisymmetric form, as presented by Pulay. Begin with Eq. (3.47) and substitute in Eqs. (3.47), then separate orders: (D.1)

$$0^{\text{th}} \text{ order. } \mathbf{F}^{(0)} \mathbf{R}^{(0)} \mathbf{S}^{(0)} = \mathbf{S}^{(0)} \mathbf{R}^{(0)} \mathbf{F}^{(0)}$$

$$1^{\text{st}} \text{ order. } \mathbf{F}^{(0)} \mathbf{R}^{(0)} \mathbf{S}^{(1)} + \mathbf{F}^{(0)} \mathbf{R}^{(1)} \mathbf{S}^{(0)} + \mathbf{F}^{(1)} \mathbf{R}^{(0)} \mathbf{S}^{(0)} = \mathbf{S}^{(0)} \mathbf{R}^{(0)} \mathbf{F}^{(1)} + \mathbf{S}^{(0)} \mathbf{R}^{(1)} \mathbf{F}^{(0)} + \mathbf{S}^{(1)} \mathbf{R}^{(0)} \mathbf{F}^{(0)}$$

$$2^{\text{nd}} \text{ order. } \mathbf{F}^{(0)} \mathbf{R}^{(1)} \mathbf{S}^{(1)} + \mathbf{F}^{(1)} \mathbf{R}^{(0)} \mathbf{S}^{(1)} + \mathbf{F}^{(1)} \mathbf{R}^{(1)} \mathbf{S}^{(0)} = \mathbf{S}^{(0)} \mathbf{R}^{(1)} \mathbf{F}^{(1)} + \mathbf{S}^{(1)} \mathbf{R}^{(0)} \mathbf{F}^{(1)} + \mathbf{S}^{(1)} \mathbf{R}^{(1)} \mathbf{F}^{(0)}$$

$$3^{\text{rd}} \text{ order. } \mathbf{F}^{(1)} \mathbf{R}^{(1)} \mathbf{S}^{(1)} = \mathbf{S}^{(1)} \mathbf{R}^{(1)} \mathbf{F}^{(1)}$$

Similarly, begin with Eq. (3.49) and substitute in Eqs. (3.47), and separate orders: (D.2)

$$0^{\text{th}} \text{ order. } \mathbf{R}^{(0)} \mathbf{S}^{(0)} \mathbf{R}^{(0)} = \mathbf{R}^{(0)}$$

$$1^{\text{st}} \text{ order. } \mathbf{R}^{(0)} \mathbf{S}^{(0)} \mathbf{R}^{(1)} + \mathbf{R}^{(0)} \mathbf{S}^{(1)} \mathbf{R}^{(0)} + \mathbf{R}^{(1)} \mathbf{S}^{(0)} \mathbf{R}^{(0)} = \mathbf{R}^{(1)}$$

$$2^{\text{nd}} \text{ order. } \mathbf{R}^{(0)} \mathbf{S}^{(1)} \mathbf{R}^{(1)} + \mathbf{R}^{(1)} \mathbf{S}^{(0)} \mathbf{R}^{(1)} + \mathbf{R}^{(1)} \mathbf{S}^{(1)} \mathbf{R}^{(0)} + \mathbf{R}^{(1)} \mathbf{S}^{(1)} \mathbf{R}^{(0)} = \mathbf{R}^{(2)}$$

The other orders have been presented for completeness, but we are only interested in first order expressions;

$$\begin{aligned} \mathbf{F}^{(0)} \mathbf{R}^{(0)} \mathbf{S}^{(1)} + \mathbf{F}^{(0)} \mathbf{R}^{(1)} \mathbf{S}^{(0)} + \mathbf{F}^{(1)} \mathbf{R}^{(0)} \mathbf{S}^{(0)} &= \mathbf{S}^{(0)} \mathbf{R}^{(0)} \mathbf{F}^{(1)} + \mathbf{S}^{(0)} \mathbf{R}^{(1)} \mathbf{F}^{(0)} + \mathbf{S}^{(1)} \mathbf{R}^{(0)} \mathbf{F}^{(0)} \\ \mathbf{R}^{(0)} \mathbf{S}^{(0)} \mathbf{R}^{(1)} + \mathbf{R}^{(0)} \mathbf{S}^{(1)} \mathbf{R}^{(0)} + \mathbf{R}^{(1)} \mathbf{S}^{(0)} \mathbf{R}^{(0)} &= \mathbf{R}^{(1)} \end{aligned} \quad (3.53a,b)$$

In order to solve these equations, we define projection operators that are constructed from the unperturbed density matrix:

$$\begin{aligned} \tilde{\mathbf{R}}_1 &= \overline{\mathbf{R}}^{(0)} = \sum_I^{\text{occ}} \tilde{\mathbf{c}}_I \tilde{\mathbf{c}}_I^\dagger && \text{occupied orbitals} \\ \tilde{\mathbf{R}}_2 &= \mathbf{1} - \overline{\mathbf{R}}^{(0)} = \sum_J^{\text{unocc}} \tilde{\mathbf{c}}_J \tilde{\mathbf{c}}_J^\dagger && \text{unoccupied orbitals} \end{aligned} \quad (3.54a,b)$$

As an example, consider an orthonormal space of two occupied orbitals and two unoccupied:

$$\tilde{\mathbf{R}}_1 = \overline{\mathbf{R}}^{(0)} = \begin{pmatrix} 1 & 0 & 0 & 0 \\ 0 & 1 & 0 & 0 \\ 0 & 0 & 0 & 0 \\ 0 & 0 & 0 & 0 \end{pmatrix}; \quad \tilde{\mathbf{R}}_2 = \mathbf{1} - \overline{\mathbf{R}}^{(0)} = \begin{pmatrix} 1 & 0 & 0 & 0 \\ 0 & 1 & 0 & 0 \\ 0 & 0 & 1 & 0 \\ 0 & 0 & 0 & 1 \end{pmatrix} - \begin{pmatrix} 1 & 0 & 0 & 0 \\ 0 & 1 & 0 & 0 \\ 0 & 0 & 0 & 0 \\ 0 & 0 & 0 & 0 \end{pmatrix} = \begin{pmatrix} 0 & 0 & 0 & 0 \\ 0 & 0 & 0 & 0 \\ 0 & 0 & 1 & 0 \\ 0 & 0 & 0 & 1 \end{pmatrix}$$

The first order equations in the orthogonal basis are (D.3)

$$\begin{aligned} \tilde{\mathbf{F}}^{(0)} \tilde{\mathbf{R}}^{(0)} \tilde{\mathbf{S}}^{(1)} + \tilde{\mathbf{F}}^{(0)} \tilde{\mathbf{R}}^{(1)} + \tilde{\mathbf{F}}^{(1)} \tilde{\mathbf{R}}^{(0)} &= \tilde{\mathbf{R}}^{(0)} \tilde{\mathbf{F}}^{(1)} + \tilde{\mathbf{R}}^{(1)} \tilde{\mathbf{F}}^{(0)} + \tilde{\mathbf{S}}^{(1)} \tilde{\mathbf{R}}^{(0)} \tilde{\mathbf{F}}^{(0)} \\ \tilde{\mathbf{R}}^{(0)} \tilde{\mathbf{R}}^{(1)} + \tilde{\mathbf{R}}^{(0)} \tilde{\mathbf{S}}^{(1)} \tilde{\mathbf{R}}^{(0)} + \tilde{\mathbf{R}}^{(1)} \tilde{\mathbf{R}}^{(0)} &= \tilde{\mathbf{R}}^{(1)} \end{aligned} \quad (3.55a,b)$$

since $\tilde{\mathbf{S}}^{(0)}$ is simply the unit matrix. Then define the projection of an arbitrary matrix, where $i, j = 1, 2$:

$$\mathbf{M}_{ij} = \tilde{\mathbf{R}}_i \mathbf{M} \tilde{\mathbf{R}}_j \quad (3.56)$$

Such that $\mathbf{M} = \mathbf{M}_{11} + \mathbf{M}_{12} + \mathbf{M}_{21} + \mathbf{M}_{22}$; Schematically, this translates exactly to

Apply this to the second first-order equation, Eq. (3.55b), to obtain the four projections: (D.4)

$$\begin{aligned} (1,1) \text{ projection: } \tilde{\mathbf{R}}_{11}^{(1)} &= -\tilde{\mathbf{S}}_{11}^{(1)} \\ (1,2) \text{ projection: } \tilde{\mathbf{R}}_{12}^{(1)} &= \tilde{\mathbf{R}}_{12}^{(1)} \\ (2,2) \text{ projection: } 0 &= \tilde{\mathbf{R}}_{22}^{(1)} \end{aligned} \quad (3.57)$$

note that (1,2) projection is undetermined, and further that

$$\begin{aligned} \left(\tilde{\mathbf{R}}_{21}^{(1)} \right)^+ &= \left(\tilde{\mathbf{R}}_2 \tilde{\mathbf{R}}^{(1)} \tilde{\mathbf{R}}_1 \right)^+ = \tilde{\mathbf{R}}_1^+ \tilde{\mathbf{R}}^{(1)+} \tilde{\mathbf{R}}_2^+ = \tilde{\mathbf{R}}_1 \tilde{\mathbf{R}}^{(1)} \tilde{\mathbf{R}}_2 = \tilde{\mathbf{R}}_{12}^{(1)} \\ \left(\tilde{\mathbf{R}}_{12}^{(1)} \right)^+ &= \left(\tilde{\mathbf{R}}_1 \tilde{\mathbf{R}}^{(1)} \tilde{\mathbf{R}}_2 \right)^+ = \tilde{\mathbf{R}}_2^+ \tilde{\mathbf{R}}^{(1)+} \tilde{\mathbf{R}}_1^+ = \tilde{\mathbf{R}}_2 \tilde{\mathbf{R}}^{(1)} \tilde{\mathbf{R}}_1 = \tilde{\mathbf{R}}_{21}^{(1)} \end{aligned} \quad (3.58)$$

In order to fix $\tilde{\mathbf{R}}_{12}^{(1)}$, we use the first first-order equation above, Eq. (3.55a), and take the (1,2) projection: (D.5)

$$\tilde{\mathbf{F}}^{(0)} \tilde{\mathbf{x}} - \tilde{\mathbf{x}} \tilde{\mathbf{F}}^{(0)} = \tilde{\mathbf{F}}_{12}^{(1)} - \tilde{\mathbf{F}}^{(0)} \tilde{\mathbf{S}}_{12}^{(1)} \quad (3.59)$$

where we have replaced \tilde{x} for $\tilde{\mathbf{R}}_{12}^{(1)}$. This equation can be solved by expanding \tilde{x} in the space of orthonormal coefficients, $\tilde{\mathbf{T}}$, and solving for the unknown coefficients A_{ij} . Its solution is (D.6)

$$\tilde{x} = \sum_{I}^{\text{occ}} \sum_{J}^{\text{unocc}} A_{ij} \tilde{\mathbf{c}}_I \tilde{\mathbf{c}}_J^+ = \sum_{I}^{\text{occ}} \sum_{J}^{\text{unocc}} \frac{\tilde{\mathbf{c}}_I^+ (\tilde{\mathbf{F}}_{12}^{(1)} - \tilde{\mathbf{F}}^{(0)} \tilde{\mathbf{S}}_{12}^{(1)}) \tilde{\mathbf{c}}_J}{(e_I - e_J)} \tilde{\mathbf{c}}_I \tilde{\mathbf{c}}_J^+ \quad (3.60)$$

where e_I is the energy of orbital I. Then pull out the projection operators:

$$\tilde{x} = \sum_{I}^{\text{occ}} \sum_{J}^{\text{unocc}} \frac{\tilde{\mathbf{c}}_I^+ \tilde{\mathbf{R}}_1 (\tilde{\mathbf{F}}^{(1)} - \tilde{\mathbf{F}}^{(0)} \tilde{\mathbf{S}}^{(1)}) \tilde{\mathbf{R}}_2 \tilde{\mathbf{c}}_J}{(e_I - e_J)} \tilde{\mathbf{c}}_I \tilde{\mathbf{c}}_J^+ \quad (3.61)$$

and recall that these projection operators can also be expressed in terms of the column vectors, Eq. (3.54a,b), such that (D.7)

$$\tilde{x} = \sum_{K}^{\text{occ}} \sum_{L}^{\text{unocc}} \frac{\tilde{\mathbf{c}}_K^+ (\tilde{\mathbf{F}}^{(1)} - e_K \tilde{\mathbf{S}}^{(1)}) \tilde{\mathbf{c}}_L}{(e_K - e_L)} \tilde{\mathbf{c}}_K \tilde{\mathbf{c}}_L^+ \quad (3.62)$$

Then the first-order density matrix is given by the sum of the four projected terms, where here we note that a perturbation due to a magnetic field should be pure imaginary; i.e. antisymmetric; one can demonstrate this is true by explicitly pulling out the imaginary parts of Eqs. (3.48) and (3.49) - we have (D.8)

$$\begin{aligned} \tilde{\mathbf{R}}^{(1)} &= \tilde{\mathbf{R}}_{11}^{(1)} + \tilde{\mathbf{R}}_{12}^{(1)} + \tilde{\mathbf{R}}_{21}^{(1)} + \tilde{\mathbf{R}}_{22}^{(1)} = -\tilde{\mathbf{S}}_{11}^{(1)} + \tilde{x} + \tilde{x}^+ \rightarrow -i\tilde{\mathbf{S}}_{11}^{(1,0)} + i\tilde{x} + (i\tilde{x})^+ \\ &= -i\tilde{\mathbf{R}}^{(0)} \tilde{\mathbf{S}}^{(1,0)} \tilde{\mathbf{R}}^{(0)} + i \sum_{K}^{\text{occ}} \sum_{L}^{\text{unocc}} \frac{\tilde{\mathbf{c}}_K^+ (\tilde{\mathbf{F}}^{(1,0)} - e_K \tilde{\mathbf{S}}^{(1,0)}) \tilde{\mathbf{c}}_L}{(e_K - e_L)} (\tilde{\mathbf{c}}_K \tilde{\mathbf{c}}_L^+ - \tilde{\mathbf{c}}_L \tilde{\mathbf{c}}_K^+) \end{aligned} \quad (3.63)$$

At this point, let us take a moment and consider what we have derived. In starting with the expansions in Eqs. (3.47), we have written the perturbations in a general way. Since we have seen that the first-order perturbation due to a magnetic field

is pure imaginary, i.e. antisymmetric, it has been shown that the resulting first-order density matrix, Eq. (3.63) is also pure imaginary. We therefore follow Ditchfield's notation by using an expression exactly analogous to Eq. (3.11):

$$\frac{\partial \tilde{\mathbf{R}}}{\partial \mathbf{H}} = \tilde{\mathbf{R}}^{(1)} = i\tilde{\mathbf{R}}^{(1,0)} \Rightarrow \tilde{\mathbf{R}}^{(1,0)} = -i\tilde{\mathbf{R}}^{(1)}$$

And so to obtain the full perturbation due to the magnetic field, we multiply Eq. (3.63) on the RHS by $-i$:

$$\tilde{\mathbf{R}}^{(1,0)} = -\tilde{\mathbf{R}}^{(0)}\tilde{\mathbf{S}}^{(1,0)}\tilde{\mathbf{R}}^{(0)} + \sum_{\substack{occ \\ K}} \sum_{\substack{unocc \\ L}} \frac{\tilde{\mathbf{c}}_K^+ (\tilde{\mathbf{F}}^{(1,0)} - e_K \tilde{\mathbf{S}}^{(1,0)}) \tilde{\mathbf{c}}_L}{(e_K - e_L)} (\tilde{\mathbf{c}}_K \tilde{\mathbf{c}}_L^+ - \tilde{\mathbf{c}}_L \tilde{\mathbf{c}}_K^+) \quad (3.64)$$

then convert to the usual density matrix using $\overline{\mathbf{R}} = \frac{1}{2} \overline{\mathbf{P}}$:

$$\tilde{\mathbf{P}}^{(1,0)} = -\frac{1}{2} \tilde{\mathbf{P}}^{(0)} \tilde{\mathbf{S}}^{(1,0)} \tilde{\mathbf{P}}^{(0)} + 2 \sum_{\substack{occ \\ K}} \sum_{\substack{unocc \\ L}} \frac{\tilde{\mathbf{c}}_K^+ (\tilde{\mathbf{F}}^{(1,0)} - e_K \tilde{\mathbf{S}}^{(1,0)}) \tilde{\mathbf{c}}_L}{(e_K - e_L)} (\tilde{\mathbf{c}}_K \tilde{\mathbf{c}}_L^+ - \tilde{\mathbf{c}}_L \tilde{\mathbf{c}}_K^+) \quad (3.65)$$

Note that this result is not exactly that given by Wolinski, Hinton, and Pulay, but this is because of an error in the original publication, discovered in the course of this derivation, and confirmed by Wolinski.⁵³ (The factor of two in the second term has been confirmed; the sign change in the first term has not, but is consistent with the antisymmetric nature of the perturbation.) Eq. (3.65) is for the case of an orthogonal basis set, but an exactly analogous expression is found for the nonorthogonal set using the transformation Eq. (3.52b). Therefore, in the notation used earlier [see, for example, Eqs. (3.48-6)], Eq. (3.65) has the form

$$\mathbf{P}_\alpha^{(1,0)} = -\frac{1}{2} \mathbf{P}^{(0)} \mathbf{S}_\alpha^{(1,0)} \mathbf{P}^{(0)} + 2 \sum_{\substack{occ \\ K}} \sum_{\substack{unocc \\ L}} \frac{\mathbf{c}_K^+ (\mathbf{F}_\alpha^{(1,0)} - e_K \mathbf{S}_\alpha^{(1,0)}) \mathbf{c}_L}{(e_K - e_L)} (\mathbf{c}_K \mathbf{c}_L^+ - \mathbf{c}_L \mathbf{c}_K^+) .$$

IV. McMurchie-Davidson Integrals

In order to evaluate the wide variety of one- and two-electron integrals given by Eqs. (3.38, 3.39, 3.48, 3.50, and 3.52) we require a very flexible integration scheme. The current section will outline the theory of McMurchie-Davidson⁵⁴ integral evaluation, and describe a modified coding algorithm that incorporates the shell structure of integral evaluation due to Dupuis. As in the previous sections, the reader will be referred to Appendix E for detailed derivations.

A. One-Electron Integrals

A standard unnormalized Cartesian Gaussian basis function centered on point \mathbf{A} ⁵⁵ in space is given by the general formula

$$\phi_A = x_A^n y_A^l z_A^m e^{-\alpha_A r_A^2} \quad (3.66)$$

where $r_A = \sqrt{x_A^2 + y_A^2 + z_A^2}$ and $\mathbf{r}_A = \mathbf{r} - \mathbf{A}$. Note that the angular momentum is given by the prefactor of the Gaussian; i.e. if $n + l + m = 0$, it is an *s*-function; if $n + l + m = 1$, it is a *p*-function, etc. A common quantity then is the charge distribution of two functions centered at different points:

$$\begin{aligned} \Omega_{AB} &= \phi_A \phi_B = x_A^n y_A^l z_A^m e^{-\alpha_A r_A^2} x_B^{\bar{n}} y_B^{\bar{l}} z_B^{\bar{m}} e^{-\alpha_B r_B^2} \\ &= x_A^n x_B^{\bar{n}} y_A^l y_B^{\bar{l}} z_A^m z_B^{\bar{m}} e^{-(\alpha_A r_A^2 + \alpha_B r_B^2)} \end{aligned} \quad (3.67)$$

Where we then note that the product of two Gaussians is another Gaussian, as shown by Boys:

$$\begin{aligned} e^{-(\alpha_A r_A^2 + \alpha_B r_B^2)} &= e^{-\frac{\alpha_A \alpha_B}{\alpha_A + \alpha_B} |\mathbf{A} - \mathbf{B}|^2} e^{-(\alpha_A + \alpha_B) r_P^2} \\ &= E_{AB} e^{-\alpha_P r_P^2} \end{aligned} \quad (3.68)$$

where

$$\mathbf{P} = \frac{\alpha_A \mathbf{A} + \alpha_B \mathbf{B}}{\alpha_A + \alpha_B} \quad (3.69)$$

At this point, we introduce an operator, which when acting on a Gaussian function, is the main feature of the McMurchie-Davidson method:

$$\mathbf{\Lambda}_j e^{-\alpha_p x_p^2} \equiv \left(\frac{\partial}{\partial P_x} \right)^j e^{-\alpha_p x_p^2} \quad (3.69)$$

The power and utility of the above definition is exposed when we relate it to the Hermite polynomials, given by the following generating function:

$$H_j(x) = (-1)^j e^{x^2} \left(\frac{\partial}{\partial x} \right)^j e^{-x^2} \quad (3.71)$$

it follows that (E.1)

$$\mathbf{\Lambda}_j e^{-\alpha_p x_p^2} = \alpha_p^{j/2} H_j(\alpha_p^{1/2} x_p) e^{-\alpha_p x_p^2} \quad (3.72)$$

Using the recurrence relations for Hermite polynomials, we can further derive the relation (E.2)

$$x_A \mathbf{\Lambda}_N = N \mathbf{\Lambda}_{N-1} + \overline{P A_x} \mathbf{\Lambda}_N + \frac{\mathbf{\Lambda}_{N+1}}{2\alpha_p} \quad (3.73)$$

where it is understood that the operators act on Gaussian functions, and $\overline{P A_x} = P_x - A_x$, where P_x is the x -coordinate of point P .

Since these operators are a function of a complete set of orthogonal functions, we can expand the Cartesian products in Eq. (3.67) in terms of them: [note that an n^{th} degree function of x requires an expansion space of Hermite polynomials also no greater than degree n , since $H_n = H_n(x^n, x^{n-2}, x^{n-4}, \text{etc.})$]

$$x_A^n x_B^{\bar{n}} = \sum_{N=0}^{n+\bar{n}} d_N^{n\bar{n}} \Lambda_N \quad (3.74)$$

Where it is understood that $d_N^{n\bar{n}} = 0$ unless $0 \leq N \leq (n + \bar{n})$, and $d_0^{00} = 1$ since $\Lambda_0 = 1$. Using the above recurrence relation, Eq. (3.73), we can find a similar relation for the coefficients of the expansion in Eq. (3.74). Consider

$$x_A^{n+1} x_B^{\bar{n}} = \sum_{N=0}^{n+\bar{n}+1} d_N^{n+1,\bar{n}} \Lambda_N = \sum_{N=0}^{n+\bar{n}} d_N^{n\bar{n}} x_A \Lambda_N \quad (3.75)$$

which allows us to identify (E.3):

$$d_N^{n+1,\bar{n}} = d_{N+1}^{n\bar{n}} (N+1) + d_N^{n\bar{n}} \overline{PA_x} + \frac{d_{N-1}^{n\bar{n}}}{2\alpha_p} \quad (3.76)$$

therefore one can use the above expression to quickly calculate a table of $d_N^{n\bar{n}}$ for use in later summations. Eq. (3.76) is specific to the x -coordinate; there are exactly analogous expressions for y and z , introduced here:

$$y_A^l y_B^{\bar{l}} = \sum_{L=0}^{l+\bar{l}} e_L^{l\bar{l}} \Lambda_L \quad ; \quad z_A^m z_B^{\bar{m}} = \sum_{M=0}^{m+\bar{m}} f_M^{m\bar{m}} \Lambda_M \quad (3.77 ; 3.78)$$

Thus the original charge distribution, Eq. (3.67) can be written as

$$\begin{aligned}
\Omega_{AB} &= \phi_A \phi_B = x_A^n x_B^{\bar{n}} y_A^l y_B^{\bar{l}} z_A^m z_B^{\bar{m}} e^{-(\alpha_A r_A^2 + \alpha_B r_B^2)} \\
&= \left(\sum_{N=0}^{n+\bar{n}} d_N^{n\bar{n}} \mathbf{\Lambda}_N \right) \left(\sum_{L=0}^{l+\bar{l}} e_L^{l\bar{l}} \mathbf{\Lambda}_L \right) \left(\sum_{M=0}^{m+\bar{m}} f_M^{m\bar{m}} \mathbf{\Lambda}_M \right) e^{-(\alpha_A r_A^2 + \alpha_B r_B^2)} \\
&= E_{AB} \sum_{N=0}^{n+\bar{n}} \sum_{L=0}^{l+\bar{l}} \sum_{M=0}^{m+\bar{m}} d_N^{n\bar{n}} e_L^{l\bar{l}} f_M^{m\bar{m}} \mathbf{\Lambda}_N \mathbf{\Lambda}_L \mathbf{\Lambda}_M e^{-\alpha_P r_P^2}
\end{aligned} \tag{3.79}$$

We will return to the integral of the charge distribution in a moment. Consider first the more complex integrand

$$\phi_A \nabla \phi_B \tag{3.80}$$

and its x -component: (E.4)

$$\begin{aligned}
\phi_A \frac{\partial}{\partial x} \phi_B &= \phi_A \frac{\partial}{\partial x} x_B^{\bar{n}} y_B^{\bar{l}} z_B^{\bar{m}} e^{-\alpha_B r_B^2} \\
&= (\bar{n} x_A^n x_B^{\bar{n}-1} - 2\alpha_B x_A^n x_B^{\bar{n}+1}) y_A^l y_B^{\bar{l}} z_A^m z_B^{\bar{m}} e^{-(\alpha_A r_A^2 + \alpha_B r_B^2)}
\end{aligned} \tag{3.81}$$

Then, using Eq. (3.75), we see the utility of the recursion relation for the coefficients:

$$\begin{aligned}
\phi_A \frac{\partial}{\partial x} \phi_B &= \left[\bar{n} \left(\sum_{N=0}^{n+\bar{n}-1} d_N^{n\bar{n}-1} \mathbf{\Lambda}_N \right) - 2\alpha_B \left(\sum_{N=0}^{n+\bar{n}+1} d_N^{n\bar{n}+1} \mathbf{\Lambda}_N \right) \right] y_A^l y_B^{\bar{l}} z_A^m z_B^{\bar{m}} e^{-(\alpha_A r_A^2 + \alpha_B r_B^2)} \\
&= E_{AB} \sum_{N=0}^{n+\bar{n}+1} \sum_{L=0}^{l+\bar{l}} \sum_{M=0}^{m+\bar{m}} \left[(\bar{n} d_N^{n\bar{n}-1} - 2\alpha_B d_N^{n\bar{n}+1}) e_L^{l\bar{l}} f_M^{m\bar{m}} \right. \\
&\quad \left. \times \mathbf{\Lambda}_N(x_P) \mathbf{\Lambda}_L(y_P) \mathbf{\Lambda}_M(z_P) e^{-\alpha_P r_P^2} \right]
\end{aligned} \tag{3.82}$$

since $d_{n+\bar{n}}^{n\bar{n}-1} = d_{n+\bar{n}+1}^{n\bar{n}-1} = 0$. This illustrates the basic method for modifying integrands.

The next step is to integrate over all space. Consider the integral of the charge distribution:

$$\begin{aligned}
\int d\mathbf{r} \Omega_{AB} &= \int d\mathbf{r} E_{AB} \sum_{N=0}^{n+\bar{n}} \sum_{L=0}^{l+\bar{l}} \sum_{M=0}^{m+\bar{m}} d_N^{n\bar{n}} e_L^{l\bar{l}} f_M^{m\bar{m}} \Lambda_N \Lambda_L \Lambda_M e^{-\alpha_p r_p^2} \\
&= E_{AB} \sum_{N=0}^{n+\bar{n}} \sum_{L=0}^{l+\bar{l}} \sum_{M=0}^{m+\bar{m}} d_N^{n\bar{n}} e_L^{l\bar{l}} f_M^{m\bar{m}} \int d\mathbf{r} \Lambda_N \Lambda_L \Lambda_M e^{-\alpha_p x_p^2} e^{-\alpha_p y_p^2} e^{-\alpha_p z_p^2} \\
&= E_{AB} \sum_{N=0}^{n+\bar{n}} \sum_{L=0}^{l+\bar{l}} \sum_{M=0}^{m+\bar{m}} d_N^{n\bar{n}} e_L^{l\bar{l}} f_M^{m\bar{m}} \int dx \Lambda_N e^{-\alpha_p x_p^2} \int dy \Lambda_L e^{-\alpha_p y_p^2} \int dz \Lambda_M e^{-\alpha_p z_p^2}
\end{aligned} \tag{3.83}$$

where we note that, for example,

$$\int dx \Lambda_N e^{-\alpha_p x_p^2} = \int dx \left(\frac{\partial}{\partial P_x} \right)^N e^{-\alpha_p x_p^2} \tag{3.84}$$

can easily be evaluated since the Hermite polynomials are orthogonal under a Gaussian weighting function:

$$\int dx e^{-x^2} H_N(x) H_M(x) = 2^N N! \sqrt{\pi} \delta_{N,M} \tag{3.85}$$

Therefore, using Eq. (3.72),

$$\begin{aligned}
\int dx \Lambda_N e^{-\alpha_p x_p^2} &= \int dx \alpha_p^{N/2} H_N(\alpha_p^{1/2} x_p) e^{-\alpha_p x_p^2} \\
&= \int d\left(\frac{\alpha_p^{1/2} x_p}{\alpha_p^{1/2}}\right) \alpha_p^{N/2} H_N(\alpha_p^{1/2} x_p) e^{-\alpha_p x_p^2} \\
&= \alpha_p^{-1/2} \alpha_p^{N/2} \int d(\alpha_p^{1/2} x_p) H_N(\alpha_p^{1/2} x_p) H_0(\alpha_p^{1/2} x_p) e^{-\alpha_p x_p^2} \\
&= \alpha_p^{-1/2} \alpha_p^{N/2} 2^N N! \sqrt{\pi} \delta_{N,0} = \delta_{N,0} \alpha_p^{-1/2} \sqrt{\pi} = \delta_{N,0} \left(\frac{\pi}{\alpha_p} \right)^{1/2}
\end{aligned} \tag{3.86}$$

where we have noted that $H_0(x) = 1$. This result simplifies Eq. (3.83):

$$\begin{aligned}
\int d\mathbf{r} \Omega_{AB} &= E_{AB} \sum_{N=0}^{n+\bar{n}} \sum_{L=0}^{l+\bar{l}} \sum_{M=0}^{m+\bar{m}} d_N^{n\bar{n}} e_L^{l\bar{l}} f_M^{m\bar{m}} \left(\delta_{N,0} \left(\frac{\pi}{\alpha_p} \right)^{1/2} \delta_{L,0} \left(\frac{\pi}{\alpha_p} \right)^{1/2} \delta_{M,0} \left(\frac{\pi}{\alpha_p} \right)^{1/2} \right) \\
&= E_{AB} d_0^{n\bar{n}} e_0^{l\bar{l}} f_0^{m\bar{m}} \left(\frac{\pi}{\alpha_p} \right)^{3/2}
\end{aligned} \tag{3.87}$$

and the overlap integral is thus evaluated. Note that the same procedure can be used for the derivative integrand, Eq. (3.80):

$$\begin{aligned}
\int d\mathbf{r} \phi_A \frac{\partial}{\partial x} \phi_B &= E_{AB} \sum_{N=0}^{n+\bar{n}+1} \sum_{L=0}^{l+\bar{l}} \sum_{M=0}^{m+\bar{m}} (\bar{n} d_N^{n,\bar{n}-1} - 2\alpha_B d_N^{n,\bar{n}+1}) e_L^{l\bar{l}} f_M^{m\bar{m}} \int d\mathbf{r} \Lambda_N \Lambda_L \Lambda_M e^{-\alpha_p r_p^2} \\
&= E_{AB} \left(\frac{\pi}{\alpha_p} \right)^{3/2} \sum_{N=0}^{n+\bar{n}+1} \sum_{L=0}^{l+\bar{l}} \sum_{M=0}^{m+\bar{m}} (\bar{n} d_N^{n,\bar{n}-1} - 2\alpha_B d_N^{n,\bar{n}+1}) e_L^{l\bar{l}} f_M^{m\bar{m}} \delta_{N,0} \delta_{L,0} \delta_{M,0} \\
&= E_{AB} \left(\frac{\pi}{\alpha_p} \right)^{3/2} (\bar{n} d_0^{n,\bar{n}-1} - 2\alpha_B d_0^{n,\bar{n}+1}) e_0^{l\bar{l}} f_0^{m\bar{m}}
\end{aligned} \tag{3.88}$$

One can also make use of the general recurrence relation, Eq. (3.73) to evaluate the more complex dipole moment expectation value: (E.5)

$$\int d\mathbf{r} \phi_A x_C \phi_B = E_{AB} \left(\frac{\pi}{\alpha_p} \right)^{3/2} \sum_{N=0}^1 d_N^{n\bar{n}} e_0^{l\bar{l}} f_0^{m\bar{m}} [\delta_{N,1} + \overline{PC_x} \delta_{N,0}] \tag{3.89}$$

Two applications of the recurrence relation leads to an evaluation of the second moments: (E.6)

$$\int d\mathbf{r} \phi_A x_C^2 \phi_B = E_{AB} \left(\frac{\pi}{\alpha_p} \right)^{3/2} \sum_{N=0}^2 d_N^{n\bar{n}} e_0^{l\bar{l}} f_0^{m\bar{m}} \left[2\delta_{N,2} + 2\overline{PC_x} \delta_{N,1} + \left(\overline{PC_x}^2 + \frac{1}{2\alpha_p} \right) \delta_{N,0} \right] \tag{3.90}$$

Note that a similar procedure can be used for $x_C y_C, y_C z_C, y_C^2$, etc.

Consider now a one-electron integral of the form

$$\begin{aligned}
\int d\mathbf{r} \phi_A r_C^{-1} \phi_B &= E_{AB} \sum_{N=0}^{n+\bar{n}} \sum_{L=0}^{l+\bar{l}} \sum_{M=0}^{m+\bar{m}} d_N^{n\bar{n}} e_L^{l\bar{l}} f_M^{m\bar{m}} \int d\mathbf{r} r_C^{-1} \mathbf{\Lambda}_N(x_p) \mathbf{\Lambda}_L(y_p) \mathbf{\Lambda}_M(z_p) e^{-\alpha_p r_p^2} \\
&= E_{AB} \sum_{N=0}^{n+\bar{n}} \sum_{L=0}^{l+\bar{l}} \sum_{M=0}^{m+\bar{m}} d_N^{n\bar{n}} e_L^{l\bar{l}} f_M^{m\bar{m}} \left(\frac{\partial}{\partial P_x} \right)^N \left(\frac{\partial}{\partial P_y} \right)^L \left(\frac{\partial}{\partial P_z} \right)^M \int d\mathbf{r} r_C^{-1} e^{-\alpha_p r_p^2}
\end{aligned} \tag{3.91}$$

Boys has shown,⁵⁶ and we can easily verify that (E.7)

$$\int d\mathbf{r} r_C^{-1} e^{-\alpha_p r_p^2} = \left(\frac{2\pi}{\alpha_p} \right) \int_0^1 du e^{-\alpha_p \bar{C}P^2 u^2} = \left(\frac{2\pi}{\alpha_p} \right) F_0(\alpha_p \bar{C}P^2) \tag{3.92}$$

we then define

$$R_{NLM} = \left(\frac{\partial}{\partial P_x} \right)^N \left(\frac{\partial}{\partial P_y} \right)^L \left(\frac{\partial}{\partial P_z} \right)^M F_0(\alpha_p \bar{C}P^2) \tag{3.93}$$

$F_0(x)$ is related to the incomplete Gamma function, for which standard methods of evaluation are available.⁵⁷ Using these definitions, Eq. (3.91) becomes

$$\int d\mathbf{r} \phi_A r_C^{-1} \phi_B = E_{AB} \sum_{N=0}^{n+\bar{n}} \sum_{L=0}^{l+\bar{l}} \sum_{M=0}^{m+\bar{m}} d_N^{n\bar{n}} e_L^{l\bar{l}} f_M^{m\bar{m}} \left(\frac{2\pi}{\alpha_p} \right) R_{NLM} \tag{3.94}$$

Note that the values of R_{NLM} can also be obtained with the help of a recursion relation, since they are related to the Hermite polynomials: (E.8)

$$R_{0,0,M+1,j} = cR_{0,0,M,j+1} + MR_{0,0,M-1,j+1} \tag{3.95}$$

$$R_{0,L+1,M,j} = bR_{N,L,M,j+1} + LR_{N-1,L,M,j+1} \tag{3.96}$$

$$R_{N+1,L,M,j} = aR_{N,L,M,j+1} + NR_{N-1,L,M,j+1} \tag{3.97}$$

Electric and magnetic field integrals typically involve factors of x_C/r_C^3 , and these can be evaluated using the above method if we note that

$$\frac{\partial r_C^{-1}}{\partial C_x} = \left(\frac{\partial x_C}{\partial C_x} \right) \left(\frac{\partial r_C}{\partial x_C} \right) \left(\frac{\partial r_C^{-1}}{\partial r_C} \right) = (-1) \left(\frac{x_C}{r_C} \right) \left(-\frac{1}{r_C^2} \right) = \frac{x_C}{r_C^3} \quad (3.98)$$

then the general integral is given by

$$\int d\mathbf{r} \phi_A \frac{x_C}{r_C^3} \phi_B = \int d\mathbf{r} \phi_A \frac{\partial r_C^{-1}}{\partial C_x} \phi_B = \frac{\partial}{\partial C_x} E_{AB} \sum_{N=0}^{n+\bar{n}} \sum_{L=0}^{l+\bar{l}} \sum_{M=0}^{m+\bar{m}} d_N^{n\bar{n}} e_L^{l\bar{l}} f_M^{m\bar{m}} \left(\frac{2\pi}{\alpha_p} \right) R_{NLM} \quad (3.99)$$

But since R_{NLM} is a function of $(\alpha_p \overline{CP}^2)$, which itself depends on $C_x - P_x$, we have

$$\begin{aligned} f(\alpha_p \overline{CP}^2) &= f(T) \\ \Rightarrow \frac{\partial f}{\partial C_x} &= \frac{\partial T}{\partial C_x} \frac{\partial f}{\partial T} = -\frac{\partial T}{\partial P_x} \frac{\partial f}{\partial T} = -\frac{\partial f}{\partial P_x} \end{aligned} \quad (3.100)$$

since

$$\frac{\partial T}{\partial C_x} = 2\alpha_p \frac{\partial}{\partial C_x} (C_x - P_x) = -\frac{\partial T}{\partial P_x} \quad (3.101)$$

for any function of T . So then Eq. (3.99) becomes

$$\begin{aligned} \int d\mathbf{r} \phi_A \frac{x_C}{r_C^3} \phi_B &= -\frac{\partial}{\partial P_x} E_{AB} \sum_{N=0}^{n+\bar{n}} \sum_{L=0}^{l+\bar{l}} \sum_{M=0}^{m+\bar{m}} d_N^{n\bar{n}} e_L^{l\bar{l}} f_M^{m\bar{m}} \left(\frac{2\pi}{\alpha_p} \right) \left(\frac{\partial}{\partial P_x} \right)^N \left(\frac{\partial}{\partial P_y} \right)^L \left(\frac{\partial}{\partial P_z} \right)^M F_0(T) \\ &= -E_{AB} \sum_{N=0}^{n+\bar{n}} \sum_{L=0}^{l+\bar{l}} \sum_{M=0}^{m+\bar{m}} d_N^{n\bar{n}} e_L^{l\bar{l}} f_M^{m\bar{m}} \left(\frac{2\pi}{\alpha_p} \right) R_{N+1,L,M} \end{aligned} \quad (3.102)$$

where $F_0(T)$ was defined in Eq. (3.92).

We have now developed the theory to the point where the needed integrals, given by Eqs. (3.38, 3.39, 3.48, 3.50, 3.52) can be evaluated. Consider the x -component of the matrix element of the one-electron spin-orbit operator:

$$\begin{aligned}
\langle \phi_A | \frac{(\mathbf{r}_C \times \nabla)_x}{r_C^3} | \phi_B \rangle &= \int d\mathbf{r} \phi_A \frac{(\mathbf{r}_C \times \nabla)_x}{r_C^3} \phi_B \\
&= \int d\mathbf{r} \phi_A \left(\frac{y_C \nabla_z}{r_C^3} \right) \phi_B - \int d\mathbf{r} \phi_A \left(\frac{z_C \nabla_y}{r_C^3} \right) \phi_B
\end{aligned} \tag{3.103}$$

We can explicitly treat just one of these integrals to define the general procedure:

$$\begin{aligned}
\int d\mathbf{r} \phi_A \left(\frac{y_C \nabla_z}{r_C^3} \right) \phi_B &= \int d\mathbf{r} \phi_A \frac{y_C}{r_C^3} \frac{\partial}{\partial z} \phi_B = \int d\mathbf{r} \phi_A \frac{y_C}{r_C^3} \frac{\partial}{\partial z} \phi_B = \int d\mathbf{r} \phi_A \frac{\partial r_C^{-1}}{\partial C_y} \frac{\partial}{\partial z} \phi_B \\
&= \frac{\partial}{\partial C_y} \int d\mathbf{r} \phi_A r_C^{-1} \frac{\partial}{\partial z} \phi_B \\
&= \frac{\partial}{\partial C_y} E_{AB} \sum_{N=0}^{n+\bar{n}} \sum_{L=0}^{l+\bar{l}} \sum_{M=0}^{m+\bar{m}+1} \left[d_N^{m\bar{m}} e_L^{\bar{l}} \left(\bar{m} f_M^{m, \bar{m}-1} - 2\alpha_B f_M^{m, \bar{m}+1} \right) \right. \\
&\quad \left. \times \mathbf{\Lambda}_N(x_p) \mathbf{\Lambda}_L(y_p) \mathbf{\Lambda}_M(z_p) \int d\mathbf{r} r_C^{-1} e^{-\alpha_p r_p^2} \right]
\end{aligned} \tag{3.104}$$

using Eq. (3.82). For convenience, let us define $F_M^m = (\bar{m} f_M^{m, \bar{m}-1} - 2\alpha_B f_M^{m, \bar{m}+1})$:

$$\int d\mathbf{r} \phi_A \left(\frac{y_C \nabla_z}{r_C^3} \right) \phi_B = -E_{AB} \sum_{N=0}^{n+\bar{n}} \sum_{L=0}^{l+\bar{l}} \sum_{M=0}^{m+\bar{m}+1} d_N^{m\bar{m}} e_L^{\bar{l}} F_M^m \left(\frac{2\pi}{\alpha_p} \right) R_{N, L+1, M} \tag{3.105}$$

where we have used Eqs. (3.92), (3.93), and (3.101).

The next class of integral is given by

$$\langle z_v \phi_v | \frac{y_B \nabla_z}{r_B^3} | \phi_\lambda \rangle = \int d\mathbf{r} z_A \phi_A \left(\frac{y_C \nabla_z}{r_C^3} \right) \phi_B \tag{3.106}$$

which is simply the previous integral with a higher angular momentum on basis function A . In this case, m should be replaced by $m+1$ to account for the extra z on function A :

$$\int d\mathbf{r} z_A \phi_A \left(\frac{y_C \nabla_z}{r_C^3} \right) \phi_B = -E_{AB} \sum_{N=0}^{n+\bar{n}} \sum_{L=0}^{l+\bar{l}} \sum_{M=0}^{m+\bar{m}+2} d_N^{m\bar{m}} e_L^{\bar{l}} F_M^{m+1} \left(\frac{2\pi}{\alpha_p} \right) R_{N, L+1, M} \tag{3.107}$$

The final class of integral is given by

$$\langle \phi_v | \frac{\mathbf{r}_\lambda \cdot \mathbf{r}_B \delta_{\alpha\beta} - (\mathbf{r}_\lambda)_\alpha (\mathbf{r}_B)_\beta}{r_B^3} | \phi_\lambda \rangle \quad (3.108)$$

If we take the xx -component of this, we have

$$\langle \phi_A | \frac{r_{Bx}r_{Cx} + r_{By}r_{Cy} + r_{Bz}r_{Cz} - r_{Bx}r_{Cx}}{r_C^3} | \phi_B \rangle = \langle \phi_A | \frac{y_B y_C}{r_C^3} | \phi_B \rangle + \langle \phi_A | \frac{z_B z_C}{r_C^3} | \phi_B \rangle \quad (3.109)$$

which is analogous to Eq. (3.102) with a higher angular momentum on function B . We therefore modify Eq. (3.102) accordingly:

$$\langle \phi_A | \frac{y_B y_C}{r_C^3} | \phi_B \rangle = -E_{AB} \sum_{N=0}^{n+\bar{n}} \sum_{L=0}^{l+\bar{l}+1} \sum_{M=0}^{m+\bar{m}} d_N^{\bar{n}} e_L^{l, \bar{l}+1} f_M^{m \bar{m}} \left(\frac{2\pi}{\alpha_p} \right) R_{N, L+1, M} \quad (3.110)$$

B. Two-Electron Integrals

In order to calculate the needed two-electron integrals, one follows a nearly identical formalism as given for the one-electron case. Because of the strong similarity, we need only summarize the important equations. The basis functions are given by

$$\begin{aligned} \phi_A &= x_A^n y_A^l z_A^m e^{-\alpha_A r_A^2} & \phi_B &= x_B^{\bar{n}} y_B^{\bar{l}} z_B^{\bar{m}} e^{-\alpha_B r_B^2} \\ \phi_C &= x_C^{n'} y_C^{l'} z_C^{m'} e^{-\alpha_C r_C^2} & \phi_D &= x_D^{\bar{n}'} y_D^{\bar{l}'} z_D^{\bar{m}'} e^{-\alpha_D r_D^2} \end{aligned} \quad (3.111)$$

Typically, these functions are constructed as a linear combination of so-called *primitive* Gaussian functions. This is also true for the one-electron case, although it was not explicitly included in the derivations. We include it here, however, for completeness and to make a point on the algorithm later on:

$$\begin{aligned}
\phi_A &= \sum_i^I d_{iA} x_A^n y_A^l z_A^m e^{-\alpha_A^i r_A^2} & \phi_B &= \sum_j^J d_{jB} x_B^{\bar{n}} y_B^{\bar{l}} z_B^{\bar{m}} e^{-\alpha_B^j r_B^2} \\
\phi_C &= \sum_g^G d_{gC} x_C^{n'} y_C^{l'} z_C^{m'} e^{-\alpha_C^g r_C^2} & \phi_D &= \sum_h^H d_{hD} x_D^{\bar{n}'} y_D^{\bar{l}'} z_D^{\bar{m}'} e^{-\alpha_D^h r_D^2}
\end{aligned} \tag{3.112}$$

where the d_{iA} are the contraction coefficients. Note also that the exponents can vary from primitive to primitive. We thus have the following charge distributions; the first for electron one, and the second for electron two:

$$\begin{aligned}
\Omega_{AB} &= \sum_i^I \sum_j^J d_{iA} d_{jB} E_{AB}^{ij} \sum_{N=0}^{n+\bar{n}} \sum_{L=0}^{l+\bar{l}} \sum_{M=0}^{m+\bar{m}} f_M^{m\bar{m}} e_L^{\bar{l}} d_N^{m\bar{m}} \mathbf{\Lambda}_N \mathbf{\Lambda}_L \mathbf{\Lambda}_M e^{-\alpha_P r_P^2} \\
\Omega_{CD} &= \sum_g^G \sum_h^H d_{gC} d_{hD} E_{CD}^{gh} \sum_{N'=0}^{n'+\bar{n}'} \sum_{L'=0}^{l'+\bar{l}'} \sum_{M'=0}^{m'+\bar{m}'} f_{M'}^{m'\bar{m}'} e_{L'}^{l'} d_{N'}^{n'\bar{n}'} \mathbf{\Lambda}_{N'} \mathbf{\Lambda}_{L'} \mathbf{\Lambda}_{M'} e^{-\alpha_Q r_Q^2}
\end{aligned} \tag{3.113}$$

such that the general two-electron, four-center integral can be written as

$$\begin{aligned}
(\phi_A \phi_B | \phi_C \phi_D) &= \int d\mathbf{r} \Omega_{AB} r_{12}^{-1} \Omega_{CD} \\
&= \sum_i^I \sum_j^J \sum_g^G \sum_h^H d_{iA} d_{jB} d_{gC} d_{hD} E_{CD}^{gh} E_{AB}^{ij} \sum_{N=0}^{n+\bar{n}} \sum_{L=0}^{l+\bar{l}} \sum_{M=0}^{m+\bar{m}} \sum_{N'=0}^{n'+\bar{n}'} \sum_{L'=0}^{l'+\bar{l}'} \sum_{M'=0}^{m'+\bar{m}'} d_N^{n\bar{n}} e_L^{\bar{l}} f_M^{m\bar{m}} d_{N'}^{n'\bar{n}'} e_{L'}^{l'} f_{M'}^{m'\bar{m}'} \\
&\quad \times \left(\frac{\partial}{\partial P_x} \right)^N \left(\frac{\partial}{\partial P_y} \right)^L \left(\frac{\partial}{\partial P_z} \right)^M \left(\frac{\partial}{\partial Q_x} \right)^{N'} \left(\frac{\partial}{\partial Q_y} \right)^{L'} \left(\frac{\partial}{\partial Q_z} \right)^{M'} \int d\mathbf{r} r_{12}^{-1} e^{-\alpha_P r_P^2} e^{-\alpha_Q r_Q^2}
\end{aligned} \tag{3.114}$$

However, Boys has shown that⁵⁸

$$\int d\mathbf{r} r_{12}^{-1} e^{-\alpha_P r_P^2} e^{-\alpha_Q r_Q^2} = \frac{2\pi^{5/2}}{\alpha_P \alpha_Q (\alpha_P + \alpha_Q)^{1/2}} F_0(T) \tag{3.115}$$

where $T = \frac{\alpha_P \alpha_Q}{\alpha_P + \alpha_Q} \overline{PQ}^2$. And since T is a function of $\mathbf{P} - \mathbf{Q}$,

$$-\left(\frac{\partial}{\partial P_x}\right)^N g(T) = \left(\frac{\partial}{\partial Q_x}\right)^N g(T) \quad (3.116)$$

in a manner similar to Eq. (3.101). Therefore

$$(\phi_A \phi_B | \phi_C \phi_D) = \lambda \sum_i^I \sum_j^J \sum_g^G \sum_h^H \sum_k^k \sum_{k'} D_k^{ij} D_{k'}^{gh} (-1)^{N'+L'+M'} R_{N+N', L+L', M+M'} \quad (3.117)$$

where we have used the abbreviations

$$\begin{aligned} D_k^{ij} &= d_{iA} d_{jB} E_{AB}^{ij} d_N^{m\bar{m}} e_L^{\bar{l}} f_M^{m\bar{m}} & \sum_k &\Rightarrow \sum_{N=0}^{n+\bar{n}} \sum_{L=0}^{l+\bar{l}} \sum_{M=0}^{m+\bar{m}} \\ D_{k'}^{gh} &= d_{gC} d_{hD} E_{CD}^{gh} d_{N'}^{n'\bar{n}'} e_{L'}^{\bar{l}'} f_{M'}^{m'\bar{m}'} & \sum_{k'} &\Rightarrow \sum_{N'=0}^{n'+\bar{n}'} \sum_{L'=0}^{l'+\bar{l}'} \sum_{M'=0}^{m'+\bar{m}'} \\ \lambda &= \frac{2\pi^{5/2}}{\alpha_p \alpha_Q (\alpha_p + \alpha_Q)^{1/2}} \end{aligned} \quad (3.118)$$

The desired integrals are then an easy modification of this result;

$$\begin{aligned} (x_A \phi_A \phi_B | \phi_C \phi_D) &= \lambda \sum_k^{n+1} \sum_{k'} D_k^{ij(n+1)} D_{k'}^{gh} (-1)^{N'+L'+M'} R_{N+N', L+L', M+M'} \\ (\phi_A \phi_B | x_C \phi_C \phi_D) &= \lambda \sum_k^{n'+1} \sum_{k'} D_k^{ij} D_{k'}^{gh(n'+1)} (-1)^{N'+L'+M'} R_{N+N', L+L', M+M'} \end{aligned} \quad (3.119)$$

In implementing Eq. (3.119), a modified version of the algorithm given by McMurchie and Davidson has been used, in that the shell structure advocated by Dupuis is introduced at the highest level. This allows for efficient evaluation of the contraction coefficients and other quantities related to a given shell. Fig. 3.2 illustrates the basic approach schematically.

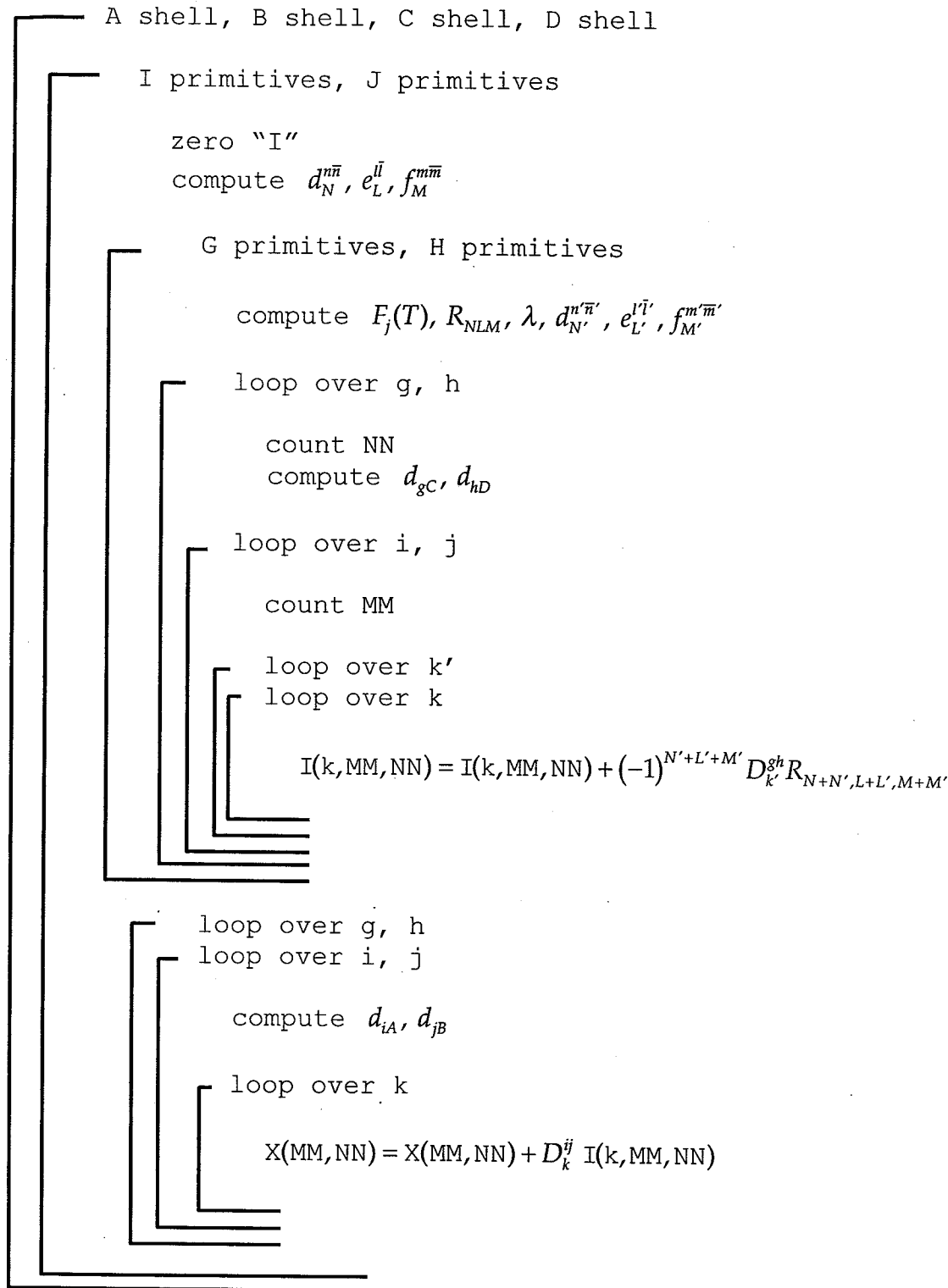


Fig. (3.2) Loop structure for two-electron integrals.

V. Strategies for Incorporating Solvent Effects

There are several potential approaches for incorporating the EFP method (see Ch. 4) and the GIAO chemical shift formalism. A few of these methods will be discussed in this section.

The simplest approximation is to take the previously derived expression for chemical shifts, Eq. (3.37), and substitute the density matrix modified by the presence of the EFPs for its *ab initio* counterpart:

$$\begin{aligned}\sigma_{B\alpha\beta} &= \sum_{v\lambda} \left\{ \left(P_{v\lambda}^{(1,0)} \right)_\alpha \left(H_{Bv\lambda}^{(0,1)} \right)_\beta + P_{v\lambda}^{(0)} \left(H_{Bv\lambda}^{(1,1)} \right)_{\alpha\beta} \right\} \\ &\rightarrow \sum_{v\lambda} \left\{ \left(P_{v\lambda}^{(1,0)} \right)^{EFP} \left(H_{Bv\lambda}^{(0,1)} \right)_\beta + P_{v\lambda}^{EFP} \left(H_{Bv\lambda}^{(1,1)} \right)_{\alpha\beta} \right\}\end{aligned}\quad (3.120)$$

where the first order density matrix, Eq. (3.65) has been similarly modified:

$$\tilde{\mathbf{P}}^{(1,0),EFP} = -\frac{1}{2} \tilde{\mathbf{P}}^{EFP} \tilde{\mathbf{S}}^{(1,0)} \tilde{\mathbf{P}}^{EFP} + 2 \sum_K^{\text{occ}} \sum_L^{\text{unocc}} \frac{\tilde{\mathbf{c}}_K^+ \left(\tilde{\mathbf{F}}^{(1,0)} - e_K \tilde{\mathbf{S}}^{(1,0)} \right) \tilde{\mathbf{c}}_L}{(e_K - e_L)} \left(\tilde{\mathbf{c}}_K \tilde{\mathbf{c}}_L^+ - \tilde{\mathbf{c}}_L \tilde{\mathbf{c}}_K^+ \right) \quad (3.121)$$

In this way, solvent effects are certainly introduced; it remains to be seen to what degree this approximation is reasonable.

In addition to the above, a second level of approximation is to modify the vector potential as it appears in the HF core Hamiltonian, Eq. (3.27), after application of the commutator Eq. (C.9.1), such that it includes contributions from the fragments:

$$H_{v\lambda} \propto \mathbf{A}'(\mathbf{r}_\lambda) = \frac{1}{2} \mathbf{H} \times \mathbf{r}_\lambda + \sum_B \frac{\mathbf{\mu}_B \times \mathbf{r}_B}{r_B^3} + \mathbf{A}_{EFP} \quad (3.122)$$

From this point, one might envision several approximations to \mathbf{A}_{EFP} ; a relatively simple form is to consider the effect of the nuclear magnetic moments of the "nuclei" of the fragments:

$$\mathbf{A}_{EFP} = \sum_I^{\text{EFP nuclei}} \frac{\boldsymbol{\mu}_I \times \mathbf{r}_I}{r_I^3} \quad (3.123)$$

where I counts the EFP nuclear points. This formulation would lead to the following simple modification of the vector potential [c.f. (C.9)]:

$$\frac{1}{2} \mathbf{H} \times \mathbf{r}_\lambda + \sum_B \frac{\boldsymbol{\mu}_B \times \mathbf{r}_B}{r_B^3} \rightarrow \frac{1}{2} \mathbf{H} \times \mathbf{r}_\lambda + \sum_J^{\text{ab initio \& EFP nuclei}} \frac{\boldsymbol{\mu}_J \times \mathbf{r}_J}{r_J^3} \quad (3.124)$$

where J counts over all the *ab initio* nuclei, as before, in addition to the EFP nuclei. Since this term in the end depends only on the location of the nuclei (the integrals are taken at zero field strength) this would incorporate the nuclear magnetic moment contribution of the fragments to the chemical shifts in an ‘exact’ (although incomplete) way. The next level of approximation would be to find an analogous form for the first term of Eq. (3.122) - the interaction of the external magnetic field with the fragments. For the *ab initio* case, the magnetic field is crossed with vectors associated with the centers of the Gaussian basis functions, λ . For the EFP case, it is tempting to choose either the points of expansion for the DMA [see Fig. (4.1)], or the centroids of the localized orbitals [see Fig. (4.2)] instead of the Gaussian centers of the basis set and proceed as in the *ab initio* case, but this will lead to difficulties. For the *ab initio* case, the factor \mathbf{r}_λ ultimately leads to an integral where the angular momentum on basis function λ has been increased, i.e. $s \rightarrow p, p \rightarrow d$, etc. Since the EFP points are not associated with the *ab initio* basis set, choosing these points will lead to integrals with no physical meaning. Clearly, this would not be a productive path for future work.

Instead, one might consider calculating the effect of the external magnetic field on the fragment when the fragment is constructed; i.e. during a “MAKEFP” run. Such a calculation is an *ab initio* one, and therefore the standard GIAO method may be used. The difference would be to omit the second term of the vector potential. Thus the Hamiltonian would have the form

$$H_{\nu\lambda} \propto \mathbf{A}'(\mathbf{r}_\lambda) = \frac{1}{2} \mathbf{H} \times \mathbf{r}_\lambda \quad (3.125)$$

There are two problems with this approach; first, the removal of the second term removes the dependence on the nuclear magnetic moments, and thus makes a straight-forward evaluation of the second derivative tensor difficult. Second, this formulation does not allow for *ab initio* - fragment interaction in terms of magnetic properties. Therefore, one must be aware of the need to represent cross-terms between the *ab initio* and fragment parts of the system.

The final method for integrating the EFP method with the GIAO formalism is simple to describe, but quite possibly difficult to execute. The electrostatic and polarization terms of the EFP potential are ultimately constructed from a finite basis set, as described in the previous paragraph. One could replace this basis set with GIAOs, rederive the EFP terms, and take the second derivative of the full *ab initio* - EFP Hamiltonian, Eq. (4.1). While simple on paper, this most likely has several hidden difficulties that may even make the method intractable. Certainly further research would be required to answer the feasibility question. In its present form, the exchange repulsion/charge penetration term of the EFP method is fitted, and this would also have to be redone for the GIAO case.

VI. Summary and Conclusions

The gauge invariant atomic orbital method has been rederived in an alternate way and presented in detail. The resulting one- and two- electron integrals have been evaluated using a modified algorithm for the McMurchie-Davidson method. The previously published expression for the first-order density matrix has been rederived and corrected in the context of antisymmetric perturbation theory for field-dependent, nonorthogonal basis sets. Several approaches have been presented for incorporating the GIAO method with the Effective Fragment Potential method, in order to achieve the ultimate goal of predicting chemical shifts in solution.

CHAPTER 4: THE SOLVATION OF FORMIC AND ACETIC ACIDS

A paper to be submitted to the Journal of the American Chemical Society

Abstract

The solvation of formic and acetic acids has been studied by treating the weak acid with a restricted Hartree-Fock (RHF/6-31++G(d,p)) *ab initio* wavefunction, and the solvent waters with the Effective Fragment Potential (EFP) model for discrete solvation. The acidic O-H bond length, frequency, and Mulliken charges are measured at each local minimum as a function of added solvent molecules. Boltzmann averages of these data allow for the calculation of a potential of mean force, which can give a quantitative description of the mechanism of dissociation. Monte Carlo or molecular mechanics methods are necessary to adequately sample the configuration space if more than four or five waters are present.

I. Introduction

The purpose of this chapter is to examine the solvation of formic and acetic acids. There are several questions to be answered in a study of this kind; namely, what is the effect of solvation on an electrolyte? In other words, how does the electronic structure of the electrolyte change as an increasing number of discrete solvent molecules are added to the system? What is the mechanism of dissociation? Being an electrolyte, we expect a certain fraction of the solute molecules to dissociate into ions at equilibrium. Can we propose a mechanism for this ionization? Finally, how does the physics of dissociation differ between strong and weak electrolytes? The current study focuses on weak acids, but we can compare with previous studies on sodium chloride⁵⁹ and ongoing studies of strong acids such as HCl and NaOH.

II. Theoretical Methods

Our task is to obtain a quantitative description of the dissolved state of the electrolyte. This will be done via the so-called potential of mean force, for which there are two approaches: first, consider Fig. (4.1).

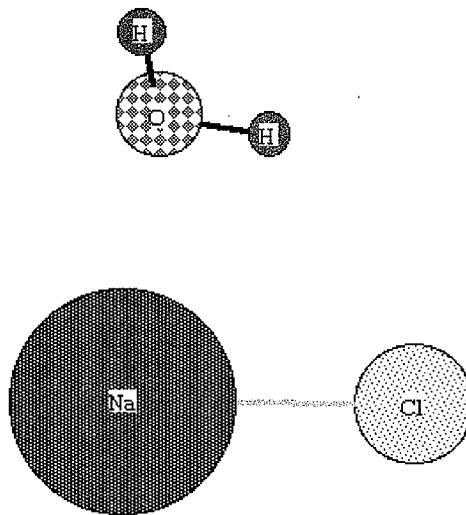


Fig. (4.1) Sodium chloride with a single solvent molecule.

In this approach, the bond distance between the two atoms of the diatomic solute, sodium chloride, is fixed at a certain value. Then the system of solute and solvent (shown as a single water molecule) is optimized under the restriction of the fixed Na-Cl bond length. Then, the bond length is increased slightly and fixed again, followed by optimization. This is repeated until the ions Na^+ and Cl^- are dissociated, and the entire procedure is repeated for two solvent molecules, then three, etc. At each step, the potential and other physical properties such as Mulliken charges are calculated. This is a computationally demanding and time consuming procedure.

The second approach is to measure the bond length, potential, vibrational frequencies, and other physical properties as a function of the number of solvent molecules added. For an increasing number of solvent molecules, there is an exponential increase in the number of minima on the potential energy surface. For this study, an attempt is made to find as many possible minima manually, and then average the results using Boltzmann's method:

$$\text{Avg}(\xi) = \frac{1}{N} \sum_i^N \xi_i e^{-\frac{\Delta G_i}{RT}} \quad (4.1)$$

where ξ_i is the value of some physical property (Mulliken charge, vibrational frequency, etc.) for the i^{th} minimum on the potential energy surface, and further,

$$\begin{aligned} \Delta G_i &= G_i - G_0 \\ G_i &\equiv E_{\text{final}} + E_{\text{corr}}(298.15) \text{ for } i^{\text{th}} \text{ structure} \\ G_0 &\equiv E_{\text{final}} + E_{\text{corr}}(298.15) \text{ for lowest - energy structure} \end{aligned} \quad (4.2a,b,c)$$

Here, G represents the Gibbs free energy, E_{final} is the electronic energy of the system, and E_{corr} is the the temperature correction to the electronic energy based on the rigid rotor, ideal gas, and simple harmonic oscillator approximations. It should be noted that for systems with such a shallow potential energy surface, the simple harmonic oscillator is a poor model, and this calls into question the validity of this traditional thermodynamic calculations on small clusters of molecules. For the purposes of averaging, however, we will use these approximations as shown in Eqs. (4.2).

The manual technique used for finding the maximum number of minima in configuration space is as follows: Consider a coordinate system centered on the carbonyl carbon in the weak acid. The x -axis is represented by a line from this origin to the nucleus of the oxygen bonded to the acidic hydrogen, as seen in Fig. (4.2).

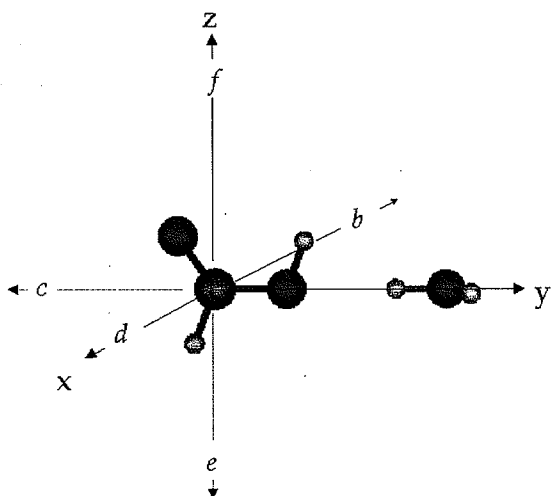


Fig. (4.2) Definition of the coordinate system and initial fragment points. The fragment shown is at point *a*.

With this coordinate system in place, six points can be defined, as shown in Fig. (4.2). These points are roughly 3.0-3.5 Å from the origin, and they are the starting points for the introduction of fragment solvent molecules. The procedure is as follows: an isolated solute molecule's geometry is optimized, and then six independent optimizations are run with a single water fragment at each of the six points in Fig. (4.2). Of these optimizations, the *unique* geometries obtained are taken as the starting point for optimizations with two fragment waters, introducing the second water at each of the six positions, as before. This procedure is then repeated for three, four, and five waters. The number of unique geometries increases exponentially, as shown in Table (4.1)

Waters	Formic Acid			Acetic Acid		
	Total unique structures	Struc. w/ 1 saddle pt.	Struc. w/ >1 saddle pt.	Total unique structures	Struc. w/ 1 saddle pt.	Struc. w/ >1 saddle pt.
1	2	0	0	3	0	1
2	6	2	0	8	4	1
3	18	3	0	32	13	4
4	62	13	4	105	38	6
5	241	69	16	-	-	-

Table (4.1) Number of unique geometries with increasing number of fragment water molecules. Those structures with saddle points are indicated.

Note that this manual method quickly becomes intractable, as formic acid with six waters would require $(241 \times 6 =) 1,446$ input files. For the Boltzmann averages to follow, only positive definite geometries are included in the averaging. For all calculations, the *ab initio* solute is treated with RHF/6-31++G(d,p) and all solute molecules are represented by fragments.

III. Preliminary Results

With only four and five solvent molecules for acetic and formic acid, respectively, it is unrealistic to draw major conclusions, as full dissociation is not nearly approached. As seen in the last section, it is not feasible to continue to search for minima manually, and so this work is waiting for Monte Carlo or molecular dynamics codes written explicitly for use with the EFP method to become available. Preliminary results can be presented, however.

waters	$\langle R \rangle$ (Å)	$\langle v \rangle$ (cm ⁻¹)	Mull.Ch. O	Mull.Ch. H
0	0.9484	4125	-0.5201	0.4035
1	0.9526	4013	-0.5436	0.4486
2	0.9527	3964	-0.5543	0.4608
3	0.9527	3905	-0.5825	0.4815
4	0.9527	3893	-0.5902	0.4866
5	0.9534	3864	-0.5951	0.4965

Table (4.2) Boltzmann averages over the positive definite structures of solvated and unsolvated formic acid.

waters	$\langle R \rangle$ (Å)	$\langle v \rangle$ (cm ⁻¹)	Mull.Ch. O	Mull.Ch. H
0	0.9459	4111	-0.5100	0.5000
1	0.9512	4043	-0.5561	0.4538
2	0.9497	4038	-0.5451	0.4370
3	0.9475	3974	-0.5745	0.4608
4	0.9491	3932	-0.5916	0.4810

Table (4.3) Boltzmann averages over the positive definite structures of solvated and unsolvated acetic acid.

In Tables (4.2) and (4.3), the distance $\langle R \rangle$ is the Boltzmann average of the bond length between the oxygen and the acidic hydrogen in the weak acid. $\langle v \rangle$ is the Boltzmann average of the vibrational frequency of the same bond. Next is the Mulliken charge on the oxygen on the pair in question, followed by the acidic hydrogen. Note that all these quantities evolve as one would expect for a bond undergoing dissociation; the bond length generally increases, the vibrational frequencies decrease, indicating a more loosely bound system, and the Mulliken charge on oxygen decreases towards -1, whereas the hydrogen charge increases towards unity. One could also note that the Gibbs free energy also decreases, but the approximations that go into calculating this quantity, especially the harmonic oscillator approximation, break down badly for a system with so shallow a potential energy surface. It is for this reason that we exclude these values at this time.

Although in general the quantities discussed above proceed in an expected way, there are bumps along the road; see for example the increase in bond length in going from three to four waters for acetic acid. This may be due to an incomplete sampling of the configuration space by the manual method described, and results of Monte Carlo and molecular mechanics routines should be quite revealing, and we hope to continue this study in the near future.

CHAPTER 5: TOWARDS MULTI-REFERENCE EQUIVALENTS OF THE G2 AND G3 METHODS

Taken from a paper that has been published in the *Journal of Chemical Physics*.

Reprinted with permission from the *Journal of Chemical Physics* 115(19),

November 15, 2001, pp 8758-8772.

Copyright 2000 American Institute of Physics

Theis I. Sølling, David M. Smith and Leo Radom
Mark A. Freitag and Mark S. Gordon

Abstract

The effect of replacing the standard single-determinant reference wave functions in variants of G2 and G3 theory by multi-reference (MR) wave functions based on a full-valence complete active space has been investigated. Twelve methods of this type have been introduced and comparisons, based on a slightly reduced G2-1 test set, are made both internally and with the equivalent single-reference methods. We use CASPT2 as the standard MR-MP2 method and MRCI+Q as the higher correlation procedure in these calculations. We find that MR-G2(MP2,SVP), MR-G2(MP2) and MR-G3(MP2) perform comparably with their single-reference analogs, G2(MP2,SVP), G2(MP2) and G3(MP2), with mean absolute deviations (MADs) from the experimental data of 1.41, 1.54 and 1.23 kcal mol⁻¹, compared with 1.60, 1.59 and 1.19 kcal mol⁻¹, respectively. The additivity assumptions in the MR-G_n methods have been tested by carrying out MR-G2/MRCI+Q and MR-G3/MRCI+Q calculations, which correspond to large-basis-set MRCI+Q + ZPVE + HLC calculations. These give MADs of 1.84 and 1.58 kcal mol⁻¹, respectively, i.e. the agreement with experiment is somewhat worse than that obtained with the MR-G2(MP2) and MR-G3(MP2) methods. In a third series of calculations, we have examined pure MP2 and MR-MP2 analogs of the G2 and G3 procedures by carrying out large-basis-set MP2 and CASPT2 (+ ZPVE + HLC) calculations. The resultant methods, which we denote G2/MP2, G3/MP2, MR-G2/MP2 and MR-G3/MP2, give MADs of 4.19, 3.36, 2.01 and 1.66 kcal mol⁻¹, respectively. Finally, we have examined the effect of using MCQDPT2 in place of CASPT2 in five of our MR-G_n procedures, and find that there is a small but

consistent deterioration in performance. Our calculations suggest that the MR-G3(MP2) and MR-G3/MP2 procedures may be useful in situations where a multi-reference approach is desirable.

I. Introduction

The prediction of thermodynamic properties, such as atomization energies, ionization energies, electron affinities and heats of formation, to "chemical accuracy" has long been a goal of quantum chemists, and there has been great progress in this direction in recent years.⁶⁰ Methods that have been developed in an attempt to achieve this goal, include the Gaussian series (G_n , $n = 1, 2$ or 3) of model chemistries developed by Curtiss, Raghavachari, Pople and co-workers,^{61,62,63} the complete-basis-set (CBS) methods of Petersson and co-workers,⁶⁴ the BAC-MPX ($X = 2$ or 4) methods due to Melius and co-workers,⁶⁵ the W1, W2 and related methods of Martin,⁶⁶ and the extrapolation procedures due to Dunning, Feller, Dixon, Peterson and co-workers.⁶⁷ The G2 and G3 methods and their variants,^{62,63} in particular, have become very popular among both theoreticians and experimentalists, because of their ability to predict accurate thermodynamics for a wide variety of chemical compounds.

One potential drawback of the G_n approaches is that they are based on the presumption that the chemical species of interest can be well described by a single configuration, i.e. it can be well represented by a single Lewis structure. There are, however, many systems for which this assumption may not be appropriate.⁶⁸ Important examples include transition structures for many chemical reactions, regions of potential energy surfaces in which bonds are dissociating or forming near conical intersections, as well as the vast majority of electronic excited states.⁶⁸ In addition, first-row transition metal complexes and unsaturated compounds that contain transition metals are also often not well described by a single-determinant wavefunction. For such species with pronounced multi-reference character, the G_n methods may not provide accurate thermodynamic quantities.⁶⁸

The aim of the various G_n models is generally to estimate energies at a high correlation level, typically quadratic configuration interaction (QCISD(T)),⁶⁹ with a large basis set. This is achieved by starting with a modest-basis-set QCISD(T)

calculation and estimating the effect of moving to a larger basis set at the MP2 and/or MP4 levels, i.e. assuming the additivity of basis set and correlation effects. In addition, a zero-point vibrational energy correction is incorporated, as well as a "higher level correction", which is intended to account for any remaining deficiencies in level of theory and basis set. In a multi-reference (MR) G_n approach, the analog of MP2 would be MR-MP2 while the analog of QCI would ideally be MR-QCI. Unfortunately, codes for carrying out MR-QCI (or related coupled cluster (MR-CC)) calculations are not widely available at the present time. We have selected multi-reference configuration interaction with single and double substitutions (MR-CISD) as the best current alternative.

In the following, we present multi-reference analogs of both the G2 and G3 methods using reduced Møller-Plesset orders, based on the MR-MP2 and MR-CI levels of theory and the same basis sets that have been used in the original G2 and G3 methods. Since the multi-reference methods (outlined in Section II) are largely untested with respect to their ability to reliably predict accurate thermodynamic quantities in the manner of the G_n methods, Section III contains a detailed assessment of their performance on a slightly modified G2-1 test set. We also examine the performance of pure MP2 and MR-MP2 analogs of G2 and G3 theory. Conclusions that emerge from our study are presented in Section IV.

II. Methods

A. Relationship between the G_n and MR- G_n methods

The simplest version of the G2 method, referred to as G2(MP2,SVP),⁶² is based on the following additivity approximation to estimate the QCISD(T) energy for the extended 6-311+G(3df,2p) basis set:

$$\begin{aligned} E[QCISD(T)/6-311+G(3df,2p)] \approx & E[QCISD(T)/6-31G(d)] + \\ & E[MP2/6-311+G(3df,2p)] - E[MP2/6-31G(d)] \quad (5.1) \end{aligned}$$

The G2(MP2,SVP) energy is derived by adding to this, firstly a zero-point

vibrational energy (ZPVE) obtained from scaled (by 0.8929) HF/6-31G(d) vibrational frequencies, and secondly a "higher level correction" (HLC). The HLC is an empirical correction which is determined by minimizing the mean absolute deviation (MAD) between experiment and theory for the thermochemical quantities in a test set of molecules (see below).

The multi-reference versions of the G_n schemes are based on the same premise as the single-reference version, namely that the effects of improvements in the basis set and treatment of electron correlation are additive. In our initial set of MR- G_n procedures, we retain the same geometries (MP2(full)/6-31G(*d*)) and ZPVEs (scaled HF/6-31G(*d*)) as in the G_n methods and these are thus taken from the G2 data base.⁷⁰ This makes it easier to identify inherent MR- G_n differences. The current single-configuration levels of theory are replaced by multi-reference analogs as follows:

$$\text{SCF} \Rightarrow \text{MCSCF} \quad (5.2)$$

$$\text{MP2} \Rightarrow \text{MR-MP2} \quad (5.3)$$

$$\text{QCISD(T)} \Rightarrow \text{MR-CISD} \quad (5.4)$$

MCSCF refers to multi-configuration (MC) self-consistent-field (SCF) calculations based on the CASSCF⁷¹ or FORS⁷² prescription. We include all valence electrons and valence orbitals in the "active space". For example, the active spaces for methane, ammonia and water are [8,8], [8,7], and [8,6], respectively, where the first number is the number of active electrons and the second number refers to the number of active orbitals. By choosing a full-valence CASSCF approach, we obtain a procedure that is well-defined for any species, but the downside is that the cost rises very rapidly with molecular size. Our standard MR-MP2 multi-reference second-order perturbation theory method is the CASPT2 procedure developed by Roos and co-workers.^{73,74} We also examine results obtained with the multi-configuration quasi-degenerate second-order perturbation theory method, MCQDPT2, developed by Nakano.⁷⁵ We note that analytic gradients for MCQDPT2 have been derived, also by Nakano,⁷⁶ and are currently being implemented into the electronic structure code GAMESS.⁷⁷ This may be important in more refined versions of MR- G_n in which the

geometries are re-optimized at MR-MP2 (rather than simply using the MP2 geometries of G_n theory).

The remaining step in the MR- G_n model requires a multi-reference energy calculation at a level of theory that is comparable to QCISD(T). The obvious choice would be MR-QCISD(T). While several groups have worked on multi-reference coupled cluster methods,⁷⁸ there are no efficient, general MR-CCSD(T) codes available at the present time. So, while in the long term it is desirable to use MR-QCISD(T) or MR-CCSD(T) for this step of the method, in the short term we will use the internally-contracted MR-CISD (of Werner and Knowles)⁷⁹ with the Davidson cluster correction (Q). We will refer to this method as MRCI+Q throughout the present work.

In this manner, we have constructed the MR-G2-type and MR-G3-type methods defined by Eqs. (5.5), (5.6) and (5.7):

$$\begin{aligned} E[\text{MR-G2(MP2,SVP)}] &= E[\text{MRCI+Q/6-31G}(d)] \\ &+ (E[\text{CASPT2/6-311+G}(3df,2p)] - E[\text{CASPT2/6-31G}(d)]) \\ &+ \text{ZPVE} + \text{HLC} \end{aligned} \quad (5.5)$$

$$\begin{aligned} E[\text{MR-G2(MP2)}] &= E[\text{MRCI+Q/6-311G}(d,p)] \\ &+ (E[\text{CASPT2/6-311+G}(3df,2p)] - E[\text{CASPT2/6-311G}(d,p)]) \\ &+ \text{ZPVE} + \text{HLC} \end{aligned} \quad (5.6)$$

$$\begin{aligned} E[\text{MR-G3(MP2)}] &= E[\text{MRCI+Q/6-31G}(d)] \\ &+ (E[\text{CASPT2/G3MP2large}] - E[\text{CASPT2/6-31G}(d)]) \\ &+ \Delta E(\text{SO}) + \text{ZPVE} + \text{HLC} \end{aligned} \quad (5.7)$$

The spin-orbit correction ($\Delta E(\text{SO})$) used in our MR-G3(MP2) calculations (Eq. (5.7)) is the same as that used in G3 theory.⁶³

In order to investigate the additivity assumptions in Eqs. (5.5)-(5.7), we have also constructed the multi-reference equivalents of the G2/QCI method^{62,80} and its G3 analog⁸¹ [Eqs. (5.8) and (5.9)]:

$$E[MR\text{-}G2/MRCI+Q] = E[MRCI+Q/6-311+G(3df,2p)] + ZPVE + HLC \quad (5.8)$$

$$E[MR\text{-}G3/MRCI+Q] = E[MRCI+Q/G3MP2large] + \Delta E(SO) + ZPVE + HLC \quad (5.9)$$

In a third set of calculations, we have investigated the performance of pure MP2 and MR-MP2 analogs of G2- and G3-type procedures, denoting such methods as G2/MP2, G3/MP2, MR-G2/MP2 and MR-G3/MP2.⁸¹ For example, the multi-reference versions correspond to large-basis-set CASPT2 calculations:

$$E[MR\text{-}G2/MP2] = E[CASPT2/6-311+G(3df,2p)] + ZPVE + HLC \quad (5.10)$$

and

$$E[MR\text{-}G3/MP2] = E[CASPT2/G3MP2large] + \Delta E(SO) + ZPVE + HLC \quad (5.11)$$

The single-reference analogs are obtained as:

$$E[G2/MP2] = E[MP2/6-311+G(3df,2p)] + ZPVE + HLC \quad (5.12)$$

and

$$E[G3/MP2] = E[MP2/G3MP2large] + \Delta E(SO) + ZPVE + HLC \quad (5.13)$$

Finally, we have examined for five of the methods, the effect of using MCQDPT2 in place of CASPT2. For example, MR(QD)-G2(MP2,SVP) is defined by:

$$E[MR(QD)\text{-}G2(MP2,SVP)] = E[MRCI+Q/6-31G(d)] + (E[MCQDPT2/6-311+G(3df,2p)] - E[MCQDPT2/6-31G(d)]) + ZPVE + HLC \quad (5.5a)$$

Similar definitions apply to MCQDPT2 analogs of MR-G2(MP2), MR-G3(MP2), MR-G2/MP2 and MR-G3/MP2.

Unless otherwise noted, all energy calculations were carried out using MOLPRO 96⁸² and MOLPRO 98.⁸² MOLPRO is currently the most efficient code available for such calculations. The MCQDPT2 calculations were performed with GAMESS.⁷⁷ The total energies for all the systems investigated in the present study, as well as the MCQDPT2 tables of relative energies, are available in Appendix F.

B. The higher level correction

The G2 and G3 methods involve different forms of higher level corrections. The derivation of the parameters involved in the G2 and G3 methods are therefore discussed separately below. The justification and possible problems associated with the use of the higher level correction have previously been discussed by Pople et al.⁶¹

A slightly reduced version of the G2-1 test set⁶² was used to obtain the higher-level-correction parameters and to assess the performance of the various methods. The reduced set includes 123 of the 125 energy comparisons of the standard G2-1 set. The heats of formation of ethane and disilane were omitted because the [14,14] full-valence active space in these two cases makes the MR-CI calculations computationally too demanding.

The G2 higher level correction has the form shown in Eq. (5.14), where n_α and n_β are the number of α and β valence electrons, respectively:

$$\text{HLC} = -An_\beta - Bn_\alpha \quad (5.14)$$

We have used this form in all the G2-type methods examined in the present study. The B parameter is constrained to be 0.19 mHartrees in all cases so as to give the correct energy for the hydrogen atom, while the A parameter is chosen to give the smallest mean absolute deviation from experiment for the 123 energy comparisons in our slightly reduced G2-1 test set. We have employed the same minimization procedure as Curtiss,⁸³ and we are able to reproduce the higher level correction and the mean absolute deviation reported by Curtiss et al. for the

G2(MP2) method from the raw electronic energies.⁶² The optimized *A* parameters for the various G2-type methods are listed in Table (5.1).

In the G3 method, there are separately optimized higher-level-correction terms for molecules and atoms. They have the form shown in Eq. (5.15) (molecules) and Eq. (5.16) (atoms):

$$\text{HLC} = -An_{\beta} - B(n_{\alpha} - n_{\beta}) \quad (5.15)$$

$$\text{HLC} = -Cn_{\beta} - D(n_{\alpha} - n_{\beta}) \quad (5.16)$$

We have used the same form of the HLC for all the G3-type methods examined here. The *A*, *B*, *C* and *D* parameters are all obtained by minimization of the mean absolute deviation between experiment and theory for the 123 thermochemical quantities in the reduced G2-1 test set. Again, we have employed the same minimization procedure as Curtiss.⁸³ The optimized parameters for the six G3-type methods are listed in Table (5.2). Starting from the raw electronic energies of the 299 energies in the entire G2/97 test set, our procedure reproduces (for both G3(MP2) and G3) the higher-level-correction parameters and the mean absolute deviations reported by Curtiss et al.⁶³

III. Results and Discussion

Having optimized the higher-level-correction parameters for 12 different MR-*Gn* procedures (as well as two related single-reference *Gn* procedures), we are now in a position to assess their performance. Thermochemical properties that are examined include heats of formation (ΔH_f^0), ionization energies (IE), electron affinities (EA) and proton affinities (PA).

A. MR-G2(MP2,SVP), MR-G2(MP2) and MR-G3(MP2)

Relative energies calculated at the MR-G2(MP2,SVP), MR-G2(MP2) and MR-G3(MP2) levels are presented in Tables (5.3-5), while a statistical analysis, including

a comparison with corresponding single-reference (SR) methods, is shown in Tables (5.6) and (5.7).

Examination of Table (5.6) shows that, in comparison with the corresponding single-reference methods, results for the three MR procedures are all slightly worse for heats of formation, significantly better for ionization energies and electron affinities, and significantly worse for proton affinities. The overall mean absolute deviations (MADs) are quite similar for MR-G2(MP2) compared with G2(MP2) and for MR-G3(MP2) compared with G3(MP2). However, MR-G2(MP2,SVP) produces better overall results than G2(MP2,SVP).

Of the 123 energy comparisons, there are 10 cases of deviations of ≥ 3 kcal mol⁻¹ for MR-G2(MP2,SVP), 15 cases for MR-G2(MP2), and 11 cases for MR-G3(MP2). Of these, eight are common to all three methods: the heats of formation of Li₂, Na₂ and SO₂, the ionization energies of Be, Na and S, the electron affinity of CH₃ and the proton affinity of H₂O. In comparison, there are 21 cases of deviations of ≥ 3 kcal mol⁻¹ for G2(MP2,SVP), 12 cases for G2(MP2), and 10 cases for G3(MP2). Six of the eight deviant cases with the MR-G_n methods are also poor with G3(MP2): the heats of formation of Li₂, Na₂ and SO₂, and the ionization energies of Be, Na and S. The poor results obtained for SO₂ in G2-type calculations have been shown previously by Martin⁸⁴ to be the result of inadequate basis sets.

Notably poorer performance by the MR procedures (compared with SR) is observed for the electron affinity of CH₃, and for the proton affinities of NH₃ and H₂O. The electron affinity of CH₃ is calculated to be negative by all the MR procedures, in contrast to the SR methods that all correctly predict a positive electron affinity. Likewise, the proton affinities of NH₃ and H₂O are consistently poorly predicted by the MR procedures. In fact, because the errors for NH₃ and H₂O are of opposite sign, the error in the proton-transfer reaction between H₃O⁺ and NH₃ is a substantial 7.2-7.5 kcal mol⁻¹. In contrast, the corresponding SR procedures predict this proton-transfer energy with an accuracy of 1.9-2.2 kcal mol⁻¹.

MR-G3(MP2) performs best of the MR methods examined in this study. It gives results comparable to those of G3(MP2) for heats of formation, ionization energies and electron affinities, but much poorer results for proton affinities. There are significant improvements for a small number of cases for which G3(MP2) gives

larger errors: the heat of formation of CS, the ionization energy of O₂, and the electron affinities of C, O and NH.

B. MR-G2/MRCI+Q and MR-G3/MRCI+Q

The MR-G2(MP2,SVP), MR-G2(MP2) and MR-G3(MP2) procedures aim to approximate the results of MRCI+Q/6-311+G(3df,2p) or MRCI+Q/G3MP2large calculations (together with HLC and ZPVE corrections) by assuming the additivity of correlation and basis set effects. It is of interest to examine the reliability of such additivity approximations by carrying out the large-basis-set MRCI+Q calculations explicitly. This gives rise to the MR-G2/MRCI+Q and MR-G3/MRCI+Q procedures, defined by Eqs. (5.8) and (5.9), which are analogous to the G2/QCI procedure examined previously.⁶² Relative energies at the MR-G2/MRCI+Q and MR-G3/MRCI+Q levels are presented in Tables (5.8) and (5.9), with statistical summaries included in Tables (5.6) and (5.7).

Quite unexpectedly, MR-G2/MRCI+Q and MR-G3/MRCI+Q show larger overall deviations from experiment than MR-G2(MP2) and MR-G3(MP2), respectively. This means that the additivity approximations in Eqs. (5.6) and (5.7) are actually helpful in improving the results (which become worse if the additivity is removed), which must surely be a fortuitous situation. There are now 23 (MR-G2/MRCI+Q) and 15 (MR-G3/MRCI+Q) cases for which the deviations from experiment exceed 3 kcal mol⁻¹. The MR-G_n/MRCI+Q procedures perform significantly worse than the corresponding standard MR-G_n methods for heats of formation and electron affinities, slightly worse for proton affinities and comparably for ionization energies.

Significantly larger errors (compared with standard MR-G_n) are observed for both MR-G2/MRCI+Q and MR-G3/MRCI+Q for the heats of formation of SiH₂(¹A₁), SiH₄ and SO₂. In addition, MR-G2/MRCI+Q shows large errors for the heats of formation of S₂, Cl₂, SO and ClO, while MR-G3/MRCI+Q performs poorly for NaCl. Both MR-G2/MRCI+Q and MR-G3/MRCI+Q significantly underestimate electron affinities, with a noticeable deterioration in the predictions for O, F, OH, O₂, NO and PO. The proton affinities of NH₃ and H₂O continue to be poorly predicted.

C. G2/MP2 and G3/MP2

The G2/QCI procedure⁶² obtains relative energies on the basis of QCISD(T)/6-311+G(3df,2p) calculations together with ZPVE and HLC corrections. It is of interest to see how the corresponding MP2 calculations fare. With this in mind, we have analysed results corresponding to MP2/6-311+G(3df,2p) + ZPVE + HLC and MP2/G3MP2large + ZPVE + HLC. These procedures are designated G2/MP2 and G3/MP2, respectively, and are defined by Eqs. (5.12) and (5.13). Calculated relative energies are presented in Tables (5.10) and (5.11), with statistical summaries again included in Tables (5.6) and (5.7).

It is immediately clear from Tables (5.6) and (5.7) that G2/MP2 and G3/MP2 are not particularly useful levels of theory from the viewpoint of thermochemical reliability. The mean absolute deviations are 4.19 and 3.36 kcal mol⁻¹, with 69 and 53, respectively, out of the 123 energy comparisons showing deviations exceeding 3 kcal mol⁻¹. The only area where the errors are modest is for proton affinities. The G2/MP2 and G3/MP2 methods are not recommended for general use.

D. MR-G2/MP2 and MR-G3/MP2

The multi-reference analogs of G2/MP2 and G3/MP2 use large-basis-set MR-MP2 (specifically CASPT2) calculations together with ZPVE and HLC corrections. They are designated MR-G2/MP2 and MR-G3/MP2 and are defined by Eqs. (5.10) and (5.11), respectively. Results are presented in Tables (5.12) and (5.13).

Examination of the statistical summaries in Tables (5.6) and (5.7) shows a number of interesting points. In the first place, MR-G2/MP2 and MR-G3/MP2 perform significantly better than G2/MP2 and G3/MP2, with MADs of 2.01 and 1.66 kcal mol⁻¹ compared with 4.19 and 3.36 kcal mol⁻¹. They are only slightly worse than MR-G2/MRCI+Q and MR-G3/MRCI+Q (MADs of 1.84 and 1.58 kcal mol⁻¹, respectively). However, they do not perform as well as the standard MR-G_n procedures. For example, the MADs are larger than with MR-G_n(MP2) for virtually all the thermochemical properties in Table (5.6).

There are 31 (MR-G2/MP2) and 23 (MR-G3/MP2) out of 123 energy comparisons for which the error exceeds 3 kcal mol⁻¹. Large errors occur for most of the systems that were noted in connection with the standard MR-Gn procedures. However, there are additional cases for which there are noticeable errors. In the case of heats of formation, CO₂, SiO, NH₃ and O₂ now show significant errors, and the error for SO₂ has moved from large negative to small positive. The MR-Gn/MP2 ionization energies are significantly worse than corresponding MR-Gn(MP2) values, and significant errors now occur at both MR-Gn/MP2 levels for the additional systems B, NH₃ and O₂. In the case of electron affinities, there are very large deviations for CH₃ (+6.4 and +5.9 kcal mol⁻¹, respectively), and F, PO and Cl₂ also have large errors. The errors in the H₃O⁺/NH₃ proton-transfer energy are now 9.0-9.2 kcal mol⁻¹. Despite these shortcomings, the MR-G3/MP2 procedure may prove useful in situations for which single-reference methods are inadequate, especially since the use of large active spaces is more limiting for MR-CI than for MR-MP2 methods.

E. MCQDPT2 vs CASPT2

Our default MR-MP2 method is the CASPT2 procedure of the MOLPRO suite of programs.^{74,82} However, it is of interest to see how the alternative MCQDPT2 procedure that is available in the GAMESS program⁷⁷ compares. Results analogous to those of Tables (5.3), (5.4), (5.5), (5.12) and (5.13) are available in Appendix F. Statistical summaries are included in Table (5.6).

The general observation is that the CASPT2-based results and MCQDPT2-based results are normally very similar. With MR-G2(MP2,SVP), there are nine cases where the difference lies between 1 and 3 kcal mol⁻¹ and just one case (NaCl) where the difference is greater than 3 kcal mol⁻¹. With MR-G2(MP2), there are eight cases where the difference lies between 1 and 3 kcal mol⁻¹, two cases (NaCl and CH₃SH) where the difference lies between 3 and 5 kcal mol⁻¹, and one case (Cl₂) where the difference exceeds 5 kcal mol⁻¹. For MR-G3(MP2), there are five cases where the difference lies between 1 and 3 kcal mol⁻¹ and one case (NaCl) where the difference exceeds 3 kcal mol⁻¹. The differences are larger with MR-G2/MP2 and

MR-G3/MP2, with 33 and 30 cases, respectively, of differences lying between 1 and 3 kcal mol⁻¹, and two and three cases, respectively, of differences exceeding 3 kcal mol⁻¹.

Although the differences between the results of the CASPT2-based methods and MCQDPT2-based methods are relatively small, it may be seen from Table (5.6) that the CASPT2-based methods virtually always perform slightly better statistically.

F. Timing comparisons and additional comments

Because the choice of method in quantum chemistry studies often involves a compromise between accuracy and computational expense, it is important to examine the relative timings of the various MR-*Gn* procedures introduced in the present article and to make comparisons with corresponding standard single-reference *Gn* methods. It should be emphasized that the timings depend on many factors and so the present data are intended largely to enable qualitative conclusions to be drawn.

We can see from Table (5.14) that for active spaces of up to about 8 orbitals, all methods are very cheap. For 10 and 12 active orbitals, the times increase rapidly for the MR-*Gn* procedures that involve MR-CI calculations, while for 14 and 16 active orbitals, such procedures are starting to become intractable. Elimination of the MR-CI component, as in the MR-G2/MP2 and MR-G3/MP2 methods, leads to a substantial reduction in CPU time. The cost of the standard (SR) *Gn* methods goes up much more slowly than the MR methods. We should emphasize that in this initial implementation of MR-*Gn* procedures, we uniformly use a full-valence active space and this leads to the very rapid increase in computational cost with size of molecule. Clearly this will be modified in implementations that use smaller active spaces.

The relative costs of the MR methods for the larger active spaces follow the pattern:⁸⁵

$$\text{MR-G2/MP2} \sim \text{MR-G3/MP2} \ll \text{MR-G2(MP2,SVP)} \sim \text{MR-G3(MP2)}$$

$$< \text{MR-G2/MRCI+Q} \sim \text{MR-G3/MRCI+Q} \quad (5.17)$$

There is a large increase in CPU time in going from MR-G3/MP2 to MR-G3(MP2) but a much smaller further increase in going to MR-G3/MRCI+Q.

The single-reference methods show the same pattern:

$$\text{G2/MP2} \sim \text{G3/MP2} \ll \text{G2(MP2,SVP)} \sim \text{G3(MP2)} < \text{G2/QCI} \sim \text{G3/QCI} \quad (5.18)$$

The MR-G2/MRCI+Q and MR-G3/MRCI+Q procedures are the most demanding of the methods investigated in the present work in terms of both memory and CPU usage. However, our results show that these two methods are by no means the most accurate. This is not an overly comforting situation, since the aim of the other methods that we have examined is to approximate their large-basis-set MRCI+Q counterparts by means of additivity. It turns out that the MR-G2 and MR-G3 schemes that we have devised do not succeed very well in mimicking the MR-Gn/MRCI+Q results. This state of affairs fortuitously results in cheaper methods (MR-G2(MP2,SVP) and MR-G3(MP2)) that are more accurate than their more expensive counterparts (MR-G2/MRCI+Q and MR-G3/MRCI+Q).

The two MR methods for which the correlation correction is based on the 6-31G(d) split-valence basis set (MR-G2(MP2,SVP) and MR-G3(MP2)) give the most accurate results. Table (5.15) lists the ten worst predictions of the G3(MP2) method together with the corresponding MR-G3(MP2) values and vice versa. It can be seen that five out of the ten cases are common to the two lists, and that both methods give poor predictions in most of the remaining ten cases as well. Individual results have been discussed in previous sections.

Overall, the agreement between theory and experiment is best in the case of the MR-G3(MP2) method, and since this is also one of the more efficient methods in terms of resources, we recommend the use of MR-G3(MP2) for future studies of systems with significant multi-reference character. MR-G3/MP2 does not perform as well as MR-G3(MP2) but is significantly less expensive. It may be useful in

situations that would benefit from a MR treatment but for which the MR-CI calculations are not tractable.

IV. Conclusions

We have introduced twelve multi-reference equivalents of the G2 and G3 methods using reduced Møller-Plesset orders and assessed their performance on a slightly reduced G2-1 test set. Whereas single-reference G_n -type procedures aim to approximate large-basis-set QCISD(T) calculations through additivity approximations, the MR- G_n methods aim to approximate large-basis-set MRCI+Q results.

We find that models based on explicit large-basis-set MRCI+Q calculations (together with ZPVE and higher level corrections) do not perform particularly well. In addition, our results indicate that the G_n -type additivity approximations hold less well for the MR- G_n methods than they do for the parent single-reference G_n methods. This leads to the somewhat fortuitous situation in which incorporation of additivity approximations in the MR- G_n procedures results in an accuracy which is better than that of MR- G_n /MRCI+Q and is generally comparable to that of the corresponding single-reference methods.

MR-G3(MP2) is the most accurate of the MR- G_n methods that we have examined and it is also one of the least computationally demanding. The mean absolute deviation between calculated and experimental values for the test set of (123) energies is 1.22 kcal mol⁻¹, compared with 1.19 kcal mol⁻¹ for standard G3(MP2). MR-G3(MP2) performs comparably to G3(MP2) for heats of formation, ionization energies and electron affinities but significantly worse for proton affinities.

The present test set involves systems for which a single-reference treatment is reasonably adequate. It is encouraging that MR-G3(MP2) performs comparably to G3(MP2) for such systems. However, the main purpose of the present study was to develop procedures that could handle systems for which a single-reference treatment is *not* adequate. It is likely that the performance of MR-G3(MP2) will

improve relative to G3(MP2) for situations of this type. Studies of such systems are in progress.

The MR-G3/MP2 procedure (MAD = 1.66 kcal mol⁻¹), which corresponds to a large-basis set CASPT2 + ZPVE + HLC treatment, does not perform as well as MR-G3(MP2) but it is computationally much less expensive because it does not require an MR-CI calculation. It may prove useful in circumstances where a multi-reference treatment is desirable but the MR-CI calculation is not affordable.

V. Acknowledgements

We thank Professor Larry Curtiss for many helpful discussions, including advice regarding the derivation of the higher level correction. A generous allocation of time on the Fujitsu VPP300 and SGI Power Challenge computers of the Australian National University Supercomputing Facility is gratefully acknowledged. We would also like to thank the National Science Foundation International Division for providing travel funds (MSG and MAF) and the National Science Foundation Chemistry Division for supporting the research.

Table (5.1) Higher-level-correction
parameters (in mHartrees) for the MR-G2-
and G2-type methods.

Method	<i>A</i>
MR-G2(MP2.SVP)	8.250
MR(QD)-G2(MP2.SVP)	8.731
MR-G2(MP2)	7.542
MR(QD)-G2(MP2)	7.820
MR-G2/MRCI+Q	6.469
MR-G2/MP2	8.802
MR(QD)-G2/MP2	9.437
G2/MP2	4.246

Table (5.2) Higher-level-correction parameters (in mHartrees) for the MR-G3- and G3-type methods.

Method	<i>A</i>	<i>B</i>	<i>C</i>	<i>D</i>
MR-G3(MP2)	11.086	2.493	10.368	1.713
MR(QD)-G3(MP2)	11.575	2.705	10.697	1.822
MR-G3/MRCI+Q	11.158	3.605	9.564	2.912
MR-G3/MP2	12.900	1.799	13.099	1.915
MR(QD)-G3/MP2	13.135	1.819	13.177	1.749
G3/MP2	7.579	4.157	9.970	0.573

Table (5.3) MR-G2(MP2,SVP) heats of formation, ionization energies, electron affinities and proton affinities. Values in parentheses are the differences between experimental and MR-G2(MP2,SVP) values.^a

	Species	Species	Species	
Heats of formation	LiH	30.3 (+ 3.0)	PH ₃	3.1 (- 1.8)
	BeH	84.2 (- 2.5)	H ₂ S	- 5.2 (+ 0.3)
	CH	141.6 (+ 0.9)	HCl	- 23.2 (+ 1.1)
	CH ₂ ³ B ₁	94.9 (- 1.2)	Li ₂	47.4 (+ 4.2)
	CH ₂ ¹ A ₁	100.8 (+ 2.0)	LiF	- 80.5 (+ 0.4)
	CH ₃	34.5 (+ 0.5)	C ₂ H ₂	54.4 (- 0.2)
	CH ₄	- 20.0 (+ 2.1)	C ₂ H ₄	15.2 (- 2.7)
	NH	85.9 (- 0.7)	CN	106.8 (- 1.9)
	NH ₂	44.7 (+ 0.4)	HCN	31.6 (- 0.1)
	NH ₃	- 9.1 (- 1.9)	CO	- 28.5 (+ 2.1)
	OH	8.7 (+ 0.7)	HCO	9.5 (+ 0.5)
	H ₂ O	- 57.7 (- 0.1)	HCHO	- 26.4 (+ 0.4)
	HF	- 65.6 (+ 0.5)	CH ₃ OH	- 48.4 (+ 0.4)
	SiH ₂ ¹ A ₁	62.9 (+ 2.3)	N ₂	- 0.2 (+ 0.2)
	SiH ₂ ³ B ₁	87.2 (- 1.0)	N ₂ H ₄	23.8 (- 1.0)
	SiH ₃	48.2 (- 0.3)	NO	20.6 (+ 1.0)
	SiH ₄	7.5 (+ 0.7)	O ₂	1.2 (- 1.2)
	PH ₂	33.5 (- 0.4)	H ₂ O ₂	- 32.5 (+ 0.0)
Ionization energies	Li	123.4 (+ 0.9)	Cl	296.2 (+ 2.9)
	Be	219.3 (- 4.4)	CH ₄	293.0 (- 2.0)
	B	189.2 (+ 2.2)	NH ₃	233.0 (+ 1.8)
	C	257.8 (+ 1.9)	OH	300.1 (- 0.1)
	N	334.1 (+ 1.2)	OH ₂	291.2 (- 0.2)
	O	313.0 (+ 0.8)	HF	371.1 (- 1.2)
	F	402.4 (- 0.7)	SiH ₄	253.5 (+ 0.2)
	Na	114.1 (+ 4.4)	PH	233.0 (+ 1.1)
	Mg	178.7 (- 2.4)	PH ₂	224.8 (+ 1.6)
	Al	137.2 (+ 0.8)	PH ₃	228.4 (- 0.8)
	Si	186.9 (+ 1.0)	SH	237.7 (+ 1.4)
	P	241.4 (+ 0.5)	H ₂ S ² B ₁	240.4 (+ 1.0)
	S	234.4 (+ 4.5)	H ₂ S ² A ₁	294.0 (+ 0.7)
Electron affinities	C	31.6 (- 2.5)	CH ₃	- 1.7 (+ 3.5)
	O	33.6 (+ 0.1)	NH	7.9 (+ 0.9)
	F	81.0 (- 2.6)	NH ₂	17.5 (+ 0.3)
	Si	32.2 (- 0.3)	OH	42.9 (- 0.7)
	P	14.2 (+ 3.0)	SiH	27.7 (+ 1.7)
	S	46.3 (+ 1.6)	SiH ₂	23.2 (+ 2.7)
	Cl	83.9 (- 0.5)	SiH ₃	33.6 (- 1.1)
	CH	27.4 (+ 1.2)	PH	22.0 (+ 1.8)
	CH ₂	16.0 (- 1.0)	PH ₂	28.7 (+ 0.6)
Proton affinities	NH ₃	205.4 (- 2.9)	SiH ₄	153.5 (+ 0.5)
	H ₂ O	160.8 (+ 4.3)	PH ₃	185.3 (+ 1.8)
	C ₂ H ₂	153.5 (- 1.2)	H ₂ S	167.6 + 1.2)

^aValues in kcal mol⁻¹. The heats of formation are 298 K values whereas the remaining quantities refer to 0 K.

Table (5.4) MR-G2(MP2) heats of formation, ionization energies, electron affinities and proton affinities. Values in parentheses are the differences between experimental and MR-G2(MP2) values.^a

	Species	Species	Species	
Heats of formation	LiH	30.6 (+ 2.7)	PH ₃	1.3 (+ 0.0)
	BeH	83.0 (- 1.3)	H ₂ S	- 5.9 (+ 1.0)
	CH	141.4 (+ 1.1)	HCl	- 23.5 (+ 1.4)
	CH ₂ ³ B ₁	94.5 (- 0.8)	Li ₂	47.9 (+ 3.7)
	CH ₂ ¹ A ₁	100.0 (+ 2.8)	LiF	- 81.3 (+ 1.2)
	CH ₃	33.8 (+ 1.2)	C ₂ H ₂	55.9 (- 1.7)
	CH ₄	- 20.9 (+ 3.0)	C ₂ H ₄	11.4 (+ 1.1)
	NH	85.7 (- 0.5)	CN	108.4 (- 3.5)
	NH ₂	44.2 (+ 0.9)	HCN	32.9 (- 1.4)
	NH ₃	- 9.8 (- 1.2)	CO	- 27.8 (+ 1.4)
	OH	8.5 (+ 0.9)	HCO	10.2 (- 0.2)
	H ₂ O	- 58.2 (+ 0.4)	HCHO	- 26.3 (+ 0.3)
	HF	- 65.5 (+ 0.4)	CH ₃ OH	- 48.9 (+ 0.9)
	SiH ₂ ¹ A ₁	61.4 (+ 3.8)	N ₂	1.0 (- 1.0)
	SiH ₂ ³ B ₁	85.7 (+ 0.5)	N ₂ H ₄	23.2 (- 0.4)
	SiH ₃	45.8 (+ 2.1)	NO	21.3 (+ 0.3)
	SiH ₄	4.0 (+ 4.2)	O ₂	1.5 (- 1.5)
	PH ₂	32.4 (+ 0.7)	H ₂ O ₂	- 32.6 (+ 0.1)
Ionization energies	Li	123.4 (+ 0.9)	Cl	295.5 (+ 3.6)
	Be	218.9 (- 4.0)	CH ₄	293.4 (- 2.4)
	B	190.2 (+ 1.2)	NH ₃	232.9 (+ 1.9)
	C	258.5 (+ 1.2)	OH	299.5 (+ 0.5)
	N	334.1 (+ 1.2)	H ₂ O	291.0 (+ 0.0)
	O	312.3 (+ 1.5)	HF	370.3 (- 0.4)
	F	401.4 (+ 0.3)	SiH ₄	254.6 (- 0.9)
	Na	114.1 (+ 4.4)	PH	232.9 (+ 1.2)
	Mg	178.2 (- 1.9)	PH ₂	224.6 (+ 1.8)
	Al	137.2 (+ 0.8)	PH ₃	228.3 (- 0.7)
	Si	187.0 (+ 0.9)	SH	237.3 (+ 1.8)
	P	241.2 (+ 0.7)	H ₂ S ² B ₁	240.1 (+ 1.3)
	S	233.8 (+ 5.1)	H ₂ S ² A ₁	294.0 (+ 0.7)
Electron affinities	C	31.6 (- 2.5)	CH ₃	- 1.8 (+ 3.6)
	O	32.6 (+ 1.1)	NH	7.4 (+ 1.4)
	F	79.4 (- 1.0)	NH ₂	17.2 (+ 0.6)
	Si	32.3 (- 0.4)	OH	42.1 (+ 0.1)
	P	13.9 (+ 3.3)	SiH	27.8 (+ 1.6)
	S	45.7 (+ 2.2)	SiH ₂	23.1 (+ 2.8)
	Cl	83.0 (+ 0.4)	SiH ₃	33.4 (- 0.9)
	CH	27.2 (+ 1.4)	PH	21.6 (+ 2.2)
	CH ₂	16.1 (- 1.1)	PH ₂	28.1 (+ 1.2)
Proton affinities	NH ₃	205.6 (- 3.1)	SiH ₄	153.4 (+ 0.6)
	H ₂ O	161.0 (+ 4.1)	PH ₃	186.3 (+ 0.8)
	C ₂ H ₂	153.9 (- 1.6)	H ₂ S	168.4 (+ 0.4)

^aValues in kcal mol⁻¹. The heats of formation are 298 K values whereas the remaining quantities refer to 0 K.

Table (5.5) MR-G3(MP2) heats of formation, ionization energies, electron affinities and proton affinities. Values in parentheses are the differences between experimental and MR-G3(MP2) values.^a

	Species	Species	Species	
Heats of formation	LiH	30.5 (+ 2.8)	PH ₃	3.7 (- 2.4)
	BeH	83.3 (- 1.6)	H ₂ S	- 4.9 (+ 0.0)
	CH	141.2 (+ 1.3)	HCl	- 23.1 (+ 1.0)
	CH ₂ ³ B ₁	93.9 (- 0.2)	Li ₂	47.5 (+ 4.1)
	CH ₂ ¹ A ₁	101.3 (+ 1.5)	LiF	- 80.3 (+ 0.2)
	CH ₃	34.3 (+ 0.7)	C ₂ H ₂	54.7 (- 0.5)
	CH ₄	- 19.3 (+ 1.4)	C ₂ H ₄	15.8 (- 3.3)
	NH	85.0 (+ 0.2)	CN	107.3 (- 2.4)
	NH ₂	44.8 (+ 0.3)	HCN	32.4 (- 0.9)
	NH ₃	- 8.4 (- 2.6)	CO	- 27.2 (+ 0.8)
	OH	8.2 (+ 1.2)	HCO	10.2 (- 0.2)
	H ₂ O	- 57.5 (- 0.3)	HCHO	- 25.3 (- 0.7)
	HF	- 65.6 (+ 0.5)	CH ₃ OH	- 47.3 (- 0.7)
	SiH ₂ ¹ A ₁	63.0 (+ 2.2)	N ₂	0.7 (- 0.7)
	SiH ₂ ³ B ₁	86.0 (+ 0.2)	N ₂ H ₄	25.2 (- 2.4)
	SiH ₃	47.5 (+ 0.4)	NO	21.3 (+ 0.3)
	SiH ₄	7.4 (+ 0.8)	O ₂	0.2 (- 0.2)
	PH ₂	33.2 (- 0.1)	H ₂ O ₂	- 32.6 (+ 0.1)
Ionization energies	Li	124.2 (+ 0.1)	Cl	296.7 (+ 2.4)
	Be	219.6 (- 4.7)	CH ₄	293.2 (- 2.2)
	B	189.9 (+ 1.5)	NH ₃	232.7 (+ 2.1)
	C	258.5 (+ 1.2)	OH	299.6 (+ 0.4)
	N	334.5 (+ 0.8)	H ₂ O	291.0 (+ 0.0)
	O	312.9 (+ 0.9)	HF	370.6 (- 0.7)
	F	401.7 (+ 0.0)	SiH ₄	254.1 (- 0.4)
	Na	115.1 (+ 3.4)	PH	234.8 (- 0.7)
	Mg	178.9 (- 2.6)	PH ₂	226.7 (- 0.3)
	Al	138.5 (- 0.5)	PH ₃	228.9 (- 1.3)
	Si	187.9 (+ 0.0)	SH	238.6 (+ 0.5)
	P	241.8 (+ 0.1)	H ₂ S ³ B ₁	241.2 (+ 0.2)
	S	235.9 (+ 3.0)	H ₂ S ¹ A ₁	294.6 (+ 0.1)
Electron affinities	C	31.2 (- 2.1)	CH ₃	- 2.5 (+ 4.3)
	O	31.8 (+ 1.9)	NH	6.6 (+ 2.2)
	F	78.6 (- 0.2)	NH ₂	16.7 (+ 1.1)
	Si	33.2 (- 1.3)	OH	41.4 (+ 0.8)
	P	15.9 (+ 1.3)	SiH	29.7 (- 0.3)
	S	47.5 (+ 0.4)	SiH ₂	25.2 (+ 0.7)
	Cl	83.7 (- 0.3)	SiH ₃	34.3 (- 1.8)
	CH	27.7 (+ 0.9)	PH	23.3 (+ 0.5)
	CH ₂	15.1 (- 0.1)	PH ₂	29.8 (- 0.5)
Proton affinities	NH ₃	206.0 (- 3.5)	SiH ₄	153.3 (+ 0.7)
	H ₂ O	161.1 (+ 4.0)	PH ₃	184.9 (+ 2.2)
	C ₂ H ₂	153.1 (- 0.8)	H ₂ S	167.0 (+ 1.8)

^aValues in kcal mol⁻¹. The heats of formation are 298 K values whereas the remaining quantities refer to 0 K.

Table (5.6) Comparison of the mean absolute deviations (kcal mol⁻¹) from experimental data for multi- and single-reference G2- and G3-type methods.^a

Test set	ΔH_f	IE	EA	PA	Total
Number of comparisons	53	38	25	7	123
G2(MP2,SVP)	1.36	1.87	2.05	0.81	1.63
MR-G2(MP2,SVP)	1.38	1.38	1.40	1.76	1.41
MR(QD)-G2(MP2,SVP)	1.55	1.42	1.32	1.93	1.48
G2(MP2)	1.33	1.88	1.98	0.64	1.59
MR-G2(MP2)	1.56	1.49	1.55	1.54	1.54
MR(QD)-G2(MP2)	1.76	1.47	1.56	1.43	1.61
G3(MP2)	1.13	1.29	1.23	0.93	1.19
MR-G3(MP2)	1.23	1.13	1.12	1.98	1.22
MR(QD)-G3(MP2)	1.35	1.13	1.13	2.07	1.28
G2/QCI ^b	1.19	1.11	1.22	1.17	1.17
MR-G2/MRCI+Q	1.95	1.35	2.33	1.87	1.84
MR-G3/MRCI+Q	1.67	1.20	1.84	2.07	1.58
G2/MP2	5.61	3.45	2.94	1.81	4.19
MR-G2/MP2	1.69	2.29	2.32	1.70	2.01
MR(QD)-G2/MP2	2.26	2.25	2.53	2.00	2.29
G3/MP2	4.24	2.80	2.74	1.97	3.36
MR-G3/MP2	1.60	1.63	1.77	1.85	1.66
MR(QD)-G3/MP2	2.00	1.77	1.84	2.07	1.90

^a Unless otherwise noted, all data refer to the 123 energy test set. In the case of the standard G_n methods, this involved re-optimization of the HLC parameters for the reduced set, leading to results that differ slightly from published values based on the full G2-1 test set.^{3,4}

^b Data obtained from Ref. 3b and refer to the full 125 energy G2-1 test set.

Table (5.7) Comparison of mean absolute deviations (MAD, kcal mol⁻¹) from experimental data for multi- and single-reference G2- and G3-type methods.^a

Method	MAD	Method	MAD
G2(MP2,SVP)	1.60	MR-G2(MP2,SVP)	1.41
G2(MP2)	1.59	MR-G2(MP2)	1.54
G3(MP2)	1.19	MR-G3(MP2)	1.23
G2/QCI	1.17	MR-G2/MRCI+Q	1.84
G3/QCI	-	MR-G3/MRCI+Q	1.58
G2/MP2	4.19	MR-G2/MP2	2.01
G3/MP2	3.36	MR-G3/MP2	1.66

^a All data refer to the 123 molecule test set. In the case of the standard G_n methods, this involved re-optimization of the HLC parameters for the reduced set, leading to results that differ slightly from published values based on the full G2-1 test set.³⁴

^b Data obtained from Ref. 3b and refer to the full 125 energy G2-1 test set.

Table (5.8) MR-G2/MRCI+Q^a heats of formation, ionization energies, electron affinities and proton affinities. Values in parentheses are the differences between experimental and MR-G2/MRCI+Q values.^b

	Species	Species	Species	
Heats of formation	LiH	31.3 (+ 2.0)	PH ₃	- 1.0 (+ 2.3)
	BeH	83.1 (- 1.4)	H ₂ S	- 6.4 (+ 1.5)
	CH	141.0 (+ 1.5)	HCl	- 23.1 (+ 1.0)
	CH ₂ ³ B ₁	94.3 (- 1.6)	Li ₂	48.5 (+ 3.1)
	CH ₂ ¹ A ₁	99.5 (+ 3.3)	LiF	- 82.5 (+ 2.4)
	CH ₃	33.8 (+ 1.2)	C ₂ H ₂	55.8 (- 1.6)
	CH ₄	- 20.6 (+ 2.7)	C ₂ H ₄	11.6 (+ 0.9)
	NH	85.2 (+ 0.0)	CN	107.4 (- 2.5)
	NH ₂	43.7 (+ 1.4)	HCN	31.7 (- 0.2)
	NH ₃	- 10.0 (- 1.0)	CO	- 27.8 (+ 1.4)
	OH	8.6 (+ 0.8)	HCO	10.3 (- 0.3)
	H ₂ O	- 57.9 (+ 0.1)	HCHO	- 26.9 (+ 0.9)
	HF	- 65.0 (- 0.1)	CH ₃ OH	- 48.0 (+ 0.0)
	SiH ₂ ¹ A ₁	60.7 (+ 4.5)	N ₂	- 0.2 (+ 0.2)
	SiH ₂ ³ B ₁	85.2 (+ 1.0)	N ₂ H ₄	23.0 (- 0.2)
	SiH ₃	45.3 (+ 2.6)	NO	21.2 (+ 0.4)
	SiH ₄	3.8 (+ 4.4)	O ₂	3.0 (- 3.0)
	PH ₂	30.5 (+ 2.6)	H ₂ O ₂	- 31.4 (- 1.1)
Ionization energies	Li	123.4 (+ 0.9)	Cl	296.6 (+ 2.5)
	Be	218.3 (- 3.4)	CH ₄	293.1 (- 2.1)
	B	189.9 (+ 1.5)	NH ₃	232.5 (+ 2.3)
	C	258.2 (+ 1.5)	OH	299.4 (+ 0.6)
	N	333.5 (+ 1.8)	H ₂ O	290.6 (+ 0.4)
	O	312.7 (+ 1.1)	HF	369.5 (+ 0.4)
	F	401.2 (+ 0.5)	SiH ₄	255.0 (- 1.3)
	Na	114.1 (+ 4.4)	PH	232.7 (+ 1.4)
	Mg	177.5 (- 1.5)	PH ₂	224.4 (+ 2.0)
	Al	138.0 (+ 0.0)	PH ₃	228.8 (- 1.2)
	Si	187.0 (+ 0.9)	SH	238.5 (+ 0.6)
	P	240.2 (+ 1.7)	H ₂ S ² B ₁	240.8 (+ 0.6)
	S	236.1 (+ 2.8)	H ₂ S ² A ₁	294.0 (+ 0.7)
Electron affinities	C	27.0 (+ 2.1)	CH ₃	- 2.3 (+ 4.1)
	O	30.6 (+ 3.1)	NH	5.9 (+ 2.9)
	F	75.8 (+ 2.6)	NH ₂	15.8 (+ 2.0)
	Si	30.5 (+ 1.4)	OH	38.9 (+ 3.3)
	P	15.6 (+ 1.6)	SiH	27.1 (+ 2.3)
	S	46.3 (+ 1.6)	SiH ₂	23.0 (+ 2.9)
	Cl	82.7 (+ 0.7)	SiH ₃	34.1 (- 1.6)
	CH	25.5 (+ 3.1)	PH	22.4 (+ 1.4)
	CH ₂	15.5 (- 0.5)	PH ₂	28.7 (+ 0.6)
Proton affinities	NH ₃	205.7 (- 3.2)	SiH ₄	152.7 (+ 1.3)
	H ₂ O	161.1 (+ 4.0)	PH ₃	185.5 (+ 1.6)
	C ₂ H ₂	154.2 (- 1.9)	H ₂ S	167.9 (+ 0.9)

^aCorresponding to MRCI+Q/6-311+G(3df,2p) + ZPVE + HLC.

^bValues in kcal mol⁻¹. The heats of formation are 298 K values whereas the remaining quantities refer to 0 K.

Table (5.9) MR-G3/MRCI+Q^a heats of formation, ionization energies, electron affinities and proton affinities. Values in parentheses are the differences between experimental and MR-G3/MRCI+Q values^b

	Species	Species	Species	
Heats of formation	LiH	31.9 (+ 1.4)	PH ₃	- 0.1 (+ 1.4)
	BeH	81.7 (+ 0.0)	H ₂ S	- 6.6 (+ 1.7)
	CH	140.6 (+ 1.9)	HCl	- 24.3 (+ 2.2)
	CH ₂ ³ B ₁	93.5 (+ 0.2)	Li ₂	49.0 (+ 2.6)
	CH ₂ ¹ A ₁	100.5 (+ 2.3)	LiF	- 83.0 (+ 2.9)
	CH ₃	34.1 (+ 0.9)	C ₂ H ₂	56.1 (- 1.9)
	CH ₄	- 19.2 (+ 1.3)	C ₂ H ₄	12.8 (- 0.3)
	NH	84.4 (+ 0.8)	CN	107.8 (- 2.9)
	NH ₂	44.1 (+ 1.0)	HCN	32.8 (- 1.3)
	NH ₃	- 8.5 (- 2.5)	CO	- 27.2 (+ 0.8)
	OH	7.4 (+ 2.0)	HCO	10.4 (- 0.4)
	H ₂ O	- 57.9 (+ 0.1)	HCHO	- 26.0 (+ 0.0)
	HF	- 66.2 (+ 1.1)	CH ₃ OH	- 46.7 (- 1.3)
	SiH ₂ ¹ A ₁	60.7 (+ 4.5)	N ₂	1.0 (- 1.0)
	SiH ₂ ³ B ₁	83.7 (+ 2.5)	N ₂ H ₄	25.6 (- 2.8)
	SiH ₃	44.5 (+ 3.4)	NO	21.2 (+ 0.4)
	SiH ₄	3.9 (+ 4.3)	O ₂	0.4 (- 0.4)
	PH ₂	30.3 (+ 2.8)	H ₂ O ₂	- 32.4 (- 0.1)
Ionization energies	Li	124.9 (- 0.6)	Cl	297.1 (+ 2.0)
	Be	218.4 (- 3.5)	CH ₄	293.7 (- 2.7)
	B	191.4 (+ 0.0)	NH ₃	232.6 (+ 2.2)
	C	259.7 (+ 0.0)	OH	299.5 (+ 0.5)
	N	334.8 (+ 0.5)	H ₂ O	290.8 (+ 0.2)
	O	312.5 (+ 1.3)	HF	369.4 (+ 0.5)
	F	400.4 (+ 1.3)	SiH ₄	256.1 (- 2.4)
	Na	115.8 (+ 2.7)	PH	235.2 (- 1.1)
	Mg	177.6 (- 1.3)	PH ₂	227.0 (- 0.6)
	Al	139.9 (- 1.9)	PH ₃	229.8 (- 2.2)
	Si	188.6 (- 0.7)	SH	239.9 (- 0.8)
	P	241.3 (+ 0.6)	H ₂ S ² B ₁	242.1 (- 0.7)
	S	237.5 (+ 1.4)	H ₂ S ² A ₁	295.0 (- 0.3)
Electron affinities	C	27.7 (+ 1.4)	CH ₃	- 2.7 (+ 4.5)
	O	28.5 (+ 5.2)	NH	5.1 (+ 3.7)
	F	73.1 (+ 5.3)	NH ₂	15.4 (+ 2.4)
	Si	32.1 (- 0.2)	OH	37.9 (+ 4.3)
	P	17.2 (+ 0.0)	SiH	29.6 (- 0.2)
	S	47.4 (+ 0.5)	SiH ₂	25.7 (+ 0.2)
	Cl	82.2 (+ 1.2)	SiH ₃	35.2 (- 2.7)
	CH	26.7 (+ 1.9)	PH	24.2 (- 0.4)
	CH ₂	15.0 (+ 0.0)	PH ₂	30.3 (- 1.0)
Proton affinities	NH ₃	206.3 (- 3.8)	SiH ₄	152.5 (+ 1.5)
	H ₂ O	161.4 (+ 3.7)	PH ₃	185.2 (+ 1.9)
	C ₂ H ₂	153.7 (- 1.4)	H ₂ S	167.2 (+ 1.6)

^aCorresponding to MRCI+Q/G3MP2large + ZPVE + HLC.

^bValues in kcal mol⁻¹. The heats of formation are 298 K values whereas the remaining quantities refer to 0 K.

Table (5.10) G2/MP2^a heats of formation, ionization energies, electron affinities and proton affinities. Values in parentheses are the differences between experimental and G2/MP2 values.^b

	Species	Species	Species	
Heats of formation	LiH	38.4 (- 5.1)	PH ₃	12.1 (- 10.8)
	BeH	79.1 (+ 2.6)	H ₂ S	- 0.8 (- 4.1)
	CH	146.1 (- 3.6)	HCl	- 22.2 (+ 0.1)
	CH ₂ ³ B ₁	95.5 (- 1.8)	Li ₂	56.5 (- 4.9)
	CH ₂ ¹ A ₁	107.8 (- 5.0)	LiF	- 86.7 (+ 6.6)
	CH ₃	38.4 (- 3.4)	C ₂ H ₂	48.1 (+ 6.1)
	CH ₄	- 13.9 (- 4.0)	C ₂ H ₄	12.5 (+ 0.0)
	NH	89.8 (- 4.6)	CN	114.2 (- 9.3)
	NH ₂	49.3 (- 4.2)	HCN	21.6 (+ 9.9)
	NH ₃	- 7.8 (- 3.2)	CO	- 40.2 (+ 13.8)
	OH	9.6 (- 0.2)	HCO	0.3 (+ 9.7)
	H ₂ O	- 60.4 (+ 2.6)	HCHO	- 34.8 (+ 8.8)
	HF	- 69.5 (+ 4.4)	CH ₃ OH	- 51.6 (+ 3.6)
	SiH ₂ ¹ A ₁	70.3 (- 5.1)	N ₂	- 9.9 (+ 9.9)
	SiH ₂ ³ B ₁	89.2 (- 3.0)	N ₂ H ₄	25.8 (- 3.0)
	SiH ₃	53.7 (- 5.8)	NO	14.3 (+ 7.3)
	SiH ₄	16.2 (- 8.0)	O ₂	- 9.1 (+ 9.1)
	PH ₂	40.5 (- 7.4)	H ₂ O ₂	- 37.6 (+ 5.1)
Ionization Energies	Li	123.2 (+ 1.1)	Cl	295.8 (+ 3.3)
	Be	205.8 (+ 9.1)	CH ₄	291.7 (- 0.7)
	B	190.6 (+ 0.8)	NH ₃	236.7 (- 1.9)
	C	259.6 (+ 0.1)	OH	300.3 (- 0.3)
	N	336.7 (- 1.4)	H ₂ O	295.0 (- 4.0)
	O	309.8 (+ 4.0)	HF	375.3 (- 5.4)
	F	401.7 (+ 0.0)	SiH ₄	251.2 (+ 2.5)
	Na	114.1 (+ 4.4)	PH	233.2 (+ 0.9)
	Mg	169.6 (+ 6.7)	PH ₂	225.1 (+ 1.3)
	Al	134.3 (+ 3.7)	PH ₃	224.5 (+ 3.1)
	Si	185.3 (+ 2.6)	SH	236.6 (+ 2.5)
	P	241.4 (+ 0.5)	H ₂ S ³ B ₁	240.5 (+ 0.9)
	S	232.0 (+ 6.9)	H ₂ S ¹ A ₁	293.7 (+ 1.0)
Electron Affinities	C	28.7 (+ 0.4)	CH ₃	0.8 (+ 1.0)
	O	32.9 (+ 0.8)	NH	6.9 (+ 1.9)
	F	84.3 (- 5.9)	NH ₂	20.9 (- 3.1)
	Si	31.3 (+ 0.6)	OH	47.4 (- 5.2)
	P	11.7 (+ 5.5)	SiH	26.8 (+ 2.6)
	S	45.7 (+ 2.2)	SiH ₂	23.1 (+ 2.8)
	Cl	85.5 (- 2.1)	SiH ₃	29.2 (+ 3.3)
	CH	28.3 (+ 0.3)	PH	20.7 (+ 3.1)
	CH ₂	12.8 (+ 2.2)	PH ₂	28.4 (+ 0.9)
Proton Affinities	NH ₃	201.4 (+ 1.1)	SiH ₄	152.6 (+ 1.4)
	H ₂ O	162.1 (+ 3.0)	PH ₃	186.5 (+ 0.6)
	C ₂ H ₂	151.1 (+ 1.2)	H ₂ S	166.1 (+ 2.7)

^aCorresponding to MP2/6-311+G(3df,2p) + ZPVE + HLC.

^bValues in kcal mol⁻¹. The heats of formation are 298 K values whereas the remaining quantities refer to 0 K.

Table (5.11) G3/MP2^a heats of formation, ionization energies, electron affinities and proton affinities. Values in parentheses are the differences between experimental and G3/MP2 values.^b

	Species	Species	Species	
Heats of Formation	LiH	36.9 (- 3.6)	PH ₃	9.3 (- 8.0)
	BeH	78.4 (+ 3.3)	H ₂ S	- 0.3 (- 4.6)
	CH	144.2 (- 1.7)	HCl	- 18.0 (- 4.1)
	CH ₂ ³ B ₁	91.2 (+ 2.5)	Li ₂	54.9 (- 3.3)
	CH ₂ ¹ A ₁	106.9 (- 4.1)	LiF	- 82.1 (+ 2.0)
	CH ₃	35.0 (+ 0.0)	C ₂ H ₂	47.3 (+ 6.9)
	CH ₄	- 16.4 (- 1.5)	C ₂ H ₄	10.2 (+ 2.3)
	NH	85.6 (- 0.4)	CN	113.5 (- 8.7)
	NH ₂	46.2 (- 1.1)	HCN	21.4 (+ 10.1)
	NH ₃	- 10.1 (- 0.9)	CO	- 36.2 (+ 9.8)
	OH	9.5 (- 0.1)	HCO	1.9 (+ 8.1)
	H ₂ O	- 59.5 (+ 1.7)	HCHO	- 32.6 (+ 6.6)
	HF	- 65.2 (+ 0.1)	CH ₃ OH	- 51.1 (+ 3.1)
	SiH ₂ ¹ A ₁	68.7 (- 3.5)	N ₂	- 10.0 (+ 10.0)
	SiH ₂ ³ B ₁	84.6 (+ 1.6)	N ₂ H ₄	22.8 (+ 0.0)
	SiH ₃	49.6 (- 1.7)	NO	15.8 (+ 5.8)
	SiH ₄	12.7 (- 4.5)	O ₂	- 7.6 (+ 7.6)
	PH ₂	36.9 (- 3.8)	H ₂ O ₂	- 34.8 (+ 2.3)
Ionization energies	Li	123.5 (+ 0.8)	Cl	299.3 (- 0.2)
	Be	208.9 (+ 6.0)	CH ₄	291.1 (- 0.1)
	B	190.6 (+ 0.8)	NH ₃	235.6 (- 0.8)
	C	259.7 (+ 0.0)	OH	299.1 (+ 0.9)
	N	336.5 (- 1.2)	H ₂ O	294.0 (- 3.0)
	O	312.8 (+ 1.0)	HF	374.1 (- 4.2)
	F	404.1 (- 2.4)	SiH ₄	251.1 (+ 2.6)
	Na	114.4 (+ 4.1)	PH	236.0 (- 1.9)
	Mg	172.8 (+ 3.5)	PH ₂	227.9 (- 1.5)
	Al	134.8 (+ 3.2)	PH ₃	224.3 (+ 3.3)
	Si	185.5 (+ 2.4)	SH	236.6 (+ 2.5)
	P	241.1 (+ 0.8)	H ₂ S ³ B ₁	240.5 (+ 0.9)
	S	236.4 (+ 2.5)	H ₂ S ¹ A ₁	293.6 (+ 1.1)
Electron affinities	C	28.1 (+ 1.0)	CH ₃	- 0.9 (+ 2.7)
	O	34.1 (- 0.4)	NH	5.0 (+ 3.8)
	F	84.7 (- 6.3)	NH ₂	19.2 (- 1.4)
	Si	31.5 (+ 0.4)	OH	45.1 (- 2.9)
	P	16.2 (+ 1.0)	SiH	30.2 (- 0.8)
	S	49.9 (- 2.0)	SiH ₂	26.0 (- 0.1)
	Cl	88.4 (- 5.0)	SiH ₃	29.1 (+ 3.4)
	CH	30.0 (- 1.4)	PH	21.2 (+ 2.6)
	CH ₂	11.1 (+ 3.9)	PH ₂	28.8 (+ 0.5)
Proton affinities	NH ₃	201.9 (+ 0.6)	SiH ₄	152.4 (+ 1.6)
	H ₂ O	162.4 (+ 2.7)	PH ₃	186.2 (+ 0.9)
	C ₂ H ₂	150.6 (+ 1.7)	H ₂ S	165.5 (+ 3.3)

^aCorresponding to MP2/G3MP2large + ΔE(SO) + ZPVE + HLC.

^bValues in kcal mol⁻¹. The heats of formation are 298 K values whereas the remaining quantities refer to 0 K.

Table (5.12) MR-G2/MP2^a heats of formation, ionization energies, electron affinities and proton affinities. Values in parentheses are the differences between experimental and MR-G2/MP2 values.^b

	Species	Species	Species	
Heats of formation	LiH	30.0 (+ 3.3)	PH ₃	4.9 (- 3.6)
	BeH	85.6 (- 3.9)	H ₂ S	- 3.7 (- 1.2)
	CH	142.2 (+ 0.3)	HCl	- 22.7 (+ 0.6)
	CH ₂ ³ B ₁	94.3 (- 0.6)	Li ₂	47.1 (+ 4.5)
	CH ₂ ¹ A ₁	102.4 (+ 0.4)	LiF	- 82.5 (+ 2.4)
	CH ₃	35.2 (- 0.2)	C ₂ H ₂	52.4 (+ 1.8)
	CH ₄	- 18.3 (+ 0.4)	C ₂ H ₄	11.0 (+ 1.5)
	NH	86.1 (- 0.9)	CN	104.9 (+ 0.0)
	NH ₂	45.6 (- 0.5)	HCN	30.8 (+ 0.7)
	NH ₃	- 7.2 (- 3.8)	CO	- 27.3 (+ 0.9)
	OH	8.3 (+ 1.1)	HCO	9.6 (+ 0.4)
	H ₂ O	- 57.1 (- 0.7)	HCHO	- 26.1 (+ 0.1)
	HF	- 66.7 (+ 1.6)	CH ₃ OH	- 47.2 (- 0.8)
	SiH ₂ ¹ A ₁	63.5 (+ 1.7)	N ₂	0.4 (- 0.4)
	SiH ₂ ³ B ₁	86.2 (+ 0.0)	N ₂ H ₄	25.4 (- 2.6)
	SiH ₃	48.1 (- 0.2)	NO	19.5 (+ 2.1)
	SiH ₄	8.0 (+ 0.2)	O ₂	- 4.5 (+ 4.5)
	PH ₂	34.4 (- 1.3)	H ₂ O ₂	- 33.6 (+ 1.1)
Ionization energies	Li	123.4 (+ 0.9)	Cl	295.6 (+ 3.5)
	Be	219.5 (- 4.6)	CH ₄	291.4 (- 0.4)
	B	186.5 (+ 4.9)	NH ₃	230.6 (+ 4.2)
	C	256.1 (+ 3.6)	OH	299.4 (+ 0.6)
	N	334.0 (+ 1.3)	H ₂ O	290.1 (+ 0.9)
	O	312.0 (+ 1.8)	HF	372.2 (- 2.3)
	F	402.7 (- 1.0)	SiH ₄	252.1 (+ 1.6)
	Na	114.1 (+ 4.4)	PH	232.5 (+ 1.6)
	Mg	178.7 (- 2.4)	PH ₂	224.0 (+ 2.4)
	Al	134.1 (+ 3.9)	PH ₃	225.9 (+ 1.7)
	Si	185.2 (+ 2.7)	SH	236.5 (+ 2.6)
	P	241.4 (+ 0.5)	H ₂ S ² B ₁	238.9 (+ 2.5)
	S	233.6 (+ 5.3)	H ₂ S ² A ₁	293.1 (+ 1.6)
Electron affinities	C	31.4 (- 2.3)	CH ₃	- 4.6 (+ 6.4)
	O	34.3 (- 0.6)	NH	6.9 (+ 1.9)
	F	83.5 (- 5.1)	NH ₂	16.0 (+ 1.8)
	Si	31.7 (+ 0.2)	OH	43.9 (- 1.7)
	P	13.4 (+ 3.8)	SiH	26.8 (+ 2.6)
	S	45.7 (+ 2.2)	SiH ₂	22.0 (+ 3.9)
	Cl	84.2 (- 0.8)	SiH ₃	30.8 (+ 1.7)
	CH	27.0 (+ 1.6)	PH	20.7 (+ 3.1)
	CH ₂	13.4 (+ 1.6)	PH ₂	27.0 (+ 2.3)
Proton affinities	NH ₃	207.6 (- 5.1)	SiH ₄	154.6 (- 0.6)
	H ₂ O	161.2 (+ 3.9)	PH ₃	186.9 (+ 0.2)
	C ₂ H ₂	153.6 (- 1.3)	H ₂ S	168.5 (+ 0.3)

^aCorresponding to CASPT2/6-311+G(3df,2p) + ZPVE + HLC.

^bValues in kcal mol⁻¹. The heats of formation are 298 K values whereas the remaining quantities refer to 0 K.

Table (5.13) MR-G3/MP2^a heats of formation, ionization energies, electron affinities and proton affinities. Values in parentheses are the differences between experimental and MR-G3(MP2)/MP2 values.^b

Species		Species		Species	
Heats of formation	LiH	29.7 (+ 3.6)	PH ₃	4.4 (- 3.1)	F ₂ - 0.4 (+ 0.4)
	BeH	85.9 (- 4.2)	H ₂ S	- 3.4 (- 1.5)	CO ₂ - 98.5 (+ 4.4)
	CH	142.4 (+ 0.1)	HCl	- 21.5 (- 0.6)	Na ₂ 28.6 (+ 5.4)
	CH ₂ ³ B ₁	94.5 (- 0.8)	Li ₂	46.7 (+ 4.9)	Si ₂ 139.8 (+ 0.1)
	CH ₂ ¹ A ₁	102.4 (+ 0.4)	LiF	- 81.1 (+ 1.0)	P ₂ 35.2 (- 0.9)
	CH ₃	35.1 (- 0.1)	C ₂ H ₂	52.1 (+ 2.1)	S ₂ 30.7 (+ 0.0)
	CH ₄	- 18.7 (+ 0.8)	C ₂ H ₄	10.6 (+ 1.9)	Cl ₂ 2.4 (- 2.4)
	NH	86.3 (- 1.1)	CN	106.0 (- 1.1)	NaCl - 47.9 (+ 4.3)
	NH ₂	45.7 (- 0.6)	HCN	31.1 (+ 0.4)	SiO - 20.6 (- 4.0)
	NH ₃	- 7.5 (- 3.5)	CO	- 25.3 (- 1.1)	CS 65.7 (+ 1.2)
	OH	8.9 (+ 0.5)	HCO	11.5 (- 1.5)	SO 0.1 (+ 1.1)
	H ₂ O	- 56.8 (- 1.0)	HCHO	- 24.8 (- 1.2)	CIO 26.2 (- 2.0)
	HF	- 65.6 (+ 0.5)	CH ₃ OH	- 46.5 (- 1.5)	CIF - 10.4 (- 2.8)
	SiH ₂ ¹ A ₁	63.1 (+ 2.1)	N ₂	0.9 (- 0.9)	CH ₃ Cl - 20.0 (+ 0.4)
	SiH ₂ ³ B ₁	86.1 (+ 0.1)	N ₂ H ₄	25.3 (- 2.5)	CH ₃ SH - 3.9 (- 1.6)
	SiH ₃	47.5 (+ 0.4)	NO	21.3 (+ 0.3)	HOCl - 16.1 (- 1.7)
	SiH ₄	6.9 (+ 1.3)	O ₂	- 2.6 (+ 2.6)	SO ₂ - 72.4 (+ 1.4)
	PH ₂	34.2 (- 1.1)	H ₂ O ₂	- 33.0 (+ 0.5)	
Ionization energies	Li	124.3 (+ 0.0)	Cl	297.3 (+ 1.8)	HCl 294.6 (- 0.6)
	Be	221.0 (- 6.1)	CH ₄	292.9 (- 1.9)	C ₂ H ₂ 265.0 (- 2.1)
	B	187.4 (+ 4.0)	NH ₃	231.5 (+ 3.3)	C ₂ H ₄ 245.4 (- 3.1)
	C	256.8 (+ 2.9)	OH	300.2 (- 0.2)	CO 321.4 (+ 1.7)
	N	334.4 (+ 0.9)	H ₂ O	291.1 (- 0.1)	N ₂ ² Σ _v ⁺ 357.0 (+ 2.3)
	O	313.1 (+ 0.7)	HF	373.0 (- 3.1)	N ₂ ² Π _u 385.1 (+ 0.0)
	F	403.3 (- 1.6)	SiH ₄	253.9 (- 0.2)	O ₂ 283.8 (- 5.5)
	Na	115.2 (+ 3.3)	PH	233.9 (+ 0.2)	P ₂ 244.9 (- 2.1)
	Mg	180.2 (- 3.9)	PH ₂	225.5 (+ 0.9)	S ₂ 216.7 (- 0.9)
	Al	135.5 (+ 2.5)	PH ₃	227.6 (+ 0.0)	Cl ₂ 265.5 (- 0.3)
	Si	186.3 (+ 1.6)	SH	238.6 (+ 0.5)	CIF 291.7 (+ 0.2)
	P	242.0 (- 0.1)	H ₂ S ³ B ₁	240.9 (+ 0.5)	CS 261.1 (+ 0.2)
	S	236.3 (+ 2.6)	H ₂ S ¹ A ₁	294.9 (- 0.2)	
Electron affinities	C	31.1 (- 2.0)	CH ₃	- 4.1 (+ 5.9)	SH 54.9 (- 0.5)
	O	33.7 (+ 0.0)	NH	6.8 (+ 2.0)	O ₂ 11.1 (- 1.0)
	F	82.4 (- 4.0)	NH ₂	16.3 (+ 1.5)	NO 3.2 (- 2.7)
	Si	32.8 (- 0.9)	OH	43.7 (- 1.5)	CN 89.7 (- 0.7)
	P	16.3 (+ 0.9)	SiH	28.4 (+ 1.0)	PO 30.1 (- 5.0)
	S	48.2 (- 0.3)	SiH ₂	23.6 (+ 2.3)	S ₂ 38.1 (+ 0.2)
	Cl	85.2 (- 1.8)	SiH ₃	32.7 (- 0.2)	Cl ₂ 61.3 (- 6.2)
	CH	27.0 (+ 1.6)	PH	23.1 (+ 0.7)	
	CH ₂	13.7 (+ 1.3)	PH ₂	29.3 (+ 0.0)	
Proton affinities	NH ₃	208.1 (- 5.6)	SiH ₄	154.3 (- 0.3)	HCl 132.6 (+ 1.0)
	H ₂ O	161.5 (+ 3.6)	PH ₃	186.5 (+ 0.6)	
	C ₂ H ₂	153.1 (- 0.8)	H ₂ S	167.8 (+ 1.0)	

^aCorresponding to CASPT2/G3MP2large + ΔE(SO) + ZPVE + HLC.

^bValues in kcal mol⁻¹. The heats of formation are 298 K values whereas the remaining quantities refer to 0 K.

Table (5.14) MR-*Gn* and *Gn* timings.^a

Method	NH ₃	C ₂ H ₂	HCHO
MR-G3/MP2	11.9	235.4	382.3
MR-G2/MP2	12.0	235.8	385.1
MR-G3(MP2)	68.5	3047.0	4160.4
MR-G2(MP2,SVP)	68.6	3047.4	4163.2
MR-G2(MP2)	84.4	3197.8	4958.3
MR-G3/MRCI+Q	90.9	3440.0	4500.9
MR-G2/MRCI+Q	93.5	3487.7	4606.4
G3/MP2	3.9	4.0	4.1
G2/MP2	3.9	4.0	4.3
G3(MP2)	27.6	29.6	32.8
G2(MP2,SVP)	27.6	29.6	33.0
G2(MP2)	40.0	32.9	41.0
G3/QCI	34.1	51.0	70.6
G2/QCI	37.6	49.6	87.7

^aIn seconds using MOLPRO 98 on a single processor of a VPP300 with 1700 Mb memory. The active-space sizes for NH₃, C₂H₂ and HCHO are (8,7), (10,10) and (12,10) for NH₃, C₂H₂ and HCHO, respectively. The *Gn* timings refer to *Gn*(CCSD) calculations, i.e. in which CCSD(T) is used in place of QCISD(T).

Table (5.15) Comparison of the ten largest deviations between experiment and the values calculated by MR-G3(MP2) and G3(MP2).^a

Quantity	MR-G3(MP2) ^b	Quantity	G3(MP2) ^c
$\Delta H_f^0(\text{SO}_2)$	- 5.0 (- 3.9)	IE(Be)	- 5.4 (- 4.7)
IE(Be)	- 4.7 (- 5.4)	EA(NH)	+ 4.5 (+ 2.2)
$\Delta H_f^0(\text{Na}_2)$	+ 4.5 (+ 3.3)	IE(O ₂)	- 4.0 (- 2.6)
EA(CH ₃)	+ 4.3 (+ 1.7)	$\Delta H_f^0(\text{SO}_2)$	- 3.9 (- 5.0)
PA(H ₂ O)	+ 4.0 (+ 1.8)	IE(S)	+ 3.6 (+ 3.0)
PA(NH ₃)	- 3.5 (- 0.4)	EA(C)	+ 3.6 (- 2.1)
IE(Na)	+ 3.4 (+ 3.2)	EA(O)	+ 3.3 (+ 1.9)
$\Delta H_f^0(\text{C}_2\text{H}_4)$	- 3.3 (+ 0.7)	$\Delta H_f^0(\text{Na}_2)$	+ 3.3 (+ 4.5)
$\Delta H_f^0(\text{NaCl})$	+ 3.0 (+ 1.5)	$\Delta H_f^0(\text{CS})$	+ 3.2 (+ 2.0)
IE(S)	+ 3.0 (+ 3.6)	IE(Na)	+ 3.2 (+ 3.4)

^aIn kcal mol⁻¹. ^bValues in parentheses are the corresponding G3(MP2) deviations from ref 4b. ^cTaken from ref. 4b; values in parentheses are the corresponding MR-G3(MP2) deviations from the present work.

CHAPTER 6: ON THE ELECTRONIC STRUCTURE OF BIS(η^5 -CYCLOPENTADIENYL) TITANIUM

A paper to be submitted to the Journal of the American Chemical Society

Mark A. Freitag and Mark S. Gordon

Abstract

Prior to the first reported synthesis of the titanium analog of ferrocene, bis(η^5 -cyclopentadienyl)Ti, there was theoretical speculation as to the electronic structure of what would become known as "titanocene." In time, the original report of a successful synthesis was apparently shown to be incorrect, and a dimeric form of the substance was postulated as the correct structure. In the present work, high level *ab initio* and DFT calculations are performed on the titanocene monomer to help answer these structural questions, and to compare with early theoretical and experimental efforts. The need for a multi-configurational wavefunction is analyzed and found to be unnecessary. The present calculations predict that the ground state of titanocene monomer is a linear triplet with freely rotating cyclopentadienyl rings, which further suggests that experimentally synthesized "titanocene" is indeed some form of the dimer.

I. Introduction

A. Historical Background

The historical account given here is presented from a distinctly theoretical point of view. For an experimental perspective, see the recent review by Beckhaus.⁸⁶

Even before Fischer and Wilkinson reported the first synthesis of what they called *di*(π -cyclopentadienyl)titanium(II) in 1956,⁸⁷ there was theoretical speculation as to the electronic structure of what would come to be known as "titanocene."

From 1953 to 1954, Dunitz and Orgel,^{88,89} Jaffé,⁹⁰ and Moffitt,⁹¹ in the light of molecular orbital theory and motivated by the recent discovery of ferrocene,⁹² considered the electronic structure of *all* bis-cyclopentadienyl compounds in general.

Moffitt assumed a D_{5d} structure for the "beautifully symmetric" ferrocene, and broke the molecule into the iron atom and cyclopentadienyl (Cp) ring fragments to evaluate the bonding. For the rings, he used a simple p -orbital basis on each carbon atom to derive a linear combination of 10 MOs: $a_{1g} + a_{2u} + e_{1g} + e_{2g} + e_{1u} + e_{2u}$. Moffitt then chose to describe the iron atom using its 4s (a_{1g}), 3d (a_{1g}, e_{1g}, e_{2g}), and 4p (e_{1u}, a_{2u}) orbitals. From there, qualitative arguments were used to estimate the orbital energies, and the resulting orbital interaction diagram was derived: in order of increasing energy, the frontier orbitals for titanocene were $(e_{1g})^4 (a_{2u})^2 (a_{1g})^2 [a_{1g}(4s)]^2 (e_{1u})^4 (e_{2g})^0$, where the e_{1u} and e_{2g} orbitals are nearly degenerate. In his model, the stability of ferrocene was accounted for by significant overlap of the e_{1g} orbitals of the Cp rings and the corresponding d_{xz} and d_{yz} orbitals of the iron atom. By extrapolation, Moffitt suggested that titanocene, with its four valence electrons, should be a diamagnetic singlet, with the two non-bonding titanium electrons assigned to the $a_{1g}(4s)$ orbital. However, Moffitt also suggested that if the Hund stabilization was significant, the paramagnetic triplet, with one electron in the metal's e_{2g} orbital, would be more stable. Titanocene had yet to be synthesized experimentally at the time of Moffitt's paper, so these predictions could not be tested.

A year later, Dunitz and Orgel⁸⁹ modified Moffitt's qualitative approximation into a "semiquantitative" model, approximating overlap integrals between the metal atom and Cp ring orbitals. These calculations changed ferrocene's MO frontier orbital energies (for titanocene occupation) from Moffitt's order to $(a_{1g})^2 (a_{2u})^2 (e_{1g})^4 (e_{2g})^2 [a_{1g}(4s)]^0 (e_{1u})^4$ in order of increasing energy, the last three orbitals being "uncertain," and approximately degenerate. This in turn changed the prediction for titanocene from a singlet to a triplet, since the two non-bonding metal electrons were assigned to the degenerate e_{2g} orbital.

Also in 1955, Fisher and Wilkinson⁸⁷ reported the first synthesis of titanocene. They were aware of the predictions of Moffitt, Dunitz and Orgel, and since they found their substance to be diamagnetic, they used Moffitt's scheme to support their observation that there were two forms of the compound: a green paramagnetic (triplet) form that converted spontaneously to a brown diamagnetic (singlet) form. Based on magnetic susceptibility experiments, they proposed that for unsolvated

titanocene, the excited triplet state must be at a level at least kT (~ 0.75 kcal) above the singlet ground state.

In 1957, another theoretical paper appeared on metal aromatic structures by Liehr and Ballhausen.⁹³ They followed Moffitt's basic treatment, and improved on Dunitz and Orgel's calculations by using one-electron Hamiltonians and the variational principle, applied to each of the important molecular orbitals. They further estimated orbital energies using crystal field theory, allowing positive point charges on the Cp rings to interact with electrons in the metal's e_{1g} orbital to simulate bonding interactions. Anti-bonding interactions were modeled with negative point charges on the Cp ring interacting with the same metal e_{1g} electrons, and non-bonding interactions were between negative point charges on the ring and electrons in the metal's $a_{1g}(4s)$, $a_{1g'}$, and e_{2g} orbitals. Using this method, they found the order of increasing energy in MOs to be $(a_{1g})^2 (a_{2u})^2 (e_{1u})^4 (e_{1g})^4 [a_{1g}(4s)]^2$. This also suggested a singlet ground state for titanocene, but the authors used an adjustable parameter and the experimental results of Fischer and Wilkinson to generate this result after the fact.

Two years later, Matsen⁹⁴ used a "strong-field, ligand-field model" to predict a singlet ground state for titanocene, again in support of the known experimental evidence at the time.

In 1960, Robertson and McConnell,⁹⁵ in a magnetic resonance study, noted that based on Fischer and Wilkinson's work, titanocene should be diamagnetic, but they argued that this does not fit their ionic model well. The model represents the Cp ligands using circular line charges, which create a field potential. This potential splits the $3d$ orbitals, and an energy difference could be calculated. Based on experimental magnetic susceptibility data, the authors assumed that of the metal's d orbitals, a_{1g} and e_{2g} should be nearly degenerate, and lie much lower in energy than the e_{1g} . The authors noted that titanocene, with two electrons in these orbitals, does not fit this assumption, since it would then most likely be paramagnetic by Hund's rule. They suggested that the observed magnetic properties may be a result of interaction with neighboring molecules in the crystal, which may "quench" the spin. They also suggested lowering the energy of one of the three d -orbitals, but

ultimately did not adopt this since the other metallocenes studied fit their model quite well. They considered titanocene an exception to their general conclusions.

An excellent review of the above theoretical approaches as they apply specifically to *ferrocene* is given by Scott and Becker.⁹⁶ They also include the Yamazaki⁹⁷ reference, which is the first theoretical treatment to use SCF theory, although that paper makes no specific reference to titanocene.

In 1964, Watt and Baye⁹⁸ reported properties of FeCp_2 , NiCp_2 , and CrCp_2 , and questioned Fischer and Wilkinson's synthesis of TiCp_2 : "[W]e have been unable to produce $(\text{C}_5\text{H}_5)_2\text{Ti}$ by their procedure, by any modification thereof, or by other methods that might reasonably be expected to provide this compound." In a later paper,⁹⁹ these same authors along with Drummond noted two other reported syntheses of titanocene, but suggest that the characterizations of each were quite weak. They used IR data to support their claim that they had indeed produced titanocene, and reported that the substance is more stable thermally than had been reported by Fischer and Wilkinson. When their diamagnetic singlet green form is heated to 200°, it turns black and appears to decompose, but then dissolves in benzene to form a green solution of titanocene which can be recrystallized. Their magnetic susceptibility experiments showed that all samples of titanocene were diamagnetic. They found the molecular weight (cryoscopically in benzene) to be 346, compared to 178.07 for $(\text{C}_5\text{H}_5)_2\text{Ti}$. ($178.07 \times 2 = 356.14$)

Calderazzo, Salzmann, and Mosimann,¹⁰⁰ based on the above results, suggested a dimeric formula for titanocene, although they were not specific regarding the details of such a structure. In a later paper, Salzmann and Mosimann¹⁰¹ suggested that the IR spectra of Watt, Baye and Drummond's compound is too complex to be consistent with a simple ferrocene-like sandwich structure. They note the spectrum has characteristics of both sigma- and pi- ring-to-metal bonding, but were unsure as to the stability of this structure in solution.

In 1969, Brintzinger and Bartell¹⁰² proposed that both Watt, Baye, and Drummond⁹⁹, and Salzmann and Mosimann¹⁰⁰ indeed had a compound $\text{C}_{10}\text{H}_{10}\text{Ti}$, but it in fact exists as a dimer and does not have the traditional sandwich structure of metallocenes. They used IR and NMR data to confirm Salzmann and Mosimann's suggestion that the Cp rings are σ bound as well as π bound to the titanium atom.

Finally, in 1978 Clack and Warren¹⁰⁹ used INDO SCF calculations to come to the same conclusions as Hoffmann about the relative frontier orbital energies.

B. The Present Approach

It is clear that there has been much interest and speculation regarding the nature of the electronic structure of "titanocene." (Here we will take "titanocene" to mean a single bis(η^5 -cyclopentadienyl)Ti fragment, abbreviated as TiCp₂.) There seems to be general agreement that attempts to prepare titanocene in the laboratory result in some form of the dimer, with or without hydride bridges, as discussed above. Still, the TiCp₂ fragment, while possibly not stable as the monomer, is still an important component of many useful catalysts, and a knowledge of its electronic structure will aid in the understanding of the chemistry of these species. Of course, it is also important to obtain an understanding of the molecular and electronic structure of TiCp₂ itself. We anticipate that future work will focus on the electronic structure of possible dimers.

Our approach will be to re-examine previous conclusions using high-level *ab initio* and density functional theory (DFT) theories to determine the structure and relative energies of the lowest energy singlet and triplet states of TiCp₂. First, the use of multi-configurational wavefunctions will be analyzed, in order to assess the need for such a wavefunction. Once it is established that single reference methods should be reliable, DFT, second order perturbation theory (MP2) and coupled cluster [CCSD(T)] methods are employed to elucidate the low-energy form of TiCp₂.

II. Methods

The all-electron 6-31G**¹¹⁰ and GAMESS PVTZ¹¹¹ basis sets were used for all atoms, including titanium.^{112,113} Geometries and numerical Hessians were obtained at the Hartree-Fock, DFT and MP2 levels of theory. For the MCSCF wavefunction, a (2,2) active space is used, where the two orbitals are the HOMO and LUMO based on the MP2 natural orbitals. Larger active spaces sets were also tested with similar results. MCSCF, ROHF, RHF, DFT (B3LYP)¹¹⁴ and closed-shell MP2 calculations

were carried out using the GAMESS¹¹⁵ suite of programs, unrestricted MP2 (UMP2) calculations were performed using Gaussian 94,¹¹⁶ and Molpro was used for the CCSD(T)¹¹⁷ and UCCSD(T)¹¹⁸ calculations. The notation RHF/6-31G** refers to a geometry optimization at this level of theory, while RHF/PVTZ//RHF/6-31G** refers to a single-point RHF/PVTZ calculation at the RHF/6-31G** geometry. Numerical Hessians were evaluated throughout, using the double-difference method, and projected to eliminate rotational and translational contaminants.¹¹⁹

For C_{2v} and C_s geometries, the Cp-Ti-Cp angle is measured by defining the plane of each Cp ring in terms of three points: the nuclei of the symmetry unique carbon and the two carbons furthest away from it in the same Cp ring. The angle between the two vectors normal to these planes is defined as the Cp-Ti-Cp angle, θ .

III. Results and Discussion

A. Preliminary Considerations

Let us first consider the symmetry characteristics of the molecule in more detail. If the Cp rings are parallel to one another and staggered, $TiCp_2$ has D_{5d} symmetry; if the rings are parallel but eclipsed, the symmetry is D_{5h} ; decreasing the Cp-Ti-Cp angle θ from 180° in D_{5h} symmetry gives C_{2v} , and similar bending from D_{5d} gives a C_s geometry. Fig. (6.1) shows the orientation of these four point groups relative to Cartesian coordinates. For the C_s geometry, the xy plane is the mirror plane. Note that upon reducing symmetry from (D_{5h}/D_{5d}) to (C_{2v}/C_s), the molecule is rotated from (y, z, x) to (x, y, z) in order to maintain the z -axis as the principle axis. Consequently, orbital designations change also. For example, a d_{xz} orbital in C_s is a d_{xy} in D_{5d} . For ease of reference, Table (6.1) summarizes this information.

D_{5d}	D_{5h}	C_{2v}	C_s	Orbital designations for D_{5d}, D_{5h}	Orbital designations for C_{2v}, C_s
A_{1g}	A_1'	A_1	A'	z^2	y^2
A_{2g}	A_2'	B_1	A''		
E_{1g}	E_1''	A_2+B_2	$A'+A''$	xz, yz	yz, xy
E_{2g}	E_2'	A_1+B_1	$A'+A''$	x^2-y^2, xy	x^2-z^2, xz
A_{1u}	A_1''	A_2	A''		
A_{2u}	A_2''	B_2	A'	z	y
E_{1u}	E_1'	A_1+B_1	$A'+A''$	x, y	z, x
E_{2u}	E_2''	A_2+B_2	$A'+A''$		

Table (6.1) Relative symmetries and labels for $TiCp_2$. See text for a note on the rotation of the Cartesian axes.

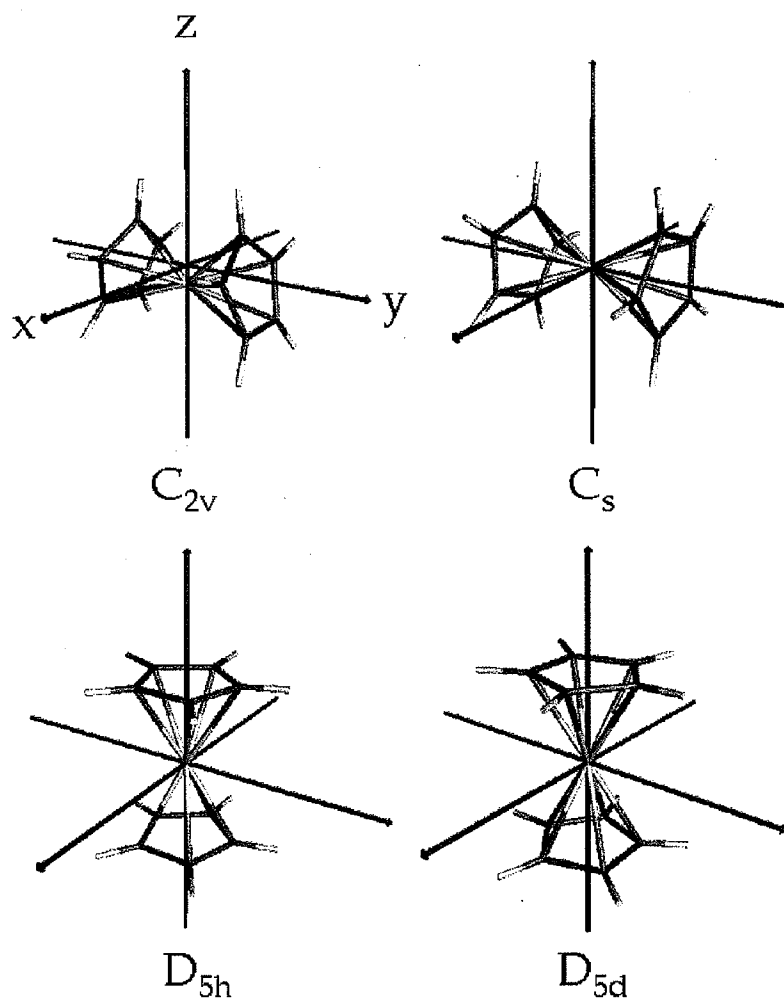


Fig. (6.1) Relative geometries of the four possible point groups of $TiCp_2$.

B. Hartree-Fock Analysis

Preliminary calculations were carried out at the Hartree-Fock level. As shown in Table (6.2), the ROHF/6-31G** 3B_1 (C_{2v}) and $^3A''$ (C_s) optimized geometries are nearly degenerate, and both lie 18.6 kcal/mol below the analogous 3A_2 (D_{5h}) state, which itself is nearly degenerate with the 3A_2 (D_{5d}) state. Similarly, the RHF 1A_1 state in C_{2v} symmetry lies just 0.1 kcal/mol below the $^1A'$ (C_s) state, and 9.4 kcal/mol below the 1A_1 (D_{5h}) and 1A_1 (D_{5d}) states, where the latter two are essentially degenerate. The 1A_1 (C_{2v}) state is 39.3 kcal/mol above the 3B_1 (C_{2v}) state at this level of theory. All of the geometries at the HF level have the Cp rings within roughly 6 degrees of being parallel. Of course, D_{5h} and D_{5d} symmetries force the rings to be exactly parallel. Inefficient overlap of the cyclopentadienyl p_y orbitals is the most likely cause for the lack of bending of the Cp-Ti-Cp angle in C_s symmetry. Numerical Hessians performed at this level show imaginary frequencies for the C_{2v} and C_s geometries, while for higher symmetry (except triplet D_{5d} which has a small imaginary frequency) the geometries are positive definite. All attempts to step off these imaginary modes (as one does in an intrinsic reaction coordinate calculation, for example) and isolate a positive definite geometry failed. This may suggest that the numerical Hessians are very sensitive to step sizes due to the low-frequency ring modes.

For the triple-zeta basis set, one sees qualitatively similar behavior. It is especially revealing that the relative RHF/PVTZ//RHF/6-31G** energies are essentially identical to those for the full RHF/PVTZ optimization, as seen in Table (6.3). This suggests that the 6-31G** geometries are adequate at the Hartree-Fock level. Based on the results in Tables (6.2) and (6.3), we conclude that HF theory predicts $TiCp_2$ has a triplet ground state with C_{2v} symmetry (3B_1) that is ~40 kcal/mol below the lowest singlet (C_{2v} 1A_1).

		$^1\text{A}_1(\text{C}_{2v})$	$^1\text{A}'(\text{C}_s)$	$^1\text{A}_1(\text{D}_{5d})$	$^1\text{A}_1(\text{D}_{5h})$	$^3\text{B}_1(\text{C}_{2v})$	$^3\text{A}''(\text{C}_s)$	$^3\text{A}_2(\text{D}_{5d})$	$^3\text{A}_2(\text{D}_{5h})$
								$(\text{e}_{2g})^2$	$(\text{e}_2)^2$
HF	E	0	0.1	9.4	9.4	-39.3	-39.3	-20.7	-20.7
	θ	173.91	180.00	-	-	178.21	180.00	-	-
	ν	95	71 ^b ,16	-	-	93,8 ^b	71 ^b ,6 ^a	10 ^b	-
DFT	E	0	2.1 ^c	19.4	19.4	-15.0	-14.2 ^c	-6.0	-6.4
	θ	158.87	167.06	-	-	171.17	180.00	-	-
	ν	161	161,119,27	127 ^a	110 ^b	153,57 ^b	193 ^b ,154 ^a ,48	118 ^a	109 ^b
(tight)		26	46	-	-	-	153 ^b ,14	23 ^b	-
MP2	E	0	1.7	13.8	13.7	-21.0	-21.0	-6.4	-6.7
	θ	148.43	180.00	-	-	176.9	179.59	-	-
	ν	28	52	10 ^b	5 ^b	n/a	n/a	n/a	n/a

^a intensity less than 0.001 debye/amu \AA^2

^b zero intensity

^c the geometry is considered converged at a RMS gradient of less than 6.9×10^{-5} hartree/bohr rather than the usual default of 3.0×10^{-5} .

Table (6.2) Energies, E (kcal/mol) are relative to the corresponding $^1\text{A}_1(\text{C}_{2v})$ state; θ is the Cp-Ti-Cp angle; ν (cm^{-1}) are the imaginary frequencies. ν (tight) are the imaginary frequencies with the tight grid - see text for explanation. The 6-31G** basis is used throughout.

		$^1A_1 (C_{2v})$	$^1A' (C_s)$	$^1A_1 (D_{5d})$	$^1A_1 (D_{5h})$	$^3B_1 (C_{2v})$	$^3A'' (C_s)$	$^3A_2 (D_{5d})$	$^3A_2 (D_{5h})$
HF/PVTZ// HF/6-31G**	E	0	0	15.1	15.1	-36.1	-36.1	-20.2	-20.2
	E	0	0	15.1	15.1	-36.1	-36.1	-20.2	-20.2
HF/PVTZ	θ	174.27	180	-	-	178.26	180.00	-	-
	v	102	32 ^b	-	4 ^b	105	77 ^b ,7 ^a	10 ^b	-
B3LYP/PVTZ// B3LYP/6-31G**	E	0	1.8	24.1	24.1	-13.3	-12.7	-7.2	-7.4
	E	0	1.8	24.1	24.4	-13.1	-12.4 ^c	-7.2	-7.4
B3LYP/PVTZ	θ	160.98	169.9	-	-	171.37	180.00	-	-
	v	167	161,129 ^a ,42	136 ^a	136 ^b	141,61 ^b	192 ^b ,151,54 ^a	128 ^a	123 ^b
(U)MP2/PVTZ// (U)MP2/6-31G**	E	0	2.0	19.9	19.7	-5.0	-4.4	-5.5	-6.3
	E	0	2.0	20.1	19.8	n/a	n/a	n/a	n/a
(U)MP2/PVTZ	θ	148.63	180	-	-	n/a	n/a	-	-
CCSD(T)/6-31G**// (U)MP2/6-31G**	E	0	0.4	4.2	3.9	-19.3	-19.2	-6.5	-6.8
	E	0	0.5	6.8	6.5	-7.5	-6.9	-7.5	-8.3

^a intensity less than 0.001 debye/amu \AA^2

^b zero intensity

^c the geometry is considered converged at a RMS gradient of less than 6.9×10^{-5} hartree/bohr rather than the usual default of 3.0×10^{-5} .

Table (6.3) Energies, E (kcal/mol) are relative to the corresponding $^1A_1 (C_{2v})$ state; θ is the Cp-Ti-Cp angle; v (cm^{-1}) are the imaginary frequencies.

C. MCSCF/GVB Theory

Based on previous calculations for TiH_2 ^{120,121} and Ti_2H_6 ¹²² one might expect TiCp_2 calculations to require a multiconfigurational wavefunction. To assess the need for such a wavefunction, the singlet MP2 natural orbitals were used as a starting point for a TCSCF calculation with the MP2 HOMO ($3d_{xz}$) and LUMO ($4p_z$) as the (2,2) active space. The resulting natural orbital occupation numbers (NOONs) in the active space show very little multiconfigurational character: 1.992 and 0.008 electrons in the HOMO and the LUMO, respectively. Using triplet TCSCF orbitals as a starting guess for singlet TCSCF results in the same occupation numbers. Even after TCSCF optimization starting from the bent MP2 structure, the NOONs changed very little: 1.995 and 0.005. For the triplet TCSCF, NOONs are 1.000 and 1.000. A second diagnostic are the NOONs resulting from a MP2 calculation itself. It has been shown¹²³ that if these occupation numbers are significantly unphysical, i.e. much greater (less) than two (zero), the system is likely to require a multiconfigurational wavefunction, since this behavior suggests the single-reference Hamiltonian has broken down. In the case of TiCp_2 , the MP2 NOONs range from 2.0018 to -0.0075, where we have included all four geometries. These are not significant deviations from the physical expectations. We therefore conclude that a single-reference wavefunction is appropriate for TiCp_2 .

D. Density Functional Theory

Density functional theory calculations shown in Table (6.2) show a quantitative, but not qualitative shift relative to the Hartree-Fock results. Comparing double-zeta results, the lowest energy structure is still the $^3\text{B}_1$ state, but it now lies only 15.0 kcal/mol below the lowest singlet ($\text{C}_{2v}\ ^1\text{A}_1$), and the $^3\text{A}_2$ states lie 9.0 kcal/mol above $^3\text{B}_1$. The triplet geometries remain within nine degrees of linear, but the singlet C_{2v} and C_s geometries bend by an additional 15.0° and 12.9° - to 158.9° and 167.06°, respectively. The imaginary frequencies remain qualitatively similar to Hartree-Fock, with some exceptions. Both the singlet and triplet C_s geometries display three imaginary frequencies using the default DFT grid size in GAMESS;

however, these become similar to the Hartree-Fock values when a tighter grid is used. Similarly, all but one (D_{5d}^{a} 3A_2) of the imaginary frequencies, with zero or very small intensities calculated using the default grid for the D_{5d} and D_{5h} geometries, disappear when the tighter grid is used - again similar to Hartree-Fock.

There are very small quantitative changes in going from a double-zeta to a triple-zeta basis set; $\sim 2^0$ in the geometries, ~ 1.5 kcal/mol in the relative energies, and ~ 10 -15 wavenumbers in the imaginary frequencies. It appears that very little is gained by increasing the size of the basis set, although the splitting between the triplet geometries is reduced to 5.9 kcal/mol. Single-point energies at double-zeta geometries agree with full triple-zeta optimizations to within 0.3 kcal/mol.

While the singlet-triplet splitting is reduced to ~ 13 kcal/mol, compared with ~ 40 kcal/mol for HF, DFT still predicts a triplet ground state for TiCp_2 .

E. Second Order Perturbation Theory

The MP2/6-31G** results [Table (6.2)] are very similar to those summarized above for DFT: The 3B_1 (C_{2v}) ground state is predicted to be ~ 15 kcal/mol below the higher symmetry triplets and ~ 21 kcal/mol below the lowest energy 1A_1 (C_{2v}) singlet state. One again finds small ($\sim 15i$ - $50i$ cm^{-1}) imaginary frequencies, due to instabilities of the numerical Hessians. This picture is significantly altered when the larger triple zeta basis set is used, as shown in Table (6.3). Now, all of the triplets are within ~ 1 kcal/mol of each other, with the higher symmetry D_{5d} and D_{5h} structures slightly *lower* in energy. The ground state is still predicted to be the triplet, but now only by ~ 6 kcal/mol relative to the C_{2v} 1A_1 singlet. The latter is still predicted to be the lowest energy singlet structure.

F. Coupled Cluster Theory

To further evaluate the relative energetics, CCSD(T) [UCCSD(T)] calculations were performed at the singlet [triplet] MP2/6-31G** [UMP2/6-31G**] geometries using the 6-31G** and PVTZ basis sets. The results are qualitatively similar to the perturbation theory results, as seen in Table (6.3). Note that because of program

limitations, the restricted D_{5d} (D_{5h}) energy is evaluated using the Abelian C_{2h} (C_{2v}) point group. Based on MP2 and HF calculations, the Abelian energy is artificially 0–10 kcal/mol low due to split degeneracies. This is not an issue for the unrestricted triplet calculations. For the 6-31G** basis set, all the triplet geometries are more stable than the lowest singlet, and the splitting between triplet $C_{2v}, C_s / D_{5d}, D_{5h}$ is 12.8 kcal/mol. As in the MP2 case, there is a qualitative shift when the PVTZ basis set is used; the triplet geometries are all still lower in energy, but in this case the lowest energy structure is the 3A_2 (D_{5h}). This further suggests that the lowest energy geometry of the monomer is indeed linear. As for MP2, there is also a significant basis set effect on the singlet-triplet splitting. The triplet is lower than the lowest energy singlet, 1A_1 (C_{2v}), by only ~8 kcal/mol at this level of theory.

IV. Conclusions

At all levels of theory, the triplet geometries are all lower than the lowest energy singlet, and as a general rule, the splitting between the high symmetry and low symmetry triplets becomes less as the level of theory is increased. In all of the above calculations where double- and triple-zeta optimizations are feasible, it is found that triple-zeta energies at double-zeta geometries reproduce the results of full triple-zeta optimizations to within 0.3 kcal/mol. At all applicable levels of theory, Hartree-Fock, B3LYP (with sufficiently tight grid) and MP2, the numerical Hessians show the high symmetry, linear geometries are positive definite or have imaginary frequencies with wavenumbers less than 20 cm⁻¹. Based on these data, we conclude that bis(η^5 -cyclopentadienyl)Ti is a paramagnetic triplet with freely rotating Cp rings. All attempts to synthesize this compound in the literature result in a diamagnetic singlet, which lends support to the suggestion that the true structure is some form of the dimer.

It is particularly enlightening to compare these results with those of the early theorists introduced in the Introduction. Recall that before Watt and Baye's failed synthesis of Fischer and Wilkinson's "titanocene," this compound was assumed to have a molecular formula of $(C_5H_5)_2Ti$, which allows us to compare directly with the early results. Fig. (6.2) shows the UHF orbital energies (in hartrees) for the 3A_2 (D_{5d})

state at the UMP2/PVTZ//UMP2/6-31G** level. Compared with these are the relative orbital energies given by Dunitz and Orgel in 1955 using *approximate* overlap integrals, and building from the group theoretical presentation given by Moffitt in 1954. It seems that their only error was an overestimation of the stability of the metal orbitals, in particular the metal's a_{1g} valence orbital. This profound and striking result is a testament to the power of group theory in the hands of clever chemists.

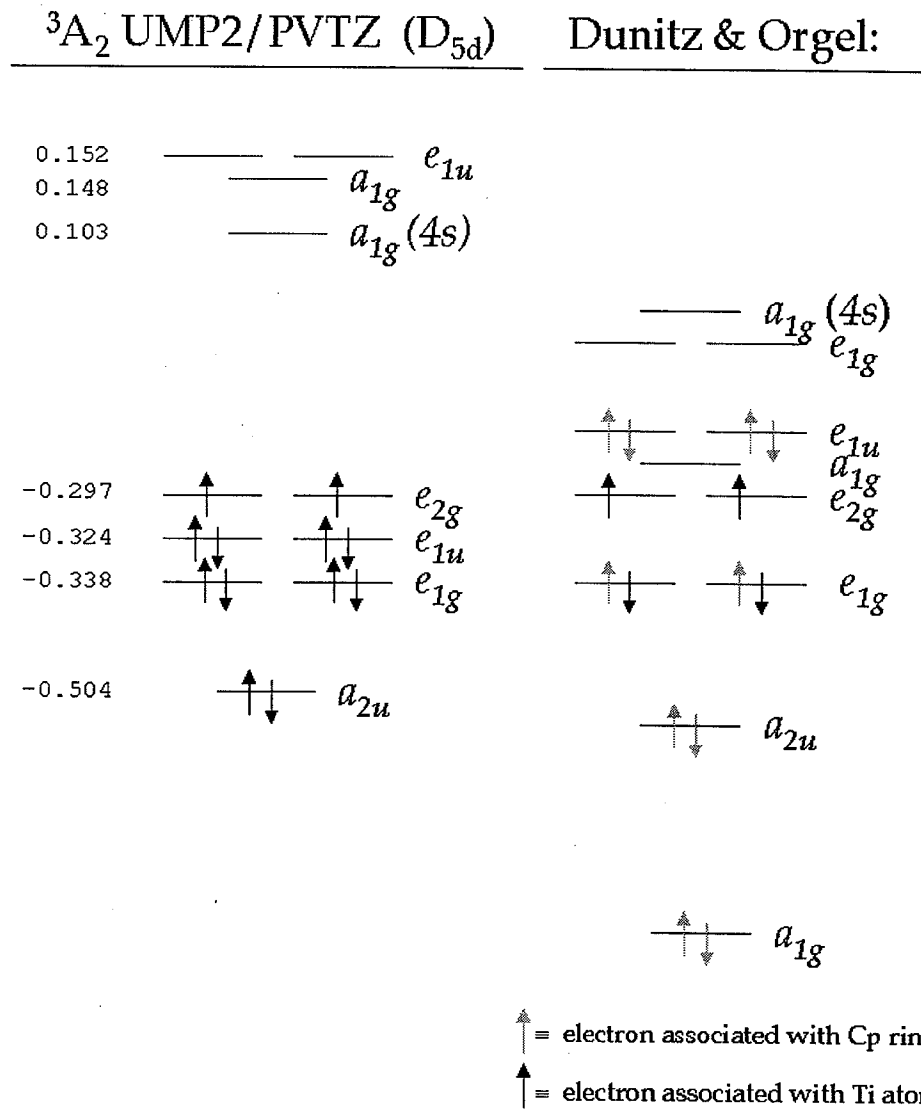


Fig. (6.2) Orbital interaction diagrams for the present work and for that given by Dunitz and Orgel in 1955. Energies are given in hartrees, but the drawing is not strictly to scale.

CHAPTER 7: GENERAL CONCLUSIONS

Schrödinger's equation, Eq. (1.1), represents the first principles of non-relativistic quantum mechanics, and is the starting point for all the studies contained in this dissertation. Let us briefly review the thread that ties this volume together.

In the General Introduction, we saw how one can integrate out the time dependence of Eq. (1.1) to leave the time-independent form of Schrödinger's equation:

$$H|\psi\rangle = E|\psi\rangle \quad (1.5)$$

Using the Born-Oppenheimer approximation, the Hamiltonian, H , was simplified, and using the orbital approximation and the antisymmetric property of the electronic wavefunction, we arrived at the Hartree-Fock equations, Eqs. (1.37). To make the resulting problem tractable, it was described how the wavefunction is further approximated by expansion in terms of well-defined basis sets. Using Hartree-Fock theory as a starting point, we explained how the method relates to unrestricted Hartree-Fock theory, MP2 perturbation theory, CI theory, MCSCF theory, coupled cluster theory, and DFT.

For many problems, especially large ones such as discrete solute/solvent interactions, the methods described in Chapter 1 become unsuitable because of the computational time required. In order to study such systems, hybrid quantum mechanics/molecular mechanics techniques have been developed, such as the Effective Fragment Potential, described in Chapter 1. One of the interactions that must be accounted for using this method is charge penetration between distributed multipolar expansions, and this is derived and tested in Chapter 2.

The Hamiltonian derived in Chapter 1, Eq. (1.7), is for an isolated system, free from the effect of perturbing fields. A powerful experimental spectroscopy, nuclear magnetic resonance (NMR) measures the so-called chemical shifts of nuclei in the presence of a magnetic field. In order to account for the effect of the magnetic field theoretically, an appropriate vector potential must be added to the Hamiltonian; this

was done in Eq. (3.1). It was described how the use of a vector potential leads to a gauge dependence in the solution of the Hartree-Fock equations when a finite basis is used, and how this dependence can be removed using Ditchfield's gauge-invariant atomic orbitals. It was explained how the physical property of chemical shifts can be defined as a second derivative of the energy with respect to the external magnetic field and the nuclear magnetic moments, and this derivative was evaluated in detail. The resulting integrals were further evaluated using the McMurchie-Davidson method, and coded into GAMESS using the modified algorithm described. The chemical shifts were also shown to depend on the first derivative of the density matrix, whose evaluation was seen to require antisymmetric perturbation theory for nonorthogonal, perturbation-dependent basis sets. This formalism was also derived in Chapter 3. Finally, it was explained how our ultimate goal is to predict chemical shifts in solution, so several possible approaches were given on how to integrate the EFP method with the GIAO formalism. The next step in future research should be to replace the *ab initio* density matrix with the density matrix in the presence of fragments and investigate the influence of the fragment solvent at this level of approximation.

A conventional application of the EFP method was given in Chapter 4, which studied the solvation of formic and acetic acids. Although the preliminary results of this study were promising, it was noted that further progress in this area awaits an appropriate Monte Carlo or molecular mechanics code because of the currently inadequate method for sampling configuration space. Once this code is available, the presented work should be repeated to investigate the degree to which the sampling of configuration space is complete. If the Monte Carlo sampling is adequate, more solvent molecules should be added until dissociation of the weak acid is achieved and can be studied in detail.

The theoretical methods described in Chapter 1 rely on various levels of approximation. It has long been the goal of the quantum chemist to obtain thermodynamic levels of accuracy; i.e. roughly within 1 kcal/mol of experiment. In order to accomplish this, many hybrid schemes have been developed, most notably Pople's G2 and G3 methods. Chapter 5 explained how this method is only useful for systems that are well-described by a single electron configuration, or loosely

speaking, a single Lewis structure. It was further explained that many interesting chemical systems require a multi-configurational wavefunction, and the chapter went on to describe multi-reference versions of several G2 and G3 techniques and reported their performance in detail. The results indicate that the G_n -type additivity approximations hold less well for the MR- G_n methods than they do for the parent single-reference G_n methods. This leads to the somewhat fortuitous situation in which incorporation of additivity approximations in the MR- G_n procedures results in an accuracy which is better than that of MR- G_n /MRCI+Q and is generally comparable to that of the corresponding single-reference methods. MR-G3(MP2) is the most accurate of the MR- G_n methods that we have examined; the mean absolute deviation between calculated and experimental values for the test set of (123) energies is 1.22 kcal mol⁻¹, compared with 1.19 kcal mol⁻¹ for standard G3(MP2).

Finally, Chapter 6 discussed the electronic structure of the complex organometallic molecule titanocene. The history of the study of this species was discussed, and the results of many high level calculations such as DFT and MP2 with a triple-zeta basis set were evaluated. At all levels of theory, the triplet geometries are all lower than the lowest energy singlet, and as a general rule, the splitting between the high symmetry and low symmetry triplets becomes less as the level of theory is increased. At all applicable levels of theory, Hartree-Fock, B3LYP (with sufficiently tight grid) and MP2, the numerical Hessians show the high symmetry, linear geometries are positive definite or have imaginary frequencies with wavenumbers less than 20 cm⁻¹. Based on these data, we conclude that bis(η^5 -cyclopentadienyl)Ti is a paramagnetic triplet with freely rotating Cp rings. All attempts to synthesize this compound in the literature result in a diamagnetic singlet, which lends support to the suggestion that the true structure is some form of the dimer. Similar calculations carried out on the suggested forms of the dimer should lead to further understanding.

As was noted earlier, all of the above results can be considered approximate solutions of Eq. (1.5) which in turn is an exact solution of Eq. (1.1). It should be noted, however that this form of Schrödinger's equation itself is approximate, as it does not incorporate relativistic effects. It has been further argued that the relativistic form of this equation, the Dirac equation, is also approximate, since in

their present state, quantum mechanics and general relativity are mutually inconsistent. (Dirac himself spent his later years searching in vain for an alternate formulation for quantum electrodynamics.¹²⁴) Having said that, however, it should be noted that quantum mechanics is the most precise physical theory known to man, and as such is unlikely to be superceded for chemical applications - it has been, and will continue to be, the quantum chemist's first principles.

APPENDIX A. CARTESIAN VS. SPHERICAL HARMONIC FUNCTIONS

There are several ways to approach the idea of spherical harmonic functions. A particularly elegant way introduced to me by Prof. David Hoffman takes advantage of the idea of a tensor, and shows the relationship between spherical and Cartesian functions very well.

Consider a Taylor expansion of a function $f(x, y, z)$:

$$f(x, y, z) = f_0 + \left(x \frac{\partial f}{\partial x} \Big|_0 + y \frac{\partial f}{\partial y} \Big|_0 + z \frac{\partial f}{\partial z} \Big|_0 \right) + \frac{1}{2} \left(x^2 \frac{\partial^2 f}{\partial x^2} \Big|_0 + xy \frac{\partial^2 f}{\partial x \partial y} \Big|_0 + \dots + z^2 \frac{\partial^2 f}{\partial z^2} \Big|_0 \right) + \dots \quad (A.1)$$

where in total there will be three linear terms, nine quadratic terms, 27 cubic terms, etc., and each derivative is evaluated at the origin. Note that since the order of differentiation is irrelevant, several of the terms given above are equivalent. The "coefficients" (components) preceding each derivative can be found using the following:

$$x^l y^m z^n \quad (A.2)$$

where $l + m + n = N$, (c.f. the original Taylor expansion given above: for the single derivative terms, $N = 1$; for the second derivative terms, $N = 2$, etc.) Further note that although there are 3^N total components, some are identical, as noted above. In fact, only

$$\frac{(N+1)(N+2)}{2} \quad (A.3)$$

components are distinct.

Consider now an arbitrary vector $r = r(x, y, z)$. [In general, $(r \dots r)$ can be thought of as one long vector with 3^N components, N being the number of r 's. c.f. Eq. (4.5).] If this vector is rotated in some way, then its new coordinates can be put in terms of its old coordinates:

$$\begin{aligned} x' &= x'(x, y, z) \\ y' &= y'(x, y, z) \\ z' &= z'(x, y, z) \end{aligned} \quad (\text{A.4})$$

Unintrusive rotations are described by a unitary (or, if all the elements of the vector are real, as in this case, orthogonal) transformation. For example:

$$\begin{aligned} x &= U_{xx'}x' + U_{xy'}y' + U_{xz'}z' \\ y &= U_{yx'}x' + U_{yy'}y' + U_{yz'}z' \quad \text{or} \quad \mathbf{U}\mathbf{r}' = \mathbf{r} \\ z &= U_{zx'}x' + U_{zy'}y' + U_{zz'}z' \end{aligned} \quad (\text{A.5})$$

Since the equations given above are linear, it follows that the old components of r , (x^l, y^m, z^n) can be written as some linear combination of the new set $(x'^{l'}, y'^{m'}, z'^{n'})$ where as before, $l' + m' + n' = N$.

So in effect, the 3^N components of $(r \dots r)$ form a 3^N -D basis for the full rotation group. Further, since the matrix that relates r to r' is unitary, (as shown above) then the $3^N \times 3^N$ matrix that relates the components of $(r \dots r)$ to $(r' \dots r')$ is also unitary. This is important because the 3^N elements of $(r \dots r)$ form the basis of a representation of the full rotation group with dimension $(N+1)(N+2)/2$, called the *Cartesian* representation.

Sets of components that form the basis for unitary representations of the full rotation group are called tensors. Tensors are then eigenvectors of the Hamiltonian and \hat{L}^2 if the potential of the system is spherically symmetric, as it is with the hydrogen atom.

Referring back to the original Taylor expansion, a zeroth rank tensor is a scalar (f_0), a first rank tensor can be written as a vector:

$$\begin{pmatrix} x \\ y \\ z \end{pmatrix} \quad (A.6)$$

A second rank tensor can be written as a matrix,

$$\begin{pmatrix} x^2 & xy & xz \\ yx & y^2 & yz \\ zx & zy & z^2 \end{pmatrix} \quad (A.7)$$

and a third rank tensor can be imagined as a cubical structure. It should be remembered that this is just a nice way to keep track of the components of the tensor; all are properly viewed as the elements of one long vector.

Here's where we make the connection to chemistry. If $N = 0$, we have a 1-D representation of the rotation group. As a constant (e.g. f_0), this representation is independent of any angle, and thus forms the basis for the totally symmetric representation, and is an eigenfunction for the hydrogen atom Hamiltonian. This function is called an *s*-function, which corresponds to the *s*-orbital an average chemist is familiar with.

If $N = 1$, the first-rank tensor has three components which form the basis of a 3-D irreducible representation. (The representation must be irreducible since each of the rotations around the x , y , and z axes don't commute with one another.) These elements are the eigenfunctions of the Hamiltonian and \hat{L}^2 that form the 3-D *p*-functions, which have the following angular dependence:

$$\begin{aligned} x &= r \sin \theta \cos \phi \\ y &= r \sin \theta \sin \phi \\ z &= r \cos \theta \end{aligned} \quad (A.8)$$

Finally our story comes back to GAMESS and the work I've been doing. If $N = 2$, the second rank tensor forms the basis of a

$$\frac{(2+1)(2+2)}{2} = 6 \quad (\text{A.9})$$

dimensional representation of the full rotation group. The question then becomes, is this 6-D representation irreducible? The answer is no, as one can demonstrate: write the second rank tensor as

$$\begin{pmatrix} x^2 - \frac{r^2}{3} & xy & xz \\ yx & y^2 - \frac{r^2}{3} & yz \\ zx & zy & z^2 - \frac{r^2}{3} \end{pmatrix} + \frac{r^2}{3} \begin{pmatrix} 1 & 0 & 0 \\ 0 & 1 & 0 \\ 0 & 0 & 1 \end{pmatrix} \quad (\text{A.10})$$

Since the second term only depends on r , it is invariant under rotations, and so is a representation of the totally symmetric group (s -functions). The remaining tensor has five independent components since $x^2 + y^2 + z^2 = r^2$, thus

$$\left(x^2 - \frac{r^2}{3} \right) + \left(y^2 - \frac{r^2}{3} \right) + \left(z^2 - \frac{r^2}{3} \right) = r^2 - r^2 = 0 \quad (\text{A.11})$$

And so the third component (usually the z) can be written in terms of x and y . (i.e. It is not linearly independent.) Note that the remaining tensor is both symmetric and traceless; it can be shown that tensors with these characteristics always form the basis of irreducible representations. And so we have a 5-D irreducible representation of the full rotation group, and the familiar d -functions and orbitals. In effect, we have used a spherical harmonic basis to form the 5-D representation, whereas a 6-D representation was required for Cartesian space. Historically, it was easier and faster to use Cartesian functions in quantum calculations, and those

functions were used rather than spherical harmonics. My project was to provide the option to use the spherical functions in GAMESS.

This was accomplished using code written by Michel Dupuis at IBM that was already used in his quantum chemistry package HONDO. GAMESS in large part grew out of HONDO, and much of the code is the same. Dupuis' code removes the linear dependencies found in the Cartesian basis, and leaves the spherical harmonic functions.

This removal of linear dependence is accomplished as follows: This is a summary of what can be found in E. Hollauer, and M. Dupuis, J. Chem. Phys. **96**, 5220, (1992).

Similar to HONDO, GAMESS obtains all the symmetry information on a given molecule by way of its Schoenflies point group symbol, and the specification of its coordinates relative to a given axis. (e.g. In GAMESS, the z -axis is the principal roatation axis, and xz is the σ_v plane, etc.) Once these data are given, GAMESS will use the appropriate character table to generate a Symmetry Adapted Linear Combination (SALC) of atomic orbitals; the atomic orbitals being the given basis set. In effect, linear combinations of the basis functions are formed such that the new functions obey the symmetry of the molecule. This is accomplished by means of a so-called SALC matrix, \mathbf{W} .

Let \mathbf{S} be the overlap matrix of the given basis set:

$$S_{\mu\nu} = \int d\tau \phi_{\mu}^* \phi_{\nu} = \langle \phi_{\mu} | \phi_{\nu} \rangle \quad (\text{A.12})$$

Then \mathbf{W} is constructed such that the overlap matrix, $\tilde{\mathbf{S}}$, of the SALC orbitals can be written as

$$\tilde{\mathbf{S}} = \mathbf{W}^* \mathbf{S} \mathbf{W} \quad (\text{A.13})$$

Once this is done, the overlap matrix of SALC orbitals is block diagonal, each block corresponding an irreducible representation of the point group of the molecule. In

this form, it is easy to diagonalize this matrix and find the eigenvalues and eigenvectors:

$$\tilde{\mathbf{S}}\tilde{\mathbf{U}} = \tilde{\mathbf{s}}\tilde{\mathbf{U}} \quad (\text{A.14})$$

It is at this point that the elimination of linearly dependent functions occurs. $\tilde{\mathbf{U}}$ is a matrix of eigenvectors of $\tilde{\mathbf{S}}$ with eigenvalues $\tilde{\mathbf{s}}$. If any of the SALC functions are linearly dependent, then a corresponding eigenvalue $\tilde{\mathbf{s}}$ will be very close to zero. (The closer to zero, the greater the degreee of linear dependence.) Any eigenfunctions whose corresponding eigenvalue is below a certain threshold are dropped, and in this way, the linearly dependent functions are removed. In GAMESS, this threshold is 1.0×10^{-6} . From this point, a matrix $\tilde{\mathbf{Q}}$ is defined and used to bring us back to the familiar pseudo-eigenvalue problem that arises from a Hartree-Fock formalism. (See Szabo and Ostlund, Section 3.4.4., p. 140.):

$$\begin{aligned} \tilde{\mathbf{Q}} &= \mathbf{W}\tilde{\mathbf{U}}\tilde{\mathbf{s}}^{-\frac{1}{2}} \\ \tilde{\mathbf{Q}}^+\mathbf{S}\tilde{\mathbf{Q}} &= \left(\mathbf{W}\tilde{\mathbf{U}}\tilde{\mathbf{s}}^{-\frac{1}{2}} \right)^+ \mathbf{S} \left(\mathbf{W}\tilde{\mathbf{U}}\tilde{\mathbf{s}}^{-\frac{1}{2}} \right) \\ &= \left(\tilde{\mathbf{s}}^{-\frac{1}{2}} \right)^+ \tilde{\mathbf{U}}^+\mathbf{W}^+\mathbf{S}\mathbf{W}\tilde{\mathbf{U}}\tilde{\mathbf{s}}^{-\frac{1}{2}} \\ &= \left(\tilde{\mathbf{s}}^{-\frac{1}{2}} \right)^+ \tilde{\mathbf{U}}^+\tilde{\mathbf{S}}\tilde{\mathbf{U}}\tilde{\mathbf{s}}^{-\frac{1}{2}} \\ &= \left(\tilde{\mathbf{s}}^{-\frac{1}{2}} \right)^+ \tilde{\mathbf{s}}\tilde{\mathbf{s}}^{-\frac{1}{2}} = \mathbf{1} \end{aligned} \quad (\text{A.15})$$

If one redefines the Fock matrix and its pseudoeigenvectors in terms of this $\tilde{\mathbf{Q}}$ matrix, then the above can be used to modify the Roothaan equation:

$$\begin{aligned}
 \tilde{\mathbf{F}} &= \tilde{\mathbf{Q}}^+ \mathbf{F} \mathbf{Q} \quad ; \quad \mathbf{C} = \tilde{\mathbf{Q}} \tilde{\mathbf{C}} \\
 \Rightarrow \mathbf{F} \mathbf{C} &= \mathbf{S} \mathbf{C} \mathbf{e} \\
 \Rightarrow \mathbf{F} \tilde{\mathbf{Q}} \tilde{\mathbf{C}} &= \mathbf{S} \tilde{\mathbf{Q}} \tilde{\mathbf{C}} \mathbf{e} \\
 \Rightarrow \tilde{\mathbf{Q}}^+ \mathbf{F} \tilde{\mathbf{Q}} \tilde{\mathbf{C}} &= \tilde{\mathbf{Q}}^+ \mathbf{S} \tilde{\mathbf{Q}} \tilde{\mathbf{C}} \mathbf{e} \\
 \Rightarrow \tilde{\mathbf{F}} \tilde{\mathbf{C}} &= \tilde{\mathbf{C}} \mathbf{e}
 \end{aligned} \tag{A.16}$$

\mathbf{Q} is block diagonal like $\tilde{\mathbf{S}}$, so that the transformed Fock matrix is also now a block diagonal $L_0 \times L_0$ matrix, where L_0 is the number of linearly independent functions (MO's). (\mathbf{Q} is $L_1 \times L_0$, where L_1 is the original number of linearly dependent functions.(AO's))

APPENDIX B. GRADIENTS(∇), DIVERGENCE($\nabla \cdot$) AND CURLS($\nabla \times$)

The following vector identities are relevant to the derivations contained in this dissertation. Many can be found in any text on vector calculus, although two (B.17 and B.18) were derived by the author in the course of his research. Short proofs are provided for clarity for those dealing specifically with the positional vector \mathbf{r} . \mathbf{F} , \mathbf{G} , \mathbf{H} , and \mathbf{I} are general vectors.

Some definitions:

$$r = (x^2 + y^2 + z^2)^{\frac{1}{2}} \quad \mathbf{r} = (\hat{\mathbf{x}}x + \hat{\mathbf{y}}y + \hat{\mathbf{z}}z) \quad \hat{\mathbf{r}} = \frac{\mathbf{r}}{r} \quad \nabla = \left(\hat{\mathbf{x}} \frac{\partial}{\partial x} + \hat{\mathbf{y}} \frac{\partial}{\partial y} + \hat{\mathbf{z}} \frac{\partial}{\partial z} \right)$$

$$\mathbf{F} \times \nabla = \begin{vmatrix} \hat{\mathbf{x}} & \hat{\mathbf{y}} & \hat{\mathbf{z}} \\ F_x & F_y & F_z \\ \frac{\partial}{\partial x} & \frac{\partial}{\partial y} & \frac{\partial}{\partial z} \end{vmatrix} = \begin{pmatrix} F_y \frac{\partial}{\partial z} - F_z \frac{\partial}{\partial y} \\ F_z \frac{\partial}{\partial x} - F_x \frac{\partial}{\partial z} \\ F_x \frac{\partial}{\partial y} - F_y \frac{\partial}{\partial x} \end{pmatrix}$$

B.1) $\mathbf{F} \times \mathbf{G} = -\mathbf{G} \times \mathbf{F}$

B.2) $\mathbf{F} \cdot (\mathbf{G} \times \mathbf{H}) = (\mathbf{F} \times \mathbf{G}) \cdot \mathbf{H} = \mathbf{G} \cdot (\mathbf{H} \times \mathbf{F}) = \mathbf{H} \cdot (\mathbf{F} \times \mathbf{G})$

B.3) $\mathbf{F} \times (\mathbf{G} \times \mathbf{H}) = \mathbf{G}(\mathbf{F} \cdot \mathbf{H}) - \mathbf{H}(\mathbf{F} \cdot \mathbf{G})$

B.4) $(\mathbf{F} \times \mathbf{G}) \cdot (\mathbf{H} \times \mathbf{I}) = (\mathbf{F} \cdot \mathbf{H})(\mathbf{G} \cdot \mathbf{I}) - (\mathbf{F} \cdot \mathbf{I})(\mathbf{G} \cdot \mathbf{H})$
 $= \sum_{\alpha\beta} F_\alpha (\mathbf{G} \cdot \mathbf{I} \delta_{\alpha\beta} - G_\alpha I_\beta) H_\beta$

B.5) $\nabla \times \nabla f = 0$

B.6) $\nabla \cdot (f\mathbf{F}) = f(\nabla \cdot \mathbf{F}) + \mathbf{F} \cdot \nabla f$

B.7) $\nabla \times (f\mathbf{F}) = f(\nabla \times \mathbf{F}) + \nabla f \times \mathbf{F}$

B.8) $\nabla \cdot (\mathbf{F} \times \mathbf{G}) = \mathbf{G}(\nabla \times \mathbf{F}) - \mathbf{F}(\nabla \times \mathbf{G})$

B.9) $\nabla \times (\nabla \times \mathbf{F}) = \nabla(\nabla \cdot \mathbf{F}) - \nabla^2 \mathbf{F}$

B.10) $\nabla \times (\mathbf{F} \times \mathbf{G}) = (\mathbf{G} \cdot \nabla) \mathbf{F} - (\mathbf{F} \cdot \nabla) \mathbf{G} - \mathbf{G}(\nabla \cdot \mathbf{F}) + \mathbf{F}(\nabla \cdot \mathbf{G})$

B.11) $\nabla(\mathbf{F} \cdot \mathbf{G}) = (\mathbf{F} \cdot \nabla) \mathbf{G} + (\mathbf{G} \cdot \nabla) \mathbf{F} + \mathbf{F} \times (\nabla \times \mathbf{G}) + \mathbf{G} \times (\nabla \times \mathbf{F})$

B.12) $\nabla r = \hat{\mathbf{r}}$

Proof:

$$\begin{aligned}
\nabla r &= \left(\hat{\mathbf{x}} \frac{\partial}{\partial x} + \hat{\mathbf{y}} \frac{\partial}{\partial y} + \hat{\mathbf{z}} \frac{\partial}{\partial z} \right) (x^2 + y^2 + z^2)^{\frac{1}{2}} \\
&= \hat{\mathbf{x}} \frac{\partial}{\partial x} (x^2 + y^2 + z^2)^{\frac{1}{2}} + \hat{\mathbf{y}} \frac{\partial}{\partial y} (x^2 + y^2 + z^2)^{\frac{1}{2}} + \hat{\mathbf{z}} \frac{\partial}{\partial z} (x^2 + y^2 + z^2)^{\frac{1}{2}} \\
&= \hat{\mathbf{x}} \frac{1}{2} (x^2 + y^2 + z^2)^{-\frac{1}{2}} 2x + \hat{\mathbf{y}} \frac{1}{2} (x^2 + y^2 + z^2)^{-\frac{1}{2}} 2y + \hat{\mathbf{z}} \frac{1}{2} (x^2 + y^2 + z^2)^{-\frac{1}{2}} 2z \\
&= \hat{\mathbf{x}} \frac{x}{r} + \hat{\mathbf{y}} \frac{y}{r} + \hat{\mathbf{z}} \frac{z}{r} = \frac{1}{r} (\hat{\mathbf{x}} x + \hat{\mathbf{y}} y + \hat{\mathbf{z}} z) = \frac{\mathbf{r}}{r} = \hat{\mathbf{r}} \quad Q.E.D.
\end{aligned}$$

$$B.13) \quad \nabla f(r) = \hat{\mathbf{r}} \frac{df(r)}{dr}$$

Proof:

$$\begin{aligned}
\nabla f(r) &= \left(\hat{\mathbf{x}} \frac{\partial}{\partial x} + \hat{\mathbf{y}} \frac{\partial}{\partial y} + \hat{\mathbf{z}} \frac{\partial}{\partial z} \right) f(r) \\
&= \hat{\mathbf{x}} \frac{\partial}{\partial x} f(r) + \hat{\mathbf{y}} \frac{\partial}{\partial y} f(r) + \hat{\mathbf{z}} \frac{\partial}{\partial z} f(r) \\
&= \hat{\mathbf{x}} \frac{df(r)}{dr} \frac{\partial r}{\partial x} + \hat{\mathbf{y}} \frac{df(r)}{dr} \frac{\partial r}{\partial y} + \hat{\mathbf{z}} \frac{df(r)}{dr} \frac{\partial r}{\partial z} \\
&= \frac{df(r)}{dr} \left(\hat{\mathbf{x}} \frac{\partial}{\partial x} + \hat{\mathbf{y}} \frac{\partial}{\partial y} + \hat{\mathbf{z}} \frac{\partial}{\partial z} \right) r = \hat{\mathbf{r}} \frac{df(r)}{dr} \quad Q.E.D.
\end{aligned}$$

$$B.14) \quad \nabla \mathbf{r} f(r) = 3f(r) + r \frac{df(r)}{dr}$$

Proof:

$$\begin{aligned}
\nabla \mathbf{r} f(r) &= \nabla (\hat{\mathbf{x}} x + \hat{\mathbf{y}} y + \hat{\mathbf{z}} z) f(r) + (\hat{\mathbf{x}} x + \hat{\mathbf{y}} y + \hat{\mathbf{z}} z) \nabla f(r) \\
&= \left(\hat{\mathbf{x}} \frac{\partial}{\partial x} + \hat{\mathbf{y}} \frac{\partial}{\partial y} + \hat{\mathbf{z}} \frac{\partial}{\partial z} \right) (\hat{\mathbf{x}} x + \hat{\mathbf{y}} y + \hat{\mathbf{z}} z) f(r) + (\hat{\mathbf{x}} x + \hat{\mathbf{y}} y + \hat{\mathbf{z}} z) \left(\hat{\mathbf{x}} \frac{\partial}{\partial x} + \hat{\mathbf{y}} \frac{\partial}{\partial y} + \hat{\mathbf{z}} \frac{\partial}{\partial z} \right) f(r) \\
&= 3f(r) + (\hat{\mathbf{x}} x + \hat{\mathbf{y}} y + \hat{\mathbf{z}} z) \hat{\mathbf{r}} \frac{df(r)}{dr} \\
&= 3f(r) + (\hat{\mathbf{x}} x + \hat{\mathbf{y}} y + \hat{\mathbf{z}} z) \frac{(\hat{\mathbf{x}} x + \hat{\mathbf{y}} y + \hat{\mathbf{z}} z)}{r} \frac{df(r)}{dr} \\
&= 3f(r) + \frac{(x^2 + y^2 + z^2)}{r} \frac{df(r)}{dr} = 3f(r) + \frac{r^2}{r} \frac{df(r)}{dr} = 3f(r) + r \frac{df(r)}{dr} \quad Q.E.D.
\end{aligned}$$

$$B.15) \quad \nabla \hat{\mathbf{r}} = \frac{2}{r}$$

Proof:

$$\begin{aligned}\nabla \hat{\mathbf{r}} &= \nabla \frac{\mathbf{r}}{r} = \frac{\nabla \mathbf{r}}{r} + \mathbf{r} \nabla \frac{1}{r} = \frac{3}{r} + \mathbf{r} \nabla \frac{1}{r} = \frac{3}{r} + \mathbf{r} \hat{\mathbf{r}} \frac{d}{dr} r^{-1} \\ &= \frac{3}{r} - \mathbf{r} \hat{\mathbf{r}} \left(\frac{1}{r^2} \right) = \frac{3}{r} - \frac{\mathbf{r} \cdot \mathbf{r}}{r} \left(\frac{1}{r^2} \right) = \frac{3}{r} - \frac{r^2}{r} \left(\frac{1}{r^2} \right) = \frac{2}{r} \quad Q.E.D.\end{aligned}$$

$$\text{B.16) } \nabla^2 \mathbf{r} r^{n-1} = \hat{\mathbf{r}} (n+2)(n-1) r^{n-2}$$

Proof:

$$\begin{aligned}\nabla^2 \mathbf{r} r^{n-1} &= \nabla \left(\nabla \mathbf{r} r^{n-1} + \mathbf{r} \nabla r^{n-1} \right) = \nabla \left(3r^{n-1} + \mathbf{r} \hat{\mathbf{r}} \frac{d}{dr} r^{n-1} \right) \\ &= \nabla [3r^{n-1} + r(n-1)r^{n-2}] = \nabla [3r^{n-1} + (n-1)r^{n-1}] = (n+2) \nabla r^{n-1} \\ &= (n+2) \nabla r^{n-1} = \hat{\mathbf{r}} (n+2)(n-1) r^{n-2} \quad Q.E.D.\end{aligned}$$

$$\text{B.17) } \nabla \frac{df(r)}{dr} = \hat{\mathbf{r}} \frac{d^2 f(r)}{dr^2}$$

Proof:

$$\nabla \frac{df(r)}{dr} = \hat{\mathbf{r}} \frac{d}{dr} \frac{df(r)}{dr} = \hat{\mathbf{r}} \frac{d^2 f(r)}{dr^2} \quad Q.E.D.$$

$$\text{B.18) } \nabla^2 \mathbf{r} f(r) = \hat{\mathbf{r}} \left[4 \frac{df(r)}{dr} + r \frac{d^2 f(r)}{dr^2} \right]$$

Proof:

$$\begin{aligned}\nabla^2 \mathbf{r} f(r) &= \nabla [\nabla \mathbf{r} f(r)] = \nabla \left[3f(r) + r \frac{df(r)}{dr} \right] \\ &= 3 \nabla f(r) + \nabla r \frac{df(r)}{dr} + r \nabla \frac{df(r)}{dr} \\ &= 3 \hat{\mathbf{r}} \frac{df(r)}{dr} + \hat{\mathbf{r}} \frac{df(r)}{dr} + r \hat{\mathbf{r}} \frac{d^2 f(r)}{dr^2} \\ &= \hat{\mathbf{r}} \left[4 \frac{df(r)}{dr} + r \frac{d^2 f(r)}{dr^2} \right] \quad Q.E.D.\end{aligned}$$

APPENDIX C. GAUGE INVARIANT ATOMIC ORBITAL DERIVATIONS

C.1) The general expression for the magnetic field induced by a current distribution in atomic units is given by the Biot-Savart Law:¹²⁵

$$\mathbf{H} = \frac{1}{c^2} \int_v dv \frac{\mathbf{j} \times \mathbf{r}}{r^3} \quad (C.1.1)$$

where \mathbf{j} is the current density (with SI units of A m^{-2}), \mathbf{r} is the point where the field is observed, and dv is an element of volume. Therefore the *volume current element* is defined as $\mathbf{j} dv$. We can further modify the form of Eq. (C.1.1) as follows:

$$\mathbf{H} = \frac{1}{c^2} \int_v dv \nabla \times \frac{\mathbf{j}}{r} \quad (C.1.2)$$

since

$$\nabla \times \frac{\mathbf{j}}{r} = \nabla \left(\frac{1}{r} \right) \times \mathbf{j} = -\frac{\mathbf{r}}{r^3} \times \mathbf{j} = \frac{\mathbf{j} \times \mathbf{r}}{r^3} \quad (C.1.3)$$

such that the curl can be pulled out of the integral to easily identify the vector potential:

$$\begin{aligned} \mathbf{H} &= \nabla \times \frac{1}{c^2} \int_v dv \frac{\mathbf{j}}{r} \\ \Rightarrow \mathbf{A} &= \frac{1}{c^2} \int_v dv \frac{\mathbf{j}}{r} = \frac{1}{c^2} I \oint_C \frac{d\mathbf{l}}{r} \end{aligned} \quad (C.1.4)$$

where we have applied the specific case for which the current is constrained to flow along a thin wire, and it is convenient to replace the current element $\mathbf{j} dv$ with $I d\mathbf{l}$, where I is the current and $d\mathbf{l}$ is a element of length. The current physical situation is given by Fig. (C.1.1):

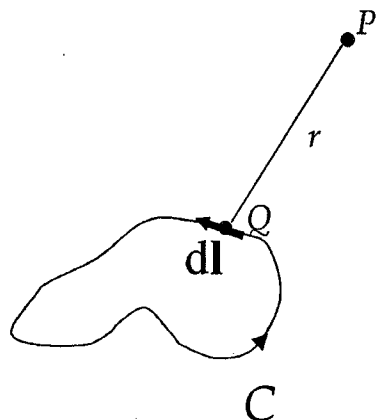


Fig. (C.1.1) Physical representation of Eq. (C.1.4)

The integration is around the closed circuit, C . Then, using Stokes' Theorem:

$$\oint_C \phi d\mathbf{L} = \int_S d\mathbf{S} \times \nabla \phi \quad (C.1.5)$$

where S is the surface area; then

$$\mathbf{A} = \frac{1}{c^2} I \int_S d\mathbf{S} \times \nabla \phi \left(\frac{1}{r} \right) \quad (C.1.6)$$

The physical picture is now given by Fig. (C.1.2):

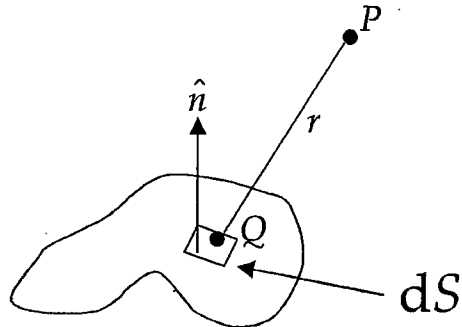


Fig. (C.1.2) Physical interpretation of Eq. (C.1.6). \hat{n} is a unit vector normal to the volume element dS .

Note that

$$\nabla_Q \left(\frac{1}{r} \right) = -\nabla_P \left(\frac{1}{r} \right) = \frac{\mathbf{r}}{r^3} \quad (C.1.7)$$

Then if we assume the current loop is very small, as in an atomic nucleus, we can assume \mathbf{r} and r to be constant, and pull them out of the integral:

$$\mathbf{A} = \frac{1}{c^2} \left(I \int_S d\mathbf{S} \right) \times \frac{\mathbf{r}}{r^3} = \frac{1}{c^2} \frac{\mathbf{\mu} \times \mathbf{r}}{r^3} \quad (C.1.8)$$

where the nuclear magnetic moment has been defined as

$$\mathbf{\mu} = I \int_S d\mathbf{S} = I \int_S \hat{n} dS = \frac{1}{2} I \oint_C \mathbf{r} \times d\mathbf{l} \quad (C.1.9)$$

[Note that Ditchfield does not associate the factor of $1/c^2$ with this term; instead, he uses a factor of $1/c$ before the *total* vector potential in Eq. (3.1), following many authors. See footnote after presentation of Eq. (3.1).]

If we expand the kinetic and magnetic parts of the Hamiltonian, Eq. (3.1), and evaluate the resulting terms:

$$\begin{aligned}
 \left(-i\nabla_j + \frac{1}{c}\mathbf{A}'(\mathbf{r}_j) \right)^2 &= \left(-i\nabla_j + \frac{1}{c}\mathbf{A}'(\mathbf{r}_j) \right) \left(-i\nabla_j + \frac{1}{c}\mathbf{A}'(\mathbf{r}_j) \right) \\
 &= -\nabla_j^2 - \frac{i}{c}(\nabla_j \cdot \mathbf{A}'(\mathbf{r}_j)) - \frac{i}{c}(\mathbf{A}'(\mathbf{r}_j) \cdot \nabla_j) + \frac{1}{c^2}\mathbf{A}'^2(\mathbf{r}_j) \\
 &= -\nabla_j^2 - \frac{i}{c}(\nabla_j \cdot \mathbf{A}'(\mathbf{r}_j)) - \frac{2i}{c}(\mathbf{A}'(\mathbf{r}_j) \cdot \nabla_j) + \frac{1}{c^2}\mathbf{A}'^2(\mathbf{r}_j)
 \end{aligned} \tag{C.2.1}$$

and since we are using the coulomb gauge, which by definition requires

$$\nabla_j \cdot \mathbf{A}'(\mathbf{r}_j) = 0 \tag{C.2.2}$$

The other terms are

$$\begin{aligned}
 \mathbf{A}'(\mathbf{r}_j) \cdot \nabla_j &= \left[\frac{1}{2}\mathbf{H} \times \mathbf{r}_j + \sum_B \frac{\boldsymbol{\mu}_B \times \mathbf{r}_{jB}}{r_{jB}^3} \right] \cdot \nabla_j \\
 &= \frac{1}{2}\mathbf{H} \times \mathbf{r}_j \cdot \nabla_j + \sum_B \frac{\boldsymbol{\mu}_B \times \mathbf{r}_{jB} \cdot \nabla_j}{r_{jB}^3} \\
 &= \frac{1}{2}\mathbf{H} \cdot \mathbf{r}_j \times \nabla_j + \sum_B \frac{\boldsymbol{\mu}_B \cdot \mathbf{r}_{jB} \times \nabla_j}{r_{jB}^3} \\
 &= \frac{1}{2} \sum_{\alpha} H_{\alpha} (\mathbf{r}_j \times \nabla_j)_{\alpha} + \sum_{\alpha, B} \frac{\mu_{B\alpha} (\mathbf{r}_{jB} \times \nabla_j)_{\alpha}}{r_{jB}^3}
 \end{aligned} \tag{C.2.3}$$

using (B.2), and

$$\begin{aligned}
\mathbf{A}'^2(\mathbf{r}_j) &= \left[\frac{1}{2} \mathbf{H} \times \mathbf{r}_j + \sum_B \frac{\boldsymbol{\mu}_B \times \mathbf{r}_{jB}}{r_{jB}^3} \right] \cdot \left[\frac{1}{2} \mathbf{H} \times \mathbf{r}_j + \sum_B \frac{\boldsymbol{\mu}_B \times \mathbf{r}_{jB}}{r_{jB}^3} \right] \\
&= \left(\frac{1}{2} \mathbf{H} \times \mathbf{r}_j \right) \cdot \left(\frac{1}{2} \mathbf{H} \times \mathbf{r}_j \right) + \left(\frac{1}{2} \mathbf{H} \times \mathbf{r}_j \right) \cdot \left(\sum_B \frac{\boldsymbol{\mu}_B \times \mathbf{r}_{jB}}{r_{jB}^3} \right) \\
&\quad + \left(\sum_B \frac{\boldsymbol{\mu}_B \times \mathbf{r}_{jB}}{r_{jB}^3} \right) \cdot \left(\frac{1}{2} \mathbf{H} \times \mathbf{r}_j \right) + \left(\sum_B \frac{\boldsymbol{\mu}_B \times \mathbf{r}_{jB}}{r_{jB}^3} \right) \cdot \left(\sum_{B'} \frac{\boldsymbol{\mu}_{B'} \times \mathbf{r}_{jB'}}{r_{jB'}^3} \right) \\
&= \sum_{\alpha, \beta} \frac{1}{2} H_\alpha \left(\mathbf{r}_j \cdot \mathbf{r}_j \delta_{\alpha\beta} - r_{j\alpha} r_{j\beta} \right) \frac{1}{2} H_\beta + \sum_{B, \alpha, \beta} \frac{1}{2} H_\alpha \frac{(\mathbf{r}_j \cdot \mathbf{r}_{jB} \delta_{\alpha\beta} - r_{j\alpha} r_{jB\beta})}{r_{jB}^3} \mu_{B\beta} \\
&\quad + \sum_{B, \alpha, \beta} \mu_{B\alpha} \frac{(\mathbf{r}_{jB} \cdot \mathbf{r}_j \delta_{\alpha\beta} - r_{jB\alpha} r_{j\beta})}{r_{jB}^3} \frac{1}{2} H_\beta + \sum_{B, B', \alpha, \beta} \mu_{B\alpha} \frac{(\mathbf{r}_{jB} \cdot \mathbf{r}_{jB'} \delta_{\alpha\beta} - r_{jB\alpha} r_{jB'\beta})}{r_{jB}^3 r_{jB'}^3} \mu_{B'\beta}
\end{aligned} \tag{C.2.4}$$

using (B.4). Note that the last term here has been dropped since it corresponds to $\mathcal{H}_\alpha^{(0,2)}$, which is not included in this discussion. (It is the mutual interaction of the nuclear magnetic moments, which is related to spin-spin coupling.) Therefore,

$$\mathbf{A}'^2(\mathbf{r}_j) = \frac{1}{4} \sum_{\alpha, \beta} H_\alpha \left(r_j^2 \delta_{\alpha\beta} - r_{j\alpha} r_{j\beta} \right) H_\beta + \sum_{B, \alpha, \beta} H_\alpha \frac{(\mathbf{r}_j \cdot \mathbf{r}_{jB} \delta_{\alpha\beta} - r_{j\alpha} r_{jB\beta})}{r_{jB}^3} \mu_{B\beta} \tag{C.2.5}$$

All of which makes Eq. (3.1)

$$\begin{aligned}
\mathcal{H}(\mathbf{H}, \boldsymbol{\mu}) &= \frac{1}{2} \sum_j \left\{ \left(-\nabla_j^2 - \frac{2i}{c} (\mathbf{A}'(\mathbf{r}_j) \cdot \nabla_j) + \frac{1}{c^2} \mathbf{A}'^2(\mathbf{r}_j) \right) - 2 \sum_B \frac{Z_B}{r_{jB}} \right\} + \sum_{j \neq l} \frac{1}{r_{jl}} + \sum_{B \neq D} \frac{Z_B Z_D}{R_{BD}} \\
&= \frac{1}{2} \sum_j \left\{ \left(-\nabla_j^2 - \frac{2i}{c} \left(\frac{1}{2} \sum_\alpha H_\alpha (\mathbf{r}_j \times \nabla_j)_\alpha + \sum_{\alpha, B} \frac{\mu_{B\alpha} (\mathbf{r}_{jB} \times \nabla_j)_\alpha}{r_{jB}^3} \right) \right) \right. \\
&\quad \left. + \frac{1}{c^2} \left(\frac{1}{4} \sum_{\alpha, \beta} H_\alpha (r_j^2 \delta_{\alpha\beta} - r_{j\alpha} r_{j\beta}) H_\beta + \sum_{B, \alpha, \beta} H_\alpha \frac{(\mathbf{r}_j \cdot \mathbf{r}_{jB} \delta_{\alpha\beta} - r_{j\alpha} r_{jB\beta})}{r_{jB}^3} \mu_{B\beta} \right) \right\} + \sum_{j \neq l} \frac{1}{r_{jl}} + \sum_{B \neq D} \frac{Z_B Z_D}{R_{BD}}
\end{aligned}$$

$$\begin{aligned}
& \left. \left(\begin{array}{l} -\frac{1}{2} \nabla_j^2 - \frac{i}{2c} \sum_{\alpha} H_{\alpha} (\mathbf{r}_j \times \nabla_j)_{\alpha} - \frac{i}{c} \sum_{\alpha, B} \frac{\mu_{B\alpha} (\mathbf{r}_{jB} \times \nabla_j)_{\alpha}}{r_{jB}^3} \\ + \frac{1}{8c^2} \sum_{\alpha, \beta} H_{\alpha} (r_j^2 \delta_{\alpha\beta} - r_{j\alpha} r_{j\beta}) H_{\beta} + \frac{1}{2c^2} \sum_{B, \alpha, \beta} H_{\alpha} \frac{(\mathbf{r}_j \cdot \mathbf{r}_{jB} \delta_{\alpha\beta} - r_{j\alpha} r_{jB\beta})}{r_{jB}^3} \mu_{B\beta} \\ - \sum_B \frac{Z_B}{r_{jB}} \end{array} \right) \right\} + \sum_{j \neq l} \frac{1}{r_{jl}} + \sum_{B \neq D} \frac{Z_B Z_D}{R_{BD}} \\
& = -\frac{1}{2} \sum_j \nabla_j^2 - \sum_B \frac{Z_B}{r_{jB}} + \sum_{j \neq l} \frac{1}{r_{jl}} + \sum_{B \neq D} \frac{Z_B Z_D}{R_{BD}} - \frac{i}{2c} \sum_{\alpha} H_{\alpha} \sum_j (\mathbf{r}_j \times \nabla_j)_{\alpha} - \frac{i}{c} \sum_{\alpha, B} \mu_{B\alpha} \sum_j \frac{(\mathbf{r}_{jB} \times \nabla_j)_{\alpha}}{r_{jB}^3} \\
& \quad + \frac{1}{8c^2} \sum_{\alpha, \beta} H_{\alpha} \sum_j (r_j^2 \delta_{\alpha\beta} - r_{j\alpha} r_{j\beta}) H_{\beta} + \frac{1}{2c^2} \sum_{B, \alpha, \beta} H_{\alpha} \sum_j \frac{(\mathbf{r}_j \cdot \mathbf{r}_{jB} \delta_{\alpha\beta} - r_{j\alpha} r_{jB\beta})}{r_{jB}^3} \mu_{B\beta}
\end{aligned}$$

C.3) Begin by using definitions similar to that in Eq. (3.11, 13) for first order terms,

$$\text{i.e. } \left. \frac{\partial P_{v\lambda}}{\partial H_{\alpha}} \right|_0 = i \left(P_{v\lambda}^{(1,0)} \right)_{\alpha} :$$

$$\begin{aligned}
\left(P_{v\lambda}^{(1,0)} \right)_{\alpha} &= -i \left. \frac{\partial P_{v\lambda}(H_{\alpha}, \mu_{B\beta})}{\partial H_{\alpha}} \right|_0 = -i \left. \frac{\partial}{\partial H_{\alpha}} \left(2 \sum_j^{occ} c_{vj}(H_{\alpha}, \mu_{B\beta}) c_{\lambda j}^*(H_{\alpha}, \mu_{B\beta}) \right) \right|_0 \\
&= -i \left. \frac{\partial}{\partial H_{\alpha}} \left(2 \sum_j^{occ} \left(c_{vj}^{(0)} + i H_{\alpha} (c_{vj}^{(1,0)})_{\alpha} + \dots \right) \left(c_{\lambda j}^{(0)} - i H_{\alpha} (c_{\lambda j}^{(1,0)})_{\alpha} + \dots \right) \right) \right|_0 \\
&= -i 2 \sum_j^{occ} -i c_{vj}^{(0)} (c_{\lambda j}^{(1,0)})_{\alpha} + i (c_{vj}^{(1,0)})_{\alpha} c_{\lambda j}^{(0)} \\
&= 2 \sum_j^{occ} (c_{vj}^{(1,0)})_{\alpha} c_{\lambda j}^{(0)} - c_{vj}^{(0)} (c_{\lambda j}^{(1,0)})_{\alpha} \\
\left(P_{Bv\lambda}^{(0,1)} \right)_{\beta} &= -i \left. \frac{\partial P_{v\lambda}(H_{\alpha}, \mu_{B\beta})}{\partial \mu_{B\beta}} \right|_0 = -i \left. \frac{\partial}{\partial \mu_{B\beta}} \left(2 \sum_j^{occ} c_{vj}(H_{\alpha}, \mu_{B\beta}) c_{\lambda j}^*(H_{\alpha}, \mu_{B\beta}) \right) \right|_0 \\
&= -i \left. \frac{\partial}{\partial \mu_{B\beta}} \left(2 \sum_j^{occ} \left(c_{vj}^{(0)} + i \mu_{B\beta} (c_{Bvj}^{(0,1)})_{\beta} + \dots \right) \left(c_{\lambda j}^{(0)} - i \mu_{B\beta} (c_{B\lambda j}^{(0,1)})_{\beta} + \dots \right) \right) \right|_0 \\
&= -2i \sum_j^{occ} -i c_{vj}^{(0)} (c_{B\lambda j}^{(0,1)})_{\beta} + i (c_{Bvj}^{(0,1)})_{\beta} c_{\lambda j}^{(0)} \\
&= 2 \sum_j^{occ} (c_{Bvj}^{(0,1)})_{\beta} c_{\lambda j}^{(0)} - c_{vj}^{(0)} (c_{B\lambda j}^{(0,1)})_{\beta}
\end{aligned}$$

C.4) Using Eq. (3.28):

$$\begin{aligned}
 \left(G_{Bv\lambda}^{(0,1)} \right)_\beta &= -i \frac{\partial G_{v\lambda}(H_\alpha, \mu_{B\beta})}{\partial \mu_{B\beta}} \Big|_0 = -i \frac{\partial}{\partial \mu_{B\beta}} \left(\sum_{\rho\sigma} P_{\rho\sigma}(H_\alpha, \mu_{B\beta}) G_{v\lambda\rho\sigma}(H_\alpha) \right) \Big|_0 \\
 &= -i \sum_{\rho\sigma} i \left(P_{B\rho\sigma}^{(0,1)} \right)_\alpha G_{v\lambda\rho\sigma}^{(0)} \\
 &= \sum_{\rho\sigma} \left(P_{B\rho\sigma}^{(0,1)} \right)_\alpha G_{v\lambda\rho\sigma}^{(0)}
 \end{aligned}$$

Since $G_{v\lambda\rho\sigma}^{(0)}$ does not depend on the nuclear magnetic moments.

C.5)

$$\begin{aligned}
 \frac{\partial E}{\partial \mu_{B\beta}} \Big|_0 &= \sum_{v\lambda} \left\{ \frac{\partial P_{v\lambda}}{\partial \mu_{B\beta}} \left(H_{v\lambda} + \frac{1}{2} G_{v\lambda} \right) + P_{v\lambda} \left(\frac{\partial H_{v\lambda}}{\partial \mu_{B\beta}} + \frac{1}{2} \frac{\partial G_{v\lambda}}{\partial \mu_{B\beta}} \right) \right\} \\
 &= \sum_{v\lambda} \left\{ i \left(P_{Bv\lambda}^{(0,1)} \right)_\beta \left(H_{v\lambda}^{(0)} + \frac{1}{2} G_{v\lambda}^{(0)} \right) + P_{v\lambda}^{(0)} \left(i \left(H_{Bv\lambda}^{(0,1)} \right)_\beta + \frac{i}{2} \left(G_{Bv\lambda}^{(0,1)} \right)_\beta \right) \right\}
 \end{aligned}$$

then, using Eqs. (3.28) and (3.32),

$$\begin{aligned}
 \frac{\partial E}{\partial \mu_{B\beta}} \Big|_0 &= \sum_{v\lambda} \left\{ i \left(P_{Bv\lambda}^{(0,1)} \right)_\beta \left(H_{v\lambda}^{(0)} + \frac{1}{2} \sum_{\rho\sigma} P_{\rho\sigma}^{(0)} G_{v\lambda\rho\sigma}^{(0)} \right) + P_{v\lambda}^{(0)} \left(i \left(H_{Bv\lambda}^{(0,1)} \right)_\beta + \frac{i}{2} \sum_{\rho\sigma} \left(P_{B\rho\sigma}^{(0,1)} \right)_\beta G_{v\lambda\rho\sigma}^{(0)} \right) \right\} \\
 &= i \sum_{v\lambda\rho\sigma} \left\{ \left(P_{Bv\lambda}^{(0,1)} \right)_\beta H_{v\lambda}^{(0)} + \frac{1}{2} \left(P_{Bv\lambda}^{(0,1)} \right)_\beta P_{\rho\sigma}^{(0)} G_{v\lambda\rho\sigma}^{(0)} + P_{v\lambda}^{(0)} \left(H_{Bv\lambda}^{(0,1)} \right)_\beta + \frac{1}{2} P_{v\lambda}^{(0)} \left(P_{B\rho\sigma}^{(0,1)} \right)_\beta G_{v\lambda\rho\sigma}^{(0)} \right\}
 \end{aligned}$$

recognizing dummy indices, we combine:

$$\begin{aligned}
 \frac{\partial E}{\partial \mu_{B\beta}} \Big|_0 &= i \sum_{v\lambda\rho\sigma} \left\{ \left(P_{Bv\lambda}^{(0,1)} \right)_\beta H_{v\lambda}^{(0)} + \left(P_{Bv\lambda}^{(0,1)} \right)_\beta P_{\rho\sigma}^{(0)} G_{v\lambda\rho\sigma}^{(0)} + P_{v\lambda}^{(0)} \left(H_{Bv\lambda}^{(0,1)} \right)_\beta \right\} \\
 &= i \sum_{v\lambda\rho\sigma} \left\{ \left(P_{Bv\lambda}^{(0,1)} \right)_\beta \left(H_{v\lambda}^{(0)} + P_{\rho\sigma}^{(0)} G_{v\lambda\rho\sigma}^{(0)} \right) + P_{v\lambda}^{(0)} \left(H_{Bv\lambda}^{(0,1)} \right)_\beta \right\} \\
 &= i \sum_{v\lambda} \left\{ \left(P_{Bv\lambda}^{(0,1)} \right)_\beta \left(H_{v\lambda}^{(0)} + G_{v\lambda}^{(0)} \right) + P_{v\lambda}^{(0)} \left(H_{Bv\lambda}^{(0,1)} \right)_\beta \right\}
 \end{aligned}$$

Finally, using Eq. (3.26),

$$\left. \frac{\partial E}{\partial \mu_{B\beta}} \right|_0 = i \sum_{v\lambda} \left\{ \left(P_{Bv\lambda}^{(0,1)} \right)_\beta F_{v\lambda}^{(0)} + P_{v\lambda}^{(0)} \left(H_{Bv\lambda}^{(0,1)} \right)_\beta \right\}$$

C.6)

$$\begin{aligned} \frac{\partial}{\partial \mu_{B\beta}} \left(\sum_{v\lambda} c_{vj}^* c_{\lambda l} S_{v\lambda} = \delta_{jl} \right) \\ \sum_{v\lambda} \left[\frac{\partial c_{vj}^*}{\partial \mu_{B\beta}} c_{\lambda l} + c_{vj}^* \frac{\partial c_{\lambda l}}{\partial \mu_{B\beta}} \right] S_{v\lambda} = \frac{\partial \delta_{jl}}{\partial \mu_{B\beta}} \end{aligned}$$

since the overlap matrix does not depend on the nuclear magnetic moments.

$$\begin{aligned} \Rightarrow \sum_{v\lambda} \left[\begin{aligned} & \frac{\partial}{\partial \mu_{B\beta}} \left(c_{vj}^{(0)} - i\mu_{B\beta} \left(c_{Bvj}^{(0,1)} \right)_\beta - \dots \right) c_{\lambda l} \\ & + c_{vj}^* \frac{\partial}{\partial \mu_{B\beta}} \left(c_{\lambda l}^{(0)} + i\mu_{B\beta} \left(c_{B\lambda l}^{(0,1)} \right)_\beta + \dots \right) \end{aligned} \right] S_{v\lambda} = 0 \\ \sum_{v\lambda} \left[-i \left(c_{Bvj}^{(0,1)} \right)_\beta c_{\lambda l}^{(0)} + i c_{vj}^{(0)} \left(c_{B\lambda l}^{(0,1)} \right)_\beta \right] S_{v\lambda}^{(0)} = 0 \\ i \sum_{v\lambda} \left[c_{vj}^{(0)} \left(c_{B\lambda l}^{(0,1)} \right)_\beta - \left(c_{Bvj}^{(0,1)} \right)_\beta c_{\lambda l}^{(0)} \right] S_{v\lambda}^{(0)} = 0 \end{aligned}$$

C.7)

$$\begin{aligned}
\left. \frac{\partial E}{\partial \mu_{B\beta}} \right|_0 &= i \sum_{\nu\lambda} \left\{ \left(P_{B\nu\lambda}^{(0,1)} \right)_\beta F_{\nu\lambda}^{(0)} + P_{\nu\lambda}^{(0)} \left(H_{B\nu\lambda}^{(0,1)} \right)_\beta \right\} \\
&= i \sum_{\nu\lambda} \left\{ 2 \sum_j \left[\left(C_{B\nu j}^{(0,1)} \right)_\beta C_{\lambda j}^{(0)} - C_{\nu j}^{(0)} \left(C_{B\lambda j}^{(0,1)} \right)_\beta \right] F_{\nu\lambda}^{(0)} + P_{\nu\lambda}^{(0)} \left(H_{B\nu\lambda}^{(0,1)} \right)_\beta \right\} \\
&= i \sum_{\nu\lambda} \left\{ 2 \sum_j \left[\left(C_{B\nu j}^{(0,1)} \right)_\beta C_{\lambda j}^{(0)} \varepsilon_j^{(0)} S_{\nu\lambda}^{(0)} - C_{\nu j}^{(0)} \varepsilon_j^{(0)} S_{\nu\lambda}^{(0)} \left(C_{B\lambda j}^{(0,1)} \right)_\beta \right] + P_{\nu\lambda}^{(0)} \left(H_{B\nu\lambda}^{(0,1)} \right)_\beta \right\} \\
&= -2 \sum_j \varepsilon_j^{(0)} \left[i \sum_{\nu\lambda} C_{\nu j}^{(0)} \left(C_{B\lambda j}^{(0,1)} \right)_\beta - \left(C_{B\nu j}^{(0,1)} \right)_\beta C_{\lambda j}^{(0)} \right] S_{\nu\lambda}^{(0)} + i \sum_{\nu\lambda} P_{\nu\lambda}^{(0)} \left(H_{B\nu\lambda}^{(0,1)} \right)_\beta \\
&= -2 \sum_j \varepsilon_j^{(0)} [0] + i \sum_{\nu\lambda} P_{\nu\lambda}^{(0)} \left(H_{B\nu\lambda}^{(0,1)} \right)_\beta \\
&= i \sum_{\nu\lambda} P_{\nu\lambda}^{(0)} \left(H_{B\nu\lambda}^{(0,1)} \right)_\beta
\end{aligned}$$

C.8) Compare the first parts of this derivation with (C.2). Begin with Eq. (3.27):

$$\frac{1}{2} \left(-i\nabla + \frac{1}{c} \mathbf{A}'(\mathbf{r}) \right)^2 = -\frac{1}{2} \nabla^2 - \frac{i}{2c} (\nabla \cdot \mathbf{A}'(\mathbf{r})) - \frac{i}{c} (\mathbf{A}'(\mathbf{r}) \cdot \nabla) + \frac{1}{2c^2} \mathbf{A}'^2(\mathbf{r})$$

where, as before, $\nabla \cdot \mathbf{A}'(\mathbf{r}) = 0$, and

$$\mathbf{A}'(\mathbf{r}) \cdot \nabla = \frac{1}{2} \sum_{\alpha} H_{\alpha} (\mathbf{r} \times \nabla)_{\alpha} + \sum_{\alpha, B} \frac{\mu_{B\alpha} (\mathbf{r}_B \times \nabla)_{\alpha}}{r_B^3}$$

and

$$\mathbf{A}'^2(\mathbf{r}) = \frac{1}{4} \sum_{\alpha, \beta} H_{\alpha} (r^2 \delta_{\alpha\beta} - r_{\alpha} r_{\beta}) H_{\beta} + \sum_{B, \alpha, \beta} H_{\alpha} \frac{(\mathbf{r} \cdot \mathbf{r}_B \delta_{\alpha\beta} - r_{\alpha} r_{B\beta})}{r_B^3} \mu_{B\beta}$$

such that

$$\begin{aligned}
\frac{1}{2} \left(-i\nabla + \frac{1}{c} \mathbf{A}'(\mathbf{r}) \right)^2 &= -\frac{1}{2} \nabla^2 - \frac{i}{c} \left(\frac{1}{2} \sum_{\alpha} H_{\alpha} (\mathbf{r} \times \nabla)_{\alpha} + \sum_{\alpha, B} \frac{\mu_{B\alpha} (\mathbf{r}_B \times \nabla)_{\alpha}}{r_B^3} \right) \\
&\quad + \frac{1}{2c^2} \left(\frac{1}{4} \sum_{\alpha, \beta} H_{\alpha} (r^2 \delta_{\alpha\beta} - r_{\alpha} r_{\beta}) H_{\beta} + \sum_{B, \alpha, \beta} H_{\alpha} \frac{(\mathbf{r} \cdot \mathbf{r}_B \delta_{\alpha\beta} - r_{\alpha} r_{B\beta})}{r_B^3} \mu_{B\beta} \right)
\end{aligned}$$

such that the derivative with respect to the nuclear magnetic moments is evaluated:

$$\begin{aligned}
 (H_{B\nu\lambda}^{(0,1)})_{\beta} &= -i \frac{\partial H_{\nu\lambda}(0, \mu_{B\beta})}{\partial \mu_{B\beta}} \Big|_0 = -i \frac{\partial}{\partial \mu_{B\beta}} \left\langle \phi_{\nu} \left| -\frac{i}{c} \left(\frac{\mu_{B\beta} (\mathbf{r}_B \times \nabla)_{\beta}}{r_B^3} \right) - \sum_B \frac{Z_B}{r_B} \right| \phi_{\lambda} \right\rangle \\
 &= \frac{i^2}{c} \left\langle \phi_{\nu} \left| \frac{(\mathbf{r}_B \times \nabla)_{\beta}}{r_B^3} \right| \phi_{\lambda} \right\rangle \\
 &= -\frac{1}{c} \left\langle \phi_{\nu} \left| \frac{L_{\beta}^B}{r_B^3} \right| \phi_{\lambda} \right\rangle
 \end{aligned}$$

C.9)

$$\begin{aligned}
 (H_{B\nu\lambda}^{(1,1)})_{\alpha\beta} &= \frac{\partial^2 H_{\nu\lambda}}{\partial H_{\alpha} \partial \mu_{B\beta}} \Big|_0 = \frac{\partial^2}{\partial H_{\alpha} \partial \mu_{B\beta}} \langle \chi_{\nu} \left| \left\{ \frac{1}{2} \left(-i\nabla + \frac{1}{c} \mathbf{A}'(\mathbf{r}) \right)^2 - \sum_B \frac{Z_B}{r_B} \right\} \right| \chi_{\lambda} \rangle \\
 &= \frac{\partial^2}{\partial H_{\alpha} \partial \mu_{B\beta}} \langle \chi_{\nu} \left| \left\{ \frac{1}{2} \left(-i\nabla + \frac{1}{c} \mathbf{A}'(\mathbf{r}) \right)^2 \right\} \right| \chi_{\lambda} \rangle \\
 &= \frac{\partial^2}{\partial H_{\alpha} \partial \mu_{B\beta}} \langle \chi_{\nu} \left| \left\{ \frac{1}{2} \boldsymbol{\pi}^2 \right\} \right| \chi_{\lambda} \rangle
 \end{aligned}$$

then, using the following commutation relation:

$$\begin{aligned}
 [\boldsymbol{\pi}, f_{\lambda}] &= \left[-i\nabla + \frac{1}{c} \mathbf{A}'(\mathbf{r}), e^{-\frac{i}{c} \mathbf{A}_{\lambda} \cdot \mathbf{r}} \right] \\
 &= \left(-i\nabla + \frac{1}{c} \mathbf{A}'(\mathbf{r}) \right) e^{-\frac{i}{c} \mathbf{A}_{\lambda} \cdot \mathbf{r}} - e^{-\frac{i}{c} \mathbf{A}_{\lambda} \cdot \mathbf{r}} \left(-i\nabla + \frac{1}{c} \mathbf{A}'(\mathbf{r}) \right) \\
 &= \left[-i \left(-\frac{i}{c} \mathbf{A}_{\lambda} \right) + \frac{1}{c} \mathbf{A}'(\mathbf{r}) \right] e^{-\frac{i}{c} \mathbf{A}_{\lambda} \cdot \mathbf{r}} - e^{-\frac{i}{c} \mathbf{A}_{\lambda} \cdot \mathbf{r}} \left(\frac{1}{c} \mathbf{A}'(\mathbf{r}) \right) \\
 &= -\frac{1}{c} \mathbf{A}_{\lambda} e^{-\frac{i}{c} \mathbf{A}_{\lambda} \cdot \mathbf{r}} = -\frac{1}{c} \mathbf{A}_{\lambda} f_{\lambda}
 \end{aligned} \tag{C.9.1}$$

we can move the point of reference of the vector potential from electron 1 to the origin of the second basis function:

$$\begin{aligned}
\langle \chi_v | \frac{1}{2} \boldsymbol{\pi}^2 | \chi_\lambda \rangle &= \langle \phi_v | f_v^* \frac{1}{2} \boldsymbol{\pi} \boldsymbol{\pi} f_\lambda | \phi_\lambda \rangle \\
&= \langle \phi_v | f_v^* \frac{1}{2} \boldsymbol{\pi} \left(f_\lambda \boldsymbol{\pi} - \frac{1}{c} f_\lambda \mathbf{A}_\lambda \right) | \phi_\lambda \rangle \\
&= \langle \phi_v | f_v^* \frac{1}{2} \boldsymbol{\pi} f_\lambda \left(\boldsymbol{\pi} - \frac{1}{c} \mathbf{A}_\lambda \right) | \phi_\lambda \rangle \\
&= \langle \phi_v | f_v^* f_\lambda \frac{1}{2} \left(\boldsymbol{\pi} - \frac{1}{c} \mathbf{A}_\lambda \right)^2 | \phi_\lambda \rangle
\end{aligned}$$

which can be simplified:

$$\begin{aligned}
\boldsymbol{\pi} - \frac{1}{c} \mathbf{A}_\lambda &= -i\nabla + \frac{1}{c} \mathbf{A}'(\mathbf{r}) - \frac{1}{c} \mathbf{A}_\lambda \\
&= -i\nabla + \frac{1}{c} \left[\frac{1}{2} \mathbf{H} \times \mathbf{r} + \sum_B \frac{\boldsymbol{\mu}_B \times \mathbf{r}_B}{r_B^3} - \frac{1}{2} \mathbf{H} \times \mathbf{R}_\lambda \right] \\
&= -i\nabla + \frac{1}{c} \left[\frac{1}{2} \mathbf{H} \times (\mathbf{r} - \mathbf{R}_\lambda) + \sum_B \frac{\boldsymbol{\mu}_B \times \mathbf{r}_B}{r_B^3} \right] \\
&= -i\nabla + \frac{1}{c} \left[\frac{1}{2} \mathbf{H} \times \mathbf{r}_\lambda + \sum_B \frac{\boldsymbol{\mu}_B \times \mathbf{r}_B}{r_B^3} \right] \\
&= -i\nabla + \frac{1}{c} \mathbf{A}'(\mathbf{r}_\lambda)
\end{aligned}$$

[note that we have **not** used the strict definition of \mathbf{A}' , Eq. (3.3a)] to finally leave

$$\langle \chi_v | \frac{1}{2} \boldsymbol{\pi}^2 | \chi_\lambda \rangle = \langle \phi_v | f_v^* f_\lambda \frac{1}{2} \left(-i\nabla + \frac{1}{c} \mathbf{A}'(\mathbf{r}_\lambda) \right)^2 | \phi_\lambda \rangle = \langle f_v^* f_\lambda \phi_v | \frac{1}{2} \boldsymbol{\pi}_\lambda^2 | \phi_\lambda \rangle \quad (C.9.2)$$

Returning to the derivative, we thus have

$$\begin{aligned}
\frac{\partial^2}{\partial H_\alpha \partial \mu_{B\beta}} \langle \chi_\nu | \frac{1}{2} \boldsymbol{\pi}^2 | \chi_\lambda \rangle &= \frac{\partial^2}{\partial H_\alpha \partial \mu_{B\beta}} \langle f_\nu^* f_\lambda \phi_\nu | \frac{1}{2} \boldsymbol{\pi}_\lambda^2 | \phi_\lambda \rangle \\
&= \frac{\partial}{\partial H_\alpha} \left[\left\langle \frac{\partial f_\nu^* f_\lambda \phi_\nu}{\partial \mu_{B\beta}} \left| \frac{1}{2} \boldsymbol{\pi}_\lambda^2 \right| \phi_\lambda \right\rangle + \left\langle f_\nu^* f_\lambda \phi_\nu \left| \frac{1}{2} \frac{\partial \boldsymbol{\pi}_\lambda^2}{\partial \mu_{B\beta}} \right| \phi_\lambda \right\rangle + \left\langle f_\nu^* f_\lambda \phi_\nu \left| \frac{1}{2} \boldsymbol{\pi}_\lambda^2 \right| \frac{\partial \phi_\lambda}{\partial \mu_{B\beta}} \right\rangle \right] \\
&= \frac{\partial}{\partial H_\alpha} \left\langle f_\nu^* f_\lambda \phi_\nu \left| \frac{1}{2} \frac{\partial \boldsymbol{\pi}_\lambda^2}{\partial \mu_{B\beta}} \right| \phi_\lambda \right\rangle \\
&= \left\langle \frac{\partial f_\nu^* f_\lambda \phi_\nu}{\partial H_\alpha} \left| \frac{1}{2} \frac{\partial \boldsymbol{\pi}_\lambda^2}{\partial \mu_{B\beta}} \right| \phi_\lambda \right\rangle + \left\langle f_\nu^* f_\lambda \phi_\nu \left| \frac{1}{2} \frac{\partial^2 \boldsymbol{\pi}_\lambda^2}{\partial H_\alpha \partial \mu_{B\beta}} \right| \phi_\lambda \right\rangle + \left\langle f_\nu^* f_\lambda \phi_\nu \left| \frac{1}{2} \frac{\partial \boldsymbol{\pi}_\lambda^2}{\partial \mu_{B\beta}} \right| \frac{\partial \phi_\lambda}{\partial H_\alpha} \right\rangle \\
&= \left\langle \phi_\nu \frac{\partial f_\nu^* f_\lambda}{\partial H_\alpha} \left| \frac{1}{2} \frac{\partial \boldsymbol{\pi}_\lambda^2}{\partial \mu_{B\beta}} \right| \phi_\lambda \right\rangle + \left\langle f_\nu^* f_\lambda \phi_\nu \left| \frac{1}{2} \frac{\partial^2 \boldsymbol{\pi}_\lambda^2}{\partial H_\alpha \partial \mu_{B\beta}} \right| \phi_\lambda \right\rangle
\end{aligned}$$

The first term is then evaluated as the following, using a analogous form of Eq. (3.9):
[See also (C.8).]

$$\begin{aligned}
\left\langle \phi_\nu \frac{\partial f_\nu^* f_\lambda}{\partial H_\alpha} \left| \frac{1}{2} \frac{\partial \boldsymbol{\pi}_\lambda^2}{\partial \mu_{B\beta}} \right| \phi_\lambda \right\rangle &= \left\langle \phi_\nu \frac{\partial f_\nu^* f_\lambda}{\partial H_\alpha} \left| \frac{1}{2} \frac{\partial}{\partial \mu_{B\beta}} \left[\left(-i \nabla + \frac{1}{c} \mathbf{A}'(\mathbf{r}_\lambda) \right)^2 \right] \right| \phi_\lambda \right\rangle \\
&= \left\langle \phi_\nu \frac{\partial f_\nu^* f_\lambda}{\partial H_\alpha} \left| \frac{1}{2} \frac{\partial}{\partial \mu_{B\beta}} \left[\begin{array}{l} -\nabla^2 - \frac{2i}{c} \left(\frac{1}{2} H_\alpha (\mathbf{r}_\lambda \times \nabla)_\alpha + \frac{\mu_{B\beta} (\mathbf{r}_B \times \nabla)_\beta}{r_B^3} \right) \\ + \frac{1}{4} H_\alpha \left[r_\lambda^2 \delta_{\alpha\beta} - (\mathbf{r}_\lambda)_\alpha (\mathbf{r}_\lambda)_\beta \right] H_\beta \\ + \frac{1}{c^2} \left[\frac{\mathbf{r}_\lambda \cdot \mathbf{r}_B \delta_{\alpha\beta} - (\mathbf{r}_\lambda)_\alpha (\mathbf{r}_B)_\beta}{r_B^3} \right] \mu_{B\beta} \end{array} \right] \right| \phi_\lambda \right\rangle \\
&= \left\langle \phi_\nu \frac{\partial f_\nu^* f_\lambda}{\partial H_\alpha} \left| \frac{1}{2} \left\{ -\frac{2i}{c} \frac{(\mathbf{r}_B \times \nabla)_\beta}{r_B^3} + \frac{1}{c^2} H_\alpha \left[\frac{\mathbf{r}_\lambda \cdot \mathbf{r}_B \delta_{\alpha\beta} - (\mathbf{r}_\lambda)_\alpha (\mathbf{r}_B)_\beta}{r_B^3} \right] \right\} \right| \phi_\lambda \right\rangle \\
&= \left\langle \phi_\nu \frac{\partial f_\nu^* f_\lambda}{\partial H_\alpha} \left| -\frac{i}{c} \frac{L_\beta^B}{r_B^3} + \frac{1}{2c^2} H_\alpha \left[\frac{\mathbf{r}_\lambda \cdot \mathbf{r}_B \delta_{\alpha\beta} - (\mathbf{r}_\lambda)_\alpha (\mathbf{r}_B)_\beta}{r_B^3} \right] \right| \phi_\lambda \right\rangle
\end{aligned}$$

and since the derivative is taken at zero field strength,

$$\left\langle \phi_\nu \frac{\partial f_\nu^* f_\lambda}{\partial H_\alpha} \left| \frac{1}{2} \frac{\partial \boldsymbol{\pi}_\lambda^2}{\partial \mu_{B\beta}} \right| \phi_\lambda \right\rangle = -\frac{i}{c} \left\langle \phi_\nu \frac{\partial f_\nu^* f_\lambda}{\partial H_\alpha} \left| \frac{L_\beta^B}{r_B^3} \right| \phi_\lambda \right\rangle$$

Then

$$\begin{aligned}
 \frac{\partial f_v^* f_\lambda}{\partial H_\alpha} &= \frac{\partial}{\partial H_\alpha} \left(e^{i[\mathbf{A}_v - \mathbf{A}_\lambda] \cdot \mathbf{r}} \right) \\
 &= \frac{\partial}{\partial H_\alpha} \exp \left(\frac{i}{c} [\mathbf{A}_v - \mathbf{A}_\lambda] \cdot \mathbf{r} \right) \\
 &= \frac{\partial}{\partial H_\alpha} \exp \left(\frac{i}{c} \left[\left(\frac{1}{2} \mathbf{H} \times \mathbf{R}_v \right) - \left(\frac{1}{2} \mathbf{H} \times \mathbf{R}_\lambda \right) \right] \cdot \mathbf{r} \right) \\
 &= \frac{\partial}{\partial H_\alpha} \exp \left(\frac{i}{c} \left[\left(\frac{1}{2} \mathbf{H} \times \mathbf{R}_v \cdot \mathbf{r} \right) - \left(\frac{1}{2} \mathbf{H} \times \mathbf{R}_\lambda \cdot \mathbf{r} \right) \right] \right)
 \end{aligned}$$

continuing,

$$\begin{aligned}
 \frac{\partial f_v^* f_\lambda}{\partial H_\alpha} &= \frac{\partial}{\partial H_\alpha} \exp \left(\frac{i}{c} \left[\left(\frac{1}{2} \mathbf{H} \cdot \mathbf{R}_v \times \mathbf{r} \right) - \left(\frac{1}{2} \mathbf{H} \cdot \mathbf{R}_\lambda \times \mathbf{r} \right) \right] \right) \\
 &= \frac{\partial}{\partial H_\alpha} \exp \left(\frac{i}{c} \left[\left(\frac{1}{2} H_\alpha \{ \mathbf{R}_v \times \mathbf{r} \}_\alpha \right) - \left(\frac{1}{2} H_\alpha \{ \mathbf{R}_\lambda \times \mathbf{r} \}_\alpha \right) \right] \right) \\
 &= \left(e^{i[\mathbf{A}_v - \mathbf{A}_\lambda] \cdot \mathbf{r}} \right) \frac{i}{c} \frac{\partial}{\partial H_\alpha} \left[\left(\frac{1}{2} H_\alpha \{ \mathbf{R}_v \times \mathbf{r} \}_\alpha \right) - \left(\frac{1}{2} H_\alpha \{ \mathbf{R}_\lambda \times \mathbf{r} \}_\alpha \right) \right] \\
 &= \frac{if_v^* f_\lambda}{2c} \left[(\mathbf{R}_v \times \mathbf{r})_\alpha - (\mathbf{R}_\lambda \times \mathbf{r})_\alpha \right] = \frac{if_v^* f_\lambda}{2c} [(\mathbf{R}_v - \mathbf{R}_\lambda) \times \mathbf{r}]_\alpha = \frac{if_v^* f_\lambda}{2c} (\mathbf{R}_{v\lambda} \times \mathbf{r})_\alpha \\
 &= \frac{i}{2c} [(\mathbf{T}_{v\lambda})_\alpha + (\mathbf{Q}_{v\lambda})_\alpha]
 \end{aligned} \tag{C.9.3}$$

Where we can verify the last step with the help of Margenau and Murphy, p. 139 (actually just the distributive property as applied to the vector products) and zero field strength for the derivative:

$$\begin{aligned}
\frac{i}{2c} \left[(\mathbf{T}_{\nu\lambda})_\alpha + (\mathbf{Q}_{\nu\lambda})_\alpha \right] &= \frac{i}{2c} \left[(\mathbf{R}_{\nu\lambda} \times \mathbf{r}_\nu) + (\mathbf{R}_\nu \times \mathbf{R}_\lambda) \right]_\alpha \\
&= \frac{i}{2c} \left[(\mathbf{R}_\nu - \mathbf{R}_\lambda) \times (\mathbf{r} - \mathbf{R}_\nu) + (\mathbf{R}_\nu \times \mathbf{R}_\lambda) \right]_\alpha \\
&= \frac{i}{2c} \left[(\mathbf{R}_\nu \times \mathbf{r}) - (\mathbf{R}_\nu \times \mathbf{R}_\nu) - (\mathbf{R}_\lambda \times \mathbf{r}) + (\mathbf{R}_\lambda \times \mathbf{R}_\nu) + (\mathbf{R}_\nu \times \mathbf{R}_\lambda) \right]_\alpha \\
&= \frac{i}{2c} \left[(\mathbf{R}_\nu \times \mathbf{r}) - (\mathbf{R}_\lambda \times \mathbf{r}) - (\mathbf{R}_\nu \times \mathbf{R}_\lambda) + (\mathbf{R}_\nu \times \mathbf{R}_\lambda) \right]_\alpha \\
&= \frac{i}{2c} \left[(\mathbf{R}_\nu \times \mathbf{r}) - (\mathbf{R}_\lambda \times \mathbf{r}) \right]_\alpha \\
&= \frac{i}{2c} \left[(\mathbf{R}_\nu - \mathbf{R}_\lambda) \times \mathbf{r} \right]_\alpha \\
&= \frac{i}{2c} (\mathbf{R}_{\nu\lambda} \times \mathbf{r})_\alpha
\end{aligned}$$

Such that the total first term is

$$\begin{aligned}
-\frac{i}{c} \left\langle \phi_\nu \frac{\partial f_\nu^* f_\lambda}{\partial H_\alpha} \left| \frac{L_\beta^B}{r_B^3} \right| \phi_\lambda \right\rangle &= -\frac{i}{c} \left\langle \phi_\nu \frac{i}{2c} \left[(\mathbf{T}_{\nu\lambda})_\alpha + (\mathbf{Q}_{\nu\lambda})_\alpha \right] \left| \frac{L_\beta^B}{r_B^3} \right| \phi_\lambda \right\rangle \\
&= \frac{1}{2c^2} \left\{ \left\langle (\mathbf{T}_{\nu\lambda})_\alpha \phi_\nu \left| \frac{L_\beta^B}{r_B^3} \right| \phi_\lambda \right\rangle + (\mathbf{Q}_{\nu\lambda})_\alpha \left\langle \phi_\nu \left| \frac{L_\beta^B}{r_B^3} \right| \phi_\lambda \right\rangle \right\}
\end{aligned}$$

Then the second term in the original derivative is

$$\begin{aligned}
\left\langle f_\nu^* f_\lambda \phi_\nu \left| \frac{1}{2} \frac{\partial^2 \mathbf{p}_\lambda^2}{\partial H_\alpha \partial \mu_{B\beta}} \right| \phi_\lambda \right\rangle &= \left\langle f_\nu^* f_\lambda \phi_\nu \left| \left\{ \frac{1}{2} \frac{\partial^2}{\partial H_\alpha \partial \mu_{B\beta}} \left[\left(-i\nabla + \frac{1}{c} \mathbf{A}'(\mathbf{r}_\lambda) \right)^2 \right] \right\} \right| \phi_\lambda \right\rangle \\
&= \left\langle f_\nu^* f_\lambda \phi_\nu \left| \left\{ \begin{aligned} &-\nabla^2 - \frac{2i}{c} \left(\frac{1}{2} H_\alpha (\mathbf{r}_\lambda \times \nabla)_\alpha + \frac{\mu_{B\beta} (\mathbf{r}_B \times \nabla)_\beta}{r_B^3} \right) \\ &+ \frac{1}{2} H_\alpha \left[r_\lambda^2 \delta_{\alpha\beta} - (\mathbf{r}_\lambda)_\alpha (\mathbf{r}_\lambda)_\beta \right] H_\beta \\ &+ \frac{1}{c^2} \left(H_\alpha \left[\frac{\mathbf{r}_\lambda \cdot \mathbf{r}_B \delta_{\alpha\beta} - (\mathbf{r}_\lambda)_\alpha (\mathbf{r}_B)_\beta}{r_B^3} \right] \mu_{B\beta} \right) \end{aligned} \right\} \right| \phi_\lambda \right\rangle
\end{aligned}$$

$$\begin{aligned}
&= \left\langle f_v^* f_\lambda \phi_v \left| \left\langle \frac{1}{2} \frac{\partial}{\partial H_\alpha} \left(-\frac{2i}{c} \left(\frac{(\mathbf{r}_B \times \nabla)_\beta}{r_B^3} \right) + \frac{1}{c^2} H_\alpha \frac{[\mathbf{r}_\lambda \cdot \mathbf{r}_B \delta_{\alpha\beta} - (\mathbf{r}_\lambda)_\alpha (\mathbf{r}_B)_\beta]}{r_B^3} \right) \right\rangle \right| \phi_\lambda \right\rangle \\
&= \left\langle f_v^* f_\lambda \phi_v \left| \left\langle \frac{1}{2} \left(\frac{1}{c^2} \frac{[\mathbf{r}_\lambda \cdot \mathbf{r}_B \delta_{\alpha\beta} - (\mathbf{r}_\lambda)_\alpha (\mathbf{r}_B)_\beta]}{r_B^3} \right) \right\rangle \right| \phi_\lambda \right\rangle \\
&= \frac{1}{2c^2} \left\langle \phi_v \left| \frac{[\mathbf{r}_\lambda \cdot \mathbf{r}_B \delta_{\alpha\beta} - (\mathbf{r}_\lambda)_\alpha (\mathbf{r}_B)_\beta]}{r_B^3} \right| \phi_\lambda \right\rangle
\end{aligned}$$

Since in the end we take the derivative at zero field strength, which removes $f^* f$. Finally, then, we see that

$$\begin{aligned}
(H_{B\lambda}^{(1,1)})_{\alpha\beta} &= \left\langle \phi_v \frac{\partial f_v^* f_\lambda}{\partial H_\alpha} \left| \frac{1}{2} \frac{\partial \mathbf{\pi}_\lambda^2}{\partial \mu_{B\beta}} \right| \phi_\lambda \right\rangle + \left\langle f_v^* f_\lambda \phi_v \left| \frac{1}{2} \frac{\partial^2 \mathbf{\pi}_\lambda^2}{\partial H_\alpha \partial \mu_{B\beta}} \right| \phi_\lambda \right\rangle \\
&= \frac{1}{2c^2} \left\{ \left\langle (\mathbf{T}_{\nu\lambda})_\alpha \phi_v \left| \frac{L_\beta^B}{r_B^3} \right| \phi_\lambda \right\rangle + (\mathbf{Q}_{\nu\lambda})_\alpha \left\langle \phi_v \left| \frac{L_\beta^B}{r_B^3} \right| \phi_\lambda \right\rangle \right\} \\
&\quad + \frac{1}{2c^2} \left\langle \phi_v \left| \frac{[\mathbf{r}_\lambda \cdot \mathbf{r}_B \delta_{\alpha\beta} - (\mathbf{r}_\lambda)_\alpha (\mathbf{r}_B)_\beta]}{r_B^3} \right| \phi_\lambda \right\rangle
\end{aligned}$$

C.10)

$$\begin{aligned}
(F_{\nu\lambda}^{(1,0)})_\alpha &= \left. \frac{\partial F_{\nu\lambda}}{\partial H_\alpha} \right|_0 = \frac{\partial}{\partial H_\alpha} (H_{\nu\lambda} + G_{\nu\lambda}) \\
&= \frac{\partial H_{\nu\lambda}}{\partial H_\alpha} + \frac{\partial G_{\nu\lambda}}{\partial H_\alpha} \\
&= \frac{\partial}{\partial H_\alpha} \left[H_{\nu\lambda}^{(0)} + iH_\alpha (H_{\nu\lambda}^{(1,0)})_\alpha + i\mu_{B\alpha} (H_{B\lambda}^{(0,1)})_\alpha + \dots \right] \\
&\quad + \frac{\partial}{\partial H_\alpha} \left[G_{\nu\lambda}^{(0)} + iH_\alpha \sum_{\rho\sigma} \left\{ (P_{\rho\sigma}^{(1,0)})_\alpha G_{\nu\lambda\rho\sigma}^{(0)} + P_{\rho\sigma}^{(0)} (G_{\nu\lambda\rho\sigma}^{(1,0)})_\alpha \right\} + i\mu_{B\alpha} \sum_{\rho\sigma} (P_{B\rho\sigma}^{(0,1)})_\alpha G_{\nu\lambda\rho\sigma}^{(0)} + \dots \right] \\
&= i \left[(H_{\nu\lambda}^{(1,0)})_\alpha + \sum_{\rho\sigma} \left\{ (P_{\rho\sigma}^{(1,0)})_\alpha G_{\nu\lambda\rho\sigma}^{(0)} + P_{\rho\sigma}^{(0)} (G_{\nu\lambda\rho\sigma}^{(1,0)})_\alpha \right\} \right]
\end{aligned}$$

C.11)

Consider the derivative resulting from (C.10):

$$\begin{aligned}
\left. \frac{\partial H_{v\lambda}}{\partial H_\alpha} \right|_0 &= \frac{\partial}{\partial H_\alpha} \left\langle \chi_v \left| \left\{ \frac{1}{2} \left(-i\nabla + \frac{1}{c} \mathbf{A}'(\mathbf{r}) \right)^2 - \sum_B \frac{Z_B}{r_B} \right\} \right| \chi_\lambda \right\rangle \\
&= \frac{\partial}{\partial H_\alpha} \left\langle \chi_v \left| \left\{ \frac{1}{2} \boldsymbol{\pi}^2 - \sum_B \frac{Z_B}{r_B} \right\} \right| \chi_\lambda \right\rangle = \frac{\partial}{\partial H_\alpha} \left[\left\langle \chi_v \left| \frac{1}{2} \boldsymbol{\pi}^2 \right| \chi_\lambda \right\rangle - \left\langle \chi_v \left| \sum_B \frac{Z_B}{r_B} \right| \chi_\lambda \right\rangle \right] \\
&= \frac{\partial}{\partial H_\alpha} \left[\left\langle f_v^* f_\lambda \phi_v \left| \frac{1}{2} \left(-i\nabla + \frac{1}{c} \mathbf{A}'(\mathbf{r}_\lambda) \right)^2 \right| \phi_\lambda \right\rangle - \sum_B \left\langle f_v^* f_\lambda \phi_v \left| \frac{Z_B}{r_B} \right| \phi_\lambda \right\rangle \right] \\
&= \frac{\partial}{\partial H_\alpha} \left\langle f_v^* f_\lambda \phi_v \left| \frac{1}{2} \boldsymbol{\pi}_\lambda^2 \right| \phi_\lambda \right\rangle - \sum_B \frac{\partial}{\partial H_\alpha} \left\langle f_v^* f_\lambda \phi_v \left| \frac{Z_B}{r_B} \right| \phi_\lambda \right\rangle \\
&= \left\langle \frac{\partial f_v^* f_\lambda}{\partial H_\alpha} \phi_v \left| \frac{1}{2} \boldsymbol{\pi}_\lambda^2 \right| \phi_\lambda \right\rangle + \left\langle f_v^* f_\lambda \phi_v \left| \frac{1}{2} \frac{\partial \boldsymbol{\pi}_\lambda^2}{\partial H_\alpha} \right| \phi_\lambda \right\rangle - \sum_B \left\langle \frac{\partial f_v^* f_\lambda}{\partial H_\alpha} \phi_v \left| \frac{Z_B}{r_B} \right| \phi_\lambda \right\rangle \\
&= \left\langle \frac{\partial f_v^* f_\lambda}{\partial H_\alpha} \phi_v \left| \frac{1}{2} \boldsymbol{\pi}_\lambda^2 - \sum_B \frac{Z_B}{r_B} \right| \phi_\lambda \right\rangle + \left\langle f_v^* f_\lambda \phi_v \left| \frac{1}{2} \frac{\partial \boldsymbol{\pi}_\lambda^2}{\partial H_\alpha} \right| \phi_\lambda \right\rangle
\end{aligned}$$

Then using (C.9.3),

$$\left. \frac{\partial H_{v\lambda}}{\partial H_\alpha} \right|_0 = \left\langle \frac{i}{2c} \left[(\mathbf{T}_{v\lambda})_\alpha + (\mathbf{Q}_{v\lambda})_\alpha \right] \phi_v \left| -\frac{1}{2} \nabla^2 - \sum_B \frac{Z_B}{r_B} \right| \phi_\lambda \right\rangle + \left\langle f_v^* f_\lambda \phi_v \left| \frac{1}{2} \frac{\partial \boldsymbol{\pi}_\lambda^2}{\partial H_\alpha} \right| \phi_\lambda \right\rangle$$

Since

$$\frac{1}{2} \boldsymbol{\pi}_\lambda^2 = \frac{1}{2} \left(-i\nabla + \frac{1}{c} \mathbf{A}'(\mathbf{r}_\lambda) \right)^2 \xrightarrow{\text{zero field}} \frac{1}{2} (-i\nabla)^2 = -\frac{1}{2} \nabla^2$$

Finally, again using the analogous form of Eq. (3.9), we have

$$\begin{aligned}
\frac{\partial H_{\nu\lambda}}{\partial H_\alpha} \Big|_0 &= \left\langle \frac{i}{2c} \left[(\mathbf{T}_{\nu\lambda})_\alpha + (\mathbf{Q}_{\nu\lambda})_\alpha \right] \phi_\nu \left| -\frac{1}{2} \nabla^2 - \sum_B \frac{Z_B}{r_B} \right| \phi_\lambda \right\rangle \\
&\quad + \left\langle f_\nu^* f_\lambda \phi_\nu \left| \frac{1}{2} \frac{\partial}{\partial H_\alpha} \left(\begin{array}{l} -\nabla^2 - \frac{2i}{c} \left(\frac{1}{2} H_\alpha (\mathbf{r}_\lambda \times \nabla)_\alpha + \frac{\mu_{B\beta} (\mathbf{r}_B \times \nabla)_\beta}{r_B^3} \right) \\ + \frac{1}{4} H_\alpha \left[r_\lambda^2 \delta_{\alpha\beta} - (\mathbf{r}_\lambda)_\alpha (\mathbf{r}_\lambda)_\beta \right] H_\beta \\ + \frac{1}{c^2} \left[\frac{\mathbf{r}_\lambda \cdot \mathbf{r}_B \delta_{\alpha\beta} - (\mathbf{r}_\lambda)_\alpha (\mathbf{r}_B)_\beta}{r_B^3} \right] \mu_{B\beta} \end{array} \right) \right| \phi_\lambda \right\rangle \\
&= \frac{i}{2c} \left\langle \left[(\mathbf{T}_{\nu\lambda})_\alpha + (\mathbf{Q}_{\nu\lambda})_\alpha \right] \phi_\nu \left| -\frac{1}{2} \nabla^2 - \sum_B \frac{Z_B}{r_B} \right| \phi_\lambda \right\rangle - \frac{i}{2c} \left\langle \phi_\nu \left| (\mathbf{r}_\lambda \times \nabla)_\alpha \right| \phi_\lambda \right\rangle \\
&= \frac{i}{2c} \left[\left\langle \left[(\mathbf{T}_{\nu\lambda})_\alpha + (\mathbf{Q}_{\nu\lambda})_\alpha \right] \phi_\nu \left| H^{core} \right| \phi_\lambda \right\rangle - \langle \phi_\nu | L_\alpha^\lambda | \phi_\lambda \rangle \right] \\
&= \frac{i}{2c} \left[\left\langle \left[(\mathbf{T}_{\nu\lambda})_\alpha \phi_\nu \left| H^{core} \right| \phi_\lambda \right\rangle + (\mathbf{Q}_{\nu\lambda})_\alpha \langle \phi_\nu | H^{core} | \phi_\lambda \rangle - \langle \phi_\nu | L_\alpha^\lambda | \phi_\lambda \rangle \right] \right]
\end{aligned}$$

Such that finally, the first derivative of the core magnetic Hamiltonian is given in terms of familiar one-electron integrals:

$$\begin{aligned}
(H_{\nu\lambda}^{(1,0)})_\alpha &= -i \frac{\partial H_{\nu\lambda}}{\partial H_\alpha} \Big|_0 = -i \left[\frac{i}{2c} \left[\left\langle (\mathbf{T}_{\nu\lambda})_\alpha \phi_\nu \left| H^{core} \right| \phi_\lambda \right\rangle + (\mathbf{Q}_{\nu\lambda})_\alpha \langle \phi_\nu | H^{core} | \phi_\lambda \rangle - \langle \phi_\nu | L_\alpha^\lambda | \phi_\lambda \rangle \right] \right] \\
&= \frac{1}{2c} \left[\left\langle (\mathbf{T}_{\nu\lambda})_\alpha \phi_\nu \left| H^{core} \right| \phi_\lambda \right\rangle + (\mathbf{Q}_{\nu\lambda})_\alpha \langle \phi_\nu | H^{core} | \phi_\lambda \rangle - \langle \phi_\nu | L_\alpha^\lambda | \phi_\lambda \rangle \right]
\end{aligned}$$

C.12)

$$\begin{aligned}
(\chi_p^* \chi_q | \chi_r^* \chi_s) &= (\chi_p^* \chi_q | \chi_r^* \chi_s)^{(0)} + i H_\alpha (\chi_p^* \chi_q | \chi_r^* \chi_s)^{(1,0)} + \dots \\
&= (\chi_p^* \chi_q | \chi_r^* \chi_s)^{(0)} + H_\alpha \frac{\partial}{\partial H_\alpha} (\chi_p^* \chi_q | \chi_r^* \chi_s) \Big|_0 + \dots
\end{aligned}$$

Thus

$$\begin{aligned}
(\chi_p^* \chi_q | \chi_r^* \chi_s)^{(1,0)} &= -i \frac{\partial}{\partial H_\alpha} (\chi_p^* \chi_q | \chi_r^* \chi_s) \Big|_0 = -i \frac{\partial}{\partial H_\alpha} (f_p^* f_q \phi_p \phi_q | f_r^* f_s \phi_r \phi_s) \Big|_0 \\
&= \left(-i \frac{\partial f_p^* f_q}{\partial H_\alpha} \phi_p \phi_q | f_r^* f_s \phi_r \phi_s \right) \Big|_0 + \left(f_p^* f_q \phi_p \phi_q | -i \frac{\partial f_r^* f_s}{\partial H_\alpha} \phi_r \phi_s \right) \Big|_0
\end{aligned}$$

then using (C.9.3), we have

$$\begin{aligned}
(\chi_p \chi_q | \chi_r \chi_s)^{(1,0)} &= \left(\left(\frac{1}{2c} \right) \{ (\mathbf{T}_{pq})_\alpha + (\mathbf{Q}_{pq})_\alpha \} \phi_p \phi_q | \phi_r \phi_s \right) + \left(\phi_p \phi_q \left(\frac{1}{2c} \right) \{ (\mathbf{T}_{rs})_\alpha + (\mathbf{Q}_{rs})_\alpha \} \phi_r \phi_s \right) \\
&= \frac{1}{2c} \left\{ (\mathbf{Q}_{pq})_\alpha (\phi_p \phi_q | \phi_r \phi_s) + ((\mathbf{T}_{pq})_\alpha \phi_p \phi_q | \phi_r \phi_s) + (\mathbf{Q}_{rs})_\alpha (\phi_p \phi_q | \phi_r \phi_s) + (\phi_p \phi_q | (\mathbf{T}_{rs})_\alpha \phi_r \phi_s) \right\} \\
&= \frac{1}{2c} \left\{ [(\mathbf{Q}_{pq})_\alpha + (\mathbf{Q}_{rs})_\alpha] (\phi_p \phi_q | \phi_r \phi_s) + ((\mathbf{T}_{pq})_\alpha \phi_p \phi_q | \phi_r \phi_s) + (\phi_p \phi_q | (\mathbf{T}_{rs})_\alpha \phi_r \phi_s) \right\}
\end{aligned}$$

APPENDIX D. ANTISSYMMETRIC PERTURBATION THEORY FOR FIELD-DEPENDENT NON-ORTHOGONAL BASES

D.1)

$$\mathbf{FRS} = \mathbf{SRF}$$

$$\begin{aligned} & \Rightarrow (\mathbf{F}^{(0)} + \mathbf{F}^{(1)})(\mathbf{R}^{(0)} + \mathbf{R}^{(1)})(\mathbf{S}^{(0)} + \mathbf{S}^{(1)}) = (\mathbf{S}^{(0)} + \mathbf{S}^{(1)})(\mathbf{R}^{(0)} + \mathbf{R}^{(1)})(\mathbf{F}^{(0)} + \mathbf{F}^{(1)}) \\ & \therefore \mathbf{F}^{(0)}\mathbf{R}^{(0)}\mathbf{S}^{(0)} + \mathbf{F}^{(0)}\mathbf{R}^{(0)}\mathbf{S}^{(1)} + \mathbf{F}^{(0)}\mathbf{R}^{(1)}\mathbf{S}^{(0)} + \mathbf{F}^{(0)}\mathbf{R}^{(1)}\mathbf{S}^{(1)} + \mathbf{F}^{(1)}\mathbf{R}^{(0)}\mathbf{S}^{(0)} + \\ & \quad \mathbf{F}^{(1)}\mathbf{R}^{(0)}\mathbf{S}^{(1)} + \mathbf{F}^{(1)}\mathbf{R}^{(1)}\mathbf{S}^{(0)} + \mathbf{F}^{(1)}\mathbf{R}^{(1)}\mathbf{S}^{(1)} \\ & = \mathbf{S}^{(0)}\mathbf{R}^{(0)}\mathbf{F}^{(0)} + \mathbf{S}^{(0)}\mathbf{R}^{(0)}\mathbf{F}^{(1)} + \mathbf{S}^{(0)}\mathbf{R}^{(1)}\mathbf{F}^{(0)} + \mathbf{S}^{(0)}\mathbf{R}^{(1)}\mathbf{F}^{(1)} + \mathbf{S}^{(1)}\mathbf{R}^{(0)}\mathbf{F}^{(0)} + \\ & \quad \mathbf{S}^{(1)}\mathbf{R}^{(0)}\mathbf{F}^{(1)} + \mathbf{S}^{(1)}\mathbf{R}^{(1)}\mathbf{F}^{(0)} + \mathbf{S}^{(1)}\mathbf{R}^{(1)}\mathbf{F}^{(1)} \end{aligned}$$

D.2)

$$\mathbf{RSR} = \mathbf{R}$$

$$\begin{aligned} & \Rightarrow (\mathbf{R}^{(0)} + \mathbf{R}^{(1)})(\mathbf{S}^{(0)} + \mathbf{S}^{(1)})(\mathbf{R}^{(0)} + \mathbf{R}^{(1)}) = (\mathbf{R}^{(0)} + \mathbf{R}^{(1)}) \\ & \therefore \mathbf{R}^{(0)}\mathbf{S}^{(0)}\mathbf{R}^{(0)} + \mathbf{R}^{(0)}\mathbf{S}^{(0)}\mathbf{R}^{(1)} + \mathbf{R}^{(0)}\mathbf{S}^{(1)}\mathbf{R}^{(0)} + \mathbf{R}^{(0)}\mathbf{S}^{(1)}\mathbf{R}^{(1)} \\ & \quad + \mathbf{R}^{(1)}\mathbf{S}^{(0)}\mathbf{R}^{(0)} + \mathbf{R}^{(1)}\mathbf{S}^{(0)}\mathbf{R}^{(1)} + \mathbf{R}^{(1)}\mathbf{S}^{(1)}\mathbf{R}^{(0)} + \mathbf{R}^{(1)}\mathbf{S}^{(1)}\mathbf{R}^{(1)} \\ & = \mathbf{R}^{(0)} + \mathbf{R}^{(1)} \end{aligned}$$

D.3)

$$\begin{aligned} & \mathbf{UF}^{(0)}\mathbf{UU}^{-1}\mathbf{R}^{(0)}\mathbf{U}^{-1}\mathbf{US}^{(1)}\mathbf{U} + \mathbf{UF}^{(0)}\mathbf{UU}^{-1}\mathbf{R}^{(1)}\mathbf{U}^{-1}\mathbf{US}^{(0)}\mathbf{U} + \mathbf{UF}^{(1)}\mathbf{UU}^{-1}\mathbf{R}^{(0)}\mathbf{U}^{-1}\mathbf{US}^{(0)}\mathbf{U} \\ & = \mathbf{US}^{(0)}\mathbf{UU}^{-1}\mathbf{R}^{(0)}\mathbf{U}^{-1}\mathbf{UF}^{(1)}\mathbf{U} + \mathbf{US}^{(0)}\mathbf{UU}^{-1}\mathbf{R}^{(1)}\mathbf{U}^{-1}\mathbf{UF}^{(0)}\mathbf{U} + \mathbf{US}^{(1)}\mathbf{UU}^{-1}\mathbf{R}^{(0)}\mathbf{U}^{-1}\mathbf{UF}^{(0)}\mathbf{U} \\ & \mathbf{U}^{-1}\mathbf{R}^{(0)}\mathbf{U}^{-1}\mathbf{US}^{(0)}\mathbf{UU}^{-1}\mathbf{R}^{(1)}\mathbf{U}^{-1} + \mathbf{U}^{-1}\mathbf{R}^{(0)}\mathbf{U}^{-1}\mathbf{US}^{(1)}\mathbf{UU}^{-1}\mathbf{R}^{(0)}\mathbf{U}^{-1} + \mathbf{U}^{-1}\mathbf{R}^{(1)}\mathbf{U}^{-1}\mathbf{US}^{(0)}\mathbf{UU}^{-1}\mathbf{R}^{(0)}\mathbf{U}^{-1} \\ & = \mathbf{U}^{-1}\mathbf{R}^{(1)}\mathbf{U}^{-1} \\ & \Rightarrow \tilde{\mathbf{F}}^{(0)}\tilde{\mathbf{R}}^{(0)}\tilde{\mathbf{S}}^{(1)} + \tilde{\mathbf{F}}^{(0)}\tilde{\mathbf{R}}^{(1)}\tilde{\mathbf{S}}^{(0)} + \tilde{\mathbf{F}}^{(1)}\tilde{\mathbf{R}}^{(0)}\tilde{\mathbf{S}}^{(0)} = \tilde{\mathbf{S}}^{(0)}\tilde{\mathbf{R}}^{(0)}\tilde{\mathbf{F}}^{(1)} + \tilde{\mathbf{S}}^{(0)}\tilde{\mathbf{R}}^{(1)}\tilde{\mathbf{F}}^{(0)} + \tilde{\mathbf{S}}^{(1)}\tilde{\mathbf{R}}^{(0)}\tilde{\mathbf{F}}^{(0)} \\ & \tilde{\mathbf{R}}^{(0)}\tilde{\mathbf{S}}^{(0)}\tilde{\mathbf{R}}^{(1)} + \tilde{\mathbf{R}}^{(0)}\tilde{\mathbf{S}}^{(1)}\tilde{\mathbf{R}}^{(0)} + \tilde{\mathbf{R}}^{(1)}\tilde{\mathbf{S}}^{(0)}\tilde{\mathbf{R}}^{(0)} = \tilde{\mathbf{R}}^{(1)} \\ & \Rightarrow \tilde{\mathbf{F}}^{(0)}\tilde{\mathbf{R}}^{(0)}\tilde{\mathbf{S}}^{(1)} + \tilde{\mathbf{F}}^{(0)}\tilde{\mathbf{R}}^{(1)} + \tilde{\mathbf{F}}^{(1)}\tilde{\mathbf{R}}^{(0)} = \tilde{\mathbf{R}}^{(0)}\tilde{\mathbf{F}}^{(1)} + \tilde{\mathbf{R}}^{(1)}\tilde{\mathbf{F}}^{(0)} + \tilde{\mathbf{S}}^{(1)}\tilde{\mathbf{R}}^{(0)}\tilde{\mathbf{F}}^{(0)} \\ & \tilde{\mathbf{R}}^{(0)}\tilde{\mathbf{R}}^{(1)} + \tilde{\mathbf{R}}^{(0)}\tilde{\mathbf{S}}^{(1)}\tilde{\mathbf{R}}^{(0)} + \tilde{\mathbf{R}}^{(1)}\tilde{\mathbf{R}}^{(0)} = \tilde{\mathbf{R}}^{(1)} \end{aligned}$$

Since $\tilde{\mathbf{S}}^{(0)} = \mathbf{1}$.

D.4) The (1,1) projection:

$$\tilde{\mathbf{x}} = \sum_I^{\text{occ}} \sum_J^{\text{unocc}} A_{IJ} \tilde{\mathbf{c}}_I \tilde{\mathbf{c}}_J^+$$

where $\tilde{\mathbf{c}}_I$ is the I^{th} (occupied) column of $\bar{\mathbf{T}}$, and $\tilde{\mathbf{c}}_J$ the J^{th} unoccupied column of $\bar{\mathbf{T}}$, since we are dealing with the occupied/unoccupied (1,2) projection. Then

$$\begin{aligned} \tilde{\mathbf{F}}^{(0)} \tilde{\mathbf{x}} - \tilde{\mathbf{x}} \tilde{\mathbf{F}}^{(0)} &= \tilde{\mathbf{F}}_{12}^{(1)} - \tilde{\mathbf{F}}^{(0)} \tilde{\mathbf{S}}_{12}^{(1)} \\ \Rightarrow \tilde{\mathbf{F}}^{(0)} \sum_I^{\text{occ}} \sum_J^{\text{unocc}} A_{IJ} \tilde{\mathbf{c}}_I \tilde{\mathbf{c}}_J^+ - \sum_I^{\text{occ}} \sum_J^{\text{unocc}} A_{IJ} \tilde{\mathbf{c}}_I \tilde{\mathbf{c}}_J^+ \tilde{\mathbf{F}}^{(0)} &= \tilde{\mathbf{F}}_{12}^{(1)} - \tilde{\mathbf{F}}^{(0)} \tilde{\mathbf{S}}_{12}^{(1)} \\ \Rightarrow \sum_I^{\text{occ}} \sum_J^{\text{unocc}} A_{IJ} \left(\tilde{\mathbf{F}}^{(0)} \tilde{\mathbf{c}}_I \tilde{\mathbf{c}}_J^+ - \tilde{\mathbf{c}}_I \tilde{\mathbf{c}}_J^+ \tilde{\mathbf{F}}^{(0)} \right) &= \tilde{\mathbf{F}}_{12}^{(1)} - \tilde{\mathbf{F}}^{(0)} \tilde{\mathbf{S}}_{12}^{(1)} \\ \Rightarrow \sum_I^{\text{occ}} \sum_J^{\text{unocc}} A_{IJ} \left(e_I \tilde{\mathbf{c}}_I \tilde{\mathbf{c}}_J^+ - \tilde{\mathbf{c}}_I \tilde{\mathbf{c}}_J^+ e_J \right) &= \tilde{\mathbf{F}}_{12}^{(1)} - \tilde{\mathbf{F}}^{(0)} \tilde{\mathbf{S}}_{12}^{(1)} \\ \Rightarrow \sum_I^{\text{occ}} \sum_J^{\text{unocc}} A_{IJ} \left(e_I - e_J \right) \tilde{\mathbf{c}}_I \tilde{\mathbf{c}}_J^+ &= \tilde{\mathbf{F}}_{12}^{(1)} - \tilde{\mathbf{F}}^{(0)} \tilde{\mathbf{S}}_{12}^{(1)} \end{aligned}$$

where we have used $\tilde{\mathbf{F}}^{(0)} \tilde{\mathbf{c}}_I = e_I \tilde{\mathbf{c}}_I$ and its adjoint. Then, to find A_{IJ} , we multiply on left and right by specific column vectors, \mathbf{c}_K^+ and \mathbf{c}_L , resp.:

$$\begin{aligned} \sum_I^{\text{occ}} \sum_J^{\text{unocc}} A_{IJ} \left(e_I - e_J \right) \tilde{\mathbf{c}}_K^+ \tilde{\mathbf{c}}_I \tilde{\mathbf{c}}_J^+ \tilde{\mathbf{c}}_L &= \tilde{\mathbf{c}}_K^+ \left(\tilde{\mathbf{F}}_{12}^{(1)} - \tilde{\mathbf{F}}^{(0)} \tilde{\mathbf{S}}_{12}^{(1)} \right) \tilde{\mathbf{c}}_L \\ \sum_I^{\text{occ}} \sum_J^{\text{unocc}} A_{IJ} \left(e_I - e_J \right) \delta_{KI} \delta_{JL} &= \tilde{\mathbf{c}}_K^+ \left(\tilde{\mathbf{F}}_{12}^{(1)} - \tilde{\mathbf{F}}^{(0)} \tilde{\mathbf{S}}_{12}^{(1)} \right) \tilde{\mathbf{c}}_L \\ \Rightarrow A_{KL} &= \frac{\tilde{\mathbf{c}}_K^+ \left(\tilde{\mathbf{F}}_{12}^{(1)} - \tilde{\mathbf{F}}^{(0)} \tilde{\mathbf{S}}_{12}^{(1)} \right) \tilde{\mathbf{c}}_L}{(e_K - e_L)} \end{aligned}$$

which can be substituted back into the original expansion:

$$\tilde{\mathbf{x}} = \sum_I^{\text{occ}} \sum_J^{\text{unocc}} A_{IJ} \tilde{\mathbf{c}}_I \tilde{\mathbf{c}}_J^+ = \sum_I^{\text{occ}} \sum_J^{\text{unocc}} \frac{\tilde{\mathbf{c}}_I^+ \left(\tilde{\mathbf{F}}_{12}^{(1)} - \tilde{\mathbf{F}}^{(0)} \tilde{\mathbf{S}}_{12}^{(1)} \right) \tilde{\mathbf{c}}_J}{(e_I - e_J)} \tilde{\mathbf{c}}_I \tilde{\mathbf{c}}_J^+$$

D.7)

$$\begin{aligned}
\tilde{x} &= \sum_{I}^{occ} \sum_{J}^{unocc} \frac{\tilde{\mathbf{c}}_I^+ \sum_{K}^{occ} \tilde{\mathbf{c}}_K \tilde{\mathbf{c}}_K^+ (\tilde{\mathbf{F}}^{(1)} - \tilde{\mathbf{F}}^{(0)} \tilde{\mathbf{S}}^{(1)}) \sum_{L}^{unocc} \tilde{\mathbf{c}}_L \tilde{\mathbf{c}}_L^+ \tilde{\mathbf{c}}_J}{(e_I - e_J)} \tilde{\mathbf{c}}_I \tilde{\mathbf{c}}_J^+ \\
&= \sum_{I}^{occ} \sum_{J}^{unocc} \sum_{K}^{occ} \sum_{L}^{unocc} \frac{\delta_{IK} \tilde{\mathbf{c}}_K^+ (\tilde{\mathbf{F}}^{(1)} - \tilde{\mathbf{F}}^{(0)} \tilde{\mathbf{S}}^{(1)}) \tilde{\mathbf{c}}_L \delta_{LJ}}{(e_I - e_J)} \tilde{\mathbf{c}}_I \tilde{\mathbf{c}}_J^+ \\
&= \sum_{K}^{occ} \sum_{L}^{unocc} \frac{\tilde{\mathbf{c}}_K^+ (\tilde{\mathbf{F}}^{(1)} - e_K \tilde{\mathbf{S}}^{(1)}) \tilde{\mathbf{c}}_L}{(e_K - e_L)} \tilde{\mathbf{c}}_K \tilde{\mathbf{c}}_L^+
\end{aligned}$$

since $\tilde{\mathbf{F}}^{(0)} \tilde{\mathbf{c}}_K^+ = e_K \tilde{\mathbf{c}}_K^+$.

D.8) If the imaginary parts of $\tilde{\mathbf{F}}^{(1)}$ and $\tilde{\mathbf{S}}^{(1)}$ are explicitly pulled out, we have

$$\begin{aligned}
\tilde{\mathbf{R}}^{(1)} &= \tilde{\mathbf{R}}_{11}^{(1)} + \tilde{\mathbf{R}}_{12}^{(1)} + \tilde{\mathbf{R}}_{21}^{(1)} + \tilde{\mathbf{R}}_{22}^{(1)} = -\tilde{\mathbf{S}}_{11}^{(1)} + \tilde{x} + \tilde{x}^+ = -i\tilde{\mathbf{S}}_{11}^{(1,0)} + i\tilde{x} + (\tilde{x})^+ \\
&= -i\tilde{\mathbf{S}}_{11}^{(1,0)} + i \sum_{K}^{occ} \sum_{L}^{unocc} \frac{\tilde{\mathbf{c}}_K^+ (\tilde{\mathbf{F}}^{(1,0)} - e_K \tilde{\mathbf{S}}^{(1,0)}) \tilde{\mathbf{c}}_L}{(e_K - e_L)} \tilde{\mathbf{c}}_K \tilde{\mathbf{c}}_L^+ - \left(i \sum_{K}^{occ} \sum_{L}^{unocc} \frac{\tilde{\mathbf{c}}_K^+ (\tilde{\mathbf{F}}^{(1,0)} - e_K \tilde{\mathbf{S}}^{(1,0)}) \tilde{\mathbf{c}}_L}{(e_K - e_L)} \tilde{\mathbf{c}}_K \tilde{\mathbf{c}}_L^+ \right)^* \\
&= -i\tilde{\mathbf{R}}^{(0)} \tilde{\mathbf{S}}^{(1,0)} \tilde{\mathbf{R}}^{(0)} + i \sum_{K}^{occ} \sum_{L}^{unocc} \frac{\tilde{\mathbf{c}}_K^+ (\tilde{\mathbf{F}}^{(1,0)} - e_K \tilde{\mathbf{S}}^{(1,0)}) \tilde{\mathbf{c}}_L \tilde{\mathbf{c}}_K \tilde{\mathbf{c}}_L^+}{(e_K - e_L)} - \frac{\tilde{\mathbf{c}}_L \tilde{\mathbf{c}}_K^+ \tilde{\mathbf{c}}_L^+ (\tilde{\mathbf{F}}^{(1,0)} - e_K \tilde{\mathbf{S}}^{(1,0)}) \tilde{\mathbf{c}}_K}{(e_K - e_L)} \\
&\quad \tilde{\mathbf{c}}_L^+ (\tilde{\mathbf{F}}^{(1,0)} - e_K \tilde{\mathbf{S}}^{(1,0)}) \tilde{\mathbf{c}}_K \text{ is a scalar...} \\
&= -i\tilde{\mathbf{R}}^{(0)} \tilde{\mathbf{S}}^{(1,0)} \tilde{\mathbf{R}}^{(0)} + i \sum_{K}^{occ} \sum_{L}^{unocc} \frac{\tilde{\mathbf{c}}_K^+ (\tilde{\mathbf{F}}^{(1,0)} - e_K \tilde{\mathbf{S}}^{(1,0)}) \tilde{\mathbf{c}}_L \tilde{\mathbf{c}}_K \tilde{\mathbf{c}}_L^+}{(e_K - e_L)} - \frac{\tilde{\mathbf{c}}_L \tilde{\mathbf{c}}_K^+ \tilde{\mathbf{c}}_K^+ (\tilde{\mathbf{F}}^{(1,0)} - e_K \tilde{\mathbf{S}}^{(1,0)}) \tilde{\mathbf{c}}_L}{(e_K - e_L)} \\
&= -i\tilde{\mathbf{R}}^{(0)} \tilde{\mathbf{S}}^{(1,0)} \tilde{\mathbf{R}}^{(0)} + i \sum_{K}^{occ} \sum_{L}^{unocc} \frac{\tilde{\mathbf{c}}_K^+ (\tilde{\mathbf{F}}^{(1,0)} - e_K \tilde{\mathbf{S}}^{(1,0)}) \tilde{\mathbf{c}}_L \tilde{\mathbf{c}}_K \tilde{\mathbf{c}}_L^+}{(e_K - e_L)} - \frac{\tilde{\mathbf{c}}_K^+ (\tilde{\mathbf{F}}^{(1,0)} - e_K \tilde{\mathbf{S}}^{(1,0)}) \tilde{\mathbf{c}}_L \tilde{\mathbf{c}}_L^+ \tilde{\mathbf{c}}_K}{(e_K - e_L)} \\
&= -i\tilde{\mathbf{R}}^{(0)} \tilde{\mathbf{S}}^{(1,0)} \tilde{\mathbf{R}}^{(0)} + i \sum_{K}^{occ} \sum_{L}^{unocc} \frac{\tilde{\mathbf{c}}_K^+ (\tilde{\mathbf{F}}^{(1,0)} - e_K \tilde{\mathbf{S}}^{(1,0)}) \tilde{\mathbf{c}}_L}{(e_K - e_L)} (\tilde{\mathbf{c}}_K \tilde{\mathbf{c}}_L^+ - \tilde{\mathbf{c}}_L \tilde{\mathbf{c}}_K^+)
\end{aligned}$$

APPENDIX E. McMURCHIE-DAVIDSON ONE- AND TWO-ELECTRON INTEGRALS

E.1) We can show in general that Eq. (3.79) holds by starting with the result and substituting in the definition for the Hermite polynomials:

$$\begin{aligned}
 \left(\frac{\partial \xi}{\partial x}\right)^j H_j(\xi) e^{-\xi^2} &= \left(\frac{\partial \xi}{\partial x}\right)^j \left[(-1)^j e^{\xi^2} \left(\frac{\partial}{\partial \xi}\right)^j e^{-\xi^2} \right] e^{-\xi^2} \\
 &= \left(\frac{\partial \xi}{\partial x}\right)^j \left[(-1)^j e^{\xi^2} \left(\frac{\partial a}{\partial \xi} \frac{\partial}{\partial a}\right)^j e^{-\xi^2} \right] e^{-\xi^2} \\
 &= \left(\frac{\partial \xi}{\partial x} \frac{\partial a}{\partial \xi}\right)^j \left[(-1)^j e^{\xi^2} \left(\frac{\partial}{\partial a}\right)^j e^{-\xi^2} \right] e^{-\xi^2} \\
 &= \left(-\frac{\partial a}{\partial x}\right)^j \left[(-1)^j e^{\xi^2} \left(\frac{\partial}{\partial a}\right)^j e^{-\xi^2} \right] e^{-\xi^2}
 \end{aligned}$$

since for a general function of two variables,

$$d\xi = \left(\frac{\partial \xi}{\partial x}\right)_a dx + \left(\frac{\partial \xi}{\partial a}\right)_x da$$

then let ξ be constant, and divide by da :

$$0 = \left(\frac{\partial \xi}{\partial x}\right)_a \left(\frac{\partial x}{\partial a}\right)_\xi + \left(\frac{\partial \xi}{\partial a}\right)_x \Rightarrow -\left(\frac{\partial \xi}{\partial a}\right)_x = \left(\frac{\partial \xi}{\partial x}\right)_a \left(\frac{\partial x}{\partial a}\right)_\xi \Rightarrow -\left(\frac{\partial a}{\partial x}\right)_\xi = \left(\frac{\partial \xi}{\partial x}\right)_a \left(\frac{\partial a}{\partial \xi}\right)_x$$

then since $\xi = \xi(x - a)$, $\left(\frac{\partial a}{\partial x}\right)_\xi = 1$, and we have

$$\begin{aligned}
\left(\frac{\partial \xi}{\partial x}\right)^j H_j(\xi) e^{-\xi^2} &= (-1)^j \left[(-1)^j e^{\xi^2} \left(\frac{\partial}{\partial a}\right)^j e^{-\xi^2} \right] e^{-\xi^2} \\
&= \left(\frac{\partial}{\partial a}\right)^j e^{-\xi^2}
\end{aligned} \tag{E.1.1}$$

Specifically, for $\xi = \xi(x - P_x) = \alpha_p^{1/2} x_p$, this implies that

$$\begin{aligned}
\left(\frac{\partial \xi}{\partial x}\right)^j H_j(\xi) e^{-\xi^2} &= \left(\frac{\partial}{\partial a}\right)^j e^{-\xi^2} \\
\Rightarrow \alpha_p^{j/2} H_j(\alpha_p^{1/2} x_p) e^{-\alpha_p x_p^2} &= \left(\frac{\partial}{\partial P_x}\right)^j e^{-\alpha_p x_p^2} = \Lambda_j e^{-\alpha_p x_p^2}
\end{aligned}$$

which was to be demonstrated. Note that for the simpler case where $\xi = \xi(x)$, we simply require

$$\begin{aligned}
\left(-\frac{\partial \xi}{\partial x}\right)^j H_j(\xi) e^{-\xi^2} &= \left(-\frac{\partial \xi}{\partial x}\right)^j (-1)^j e^{\xi^2} \left[\left(\frac{\partial}{\partial \xi}\right)^j e^{-\xi^2} \right] e^{-\xi^2} \\
&= (-1)^j \left(\frac{\partial \xi}{\partial x}\right)^j (-1)^j e^{\xi^2} \left[\left(\frac{\partial}{\partial \xi}\right)^j e^{-\xi^2} \right] e^{-\xi^2} \\
&= (-1)^j (-1)^j e^{\xi^2} \left[\left(\frac{\partial \xi}{\partial x} \frac{\partial}{\partial \xi}\right)^j e^{-\xi^2} \right] e^{-\xi^2} \\
&= \left(\frac{\partial}{\partial x}\right)^j e^{-\xi^2}
\end{aligned} \tag{E.1.2}$$

E.2) The recursion relation for Hermite polynomials is

$$\xi H_N(\xi) = N H_{N-1}(\xi) + \frac{1}{2} H_{N+1}(\xi) \tag{E.2.1}$$

and, using Eq. (3.79), substitute in $\alpha_p^{1/2} x_p$ or each term in Eq. (E.2.1):

$$\alpha_p^{1/2} x_p H_N(\alpha_p^{1/2} x_p) = \frac{x_p \Lambda_N}{\alpha_p^{\frac{N-1}{2}}}$$

$$N H_{N-1}(\alpha_p^{1/2} x_p) = \frac{N \Lambda_{N-1}}{\alpha_p^{\frac{N-1}{2}}}$$

$$\frac{1}{2} H_{N+1}(\alpha_p^{1/2} x_p) = \frac{\Lambda_{N+1}}{2 \alpha_p^{\frac{N+1}{2}}}$$

to make Eq. (E.2.1)

$$\begin{aligned} \frac{x_p \Lambda_N}{\alpha_p^{\frac{N-1}{2}}} &= \frac{N \Lambda_{N-1}}{\alpha_p^{\frac{N-1}{2}}} + \frac{\Lambda_{N+1}}{2 \alpha_p^{\frac{N+1}{2}}} \\ \Rightarrow \quad x_p \Lambda_N &= N \Lambda_{N-1} + \frac{\Lambda_{N+1}}{2 \alpha_p} \\ \Rightarrow \quad (x_A - \overline{PA_x}) \Lambda_N &= N \Lambda_{N-1} + \frac{\Lambda_{N+1}}{2 \alpha_p} \\ \Rightarrow \quad x_A \Lambda_N &= N \Lambda_{N-1} + \overline{PA_x} \Lambda_N + \frac{\Lambda_{N+1}}{2 \alpha_p} \end{aligned}$$

where we have used

$$x_p = x_A - \overline{PA_x} = x_A - (P_x - A_x) = x - A_x - P_x + A_x = x - P_x.$$

E.3) Consider

$$\begin{aligned} x_A^n x_B^{\bar{n}} &= \sum_{N=0}^{n+\bar{n}} d_N^{n\bar{n}} \Lambda_N, \text{ and by application of this,} \\ x_A^{n+1} x_B^{\bar{n}} &= \sum_{N=0}^{n+\bar{n}+1} d_N^{n+1,\bar{n}} \Lambda_N \end{aligned} \tag{E.3.1}$$

which can also be written as

$$x_A^{n+1} x_B^{\bar{n}} = \sum_{N=0}^{n+\bar{n}} d_N^{n\bar{n}} x_A \Lambda_N \tag{E.3.2}$$

Using this and Eq. (3.80), we have

$$\begin{aligned}
x_A^{n+1}x_B^{\bar{n}} &= \sum_{N=0}^{n+\bar{n}} d_N^{n\bar{n}} \left(N\Lambda_{N-1} + \overline{PA_x} \Lambda_N + \frac{\Lambda_{N+1}}{2\alpha_p} \right) \\
&= \sum_{N=0}^{n+\bar{n}} d_N^{n\bar{n}} N\Lambda_{N-1} + \sum_{N=0}^{n+\bar{n}} d_N^{n\bar{n}} \overline{PA_x} \Lambda_N + \sum_{N=0}^{n+\bar{n}} d_N^{n\bar{n}} \frac{\Lambda_{N+1}}{2\alpha_p} \\
&= \sum_{N=-1}^{n+\bar{n}-1} d_{N+1}^{n\bar{n}} (N+1)\Lambda_N + \sum_{N=0}^{n+\bar{n}} d_N^{n\bar{n}} \overline{PA_x} \Lambda_N + \sum_{N=1}^{n+\bar{n}+1} d_{N-1}^{n\bar{n}} \frac{\Lambda_N}{2\alpha_p} \\
&= d_0^{n\bar{n}}(0)\Lambda_{-1} + \sum_{N=0}^{n+\bar{n}+1} d_{N+1}^{n\bar{n}} (N+1)\Lambda_N - d_{n+\bar{n}+1}^{n\bar{n}} (n+\bar{n}+1)\Lambda_{n+\bar{n}} - d_{n+\bar{n}+2}^{n\bar{n}} (n+\bar{n}+2)\Lambda_{n+\bar{n}+1} \\
&\quad + \sum_{N=0}^{n+\bar{n}+1} d_N^{n\bar{n}} \overline{PA_x} \Lambda_N - d_{n+\bar{n}+1}^{n\bar{n}} \overline{PA_x} \Lambda_{n+\bar{n}+1} + \sum_{N=0}^{n+\bar{n}+1} d_{N-1}^{n\bar{n}} \frac{\Lambda_N}{2\alpha_p} - d_{-1}^{n\bar{n}} \frac{\Lambda_0}{2\alpha_p}
\end{aligned}$$

then from Eq. (E.3.2), $d_N^{n\bar{n}} = 0$ unless $0 > N > (n+\bar{n})$, such that

$$\begin{aligned}
x_A^{n+1}x_B^{\bar{n}} &= \sum_{N=0}^{n+\bar{n}+1} d_{N+1}^{n\bar{n}} (N+1)\Lambda_N + \sum_{N=0}^{n+\bar{n}+1} d_N^{n\bar{n}} \overline{PA_x} \Lambda_N + \sum_{N=0}^{n+\bar{n}+1} d_{N-1}^{n\bar{n}} \frac{\Lambda_N}{2\alpha_p} \\
&= \sum_{N=0}^{n+\bar{n}+1} \left[d_{N+1}^{n\bar{n}} (N+1) + d_N^{n\bar{n}} \overline{PA_x} + \frac{d_{N-1}^{n\bar{n}}}{2\alpha_p} \right] \Lambda_N
\end{aligned}$$

then, using Eq. (E.3.1),

$$x_A^{n+1}x_B^{\bar{n}} = \sum_{N=0}^{n+\bar{n}+1} d_N^{n+1,\bar{n}} \Lambda_N = \sum_{N=0}^{n+\bar{n}+1} \left[d_{N+1}^{n\bar{n}} (N+1) + d_N^{n\bar{n}} \overline{PA_x} + \frac{d_{N-1}^{n\bar{n}}}{2\alpha_p} \right] \Lambda_N$$

such that we can easily identify the recursion relation

$$d_N^{n+1,\bar{n}} = d_{N+1}^{n\bar{n}} (N+1) + d_N^{n\bar{n}} \overline{PA_x} + \frac{d_{N-1}^{n\bar{n}}}{2\alpha_p}$$

E.4) Very quickly, but included for completeness:

$$\begin{aligned}
\phi_A \frac{\partial}{\partial x} \phi_B &= \phi_A \frac{\partial}{\partial x} x_B^{\bar{n}} y_B^{\bar{l}} z_B^{\bar{m}} e^{-\alpha_B r_B^2} \\
&= \phi_A y_B^{\bar{l}} z_B^{\bar{m}} \left(\frac{\partial x_B^{\bar{n}}}{\partial x} e^{-\alpha_B r_B^2} + x_B^{\bar{n}} \frac{\partial e^{-\alpha_B (x_B^2 + y_B^2 + z_B^2)}}{\partial x} \right) \\
&= \phi_A y_B^{\bar{l}} z_B^{\bar{m}} \left(\bar{n} x_B^{\bar{n}-1} e^{-\alpha_B r_B^2} + x_B^{\bar{n}} e^{-\alpha_B r_B^2} (-\alpha_B) \frac{\partial (x_B^2 + y_B^2 + z_B^2)}{\partial x} \right) \\
&= \phi_A y_B^{\bar{l}} z_B^{\bar{m}} \left(\bar{n} x_B^{\bar{n}-1} e^{-\alpha_B r_B^2} - 2\alpha_B x_B^{\bar{n}+1} e^{-\alpha_B r_B^2} \right) \\
&= (\bar{n} x_A^n x_B^{\bar{n}-1} - 2\alpha_B x_A^n x_B^{\bar{n}+1}) y_A^l y_B^{\bar{l}} z_A^m z_B^{\bar{m}} e^{-(\alpha_A r_A^2 + \alpha_B r_B^2)}
\end{aligned}$$

E.5) For the dipole moment expectation value:

$$\begin{aligned}
\int d\mathbf{r} \phi_A x_C \phi_B &= E_{AB} \sum_{N=0}^{n+\bar{n}} \sum_{L=0}^{l+\bar{l}} \sum_{M=0}^{m+\bar{m}} d_N^{n\bar{n}} e_L^{\bar{l}} f_M^{m\bar{m}} \int d\mathbf{r} x_C \mathbf{\Lambda}_N \mathbf{\Lambda}_M e^{-\alpha_P r_P^2} \\
&= E_{AB} \sum_{N=0}^{n+\bar{n}} \sum_{L=0}^{l+\bar{l}} \sum_{M=0}^{m+\bar{m}} d_N^{n\bar{n}} e_L^{\bar{l}} f_M^{m\bar{m}} \int d\mathbf{r} \left(N \mathbf{\Lambda}_{N-1} + \overline{PC}_x \mathbf{\Lambda}_N + \frac{\mathbf{\Lambda}_{N+1}}{2\alpha_P} \right) \mathbf{\Lambda}_L \mathbf{\Lambda}_M e^{-\alpha_P r_P^2} \\
&= E_{AB} \left(\frac{\pi}{\alpha_P} \right) \sum_{N=0}^{n+\bar{n}} \sum_{L=0}^{l+\bar{l}} \sum_{M=0}^{m+\bar{m}} d_N^{n\bar{n}} e_L^{\bar{l}} f_M^{m\bar{m}} \delta_{L,0} \delta_{M,0} \int d\mathbf{r} \left(N \mathbf{\Lambda}_{N-1} + \overline{PC}_x \mathbf{\Lambda}_N + \frac{\mathbf{\Lambda}_{N+1}}{2\alpha_P} \right) e^{-\alpha_P x_P^2} \\
&= E_{AB} \left(\frac{\pi}{\alpha_P} \right) \sum_{N=0}^{n+\bar{n}} \sum_{L=0}^{l+\bar{l}} \sum_{M=0}^{m+\bar{m}} d_N^{n\bar{n}} e_L^{\bar{l}} f_M^{m\bar{m}} \delta_{L,0} \delta_{M,0} \left[N \delta_{N-1,0} \left(\frac{\pi}{\alpha_P} \right)^{1/2} + \overline{PC}_x \delta_{N,0} \left(\frac{\pi}{\alpha_P} \right)^{1/2} + \frac{\delta_{N+1,0}}{2\alpha_P} \left(\frac{\pi}{\alpha_P} \right)^{1/2} \right] \\
&= E_{AB} \left(\frac{\pi}{\alpha_P} \right)^{3/2} \sum_{N=0}^{n+\bar{n}} \sum_{L=0}^{l+\bar{l}} \sum_{M=0}^{m+\bar{m}} d_N^{n\bar{n}} e_L^{\bar{l}} f_M^{m\bar{m}} \delta_{L,0} \delta_{M,0} \left[N \delta_{N-1,0} + \overline{PC}_x \delta_{N,0} + \frac{\delta_{N+1,0}}{2\alpha_P} \right] \\
&= E_{AB} \left(\frac{\pi}{\alpha_P} \right)^{3/2} \sum_{N=0}^1 d_N^{n\bar{n}} e_0^{\bar{l}} f_0^{m\bar{m}} [\delta_{N,1} + \overline{PC}_x \delta_{N,0}]
\end{aligned}$$

the last line is true since N cannot be less than zero by virtue of its definition in Eq. (3.81) and in its relation to the Hermite polynomials.

E.6) The second moments can be evaluated by inspection if we note that

$$\begin{aligned}
x_C(x_C \Lambda_N) &= Nx_C \Lambda_{N-1} + \overline{PC}_x x_C \Lambda_N + \frac{x_C \Lambda_{N+1}}{2\alpha_p} \\
&= \left(N(N-1) \Lambda_{N-2} + N \overline{PC}_x \Lambda_{N-1} + \frac{N \Lambda_N}{2\alpha_p} \right) + \left(\overline{PC}_x N \Lambda_{N-1} + \overline{PC}_x^2 \Lambda_N + \frac{\overline{PC}_x \Lambda_{N+1}}{2\alpha_p} \right) \\
&\quad + \left(\frac{(N+1)}{2\alpha_p} \Lambda_N + \frac{\overline{PC}_x}{2\alpha_p} \Lambda_{N+1} + \frac{\Lambda_{N+2}}{4\alpha_p^2} \right) \\
&= N(N-1) \Lambda_{N-2} + 2N \overline{PC}_x \Lambda_{N-1} + \left[\frac{N}{2\alpha_p} + \overline{PC}_x^2 + \frac{(N+1)}{2\alpha_p} \right] \Lambda_N + \left[\frac{\overline{PC}_x}{\alpha_p} \right] \Lambda_{N+1} + \frac{\Lambda_{N+2}}{4\alpha_p^2}
\end{aligned}$$

and when taking the integral, for reasons outlined in (E.5), any terms with lambda indexed greater than zero will vanish, such that

$$\begin{aligned}
x_C x_C \Lambda_N &= N(N-1) \Lambda_{N-2} + 2N \overline{PC}_x \Lambda_{N-1} + \left[\frac{N}{2\alpha_p} + \overline{PC}_x^2 + \frac{(N+1)}{2\alpha_p} \right] \Lambda_N \\
&\Rightarrow 2\delta_{N,2} + 2\overline{PC}_x \delta_{N,1} + \left[\overline{PC}_x^2 + \frac{1}{2\alpha_p} \right] \delta_{N,0}
\end{aligned}$$

then the equation analogous to dipole integral is

$$\begin{aligned}
\int d\mathbf{r} \phi_A x_C^2 \phi_B &= E_{AB} \left(\frac{\pi}{\alpha_p} \right) \sum_{N=0}^{n+\bar{n}} \sum_{L=0}^{l+\bar{l}} \sum_{M=0}^{m+\bar{m}} d_N^{n\bar{n}} e_L^{\bar{l}} f_M^{m\bar{m}} \delta_{L,0} \delta_{M,0} \left[2\delta_{N,2} + 2\overline{PC}_x \delta_{N,1} + \left[\overline{PC}_x^2 + \frac{1}{2\alpha_p} \right] \delta_{N,0} \right] \\
&= E_{AB} \left(\frac{\pi}{\alpha_p} \right)^{3/2} \sum_{N=0}^2 d_N^{n\bar{n}} e_0^{\bar{l}} f_0^{m\bar{m}} \left[2\delta_{N,2} + 2\overline{PC}_x \delta_{N,1} + \left[\overline{PC}_x^2 + \frac{1}{2\alpha_p} \right] \delta_{N,0} \right]
\end{aligned}$$

with a similar procedure for $x_C y_C, y_C z_C, y_C^2$, etc.

E.7) Our task is to show that

$$\int d\mathbf{r} r_C^{-1} e^{-\alpha_p r_C^2} = \left(\frac{2\pi}{\alpha_p} \right) \int_0^1 du e^{-\alpha_p \overline{CP}^2 u^2}$$

To see this, transform to spheroidal coordinates^{126,127} where

$$r_C = \frac{\overline{CP}}{2}(\lambda - \mu) ; \quad r_P = \frac{\overline{CP}}{2}(\lambda + \mu)$$

$$d\mathbf{r} = \frac{1}{8} \overline{CP}^3 (\lambda^2 - \mu^2) d\lambda d\mu d\phi ; \quad 1 \leq \lambda < \infty , \quad -1 \leq \mu \leq 1 , \quad 0 \leq \phi \leq 2\pi$$

$$\begin{aligned} \int d\mathbf{r} r_C^{-1} e^{-\alpha_p r_p^2} &= \int_1^\infty \int_{-1}^1 \int_0^{2\pi} d\lambda d\mu d\phi \frac{1}{8} \overline{CP}^3 (\lambda^2 - \mu^2) \frac{2}{\overline{CP}(\lambda - \mu)} e^{-\alpha_p \frac{\overline{CP}^2}{4} (\lambda + \mu)^2} \\ &= \frac{\overline{CP}^2}{4} \int_1^\infty \int_{-1}^1 \int_0^{2\pi} d\lambda d\mu d\phi \frac{(\lambda - \mu)(\lambda + \mu)}{(\lambda - \mu)} e^{-\alpha_p \frac{\overline{CP}^2}{4} (\lambda + \mu)^2} \\ &= \frac{\pi \overline{CP}^2}{2} \int_1^\infty \int_{-1}^1 d\lambda d\mu (\lambda + \mu) e^{-\alpha_p \frac{\overline{CP}^2}{4} (\lambda + \mu)^2} \end{aligned}$$

Then let

$$\begin{aligned} \xi &= \lambda + \mu \\ d\xi &= d\mu \\ \Rightarrow \int_{-1}^1 d\mu (\lambda + \mu) e^{-\alpha_p \frac{\overline{CP}^2}{4} (\lambda + \mu)^2} &= \int_{\lambda-1}^{\lambda+1} d\xi \xi e^{-\alpha_p \frac{\overline{CP}^2}{4} \xi^2} \\ &= \int_{\lambda-1}^{\lambda+1} d\xi \left(-\frac{2}{\alpha_p \overline{CP}^2} \right) \frac{d}{d\xi} e^{-\alpha_p \frac{\overline{CP}^2}{4} \xi^2} \\ &= -\frac{2}{\alpha_p \overline{CP}^2} \int_{\lambda-1}^{\lambda+1} d\xi \frac{d}{d\xi} e^{-\alpha_p \frac{\overline{CP}^2}{4} \xi^2} \\ &= -\frac{2}{\alpha_p \overline{CP}^2} \left[e^{-\alpha_p \frac{\overline{CP}^2}{4} (\lambda-1)^2} - e^{-\alpha_p \frac{\overline{CP}^2}{4} (\lambda+1)^2} \right] \end{aligned}$$

such that

$$\begin{aligned} \int d\mathbf{r} r_C^{-1} e^{-\alpha_p r_p^2} &= \frac{\pi \overline{CP}^2}{2} \int_1^\infty d\lambda \frac{2}{\alpha_p \overline{CP}^2} \left[e^{-\alpha_p \frac{\overline{CP}^2}{4} (\lambda-1)^2} - e^{-\alpha_p \frac{\overline{CP}^2}{4} (\lambda+1)^2} \right] \\ &= \frac{\pi}{\alpha_p} \int_1^\infty d\lambda \left[e^{-\alpha_p \frac{\overline{CP}^2}{4} (\lambda-1)^2} - e^{-\alpha_p \frac{\overline{CP}^2}{4} (\lambda+1)^2} \right] \end{aligned}$$

Then let

$$u^2 = \frac{(\lambda+1)^2}{4} \quad du = \frac{1}{2} d\lambda$$

$$v^2 = \frac{(\lambda-1)^2}{4} \quad dv = \frac{1}{2} d\lambda$$

such that

$$\begin{aligned} \int d\mathbf{r} r_C^{-1} e^{-\alpha_p r_p^2} &= \frac{2\pi}{\alpha_p} \left[\int_0^\infty dv e^{-\alpha_p \bar{C}^2 v^2} - \int_1^\infty du e^{-\alpha_p \bar{C}^2 u^2} \right] \\ &= \frac{2\pi}{\alpha_p} \int_0^1 du e^{-\alpha_p \bar{C}^2 u^2} \end{aligned}$$

Q.E.D.

E.8) The recursion relations for R_{NLM} can be shown by considering the general definition:

$$R_{NLMj} = \left(\frac{\partial}{\partial a} \right)^N \left(\frac{\partial}{\partial b} \right)^L \left(\frac{\partial}{\partial c} \right)^M (-2\alpha)^j F_j(T) = \left(\frac{\partial}{\partial a} \right)^N \left(\frac{\partial}{\partial b} \right)^L \left(\frac{\partial}{\partial c} \right)^M (-2\alpha)^j \int_0^1 u^{2j} e^{-Tu^2} du$$

where $T = \alpha(a^2 + b^2 + c^2)$. Then using the general relation of the derivatives of the Hermite polynomials, Eq. (E.1.2), we have

$$\begin{aligned} R_{NLMj} &= (-2\alpha)^j \int_0^1 u^{2j} \left(\frac{\partial}{\partial a} \right)^N e^{-\alpha u^2 a^2} \left(\frac{\partial}{\partial b} \right)^L e^{-\alpha u^2 b^2} \left(\frac{\partial}{\partial c} \right)^M e^{-\alpha u^2 c^2} du \\ &= (-2\alpha)^j \int_0^1 \left\{ \begin{aligned} &u^{2j} \left(-\frac{\partial}{\partial a} \alpha^{1/2} u a \right)^N H_N(\alpha^{1/2} u a) e^{-\alpha u^2 a^2} \\ &\times \left(-\frac{\partial}{\partial b} \alpha^{1/2} u b \right)^L H_L(\alpha^{1/2} u b) e^{-\alpha u^2 b^2} \\ &\times \left(-\frac{\partial}{\partial c} \alpha^{1/2} u c \right)^M H_M(\alpha^{1/2} u c) e^{-\alpha u^2 c^2} du \end{aligned} \right\} \\ &= (-2\alpha)^j \int_0^1 \left\{ \begin{aligned} &u^{2j} \left(-\alpha^{1/2} u \right)^N H_N(\alpha^{1/2} u a) e^{-\alpha u^2 a^2} \\ &\times \left(-\alpha^{1/2} u \right)^L H_L(\alpha^{1/2} u b) e^{-\alpha u^2 b^2} \\ &\times \left(-\alpha^{1/2} u \right)^M H_M(\alpha^{1/2} u c) e^{-\alpha u^2 c^2} du \end{aligned} \right\} \\ &= \left(-\alpha^{1/2} \right)^{N+L+M} (-2\alpha)^j \int_0^1 u^{N+L+M+2j} H_N(\alpha^{1/2} u a) H_L(\alpha^{1/2} u b) H_M(\alpha^{1/2} u c) e^{-Tu^2} du \end{aligned}$$

From here, we consider $R_{0,0,M+1,j}$:

$$R_{0,0,M+1,j} = (-\alpha^{1/2})^{M+1} (-2\alpha)^j \int_0^1 u^{M+1+2j} H_M(\alpha^{1/2}uc) e^{-Tu^2} du$$

then using the recurrence formula $\xi H_N(\xi) = NH_{N-1}(\xi) + \frac{1}{2} H_{N+1}(\xi)$, we can write

$$\begin{aligned} R_{0,0,M+1,j} &= (-\alpha^{1/2})^{M+1} (-2\alpha)^j \int_0^1 u^{M+1+2j} H_{M+1}(\alpha^{1/2}uc) e^{-Tu^2} du \\ &= (-\alpha^{1/2})^{M+1} (-2\alpha)^j c \int_0^1 u^{M+2+2j} 2\alpha^{1/2} H_M(\alpha^{1/2}uc) e^{-Tu^2} du \\ &\quad - (-\alpha^{1/2})^{M+1} (-2\alpha)^j 2M \int_0^1 u^{M+1+2j} H_{M-1}(\alpha^{1/2}uc) e^{-Tu^2} du \\ &= (-\alpha^{1/2})^M (-2\alpha)^j c \int_0^1 u^{M+2+2j} H_M(\alpha^{1/2}uc) e^{-Tu^2} du \\ &\quad - (-\alpha^{1/2})^{M-1} (-\alpha^{1/2})^2 (-2\alpha)^j 2M \int_0^1 u^{M+1+2j} H_{M-1}(\alpha^{1/2}uc) e^{-Tu^2} du \\ &= c(-\alpha^{1/2})^M (-2\alpha)^{j+1} \int_0^1 u^{M+2+2j} H_M(\alpha^{1/2}uc) e^{-Tu^2} du \\ &\quad + M(-\alpha^{1/2})^{M-1} (-2\alpha)^{j+1} \int_0^1 u^{M+1+2j} H_{M-1}(\alpha^{1/2}uc) e^{-Tu^2} du \\ &= cR_{0,0,M,j+1} + MR_{0,0,M-1,j+1} \end{aligned}$$

similarly,

$$\begin{aligned} R_{0,L+1,M,j} &= (-\alpha^{1/2})^{L+M+1} (-2\alpha)^j \int_0^1 u^{L+1+M+2j} H_{L+1}(\alpha^{1/2}ub) H_M(\alpha^{1/2}uc) e^{-Tu^2} du \\ &= (-\alpha^{1/2})^{L+M+1} (-2\alpha)^j b \int_0^1 u^{L+M+2+2j} 2\alpha^{1/2} H_L(\alpha^{1/2}ub) H_M(\alpha^{1/2}uc) e^{-Tu^2} du \\ &\quad - (-\alpha^{1/2})^{L+M+1} (-2\alpha)^j 2L \int_0^1 u^{L+M+1+2j} H_{L-1}(\alpha^{1/2}ub) H_M(\alpha^{1/2}uc) e^{-Tu^2} du \\ &= (-\alpha^{1/2})^{L+M} (-2\alpha)^j b \int_0^1 u^{L+M+2+2j} H_L(\alpha^{1/2}ub) H_M(\alpha^{1/2}uc) e^{-Tu^2} du \\ &\quad - (-\alpha^{1/2})^{L+M-1} (-\alpha^{1/2})^2 (-2\alpha)^j 2L \int_0^1 u^{L+M+1+2j} H_{L-1}(\alpha^{1/2}ub) H_M(\alpha^{1/2}uc) e^{-Tu^2} du \\ &= b(-\alpha^{1/2})^{L+M} (-2\alpha)^{j+1} \int_0^1 u^{L+M+2+2j} H_L(\alpha^{1/2}ub) H_M(\alpha^{1/2}uc) e^{-Tu^2} du \\ &\quad + L(-\alpha^{1/2})^{L+M-1} (-2\alpha)^{j+1} \int_0^1 u^{M+1+2j} H_{L-1}(\alpha^{1/2}ub) H_M(\alpha^{1/2}uc) e^{-Tu^2} du \\ &= bR_{0,L,M,j+1} + LR_{0,L-1,M,j+1} \end{aligned}$$

and now that the method has been established, by an exactly analogous procedure, the final relation is obtained:

$$R_{N+1,L,M,j} = aR_{N,L,M,j+1} + NR_{N-1,L,M,j+1}$$

APPENDIX F. SUPPLEMENTAL TABLES FOR MRG_n THEORY

Table (F.1) MR(QD)-G2(MP2,SVP) heats of formation, ionization energies, electron affinities and proton affinities. Values in parentheses are the differences between experimental and MR(QD)-G2(MP2,SVP) values.^a

	Species	Species	Species	
Heats of Formation	LiH 30.0 (+ 3.3)	PH ₃ 3.0 (- 1.7)	F ₂ 0.3 (- 0.3)	
	BeH 84.7 (- 3.0)	H ₂ S - 5.1 (+ 0.2)	CO ₂ - 97.6 (+ 3.5)	
	CH 141.5 (+ 1.0)	HCl - 23.2 (+ 1.1)	Na ₂ 29.1 (+ 4.9)	
	CH ₂ ³ B ₁ 94.7 (- 1.0)	Li ₂ 47.1 (+ 4.5)	Si ₂ 141.4 (- 1.5)	
	CH ₂ ¹ A ₁ 100.6 (+ 2.2)	LiF - 79.8 (- 0.3)	P ₂ 34.8 (- 0.5)	
	CH ₃ 34.2 (+ 0.8)	C ₂ H ₂ 54.4 (- 0.2)	S ₂ 32.8 (- 2.1)	
	CH ₄ - 20.2 (+ 2.3)	C ₂ H ₄ 14.8 (- 2.3)	Cl ₂ 1.5 (- 1.5)	
	NH 85.4 (- 0.2)	CN 106.3 (- 1.4)	NaCl - 49.4 (+ 5.8)	
	NH ₂ 44.2 (+ 0.9)	HCN 31.7 (- 0.2)	SiO - 22.5 (- 2.1)	
	NH ₃ - 9.5 (- 1.5)	CO - 28.7 (+ 2.3)	CS 64.4 (+ 2.5)	
	OH 8.4 (+ 1.0)	HCO 9.0 (+ 1.0)	SO 3.4 (- 2.2)	
	H ₂ O - 58.0 (+ 0.2)	HCHO - 24.2 (- 1.8)	CIO 26.3 (- 2.1)	
	HF - 65.8 (+ 0.7)	CH ₃ OH - 48.9 (+ 0.9)	CIF - 12.2 (- 1.0)	
	SiH ₂ ¹ A ₁ 62.9 (+ 2.3)	N ₂ - 1.1 (+ 1.1)	CH ₃ Cl - 19.6 (+ 0.0)	
	SiH ₂ ³ B ₁ 87.5 (- 1.3)	N ₂ H ₄ 22.8 (+ 0.0)	CH ₃ SH - 8.0 (+ 2.5)	
	SiH ₃ 48.4 (- 0.5)	NO 20.1 (+ 1.5)	HOCl - 17.9 (+ 0.1)	
	SiH ₄ 7.8 (+ 0.2)	O ₂ 1.0 (- 1.0)	SO ₂ - 66.5 (- 4.5)	
	PH ₂ 33.3 (- 0.4)	H ₂ O ₂ - 33.2 (+ 0.7)		
Ionization Energies	Li 123.2 (+ 1.1)	Cl 296.4 (+ 2.7)	HCl 293.4 (+ 0.6)	
	Be 219.6 (- 4.7)	CH ₄ 293.0 (- 2.0)	C ₂ H ₂ 264.2 (- 1.3)	
	B 189.1 (+ 2.3)	NH ₃ 233.0 (+ 1.8)	C ₂ H ₄ 241.1 (+ 1.2)	
	C 257.9 (+ 1.8)	OH 300.3 (- 0.3)	CO 324.1 (- 1.0)	
	N 334.0 (+ 1.3)	OH ₂ 291.3 (- 0.3)	N ₂ ² Σ _g 359.1 (+ 0.2)	
	O 313.4 (+ 0.4)	HF 371.0 (- 1.1)	N ₂ ² Π _u 384.3 (+ 0.8)	
	F 402.6 (- 0.9)	SiH ₄ 252.7 (+ 1.0)	O ₂ 279.9 (- 1.6)	
	Na 114.1 (+ 4.4)	PH 233.4 (+ 0.7)	P ₂ 243.3 (- 0.5)	
	Mg 179.0 (- 2.7)	PH ₂ 224.8 (+ 1.6)	S ₂ 213.2 (+ 2.6)	
	Al 137.1 (+ 0.9)	PH ₃ 228.6 (- 1.0)	Cl ₂ 265.0 (+ 0.2)	
	Si 187.0 (+ 0.9)	SH 237.9 (+ 1.2)	CIF 291.6 (+ 0.3)	
	P 241.4 (+ 0.5)	H ₂ S ² B ₁ 240.3 (+ 1.1)	CS 263.2 (- 1.9)	
	S 235.0 (+ 3.9)	H ₂ S ² A ₁ 293.9 (+ 0.8)		
Electron Affinities	C 29.0 (+ 0.1)	CH ₃ - 2.1 (+ 3.9)	SH 53.2 (+ 1.2)	
	O 33.8 (- 0.1)	NH 8.1 (+ 0.7)	O ₂ 11.7 (- 1.6)	
	F 81.2 (- 2.8)	NH ₂ 17.4 (+ 0.4)	NO - 0.3 (+ 0.8)	
	Si 32.2 (- 0.3)	OH 42.9 (- 0.7)	CN 91.7 (- 2.7)	
	P 14.7 (+ 2.5)	SiH 27.9 (+ 1.5)	PO 25.1 (+ 0.0)	
	S 46.6 (+ 1.3)	SiH ₂ 22.7 (+ 3.2)	S ₂ 37.7 (+ 0.6)	
	Cl 84.0 (- 0.6)	SiH ₃ 33.3 (- 0.8)	Cl ₂ 55.4 (- 0.3)	
	CH 25.3 (+ 3.3)	PH 21.9 (+ 1.9)		
	CH ₂ 15.8 (- 0.8)	PH ₂ 28.6 (+ 0.7)		
Proton Affinities	NH ₃ 205.2 (- 2.7)	SiH ₄ 153.8 (+ 0.2)	HCl 133.2 (+ 0.4)	
	H ₂ O 160.5 (+ 4.6)	PH ₃ 184.9 (+ 2.2)		
	C ₂ H ₂ 154.6 (- 2.3)	H ₂ S 167.7 (+ 1.1)		

^aValues in kcal mol⁻¹. The heats of formation are 298 K values whereas the remaining quantities refer to 0 K.

Table (F.2) MR(QD)-G2(MP2) heats of formation, ionization energies, electron affinities and proton affinities. Values in parentheses are the differences between experimental and MR(QD)-G2(MP2) values.^a

	Species	Species	Species	
Heats of Formation	LiH	30.4 (+ 2.9)	PH ₃	1.7 (- 0.4)
	BeH	83.0 (- 1.3)	H ₂ S	- 5.2 (+ 0.3)
	CH	141.3 (+ 1.2)	HCl	- 23.1 (+ 1.0)
	CH ₂ ³ B ₁	94.4 (- 0.7)	Li ₂	47.7 (+ 3.9)
	CH ₂ ¹ A ₁	99.9 (+ 2.9)	LiF	- 81.3 (+ 1.2)
	CH ₃	33.6 (+ 1.4)	C ₂ H ₂	55.9 (- 1.7)
	CH ₄	- 21.2 (+ 3.3)	C ₂ H ₄	11.0 (+ 1.5)
	NH	85.5 (- 0.3)	CN	107.9 (- 3.0)
	NH ₂	44.0 (+ 1.1)	HCN	33.2 (- 1.7)
	NH ₃	- 10.1 (- 0.9)	CO	- 27.8 (+ 1.4)
	OH	8.6 (+ 0.8)	HCO	10.0 (+ 0.0)
	H ₂ O	- 58.1 (+ 0.3)	HCHO	- 23.8 (- 2.2)
	HF	- 65.2 (+ 0.1)	CH ₃ OH	- 49.3 (+ 1.3)
	SiH ₂ ¹ A ₁	61.6 (+ 3.6)	N ₂	0.5 (- 0.5)
	SiH ₂ ³ B ₁	86.2 (+ 0.0)	N ₂ H ₄	22.7 (+ 0.1)
	SiH ₃	46.2 (+ 1.7)	NO	21.2 (+ 0.4)
	SiH ₄	4.2 (+ 4.0)	O ₂	1.5 (- 1.5)
	PH ₂	32.7 (+ 0.4)	H ₂ O ₂	- 32.5 (+ 0.0)
Ionization energies	Li	123.4 (+ 0.9)	Cl	295.5 (+ 3.6)
	Be	219.1 (- 4.2)	CH ₄	293.3 (- 2.3)
	B	190.1 (+ 1.3)	NH ₃	232.8 (+ 2.0)
	C	258.4 (+ 1.3)	OH	299.6 (+ 0.4)
	N	334.0 (+ 1.3)	OH ₂	291.0 (+ 0.0)
	O	312.7 (+ 1.1)	HF	370.3 (- 0.4)
	F	401.6 (+ 0.1)	SiH ₄	253.6 (+ 0.1)
	Na	114.1 (+ 4.4)	PH	233.3 (+ 0.8)
	Mg	178.3 (- 2.0)	PH ₂	224.5 (+ 1.9)
	Al	137.1 (+ 0.9)	PH ₃	228.3 (- 0.7)
	Si	187.0 (+ 0.9)	SH	237.3 (+ 1.8)
	P	241.2 (+ 0.7)	H ₂ S ² B ₁	239.8 (+ 1.6)
	S	234.0 (+ 4.9)	H ₂ S ² A ₁	294.5 (+ 0.2)
Electron affinities	C	29.0 (+ 0.1)	CH ₃	- 2.1 (+ 3.9)
	O	32.8 (+ 0.9)	NH	7.4 (+ 1.4)
	F	79.6 (- 1.2)	NH ₂	17.0 (+ 0.8)
	Si	32.4 (- 0.5)	OH	42.1 (+ 0.1)
	P	15.5 (+ 1.7)	SiH	28.0 (+ 1.4)
	S	45.7 (+ 2.2)	SiH ₂	22.7 (+ 3.2)
	Cl	82.9 (+ 0.5)	SiH ₃	33.0 (- 0.5)
	CH	25.0 (+ 3.6)	PH	21.3 (+ 2.5)
	CH ₂	15.9 (- 0.9)	PH ₂	27.8 (+ 1.5)
Proton affinities	NH ₃	205.7 (- 3.2)	SiH ₄	153.9 (+ 0.1)
	H ₂ O	161.1 (+ 0.5)	PH ₃	186.3 (+ 0.8)
	C ₂ H ₂	153.7 (- 1.4)	H ₂ S	168.5 (+ 0.3)
			HCl	133.8 (- 0.2)

^aValues in kcal mol⁻¹. The heats of formation are 298 K values whereas the remaining quantities refer to 0 K.

Table (F.3) MR(QD)-G3(MP2) heats of formation, ionization energies, electron affinities and proton affinities. Values in parentheses are the differences between experimental and MR-G3(MP2) values.^a

	Species	Species	Species	
Heats of Formation	LiH	30.3 (+ 3.0)	PH ₃	4.0 (- 2.7)
	BeH	83.6 (- 1.9)	H ₂ S	- 4.8 (- 0.1)
	CH	141.1 (+ 1.4)	HCl	- 23.3 (+ 1.2)
	CH ₂ ³ B ₁	93.7 (+ 0.0)	Li ₂	47.4 (+ 4.2)
	CH ₂ ¹ A ₁	101.3 (+ 1.5)	LiF	- 79.8 (- 0.3)
	CH ₃	34.2 (+ 0.8)	C ₂ H ₂	54.1 (+ 0.1)
	CH ₄	- 19.2 (+ 1.3)	C ₂ H ₄	15.7 (- 3.2)
	NH	84.4 (+ 0.8)	CN	106.8 (- 1.9)
	NH ₂	44.3 (+ 0.8)	HCN	32.7 (- 1.2)
	NH ₃	- 8.5 (- 2.5)	CO	- 27.5 (+ 1.1)
	OH	7.6 (+ 1.8)	HCO	9.6 (+ 0.4)
	H ₂ O	- 57.8 (+ 0.0)	HCHO	- 23.0 (- 3.0)
	HF	- 66.0 (+ 0.9)	CH ₃ OH	- 47.8 (- 0.2)
	SiH ₂ ¹ A ₁	63.2 (+ 2.0)	N ₂	0.0 (+ 0.0)
	SiH ₂ ³ B ₁	86.2 (+ 0.0)	N ₂ H ₄	24.7 (- 1.9)
	SiH ₃	47.9 (+ 0.0)	NO	20.6 (+ 1.0)
	SiH ₄	8.0 (+ 0.2)	O ₂	- 0.4 (+ 0.4)
	PH ₂	33.1 (+ 0.0)	H ₂ O ₂	- 33.3 (+ 0.8)
Ionization energies	Li	124.2 (+ 0.1)	Cl	296.8 (+ 2.3)
	Be	219.7 (- 4.8)	CH ₄	293.1 (- 2.1)
	B	189.9 (+ 1.5)	NH ₃	232.6 (+ 2.2)
	C	258.6 (+ 1.1)	OH	299.8 (+ 0.2)
	N	334.4 (+ 0.9)	H ₂ O	291.0 (+ 0.0)
	O	313.1 (+ 0.7)	HF	370.5 (- 0.6)
	F	401.8 (- 0.1)	SiH ₄	254.6 (- 0.9)
	Na	115.1 (+ 3.4)	PH	235.4 (- 1.3)
	Mg	179.1 (- 2.8)	PH ₂	226.9 (- 0.5)
	Al	138.4 (- 0.4)	PH ₃	229.0 (- 1.4)
	Si	188.1 (- 0.2)	SH	238.6 (+ 0.5)
	P	241.8 (+ 0.1)	H ₂ S ² B ₁	241.1 (+ 0.3)
	S	236.3 (+ 2.6)	H ₂ S ² A ₁	294.4 (+ 0.3)
Electron affinities	C	28.6 (+ 0.5)	CH ₃	- 2.9 (+ 4.7)
	O	31.8 (+ 1.9)	NH	6.6 (+ 2.2)
	F	78.6 (- 0.2)	NH ₂	16.5 (+ 1.3)
	Si	33.2 (- 1.3)	OH	41.3 (+ 0.9)
	P	16.2 (+ 1.0)	SiH	30.0 (- 0.6)
	S	47.6 (+ 0.3)	SiH ₂	24.9 (+ 1.0)
	Cl	83.6 (- 0.2)	SiH ₃	33.8 (- 1.3)
	CH	27.9 (+ 0.7)	PH	23.0 (+ 0.8)
	CH ₂	14.8 (+ 0.2)	PH ₂	29.5 (- 0.2)
Proton affinities	NH ₃	205.7 (- 3.2)	SiH ₄	153.6 (+ 0.4)
	H ₂ O	160.7 (+ 4.4)	PH ₃	184.5 (+ 2.6)
	C ₂ H ₂	153.6 (- 1.3)	H ₂ S	167.1 (+ 1.7)

^aValues in kcal mol⁻¹. The heats of formation are 298 K values whereas the remaining quantities refer to 0 K.

Table (F.4) MR(QD)-G2/MP2a heats of formation, ionization energies, electron affinities and proton affinities. Values in parentheses are the differences between experimental and MR(QD)-G2/MP2 values.^b

	Species	Species	Species	
Heats of Formation	LiH 29.6 (+ 3.7) BeH 86.1 (- 4.4) CH 142.5 (+ 0.0) CH ₂ ³ B ₁ 94.5 (- 0.8) CH ₂ ¹ A ₁ 102.8 (+ 0.0) CH ₃ 35.6 (- 0.6) CH ₄ - 17.6 (- 0.3) NH 85.5 (- 0.3) NH ₂ 44.8 (+ 0.3) NH ₃ - 7.3 (- 3.7) OH 7.4 (+ 2.0) H ₂ O - 58.4 (+ 0.6) HF - 68.3 (+ 3.2) SiH ₂ ¹ A ₁ 64.5 (+ 0.7) SiH ₂ ³ B ₁ 87.4 (- 1.2) SiH ₃ 49.7 (- 1.8) SiH ₄ 10.1 (- 1.9) PH ₂ 34.8 (- 1.7)	PH ₃ 6.0 (- 4.7) H ₂ S - 2.8 (- 2.1) HCl - 22.4 (+ 0.3) Li ₂ 46.7 (+ 4.9) LiF - 81.2 (+ 1.1) C ₂ H ₂ 53.4 (+ 0.8) C ₂ H ₄ 12.1 (+ 0.4) CN 104.0 (+ 0.9) HCN 31.2 (+ 0.3) CO - 27.1 (+ 0.7) HCO 9.5 (+ 0.5) HCHO - 24.4 (- 1.6) CH ₃ OH - 45.8 (- 2.2) N ₂ - 0.3 (+ 0.3) N ₂ H ₄ 25.1 (- 2.3) NO 18.2 (+ 3.4) O ₂ - 6.1 (+ 6.1) H ₂ O ₂ - 36.4 (+ 3.9)	F ₂ - 3.1 (+ 3.1) CO ₂ - 105.0 (+ 10.9) Na ₂ 28.6 (+ 5.4) Si ₂ 138.1 (+ 1.8) P ₂ 34.4 (- 0.1) S ₂ 28.6 (+ 2.1) Cl ₂ 0.6 (- 0.6) NaCl - 50.7 (+ 7.1) SiO - 18.2 (- 6.4) CS 64.5 (+ 2.4) SO - 2.8 (+ 4.0) ClO 23.3 (+ 0.9) ClF - 14.0 (+ 0.8) CH ₃ Cl - 18.8 (- 0.8) CH ₃ SH - 6.5 (+ 1.0) HOCl - 19.0 (+ 1.2) SO ₂ - 78.5 (+ 7.5)	
Ionization energies	Li 123.2 (+ 1.1) Be 219.9 (- 5.0) B 186.6 (+ 4.8) C 256.2 (+ 3.5) N 334.0 (+ 1.3) O 312.4 (+ 1.4) F 403.0 (- 1.3) Na 114.1 (+ 4.4) Mg 179.1 (- 2.8) Al 134.2 (+ 3.8) Si 185.4 (+ 2.5) P 241.5 (+ 0.4) S 234.1 (+ 4.8)	Cl 295.8 (+ 3.3) CH ₄ 291.1 (- 0.1) NH ₃ 230.6 (+ 4.2) OH 299.8 (+ 0.2) H ₂ O 290.6 (+ 0.4) HF 372.4 (- 2.5) SiH ₄ 250.7 (+ 3.0) PH 233.6 (+ 0.5) PH ₂ 224.5 (+ 1.9) PH ₃ 226.4 (+ 1.2) SH 236.3 (+ 2.8) H ₂ S ³ B ₁ 238.1 (+ 3.3) H ₂ S ¹ A ₁ 293.6 (+ 1.1)	HCl 292.7 (+ 1.3) C ₂ H ₂ 263.5 (- 0.6) C ₂ H ₄ 244.4 (- 2.1) CO 319.1 (+ 4.0) N ₂ ² S _g 355.4 (+ 3.9) N ₂ ² T _u 384.1 (+ 1.0) O ₂ 283.8 (- 5.5) P ₂ 243.4 (- 0.6) S ₂ 215.5 (+ 0.3) Cl ₂ 263.3 (+ 1.9) ClF 290.0 (+ 1.9) CS 260.4 (+ 0.9)	
Electron affinities	C 28.8 (+ 0.3) O 34.5 (- 0.8) F 83.7 (- 5.3) Si 31.7 (+ 0.2) P 13.8 (+ 3.4) S 45.9 (+ 2.0) Cl 84.2 (- 0.8) CH 25.2 (+ 3.4) CH ₂ 13.8 (+ 1.2)	CH ₃ - 4.6 (+ 6.4) NH 7.2 (+ 1.6) NH ₂ 16.4 (+ 1.4) OH 44.4 (- 2.2) SiH 27.4 (+ 2.0) SiH ₂ 21.9 (+ 4.0) SiH ₃ 30.5 (+ 2.0) PH 20.1 (+ 3.7) PH ₂ 26.3 (+ 3.0)	SH 52.3 (+ 2.1) O ₂ 11.4 (- 1.3) NO 4.2 (- 3.7) CN 88.5 (+ 0.5) PO 30.2 (- 5.1) S ₂ 35.9 (+ 2.4) Cl ₂ 59.4 (- 4.3)	
Proton affinities	NH ₃ 206.5 (- 4.0) H ₂ O 159.6 (+ 5.5) C ₂ H ₂ 153.7 (- 1.4)	SiH ₄ 155.0 (- 1.0) PH ₃ 185.6 (+ 1.5) H ₂ S 168.6 (+ 0.2)	HCl 133.2 (+ 0.4)	

^aCorresponding to MRQDPT2/6-311+G(3df,2p) + ZPVE + HLC.

Table (F.5) MR(QD)-G3/MP2^a heats of formation, ionization energies, electron affinities and proton affinities. Values in parentheses are the differences between experimental and MR(QD)-G3(MP2)/MP2 values.^b

	Species	Species	Species	
Heats of formation	LiH	29.3 (+ 4.0)	PH ₃	5.6 (- 4.3)
	BeH	86.1 (- 4.4)	H ₂ S	- 2.6 (- 2.3)
	CH	142.5 (+ 0.0)	HCl	- 21.4 (- 0.7)
	CH ₂ ³ B ₁	94.4 (- 0.7)	Li ₂	46.3 (+ 5.3)
	CH ₂ ¹ A ₁	102.8 (+ 0.0)	LiF	- 80.1 (+ 0.0)
	CH ₃	35.3 (- 0.3)	C ₂ H ₂	52.5 (+ 1.7)
	CH ₄	- 17.9 (+ 0.0)	C ₂ H ₄	11.6 (+ 0.9)
	NH	85.4 (- 0.2)	CN	104.9 (+ 0.0)
	NH ₂	44.8 (+ 0.3)	HCN	31.5 (+ 0.0)
	NH ₃	- 7.5 (- 3.5)	CO	- 25.4 (- 1.0)
	OH	7.7 (+ 1.7)	HCO	11.1 (- 1.1)
	H ₂ O	- 58.2 (+ 0.4)	HCHO	- 23.3 (- 2.7)
	HF	- 67.4 (+ 2.3)	CH ₃ OH	- 45.4 (- 2.6)
	SiH ₂ ¹ A ₁	64.0 (+ 1.2)	N ₂	0.0 (+ 0.0)
	SiH ₂ ³ B ₁	87.0 (- 0.8)	N ₂ H ₄	25.0 (- 2.2)
	SiH ₃	49.0 (- 1.1)	NO	19.7 (+ 1.9)
	SiH ₄	9.0 (- 0.8)	O ₂	- 4.8 (+ 4.8)
	PH ₂	34.4 (- 1.3)	H ₂ O ₂	- 36.1 (+ 3.6)
Ionization energies	Li	124.2 (+ 0.1)	Cl	297.3 (+ 1.8)
	Be	221.1 (- 6.2)	CH ₄	292.4 (- 1.4)
	B	187.4 (+ 4.0)	NH ₃	231.3 (+ 3.5)
	C	256.9 (+ 2.8)	OH	300.4 (- 0.4)
	N	334.3 (+ 1.0)	H ₂ O	291.4 (- 0.4)
	O	313.3 (- 0.5)	HF	373.0 (- 3.1)
	F	403.41 (- 1.7)	SiH ₄	253.7 (+ 0.0)
	Na	115.1 (+ 3.4)	PH	234.9 (- 0.8)
	Mg	180.3 (- 4.0)	PH ₂	226.1 (+ 0.3)
	Al	135.5 (+ 2.5)	PH ₃	227.8 (- 0.2)
	Si	186.4 (+ 1.5)	SH	238.1 (+ 1.0)
	P	241.9 (+ 0.0)	H ₂ S ³ B ₁	240.0 (+ 1.4)
	S	236.6 (+ 2.3)	H ₂ S ¹ A ₁	295.1 (- 0.4)
Electron affinities	C	28.4 (+ 0.7)	CH ₃	- 4.3 (+ 6.1)
	O	33.7 (+ 0.0)	NH	6.8 (+ 2.0)
	F	82.4 (- 4.0)	NH ₂	16.6 (+ 1.2)
	Si	32.6 (- 0.7)	OH	43.9 (- 1.7)
	P	16.5 (+ 0.7)	SiH	29.0 (+ 0.4)
	S	48.1 (- 0.2)	SiH ₂	23.5 (+ 2.4)
	Cl	84.9 (- 1.5)	SiH ₃	32.1 (+ 0.4)
	CH	27.3 (+ 1.3)	PH	22.2 (+ 1.6)
	CH ₂	13.8 (+ 1.2)	PH ₂	28.3 (+ 1.0)
Proton affinities	NH ₃	207.0 (- 4.5)	SiH ₄	154.8 (- 0.8)
	H ₂ O	159.9 (+ 5.2)	PH ₃	185.2 (+ 1.9)
	C ₂ H ₂	152.7 (- 0.4)	H ₂ S	167.9 (+ 0.9)
HCl				
132.7 (+ 0.9)				

^aCorresponding to MRQDPT2/G3MP2large + ΔE(SO) + ZPVE + HLC

Table (F.6) MR-G2(MP2,SVP) total energies (in Hartrees).

Species	Energy	Species	Energy	Species	Energy
H	- 0.500 00	HCHO	- 114.348 23	SH ⁺	- 397.912 90
Li	- 7.432 20	CH ₃ OH	- 115.545 13	H ₂ S ⁺ (² B ₁)	- 398.552 34
Be	- 14.625 88	N ₂	- 109.407 36	H ₂ S ⁺ (² A ₁)	- 398.466 95
B	- 24.605 98	N ₂ H ₄	- 111.692 74	HCl ⁺	- 459.877 47
C	- 37.789 16	NO	- 129.753 66	C ₂ H ₂ ⁺	- 76.779 62
N	- 54.524 18	O ₂	- 150.164 11	C ₂ H ₄ ⁺	- 78.037 90
O	- 74.988 99	H ₂ O ₂	- 151.379 98	CO ⁺	- 112.673 22
F	- 99.640 51	F ₂	- 199.339 09	N ₂ ⁺ Σ_g^+	- 108.835 29
Na	- 161.846 13	CO ₂	- 188.379 71	N ₂ ⁺ Γ_u	- 108.795 33
Mg	- 199.648 70	Na ₂	- 323.726 40	O ₂ ⁺	- 149.718 30
Al	- 241.934 90	Si ₂	- 577.993 78	P ₂ ⁺	- 681.444 18
Si	- 288.937 81	P ₂	- 681.831 76	S ₂ ⁺	- 795.136 07
P	- 340.824 19	S ₂	- 795.475 72	Cl ₂ ⁺	- 919.027 11
S	- 397.659 19	Cl ₂	- 919.449 39	ClF ⁺	- 558.950 66
Cl	- 459.679 98	NaCl	- 621.685 52	CS ⁺	- 435.303 27
LiH	- 8.026 28	SiO	- 364.226 92	C ⁻	- 37.839 50
BeH	- 15.198 86	CS	- 435.722 28	O ⁻	- 75.042 48
CH	- 38.417 97	SO	- 472.841 24	F	- 99.769 57
CH ₂ (³ B ₁)	- 39.073 59	CIO	- 534.766 86	Si ⁻	- 288.989 19
CH ₂ (¹ A ₁)	- 39.064 17	ClF	- 559.415 30	P ⁻	- 340.846 89
CH ₃	- 39.750 92	CH ₃ Cl	- 499.563 47	S ⁻	- 397.733 03
CH ₄	- 40.418 01	CH ₃ SH	- 438.160 83	Cl ⁻	- 459.813 68
NH	- 55.148 92	HClO	- 535.418 06	CH ⁻	- 38.461 58
NH ₂	- 55.795 68	SO ₂	- 548.03 370	CH ₂ ⁻	- 39.099 16
NH ₃	- 56.462 15	Li ⁺	- 7.235 48	CH ₃ ⁻	- 39.748 13
OH	- 75.651 39	Be ⁺	- 14.276 33	NH ⁻	- 55.161 52
H ₂ O	- 76.338 36	B ⁺	- 24.304 50	NH ₂ ⁻	- 55.823 64
HF	- 100.356 82	C ⁺	- 37.378 28	OH ⁻	- 75.719 70
SiH	- 289.550 43	N ⁺	- 53.991 70	SiH ⁻	- 289.594 61
SiH ₂ (¹ A ₁)	- 290.171 34	O ⁺	- 74.490 17	SiH ₂ ⁻	- 290.208 25
SiH ₂ (³ B ₁)	- 290.132 65	F ⁺	- 98.999 31	SiH ₃ ⁻	- 290.829 22
SiH ₃	- 290.775 63	Na ⁺	- 161.664 29	PH ⁻	- 341.468 95
SiH ₄	- 291.421 16	Mg ⁺	- 199.364 00	PH ₂ ⁻	- 342.099 84
PH	- 341.433 82	Al ⁺	- 241.716 31	SH ⁻	- 398.376 60
PH ₂	- 342.054 09	Si ⁺	- 288.639 93	O ₂ ⁻	- 150.181 77
PH ₃	- 342.683 34	P ⁺	- 340.439 53	NO ⁻	- 129.752 14
SH	- 398.291 74	S ⁺	- 397.285 64	CN ⁻	- 92.740 67
H ₂ S	- 398.935 51	Cl ⁺	- 459.207 96	PO ⁻	- 416.071 52
HCl	- 460.344 70	CH ₄ ⁺	- 39.951 07	PO	- 416.032 54
Li ₂	- 14.909 19	NH ₃ ⁺	- 56.090 81	S ₂ ⁻	- 795.535 41
LiF	- 107.290 44	OH ⁺	- 75.173 22	Cl ₂ ⁻	- 919.535 28
C ₂ H ₂	- 77.197 56	H ₂ O ⁺	- 75.874 29	NH ₄ ⁺	- 56.789 49
C ₂ H ₄	- 78.421 69	HF ⁺	- 99.765 49	H ₃ O ⁺	- 76.594 66
CN	- 92.594 55	SiH ₄ ⁺	- 291.017 10	C ₂ H ₃ ⁺	- 77.442 21
HCN	- 93.295 32	PH ⁺	- 341.062 45	SiH ₅ ⁺	- 291.665 85
CO	- 113.189 65	PH ₂ ⁺	- 341.695 86	PH ₄ ⁺	- 342.978 57
HCO	- 113.710 29	PH ₃ ⁺	- 342.319 37	H ₃ S ⁺	- 399.202 65
				H ₂ Cl ⁺	- 460.556 89

Table (F.7) MR-G2(MP2) total energies (in Hartrees).

Species	Energy	Species	Energy	Species	Energy
H	- 0.500 00	HCHO	- 114.346 95	SH ⁺	- 397.912 66
Li	- 7.432 20	CH ₃ OH	- 115.544 73	H ₂ S ⁺ (² B ₁)	- 398.552 63
Be	- 14.624 16	N ₂	- 109.403 75	H ₂ S ⁺ (² A ₁)	- 398.466 73
B	- 24.605 23	N ₂ H ₄	- 111.691 97	HCl ⁺	- 459.876 26
C	- 37.787 70	NO	- 129.749 83	C ₂ H ₂ ⁺	- 76.779 14
N	- 54.520 47	O ₂	- 150.160 02	C ₂ H ₄ ⁺	- 78.039 21
O	- 74.985 42	H ₂ O ₂	- 151.376 57	CO ⁺	- 112.670 94
F	- 99.636 50	F ₂	- 199.333 45	N ₂ ⁺ ² Σ _g	- 108.832 49
Na	- 161.846 13	CO ₂	- 188.374 35	N ₂ ⁺ ² Π _u	- 108.792 48
Mg	- 199.646 80	Na ₂	- 323.725 70	O ₂ ⁺	- 149.714 90
Al	- 241.934 37	Si ₂	- 577.991 71	P ₂ ⁺	- 681.441 49
Si	- 288.936 96	P ₂	- 681.828 11	S ₂ ⁺	- 795.132 68
P	- 340.820 83	S ₂	- 795.471 88	Cl ₂ ⁺	- 919.022 95
S	- 397.659 24	Cl ₂	- 919.444 32	ClF ⁺	- 558.946 45
Cl	- 459.681 96	NaCl	- 621.682 75	CS ⁺	- 435.300 76
LiH	- 8.025 70	SiO	- 364.224 54	C ⁺	- 37.840 15
BeH	- 15.198 08	CS	- 435.719 74	O ⁻	- 75.039 16
CH	- 38.418 99	SO	- 472.837 28	F ⁻	- 99.764 79
CH ₂ (³ B ₁)	- 39.074 81	CIO	- 534.762 23	Si ⁻	- 288.988 68
CH ₂ (¹ A ₁)	- 39.066 05	CIF	- 559.410 00	P ⁻	- 340.845 62
CH ₃	- 39.752 74	CH ₃ Cl	- 499.561 91	S ⁻	- 397.730 58
CH ₄	- 40.420 11	CH ₃ SH	- 438.156 67	Cl ⁻	- 459.810 11
NH	- 55.148 41	HCIO	- 535.413 86	CH ⁻	- 38.462 39
NH ₂	- 55.795 65	SO ₂	- 548.026 81	CH ₂ ⁻	- 39.100 44
NH ₃	- 56.462 45	Li ⁺	- 7.235 48	CH ₃ ⁻	- 39.749 95
OH	- 75.649 91	Be ⁺	- 14.276 33	NH ⁻	- 55.160 13
H ₂ O	- 76.337 43	B ⁺	- 24.303 71	NH ₂ ⁻	- 55.823 00
HF	- 100.354 39	C ⁺	- 37.377 96	OH ⁻	- 75.717 00
SiH	- 289.551 00	N ⁺	- 53.990 96	SiH ⁻	- 289.595 30
SiH ₂ (¹ A ₁)	- 290.173 24	O ⁺	- 74.489 50	SiH ₂ ⁻	- 290.210 05
SiH ₂ (³ B ₁)	- 290.134 51	F ⁺	- 98.998 62	SiH ₃ ⁻	- 290.832 25
SiH ₃	- 290.778 96	Na ⁺	- 161.664 29	PH ⁻	- 341.468 30
SiH ₄	- 291.426 29	Mg ⁺	- 199.364 00	PH ₂ ⁻	- 342.099 78
PH	- 341.433 85	Al ⁺	- 241.715 62	SH ⁻	- 398.374 61
PH ₂	- 342.055 01	Si ⁺	- 288.639 33	O ₂ ⁻	- 150.176 18
PH ₃	- 342.685 36	P ⁺	- 340.439 10	NO ⁻	- 129.747 77
SH	- 398.290 80	S ⁺	- 397.285 16	CN ⁻	- 92.737 89
H ₂ S	- 398.935 22	Cl ⁺	- 459.206 86	PO ⁻	- 416.067 52
HCl	- 460.342 99	CH ₄ ⁺	- 39.952 62	PO	- 416.029 07
Li ₂	- 14.908 48	NH ₃ ⁺	- 56.091 31	S ₂ ⁻	- 795.530 29
LiF	- 107.289 37	OH ⁺	- 75.172 56	Cl ₂ ⁻	- 919.528 69
C ₂ H ₂	- 77.196 60	H ₂ O ⁺	- 75.873 78	NH ₄ ⁺	- 56.790 14
C ₂ H ₄	- 78.429 07	HF ⁺	- 99.764 34	H ₃ O ⁺	- 76.594 07
CN	- 92.591 94	SiH ₄ ⁺	- 291.020 54	C ₂ H ₃ ⁺	- 77.441 85
HCN	- 93.293 03	PH ⁺	- 341.062 67	SiH ₅ ⁺	- 291.670 80
CO	- 113.187 40	PH ₂ ⁺	- 341.697 10	PH ₄ ⁺	- 342.982 18
HCO	- 113.708 12	PH ₃ ⁺	- 342.321 55	H ₃ S ⁺	- 399.203 64
				H ₂ Cl ⁺	- 460.556 22

Table (F.8) MR-G3(MP2) total energies (in Hartrees).

Species	Energy	Species	Energy	Species	Energy
H	- 0.501 53	HCHO	- 114.358 18	SH ⁺	- 397.925 68
Li	- 7.433 72	CH ₃ OH	- 115.558 24	H ₂ S ⁺ (² B ₁)	- 398.565 48
Be	- 14.627 80	N ₂	- 109.415 55	H ₂ S ⁺ (² A ₁)	- 398.480 35
B	- 24.609 04	N ₂ H ₄	- 111.706 17	HCl ⁺	- 459.891 24
C	- 37.793 30	NO	- 129.762 04	C ₂ H ₂ ⁺	- 76.787 35
N	- 54.529 00	O ₂	- 150.174 86	C ₂ H ₄ ⁺	- 78.051 19
O	- 74.993 59	H ₂ O ₂	- 151.392 40	CO ⁺	- 112.679 23
F	- 99.644 67	F ₂	- 199.350 53	N ₂ ⁺ ² Σ _g	- 108.843 24
Na	- 161.847 65	CO ₂	- 188.390 27	N ₂ ⁺ ² Π _u	- 108.803 31
Mg	- 199.650 67	Na ₂	- 323.729 31	O ₂ ⁺	- 149.727 24
Al	- 241.939 01	Si ₂	- 578.008 20	P ₂ ⁺	- 681.462 00
Si	- 288.944 21	P ₂	- 681.850 43	S ₂ ⁺	- 795.157 90
P	- 340.833 85	S ₂	- 795.500 69	Cl ₂ ⁺	- 919.053 47
S	- 397.670 81	Cl ₂	- 919.477 28	ClF ⁺	- 558.967 20
Cl	- 459.693 08	NaCl	- 621.701 05	CS ⁺	- 435.318 05
LiH	- 8.028 98	SiO	- 364.239 94	C ⁻	- 37.842 94
BeH	- 15.201 72	CS	- 435.737 42	O ⁻	- 75.044 19
CH	- 38.424 29	SO	- 472.859 61	F ⁻	- 99.769 96
CH ₂ (³ B ₁)	- 39.082 28	ClO	- 534.785 51	Si ⁻	- 288.997 13
CH ₂ (¹ A ₁)	- 39.070 54	ClF	- 559.432 60	P ⁻	- 340.859 15
CH ₃	- 39.759 90	CH ₃ Cl	- 499.583 95	S ⁻	- 397.746 55
CH ₄	- 40.427 19	CH ₃ SH	- 438.181 54	Cl ⁻	- 459.826 46
NH	- 55.156 71	HClO	- 535.437 27	CH ⁻	- 38.468 45
NH ₂	- 55.803 52	SO ₂	- 548.054 86	CH ₂ ⁻	- 39.106 29
NH ₃	- 56.470 41	Li ⁺	- 7.235 84	CH ₃ ⁻	- 39.755 98
OH	- 75.658 46	Be ⁺	- 14.277 86	NH ⁻	- 55.167 26
H ₂ O	- 76.345 68	B ⁺	- 24.306 42	NH ₂ ⁻	- 55.830 14
HF	- 100.362 56	C ⁺	- 37.381 41	OH ⁻	- 75.724 50
SiH	- 289.559 19	N ⁺	- 53.995 99	SiH ⁻	- 289.606 53
SiH ₂ (¹ A ₁)	- 290.180 70	O ⁺	- 74.494 98	SiH ₂ ⁻	- 290.220 91
SiH ₂ (³ B ₁)	- 290.144 02	F ⁺	- 99.004 50	SiH ₃ ⁻	- 290.842 38
SiH ₃	- 290.787 68	Na ⁺	- 161.664 29	PH ⁻	- 341.483 83
SiH ₄	- 291.433 83	Mg ⁺	- 199.365 53	PH ₂ ⁻	- 342.114 71
PH	- 341.446 76	Al ⁺	- 241.718 32	SH ⁻	- 398.392 29
PH ₂	- 342.067 27	Si ⁺	- 288.644 77	O ₂ ⁻	- 150.191 45
PH ₃	- 342.696 60	P ⁺	- 340.448 50	NO ⁻	- 129.761 61
SH	- 398.305 88	S ⁺	- 397.294 86	CN ⁻	- 92.748 68
H ₂ S	- 398.949 83	Cl ⁺	- 459.220 24	PO ⁻	- 416.089 65
HCl	- 460.359 26	CH ₂ ⁺	- 39.959 90	PO ⁻	- 416.047 96
Li ₂	- 14.912 01	NH ₃ ⁺	- 56.099 53	S ₂ ⁻	- 795.562 43
LiF	- 107.295 79	OH ⁺	- 75.180 98	Cl ₂ ⁻	- 919.568 76
C ₂ H ₂	- 77.208 54	H ₂ O ⁺	- 75.881 95	NH ₄ ⁺	- 56.798 61
C ₂ H ₄	- 78.435 17	HF ⁺	- 99.771 95	H ₂ O ⁺	- 76.602 44
CN	- 92.602 78	SiH ₄ ⁺	- 291.028 82	C ₂ H ₃ ⁺	- 77.452 46
HCN	- 93.304 51	PH ⁺	- 341.072 53	SiH ₅ ⁺	- 291.678 14
CO	- 113.196 29	PH ₂ ⁺	- 341.705 94	PH ₄ ⁺	- 342.991 18
HCO	- 113.719 40	PH ₃ ⁺	- 342.331 82	H ₃ S ⁺	- 399.215 97
				H ₂ Cl ⁺	- 460.570 69

Table (F.9) MR-G2/MRCI+Q total energies (in Hartrees).^a

Species	Energy	Species	Energy	Species	Energy
H	- 0.500 00	HCHO	- 114.344 02	SH ⁺	- 397.913 00
Li	- 7.432 20	CH ₃ OH	- 115.539 41	H ₂ S ⁺ (² B ₁)	- 398.553 75
Be	- 14.624 16	N ₂	- 109.399 95	H ₂ S ⁺ (² A ₁)	- 398.469 06
B	- 24.605 23	N ₂ H ₄	- 111.686 51	HCl ⁺	- 459.879 54
C	- 37.787 70	NO	- 129.745 44	C ₂ H ₂ ⁺	- 76.775 99
N	- 54.520 47	O ₂	- 150.154 12	C ₂ H ₄ ⁺	- 78.035 78
O	- 74.985 42	H ₂ O ₂	- 151.371 11	CO ⁺	- 112.668 27
F	- 99.636 50	F ₂	- 199.328 61	N ₂ ⁺ $^2\Sigma_g^+$	- 108.828 46
Na	- 161.846 13	CO ₂	- 188.367 39	N ₂ ⁺ $^2\Pi_u$	- 108.789 21
Mg	- 199.646 80	Na ₂	- 323.724 65	O ₂ ⁺	- 149.710 73
Al	- 241.934 37	Si ₂	- 577.991 45	P ₂ ⁺	- 681.440 92
Si	- 288.936 96	P ₂	- 681.827 12	S ₂ ⁺	- 795.132 44
P	- 340.820 83	S ₂	- 795.470 03	Cl ₂ ⁺	- 919.025 78
S	- 397.659 24	Cl ₂	- 919.448 32	ClF ⁺	- 558.945 72
Cl	- 459.681 96	NaCl	- 621.688 06	CS ⁺	- 435.299 88
LiH	- 8.024 58	SiO	- 364.221 42	C ⁻	- 37.830 79
BeH	- 15.196 81	CS	- 435.719 00	O ⁻	- 75.034 14
CH	- 38.417 42	SO	- 472.832 65	F ⁻	- 99.757 33
CH ₂ (³ B ₁)	- 39.072 99	CIO	- 534.761 32	Si ⁻	- 288.985 54
CH ₂ (¹ A ₁)	- 39.064 65	CIF	- 559.409 97	P ⁻	- 340.845 64
CH ₃	- 39.750 55	CH ₃ Cl	- 499.561 69	S ⁻	- 397.733 10
CH ₄	- 40.417 53	CH ₃ SH	- 438.157 56	Cl ⁻	- 459.813 71
NH	- 55.146 28	HClO	- 535.413 69	CH ⁻	- 38.458 13
NH ₂	- 55.793 66	SO ₂	- 548.017 80	CH ₂ ⁻	- 39.097 74
NH ₃	- 56.459 90	Li ⁺	- 7.235 48	CH ₃ ⁻	- 39.746 83
OH	- 75.648 00	Be ⁺	- 14.276 33	NH ⁻	- 55.155 76
H ₂ O	- 76.335 11	B ⁺	- 24.302 62	NH ₂ ⁻	- 55.818 85
HF	- 100.351 75	C ⁺	- 37.376 30	OH ⁻	- 75.710 03
SiH	- 289.551 47	N ⁺	- 53.988 96	SiH ⁻	- 289.594 64
SiH ₂ (¹ A ₁)	- 290.174 07	O ⁺	- 74.487 11	SiH ₂ ⁻	- 290.210 80
SiH ₂ (³ B ₁)	- 290.135 05	F ⁺	- 98.997 17	SiH ₃ ⁻	- 290.833 79
SiH ₃	- 290.779 45	Na ⁺	- 161.664 29	PH ⁻	- 341.469 33
SiH ₄	- 291.426 23	Mg ⁺	- 199.364 00	PH ₂ ⁻	- 342.101 37
PH	- 341.433 56	Al ⁺	- 241.714 52	SH ⁻	- 398.376 95
PH ₂	- 342.055 58	Si ⁺	- 288.638 94	O ₂ ⁻	- 150.166 96
PH ₃	- 342.686 50	P ⁺	- 340.437 98	NO ⁻	- 129.738 67
SH	- 398.293 10	S ⁺	- 397.283 00	CN ⁻	- 92.733 57
H ₂ S	- 398.937 52	Cl ⁺	- 459.209 24	PO ⁻	- 416.059 25
HCl	- 460.346 60	CH ₄ ⁺	- 39.950 47	PO	- 416.026 14
Li ₂	- 14.907 44	NH ₃ ⁺	- 56.089 40	S ₂ ⁻	- 795.528 91
LiF	- 107.289 57	OH ⁺	- 75.170 82	Cl ₂ ⁻	- 919.529 20
C ₂ H ₂	- 77.192 53	H ₂ O ⁺	- 75.872 09	NH ₄ ⁺	- 56.787 75
C ₂ H ₄	- 78.424 51	HF ⁺	- 99.762 95	H ₃ O ⁺	- 76.591 87
CN	- 92.588 48	SiH ₄ ⁺	- 291.019 88	C ₂ H ₃ ⁺	- 77.438 32
HCN	- 93.289 91	PH ⁺	- 341.062 76	SiH ₅ ⁺	- 291.669 63
CO	- 113.183 63	PH ₂ ⁺	- 341.697 91	PH ₄ ⁺	- 342.982 17
HCO	- 113.703 95	PH ₃ ⁺	- 342.321 85	H ₃ S ⁺	- 399.205 03
				H ₂ Cl ⁺	- 460.559 24

^aCorresponding to MRCI+Q/6-311+(3df,2p) + ZPVE + HLC.

Table (F.10) MR-G3/MRCI+Q total energies (in Hartrees).^a

Species	Energy	Species	Energy	Species	Energy
H	- 0.502 73	HCHO	- 114.364 97	SH ⁺	- 97.931 19
Li	- 7.434 92	CH ₃ OH	- 115.565 27	H ₂ S ⁺ (² B ₁)	- 398.573 02
Be	- 14.627 03	N ₂	- 109.417 62	H ₂ S ⁺ (² A ₁)	- 398.488 62
B	- 24.610 57	N ₂ H ₄	- 111.712 91	HCl ⁺	- 459.899 41
C	- 37.795 44	NO	- 129.764 50	C ₂ H ₂ ⁺	- 76.792 46
N	- 54.530 25	O ₂	- 150.176 75	C ₂ H ₄ ⁺	- 78.059 25
O	- 74.994 65	H ₂ O ₂	- 151.396 62	CO ⁺	- 112.682 80
F	- 99.644 99	F ₂	- 199.353 10	N ₂ ⁺ ² Σ _g	- 108.845 04
Na	- 161.848 85	CO ₂	- 188.393 14	N ₂ ⁺ ² Π _u	- 108.805 76
Mg	- 199.649 74	Na ₂	- 323.729 40	O ₂ ⁺	- 149.730 22
Al	- 241.940 45	Si ₂	- 578.012 55	P ₂ ⁺	- 681.466 28
Si	- 288.946 22	P ₂	- 681.854 13	S ₂ ⁺	- 795.163 50
P	- 340.834 51	S ₂	- 795.505 27	Cl ₂ ⁺	- 919.063 11
S	- 397.674 76	Cl ₂	- 919.487 90	ClF ⁺	- 558.974 04
Cl	- 459.698 78	NaCl	- 621.710 72	CS ⁺	- 435.322 69
LiH	- 8.029 14	SiO	- 364.243 40	C ⁻	- 37.839 57
BeH	- 15.204 68	CS	- 435.742 90	O ⁻	- 75.040 10
CH	- 38.428 52	SO	- 472.862 20	F	- 99.761 46
CH ₂ (³ B ₁)	- 39.087 59	CIO	- 534.791 82	Si ⁻	- 288.997 32
CH ₂ (¹ A ₁)	- 39.076 39	CIF	- 559.439 79	P ⁻	- 340.861 92
CH ₃	- 39.766 11	CH ₃ Cl	- 499.593 17	S ⁻	- 397.750 34
CH ₄	- 40.433 91	CH ₃ SH	- 438.190 59	Cl ⁻	- 459.829 71
NH	- 55.160 16	HCIO	- 535.445 36	CH ⁻	- 38.471 13
NH ₂	- 55.808 19	SO ₂	- 548.055 57	CH ₂ ⁻	- 39.111 42
NH ₃	- 56.475 54	Li ⁺	- 7.235 84	CH ₃ ⁻	- 39.761 80
OH	- 75.661 88	Be ⁺	- 14.279 06	NH ⁻	- 55.168 29
H ₂ O	- 76.349 92	B ⁺	- 24.305 51	NH ₂ ⁻	- 55.832 71
HF	- 100.364 97	C ⁺	- 37.381 61	OH ⁻	- 75.722 21
SiH	- 289.564 69	N ⁺	- 53.996 71	SiH ⁻	- 289.611 93
SiH ₂ (¹ A ₁)	- 290.188 78	O ⁺	- 74.496 68	SiH ₂ ⁻	- 290.229 77
SiH ₂ (³ B ₁)	- 290.152 17	F ⁺	- 99.006 88	SiH ₃ ⁻	- 290.854 12
SiH ₃	- 290.798 07	Na ⁺	- 161.664 29	PH ⁻	- 341.490 56
SiH ₄	- 291.446 31	Mg ⁺	- 199.366 73	PH ₂ ⁻	- 342.123 33
PH	- 341.452 04	Al ⁺	- 241.717 49	SH ⁻	- 398.399 47
PH ₂	- 342.075 02	Si ⁺	- 288.645 59	O ₂ ⁻	- 150.189 16
PH ₃	- 342.706 86	P ⁺	- 340.449 95	NO ⁻	- 129.760 20
SH	- 398.313 42	S ⁺	- 397.296 21	CN ⁻	- 92.751 15
H ₂ S	- 398.958 77	Cl ⁺	- 459.225 33	PO ⁻	- 416.088 80
HCl	- 460.368 00	CH ₄ ⁺	- 39.965 83	PO	- 416.051 71
Li ₂	- 14.912 10	NH ₃ ⁺	- 56.104 80	S ₂ ⁻	- 795.566 88
LiF	- 107.301 65	OH ⁺	- 75.184 62	Cl ₂ ⁻	- 919.575 36
C ₂ H ₂	- 77.212 89	H ₂ O ⁺	- 75.886 49	NH ₄ ⁺	- 56.804 27
C ₂ H ₄	- 78.449 00	HF ⁺	- 99.776 22	H ₃ O ⁺	- 76.607 13
CN	- 92.605 40	SiH ₄ ⁺	- 291.038 15	C ₂ H ₃ ⁺	- 77.457 79
HCN	- 93.308 46	PH ⁺	- 341.077 30	SiH ₅ ⁺	- 291.689 27
CO	- 113.199 65	PH ₂ ⁺	- 341.713 24	PH ₄ ⁺	- 343.001 99
HCO	- 113.723 51	PH ₃ ⁺	- 342.340 68	H ₃ S ⁺	- 399.225 30
				H ₂ Cl ⁺	- 460.579 85

^aCorresponding to MRCI+Q/G3MP2large + ΔE(SO) + ZPVE + HLC.

Table (F.11) G2/MP2 total energies (in Hartrees).^a

Species	Energy	Species	Energy	Species	Energy
H	- 0.500 00	HCHO	- 114.306 70	SH ⁺	- 397.877 74
Li	- 7.432 22	CH ₃ OH	- 115.495 30	H ₂ S ⁺ (² B ₁)	- 398.513 00
Be	- 14.604 29	N ₂	- 109.373 23	H ₂ S ⁺ (² A ₁)	- 398.428 12
B	- 24.579 70	N ₂ H ₄	- 111.639 94	HCl ⁺	- 459.840 41
C	- 37.761 67	NO	- 129.711 53	C ₂ H ₂ ⁺	- 76.727 54
N	- 54.499 37	O ₂	- 150.125 81	C ₂ H ₄ ⁺	- 77.982 24
O	- 74.961 67	H ₂ O ₂	- 151.333 52	CO ⁺	- 112.627 90
F	- 99.615 61	F ₂	- 199.295 56	N ₂ ⁺ ² Σ _g	- 108.807 18
Na	- 161.846 17	CO ₂	- 188.335 55	N ₂ ⁺ ² Π _u	- 108.745 27
Mg	- 199.634 32	Na ₂	- 323.714 31	O ₂ ⁺	- 149.695 09
Al	- 241.914 43	Si ₂	- 577.936 03	P ₂ ⁺	- 681.384 10
Si	- 288.912 33	P ₂	- 681.778 06	S ₂ ⁺	- 795.077 06
P	- 340.796 32	S ₂	- 795.416 19	Cl ₂ ⁺	- 918.964 53
S	- 397.626 83	Cl ₂	- 919.387 59	CIF ⁺	- 558.898 07
Cl	- 459.646 88	NaCl	- 621.653 55	CS ⁺	- 435.223 45
LiH	- 8.013 28	SiO	- 364.193 71	C ⁻	- 37.807 46
BeH	- 15.183 32	CS	- 435.669 55	O ⁻	- 75.014 07
CH	- 38.383 35	SO	- 472.794 12	F ⁻	- 99.749 88
CH ₂ (³ B ₁)	- 39.045 16	CIO	- 534.703 65	Si ⁻	- 288.962 18
CH ₂ (¹ A ₁)	- 39.025 50	CIF	- 559.366 20	P ⁻	- 340.814 92
CH ₃	- 39.717 22	CH ₃ Cl	- 499.502 54	S ⁻	- 397.699 72
CH ₄	- 40.380 74	CH ₃ SH	- 438.093 78	Cl ⁻	- 459.783 21
NH	- 55.117 96	HCIO	- 535.365 60	CH ⁻	- 38.428 46
NH ₂	- 55.763 57	SO ₂	- 547.983 94	CH ₂ ⁻	- 39.065 51
NH ₃	- 56.435 24	Li ⁺	- 7.235 84	CH ₃ ⁻	- 39.718 45
OH	- 75.622 78	Be ⁺	- 14.276 39	NH ⁻	- 55.128 94
H ₂ O	- 76.315 34	B ⁺	- 24.276 02	NH ₂ ⁻	- 55.796 82
HF	- 100.338 04	C ⁺	- 37.347 93	OH ⁻	- 75.698 24
SiH	- 289.518 89	N ⁺	- 53.962 86	SiH ⁻	- 289.561 57
SiH ₂ (¹ A ₁)	- 290.134 16	O ⁺	- 74.467 93	SiH ₂ ⁻	- 290.170 90
SiH ₂ (³ B ₁)	- 290.104 03	F ⁺	- 98.975 49	SiH ₃ ⁻	- 290.787 92
SiH ₃	- 290.741 46	Na ⁺	- 161.664 29	PH ⁻	- 341.432 28
SiH ₄	- 291.381 83	Mg ⁺	- 199.364 08	PH ₂ ⁻	- 342.060 29
PH	- 341.399 23	Al ⁺	- 241.700 44	SH ⁻	- 398.341 36
PH ₂	- 342.015 04	Si ⁺	- 288.616 96	O ₂ ⁻	- 150.138 78
PH ₃	- 342.641 13	P ⁺	- 340.411 65	NO ⁻	- 129.706 03
SH	- 398.254 71	S ⁺	- 397.257 15	CN ⁻	- 92.704 13
H ₂ S	- 398.896 23	Cl ⁺	- 459.175 44	PO ⁻	- 416.027 62
HCl	- 460.310 00	CH ₄ ⁺	- 39.915 97	PO	- 415.991 79
Li ₂	- 14.894 74	NH ₃ ⁺	- 56.058 08	S ₂ ⁻	- 795.475 61
LiF	- 107.275 37	OH ⁺	- 75.144 28	Cl ₂ ⁻	- 919.475 64
C ₂ H ₂	- 77.152 73	H ₂ O ⁺	- 75.845 19	NH ₄ ⁺	- 56.756 20
C ₂ H ₄	- 78.371 05	HF ⁺	- 99.739 89	H ₃ O ⁺	- 76.573 63
CN	- 92.530 56	SiH ₄ ⁺	- 290.981 59	C ₂ H ₃ ⁺	- 77.393 52
HCN	- 93.258 99	PH ⁺	- 341.027 53	SiH ₅ ⁺	- 291.625 07
CO	- 113.153 50	PH ₂ ⁺	- 341.656 38	PH ₄ ⁺	- 342.938 28
HCO	- 113.670 15	PH ₃ ⁺	- 342.283 35	H ₂ S ⁺	- 399.160 89
				H ₂ Cl ⁺	- 460.518 79

^aCorresponding to MP2/6-311+(3df,2p) + ZPVE + HLC.

Table (F.12) G3/MP2 total energies (in Hartrees).^a

Species	Energy	Species	Energy	Species	Energy
H	- 0.501 72	HCHO	- 114.315 15	SH ⁺	- 397.887 01
Li	- 7.433 92	CH ₃ OH	- 115.506 54	H ₂ S ⁺ (² B ₁)	- 398.523 93
Be	- 14.608 92	N ₂	- 109.380 30	H ₂ S ⁺ (² A ₁)	- 398.439 30
B	- 24.585 80	N ₂ H ₄	- 111.651 77	HCl ⁺	- 459.851 97
C	- 37.769 14	NO	- 129.717 57	C ₂ H ₂ ⁺	- 76.735 87
N	- 54.507 85	O ₂	- 150.133 17	C ₂ H ₄ ⁺	- 77.992 91
O	- 74.972 54	H ₂ O ₂	- 151.344 35	CO ⁺	- 112.631 48
F	- 99.628 59	F ₂	- 199.305 36	N ₂ ⁺ ² S _g	- 108.812 62
Na	- 161.847 88	CO ₂	- 188.344 30	N ₂ ⁺ ² I _u	- 108.750 89
Mg	- 199.639 10	Na ₂	- 323.717 00	O ₂ ⁺	- 149.701 82
Al	- 241.921 52	Si ₂	- 577.947 13	P ₂ ⁺	- 681.399 43
Si	- 288.921 87	P ₂	- 681.795 66	S ₂ ⁺	- 795.096 20
P	- 340.809 24	S ₂	- 795.436 90	Cl ₂ ⁺	- 918.987 93
S	- 397.644 26	Cl ₂	- 919.413 84	ClF ⁺	- 558.911 61
Cl	- 459.667 20	NaCl	- 621.668 17	CS ⁺	- 435.235 63
LiH	- 8.015 74	SiO	- 364.205 52	C ⁻	- 37.815 28
BeH	- 15.186 49	CS	- 435.683 67	O ⁻	- 75.024 82
CH	- 38.387 84	SO	- 472.808 38	F ⁻	- 99.761 51
CH ₂ (³ B ₁)	- 39.050 57	CIO	- 534.719 63	Si ⁻	- 288.973 32
CH ₂ (¹ A ₁)	- 39.031 14	CIF	- 559.381 82	P ⁻	- 340.832 87
CH ₃	- 39.724 13	CH ₃ Cl	- 499.521 40	S ⁻	- 397.721 71
CH ₄	- 40.389 02	CH ₃ SH	- 438.112 92	Cl ⁻	- 459.807 23
NH	- 55.122 60	HCIO	- 535.383 19	CH ⁻	- 38.432 59
NH ₂	- 55.769 33	SO ₂	- 548.003 16	CH ₂ ⁻	- 39.070 69
NH ₃	- 56.442 57	Li ⁺	- 7.235 84	CH ₃ ⁻	- 39.725 14
OH	- 75.627 84	Be ⁺	- 14.278 10	NH ⁻	- 55.132 90
H ₂ O	- 76.321 68	B ⁺	- 24.280 69	NH ₂ ⁻	- 55.802 32
HF	- 100.342 85	C ⁺	- 37.354 04	OH ⁻	- 75.702 11
SiH	- 289.524 80	N ⁺	- 53.970 36	SiH ⁻	- 289.569 82
SiH ₂ (¹ A ₁)	- 290.143 00	O ⁺	- 74.476 17	SiH ₂ ⁻	- 290.181 25
SiH ₂ (³ B ₁)	- 290.112 04	F ⁺	- 98.986 76	SiH ₃ ⁻	- 290.800 27
SiH ₃	- 290.751 52	Na ⁺	- 161.664 29	PH ⁻	- 341.444 78
SiH ₄	- 291.393 89	Mg ⁺	- 199.365 79	PH ₂ ⁻	- 342.074 25
PH	- 341.408 65	Al ⁺	- 241.705 42	SH ⁻	- 398.356 10
PH ₂	- 342.025 95	Si ⁺	- 288.624 90	O ₂ ⁻	- 150.146 08
PH ₃	- 342.653 57	P ⁺	- 340.423 77	NO ⁻	- 129.712 06
SH	- 398.266 54	S ⁺	- 397.269 61	CN ⁻	- 92.710 94
H ₂ S	- 398.909 66	Cl ⁺	- 459.193 67	PO ⁻	- 416.041 36
HCl	- 460.323 62	CH ₄ ⁺	- 39.922 68	PO	- 415.995 88
Li ₂	- 14.897 25	NH ₃ ⁺	- 56.064 66	S ₂ ⁻	- 795.499 61
LiF	- 107.279 60	OH ⁺	- 75.148 73	Cl ₂ ⁻	- 919.504 11
C ₂ H ₂	- 77.162 43	H ₂ O ⁺	- 75.850 72	NH ₄ ⁺	- 56.764 36
C ₂ H ₄	- 78.383 15	HF ⁺	- 99.744 25	H ₃ O ⁺	- 76.580 51
CN	- 92.536 46	SiH ₄ ⁺	- 290.991 29	C ₂ H ₃ ⁺	- 77.402 49
HCN	- 93.266 96	PH ⁺	- 341.035 68	SiH ₅ ⁺	- 291.636 68
CO	- 113.158 97	PH ₂ ⁺	- 341.665 90	PH ₄ ⁺	- 342.950 32
HCO	- 113.676 63	PH ₃ ⁺	- 342.293 79	H ₃ S ⁺	- 399.173 44
				H ₂ Cl ⁺	- 460.531 69

^aCorresponding to MP2/G3MP2large + ΔE(SO) + ZPVE + HLC.

Table (F.13) MR-G2/MP2 total energies (in Hartrees).^a

Species	Energy	Species	Energy	Species	Energy
H	- 0.500 00	HCHO	- 114.332 13	SH ⁺	- 397.901 87
Li	- 7.432 20	CH ₃ OH	- 115.527 53	H ₂ S ⁺ (² B ₁)	- 398.540 71
Be	- 14.626 12	N ₂	- 109.390 61	H ₂ S ⁺ (² A ₁)	- 398.454 25
B	- 24.601 96	N ₂ H ₄	- 111.674 42	HCl ⁺	- 459.864 56
C	- 37.781 89	NO	- 129.739 29	C ₂ H ₂ ⁺	- 76.769 21
N	- 54.516 32	O ₂	- 150.156 58	C ₂ H ₄ ⁺	- 78.025 01
O	- 74.980 67	H ₂ O ₂	- 151.365 09	CO ⁺	- 112.662 66
F	- 99.635 00	F ₂	- 199.331 04	N ₂ ⁺ ² Σ _g	- 108.823 94
Na	- 161.846 13	CO ₂	- 188.363 81	N ₂ ⁺ ² Π _u	- 108.779 12
Mg	- 199.648 72	Na ₂	- 323.726 92	O ₂ ⁺	- 149.705 47
Al	- 241.930 13	Si ₂	- 577.977 21	P ₂ ⁺	- 681.423 66
Si	- 288.929 01	P ₂	- 681.811 19	S ₂ ⁺	- 795.115 04
P	- 340.813 89	S ₂	- 795.457 92	Cl ₂ ⁺	- 919.005 30
S	- 397.647 33	Cl ₂	- 919.424 85	ClF ⁺	- 558.936 32
Cl	- 459.667 29	NaCl	- 621.676 75	CS ⁺	- 435.289 08
LiH	- 8.026 74	SiO	- 364.205 81	C ⁻	- 37.831 91
BeH	- 15.194 74	CS	- 435.702 91	O ⁻	- 75.035 29
CH	- 38.409 72	SO	- 472.828 94	F	- 99.768 10
CH ₂ (³ B ₁)	- 39.067 28	CIO	- 534.749 43	Si ⁻	- 288.979 55
CH ₂ (¹ A ₁)	- 39.054 34	CIF	- 559.398 45	P ⁻	- 340.835 21
CH ₃	- 39.742 56	CH ₃ Cl	- 499.543 74	S ⁻	- 397.720 22
CH ₄	- 40.408 06	CH ₃ SH	- 438.136 61	Cl ⁻	- 459.801 43
NH	- 55.140 83	HCIO	- 535.397 24	CH ⁻	- 38.452 81
NH ₂	- 55.786 44	SO ₂	- 548.018 34	CH ₂ ⁻	- 39.088 70
NH ₃	- 56.451 26	Li ⁺	- 7.235 48	CH ₃ ⁻	- 39.735 24
OH	- 75.643 80	Be ⁺	- 14.276 33	NH ⁻	- 55.151 77
H ₂ O	- 76.329 07	B ⁺	- 24.304 71	NH ₂ ⁻	- 55.811 87
HF	- 100.353 06	C ⁺	- 37.373 85	OH ⁻	- 75.713 73
SiH	- 289.541 56	N ⁺	- 53.984 11	SiH ⁻	- 289.584 32
SiH ₂ (¹ A ₁)	- 290.161 62	O ⁺	- 74.483 50	SiH ₂ ⁻	- 290.196 66
SiH ₂ (³ B ₁)	- 290.125 56	F ⁺	- 98.993 20	SiH ₃ ⁻	- 290.816 17
SiH ₃	- 290.767 05	Na ⁺	- 161.664 29	PH ⁻	- 341.455 97
SiH ₄	- 291.411 58	Mg ⁺	- 199.364 00	PH ₂ ⁻	- 342.085 32
PH	- 341.423 05	Al ⁺	- 241.716 42	SH ⁻	- 398.362 65
PH ₂	- 342.042 31	Si ⁺	- 288.633 90	O ₂ ⁻	- 150.173 43
PH ₃	- 342.670 16	P ⁺	- 340.429 11	NO ⁻	- 129.744 04
SH	- 398.278 75	S ⁺	- 397.275 14	CN ⁻	- 92.723 73
H ₂ S	- 398.921 39	Cl ⁺	- 459.196 28	PO ⁻	- 416.060 21
HCl	- 460.331 29	CH ₄ ⁺	- 39.943 61	PO ⁻	- 416.014 30
Li ₂	- 14.909 71	NH ₃ ⁺	- 56.083 77	S ₂ ⁻	- 795.514 71
LiF	- 107.288 04	OH ⁺	- 75.166 64	Cl ₂ ⁻	- 919.517 65
C ₂ H ₂	- 77.186 29	H ₂ O ⁺	- 75.866 84	NH ₄ ⁺	- 56.782 06
C ₂ H ₄	- 78.413 89	HF ⁺	- 99.759 90	H ₃ O ⁺	- 76.585 93
CN	- 92.582 51	SiH ₄ ⁺	- 291.009 89	C ₂ H ₃ ⁺	- 77.431 03
HCN	- 93.281 48	PH ⁺	- 341.052 47	SiH ₅ ⁺	- 291.657 92
CO	- 113.172 22	PH ₂ ⁺	- 341.685 29	PH ₄ ⁺	- 342.967 98
HCO	- 113.694 60	PH ₃ ⁺	- 342.310 22	H ₃ S ⁺	- 399.189 84
				H ₂ Cl ⁺	- 460.543 42

^aCorresponding to CASPT2/6-311+G(3df,2p) + ZPVE + HLC.

Table (F.14) MR-G3/MP2 total energies (in Hartrees).^a

Species	Energy	Species	Energy	Species	Energy
H	- 0.501 73	HCHO	- 114.349 65	SH ⁺	- 397.915 78
Li	- 7.433 92	CH ₃ OH	- 115.549 47	H ₂ S ⁺ (² B ₁)	- 398.556 94
Be	- 14.630 21	N ₂	- 109.405 11	H ₂ S ⁺ (² A ₁)	- 398.470 74
B	- 24.607 41	N ₂ H ₄	- 111.696 69	HCl ⁺	- 459.881 42
C	- 37.788 61	NO	- 129.753 29	C ₂ H ₂ ⁺	- 76.781 30
N	- 54.523 93	O ₂	- 150.172 26	C ₂ H ₄ ⁺	- 78.043 92
O	- 74.990 03	H ₂ O ₂	- 151.386 34	CO ⁺	- 112.673 03
F	- 99.645 91	F ₂	- 199.351 32	N ₂ ⁺ $^2\Sigma_g$	- 108.836 24
Na	- 161.847 86	CO ₂	- 188.384 47	N ₂ ⁺ $^2\Pi_u$	- 108.791 46
Mg	- 199.652 86	Na ₂	- 323.731 09	O ₂ ⁺	- 149.720 03
Al	- 241.936 62	Si ₂	- 577.994 03	P ₂ ⁺	- 681.445 84
Si	- 288.938 00	P ₂	- 681.836 17	S ₂ ⁺	- 795.142 49
P	- 340.826 33	S ₂	- 795.487 82	Cl ₂ ⁺	- 919.038 54
S	- 397.663 71	Cl ₂	- 919.461 57	ClF ⁺	- 558.959 73
Cl	- 459.687 13	NaCl	- 621.697 32	CS ⁺	- 435.308 21
LiH	- 8.030 70	SiO	- 364.225 13	C ⁻	- 37.838 14
BeH	- 15.200 17	CS	- 435.724 37	O ⁻	- 75.043 74
CH	- 38.417 86	SO	- 472.852 24	F ⁻	- 99.777 21
CH ₂ (³ B ₁)	- 39.077 11	CIO	- 534.774 97	Si ⁻	- 288.990 27
CH ₂ (¹ A ₁)	- 39.064 49	CIF	- 559.424 58	P ⁻	- 340.852 23
CH ₃	- 39.754 63	CH ₃ Cl	- 499.573 05	S ⁻	- 397.740 47
CH ₄	- 40.422 29	CH ₃ SH	- 438.166 16	Cl ⁻	- 459.822 93
NH	- 55.149 76	HClO	- 535.425 28	CH ⁻	- 38.460 82
NH ₂	- 55.797 37	SO ₂	- 548.050 85	CH ₂ ⁻	- 39.098 93
NH ₃	- 56.464 57	Li ⁺	- 7.235 84	CH ₃ ⁻	- 39.748 13
OH	- 75.653 95	Be ⁺	- 14.278 06	NH ⁻	- 55.160 61
H ₂ O	- 76.341 44	B ⁺	- 24.308 81	NH ₂ ⁻	- 55.823 42
HF	- 100.363 85	C ⁺	- 37.379 36	OH ⁻	- 75.723 58
SiH	- 289.552 14	N ⁺	- 53.990 99	SiH ⁻	- 289.597 38
SiH ₂ (¹ A ₁)	- 290.174 77	O ⁺	- 74.491 09	SiH ₂ ⁻	- 290.212 41
SiH ₂ (³ B ₁)	- 290.138 07	F ⁺	- 99.003 16	SiH ₃ ⁻	- 290.834 38
SiH ₃	- 290.782 19	Na ⁺	- 161.664 29	PH ⁺	- 341.473 94
SiH ₄	- 291.429 30	Mg ⁺	- 199.365 73	PH ₂ ⁻	- 342.105 23
PH	- 341.437 13	Al ⁺	- 241.720 61	SH ⁻	- 398.383 40
PH ₂	- 342.058 59	Si ⁺	- 288.641 12	O ₂ ⁻	- 150.189 99
PH ₃	- 342.688 47	P ⁺	- 340.440 67	NO ⁻	- 129.758 43
SH	- 398.295 97	S ⁺	- 397.287 14	CN ⁻	- 92.738 06
H ₂ S	- 398.940 77	Cl ⁺	- 459.213 32	PO ⁻	- 416.083 27
HCl	- 460.350 90	CH ₄ ⁺	- 39.955 54	PO	- 416.035 34
Li ₂	- 14.913 80	NH ₃ ⁺	- 56.095 58	S ₂ ⁻	- 795.548 61
LiF	- 107.298 44	OH ⁺	- 75.175 53	Cl ₂ ⁻	- 919.559 27
C ₂ H ₂	- 77.203 58	H ₂ O ⁺	- 75.877 59	NH ₄ ⁺	- 56.796 23
C ₂ H ₄	- 78.434 95	HF ⁺	- 99.769 45	H ₃ O ⁺	- 76.598 76
CN	- 92.595 10	SiH ₄ ⁺	- 291.024 70	C ₂ H ₃ ⁺	- 77.447 59
HCN	- 93.296 99	PH ⁺	- 341.064 38	SiH ₅ ⁺	- 291.675 26
CO	- 113.185 17	PH ₂ ⁺	- 341.699 16	PH ₄ ⁺	- 342.985 64
HCO	- 113.709 32	PH ₃ ⁺	- 342.325 76	H ₃ S ⁺	- 399.208 21
					- 460.562 27

^aCorresponding to CASPT2/G3MP2large + ΔE(SO) + ZPVE + HLC.

Table (F.15) MR(QD)-G2(MP2,SVP) total energies (in Hartrees).

Species	Energy	Species	Energy	Species	Energy
H	- 0.500 00	HCHO	- 114.346 31	SH ⁺	- 397.914 07
Li	- 7.432 20	CH ₃ OH	- 115.547 49	H ₂ S ⁺ (2B ₁)	- 398.553 81
Be	- 14.626 36	N ₂	- 109.409 42	H ₂ S ⁺ (2A ₁)	- 398.468 44
B	- 24.606 34	N ₂ H ₄	- 111.694 94	HCl ⁺	- 459.879 06
C	- 37.789 63	NO	- 129.755 99	C ₂ H ₂ ⁺	- 76.777 60
N	- 54.524 52	O ₂	- 150.166 71	C ₂ H ₄ ⁺	- 78.039 14
O	- 74.990 12	H ₂ O ₂	- 151.383 38	CO ⁺	- 112.675 16
F	- 99.642 13	F ₂	- 199.342 62	N ₂ ⁺ 2Σ _g	- 108.837 19
Na	- 161.846 13	CO ₂	- 188.384 20	N ₂ ⁺ 2Π _u	- 108.796 99
Mg	- 199.649 18	Na ₂	- 323.726 88	O ₂ ⁺	- 149.720 69
Al	- 241.935 19	Si ₂	- 577.992 31	P ₂ ⁺	- 681.446 16
Si	- 288.938 40	P ₂	- 681.833 87	S ₂ ⁺	- 795.138 46
P	- 340.824 79	S ₂	- 795.478 27	Cl ₂ ⁺	- 919.030 05
S	- 397.660 57	Cl ₂	- 919.452 30	ClF ⁺	- 558.953 50
Cl	- 459.681 77	NaCl	- 621.692 69	CS ⁺	- 435.304 86
LiH	- 8.026 73	SiO	- 364.228 65	C ⁻	- 37.835 88
BeH	- 15.196 54	CS	- 435.724 28	O ⁻	- 75.043 96
CH	- 38.418 56	SO	- 472.843 85	F	- 99.771 49
CH ₂ (3B ₁)	- 39.074 33	ClO	- 534.769 49	Si ⁻	- 288.989 74
CH ₂ (1A ₁)	- 39.064 86	ClF	- 559.418 22	P ⁻	- 340.848 20
CH ₃	- 39.751 79	CH ₃ Cl	- 499.562 91	S ⁻	- 397.734 76
CH ₄	- 40.418 71	CH ₃ SH	- 438.163 60	Cl ⁻	- 459.815 60
NH	- 55.150 04	HClO	- 535.421 10	CH ⁻	- 38.458 80
NH ₂	- 55.796 88	SO ₂	- 548.038 49	CH ₂ ⁻	- 39.099 58
NH ₃	- 56.463 15	Li ⁺	- 7.235 84	CH ₃ ⁻	- 39.748 45
OH	- 75.653 12	Be ⁺	- 14.276 34	NH ⁻	- 55.162 91
H ₂ O	- 76.340 08	B ⁺	- 24.304 98	NH ₂ ⁻	- 55.824 65
HF	- 100.358 74	C ⁺	- 37.378 72	OH ⁻	- 75.721 46
SiH	- 289.550 78	N ⁺	- 53.992 24	SiH ⁻	- 289.595 16
SiH ₂ (1A ₁)	- 290.171 97	O ⁺	- 74.490 70	SiH ₂ ⁻	- 290.208 18
SiH ₂ (3B ₁)	- 290.132 79	F ⁺	- 99.000 56	SiH ₃ ⁻	- 290.828 85
SiH ₃	- 290.775 84	Na ⁺	- 161.664 29	PH ⁻	- 341.469 98
SiH ₄	- 291.421 37	Mg ⁺	- 199.364 00	PH ₂ ⁻	- 342.100 59
PH	- 341.435 08	Al ⁺	- 241.716 79	SH ⁻	- 398.377 95
PH ₂	- 342.054 94	Si ⁺	- 288.640 37	O ₂ ⁻	- 150.185 41
PH ₃	- 342.684 01	P ⁺	- 340.440 17	NO ⁻	- 129.755 50
SH	- 398.293 20	S ⁺	- 397.286 14	CN ⁻	- 92.742 37
H ₂ S	- 398.936 83	Cl ⁺	- 459.209 39	PO ⁻	- 416.074 35
HCl	- 460.346 55	CH ₄ ⁺	- 39.951 80	PO	- 416.034 30
Li ₂	- 14.909 68	NH ₃ ⁺	- 56.091 85	S ₂ ⁻	- 795.538 35
LiF	- 107.290 90	OH ⁺	- 75.174 49	Cl ₂ ⁻	- 919.540 64
C ₂ H ₂	- 77.198 64	H ₂ O ⁺	- 75.875 80	NH ₄ ⁺	- 56.790 10
C ₂ H ₄	- 78.423 32	HF ⁺	- 99.767 43	H ₃ O ⁺	- 76.595 83
CN	- 92.596 17	SiH ₄ ⁺	- 291.018 61	C ₂ H ₃ ⁺	- 77.445 05
HCN	- 93.295 97	PH ⁺	- 341.063 07	SiH ₅ ⁺	- 291.666 50
CO	- 113.191 67	PH ₂ ⁺	- 341.696 75	PH ₄ ⁺	- 342.978 66
HCO	- 113.712 70	PH ₃ ⁺	- 342.319 67	H ₃ S ⁺	- 399.204 06
				H ₂ Cl ⁺	- 460.558 79

Table (F.16) MR(QD)-G2(MP2) total energies (in Hartrees).

Species	Energy	Species	Energy	Species	Energy
H	- 0.500 00	HCHO	- 114.343 85	SH ⁺	- 397.913 28
Li	- 7.432 20	CH ₃ OH	- 115.546 27	H ₂ S ⁺ (² B ₁)	- 398.553 11
Be	- 14.625 53	N ₂	- 109.404 68	H ₂ S ⁺ (² A ₁)	- 398.465 95
B	- 24.606 96	N ₂ H ₄	- 111.692 92	HCl ⁺	- 459.877 23
C	- 37.789 99	NO	- 129.750 88	C ₂ H ₂ ⁺	- 76.777 30
N	- 54.523 42	O ₂	- 150.161 38	C ₂ H ₄ ⁺	- 78.038 59
O	- 74.987 89	H ₂ O ₂	- 151.377 79	CO ⁺	- 112.671 93
F	- 99.639 40	F ₂	- 199.335 36	N ₂ ⁺ Σ_g^+	- 108.833 50
Na	- 161.846 13	CO ₂	- 188.376 57	N ₂ ⁺ Π_u	- 108.792 96
Mg	- 199.648 23	Na ₂	- 323.725 99	O ₂ ⁺	- 149.716 01
Al	- 241.934 34	Si ₂	- 577.988 67	P ₂ ⁺	- 681.442 52
Si	- 288.937 61	P ₂	- 681.829 21	S ₂ ⁺	- 795.133 97
P	- 340.823 81	S ₂	- 795.473 43	Cl ₂ ⁺	- 919.024 72
S	- 397.658 82	Cl ₂	- 919.445 83	ClF ⁺	- 558.948 01
Cl	- 459.679 07	NaCl	- 621.688 82	CS ⁺	- 435.301 58
LiH	- 8.026 02	SiO	- 364.224 89	C ⁻	- 37.836 25
BeH	- 15.198 42	CS	- 435.720 77	O ⁻	- 75.040 23
CH	- 38.419 20	SO	- 472.838 84	F	- 99.766 32
CH ₂ (³ B ₁)	- 39.075 15	CIO	- 534.763 63	Si ⁻	- 288.989 31
CH ₂ (¹ A ₁)	- 39.066 39	CIF	- 559.411 28	P ⁻	- 340.848 47
CH ₃	- 39.753 24	CH ₃ Cl	- 499.560 26	S ⁻	- 397.731 71
CH ₄	- 40.420 67	CH ₃ SH	- 438.163 54	Cl ⁻	- 459.811 23
NH	- 55.148 81	HClO	- 535.415 11	CH ⁻	- 38.458 97
NH ₂	- 55.796 07	SO ₂	- 548.029 23	CH ₂ ⁻	- 39.100 54
NH ₃	- 56.462 94	Li ⁺	- 7.235 48	CH ₃ ⁻	- 39.749 95
OH	- 75.650 53	Be ⁺	- 14.276 34	NH ⁻	- 55.160 64
H ₂ O	- 76.337 96	B ⁺	- 24.303 99	NH ₂ ⁻	- 55.823 19
HF	- 100.355 11	C ⁺	- 37.378 21	OH ⁻	- 75.717 59
SiH	- 289.550 84	N ⁺	- 53.991 19	SiH ⁻	- 289.595 41
SiH ₂ (¹ A ₁)	- 290.173 23	O ⁺	- 74.489 64	SiH ₂ ⁻	- 290.209 36
SiH ₂ (³ B ₁)	- 290.134 14	F ⁺	- 98.999 35	SiH ₃ ⁻	- 290.831 28
SiH ₃	- 290.778 67	Na ⁺	- 161.664 29	PH ⁻	- 341.468 46
SiH ₄	- 291.426 26	Mg ⁺	- 199.364 06	PH ₂ ⁻	- 342.099 35
PH	- 341.434 55	Al ⁺	- 241.715 89	SH ⁻	- 398.374 80
PH ₂	- 342.055 00	Si ⁺	- 288.639 54	O ₂ ⁻	- 150.178 30
PH ₃	- 342.685 09	P ⁺	- 340.439 42	NO ⁻	- 129.749 83
SH	- 398.291 44	S ⁺	- 397.285 96	CN ⁻	- 92.738 78
H ₂ S	- 398.935 27	Cl ⁺	- 459.208 13	PO ⁻	- 416.069 09
HCl	- 460.343 59	CH ₄ ⁺	- 39.953 19	PO	- 416.029 56
Li ₂	- 14.908 77	NH ₃ ⁺	- 56.091 89	S ₂ ⁻	- 795.531 99
LiF	- 107.290 54	OH ⁺	- 75.173 03	Cl ₂ ⁻	- 919.539 94
C ₂ H ₂	- 77.196 90	H ₂ O ⁺	- 75.874 30	NH ₄ ⁺	- 56.790 77
C ₂ H ₄	- 78.430 10	HF ⁺	- 99.765 06	H ₃ O ⁺	- 76.594 67
CN	- 92.592 87	SiH ₄ ⁺	- 291.022 08	C ₂ H ₃ ⁺	- 77.441 84
HCN	- 93.292 75	PH ⁺	- 341.062 75	SiH ₅ ⁺	- 291.671 44
CO	- 113.188 34	PH ₂ ⁺	- 341.697 24	PH ₄ ⁺	- 342.981 99
HCO	- 113.709 32	PH ₃ ⁺	- 342.321 26	H ₃ S ⁺	- 399.203 81
				H ₂ Cl ⁺	- 460.556 78

Table (F.17) MR(QD)-G3(MP2) total energies (in Hartrees).

Species	Energy	Species	Energy	Species	Energy
H	- 0.501 64	HCHO	- 114.356 37	SH ⁺	- 397.927 29
Li	- 7.433 83	CH ₃ OH	- 115.561 02	H ₂ S ⁺ (² B ₁)	- 398.567 00
Be	- 14.628 12	N ₂	- 109.417 68	H ₂ S ⁺ (² A ₁)	- 398.482 04
B	- 24.609 40	N ₂ H ₄	- 111.708 42	HCl ⁺	- 459.893 08
C	- 37.793 86	NO	- 129.764 68	C ₂ H ₂ ⁺	- 76.788 65
N	- 54.529 52	O ₂	- 150.177 97	C ₂ H ₄ ⁺	- 78.052 73
O	- 74.994 63	H ₂ O ₂	- 151.395 90	CO ⁺	- 112.681 42
F	- 99.645 95	F ₂	- 199.354 12	N ₂ ⁺ Σ_g^+	- 108.845 40
Na	- 161.847 76	CO ₂	- 188.394 86	N ₂ ⁺ Π_u	- 108.803 81
Mg	- 199.650 99	Na ₂	- 323.729 80	O ₂ ⁺	- 149.729 92
Al	- 241.939 26	Si ₂	- 578.007 54	P ₂ ⁺	- 681.464 29
Si	- 288.944 87	P ₂	- 681.852 66	S ₂ ⁺	- 795.160 59
P	- 340.834 63	S ₂	- 795.503 72	Cl ₂ ⁺	- 919.056 69
S	- 397.672 15	Cl ₂	- 919.480 25	ClF ⁺	- 558.970 31
Cl	- 459.694 58	NaCl	- 621.708 05	CS ⁺	- 435.319 91
LiH	- 8.029 44	SiO	- 364.241 78	C ⁻	- 37.839 51
BeH	- 15.201 62	CS	- 435.739 50	O ⁻	- 75.045 34
CH	- 38.425 15	SO	- 472.862 71	F	- 99.771 28
CH ₂ (³ B ₁)	- 39.083 49	CIO	- 534.788 42	Si ⁻	- 288.997 85
CH ₂ (¹ A ₁)	- 39.071 29	CIF	- 559.435 58	P ⁻	- 340.860 44
CH ₃	- 39.761 05	CH ₃ Cl	- 499.586 54	S ⁻	- 397.748 00
CH ₄	- 40.428 01	CH ₃ SH	- 438.184 20	Cl ⁻	- 459.827 78
NH	- 55.158 31	HCIO	- 535.440 41	CH ⁻	- 38.469 55
NH ₂	- 55.805 00	SO ₂	- 548.059 77	CH ₂ ⁻	- 39.107 04
NH ₃	- 56.471 42	Li ⁺	- 7.235 84	CH ₃ ⁻	- 39.756 39
OH	- 75.660 43	Be ⁺	- 14.277 97	NH ⁻	- 55.168 90
H ₂ O	- 76.347 47	B ⁺	- 24.306 75	NH ₂ ⁻	- 55.831 22
HF	- 100.364 51	C ⁺	- 37.381 80	OH ⁻	- 75.726 31
SiH	- 289.559 75	N ⁺	- 53.996 60	SiH ⁻	- 289.607 50
SiH ₂ (¹ A ₁)	- 290.181 33	O ⁺	- 74.495 68	SiH ₂ ⁻	- 290.221 03
SiH ₂ (³ B ₁)	- 290.144 58	F ⁺	- 99.005 65	SiH ₃ ⁻	- 290.841 94
SiH ₃	- 290.788 10	Na ⁺	- 161.664 29	PH ⁻	- 341.485 10
SiH ₄	- 291.434 06	Mg ⁺	- 199.365 63	PH ₂ ⁻	- 342.115 42
PH	- 341.448 48	Al ⁺	- 241.718 65	SH ⁻	- 398.393 64
PH ₂	- 342.068 38	Si ⁺	- 288.645 17	O ₂ ⁻	- 150.195 39
PH ₃	- 342.697 26	P ⁺	- 340.449 24	NO ⁻	- 129.765 47
SH	- 398.307 59	S ⁺	- 397.295 56	CN ⁻	- 92.750 46
H ₂ S	- 398.951 18	Cl ⁺	- 459.221 62	PO ⁻	- 416.092 97
HCl	- 460.361 13	CH ₄ ⁺	- 39.960 90	PO	- 416.050 01
Li ₂	- 14.912 50	NH ₃ ⁺	- 56.100 82	S ₂ ⁻	- 795.565 66
LiF	- 107.296 31	OH ⁺	- 75.182 70	Cl ₂ ⁻	- 919.572 48
C ₂ H ₂	- 77.210 74	H ₂ O ⁺	- 75.883 69	NH ₄ ⁺	- 56.799 23
C ₂ H ₄	- 78.436 93	HF ⁺	- 99.774 10	H ₃ O ⁺	- 76.603 63
CN	- 92.604 66	SiH ₄ ⁺	- 291.028 37	C ₂ H ₃ ⁺	- 77.455 51
HCN	- 93.305 19	PH ⁺	- 341.073 40	SiH ₅ ⁺	- 291.678 82
CO	- 113.198 38	PH ₂ ⁺	- 341.706 86	PH ₄ ⁺	- 342.991 32
HCO	- 113.722 06	PH ₃ ⁺	- 342.332 36	H ₃ S ⁺	- 399.217 40
				H ₂ Cl ⁺	- 460.572 61

Table (F.18) MR(QD)-G2/MP2 total energies (in Hartrees).^a

Species	Energy	Species	Energy	Species	Energy
H	- 0.500 00	HCHO	- 114.332 35	SH ⁺	- 397.903 92
Li	- 7.432 20	CH ₃ OH	- 115.528 14	H ₂ S ⁺ (² B ₁)	- 398.542 62
Be	- 14.626 75	N ₂	- 109.393 93	H ₂ S ⁺ (² A ₁)	- 398.454 31
B	- 24.602 74	N ₂ H ₄	- 111.677 07	HCl ⁺	- 459.866 88
C	- 37.782 99	NO	- 129.744 19	C ₂ H ₂ ⁺	- 76.766 89
N	- 54.517 38	O ₂	- 150.162 59	C ₂ H ₄ ⁺	- 78.024 90
O	- 74.982 44	H ₂ O ₂	- 151.373 12	CO ⁺	- 112.666 27
F	- 99.637 21	F ₂	- 199.338 17	N ₂ ⁺ ² S _g	- 108.827 50
Na	- 161.846 13	CO ₂	- 188.374 03	N ₂ ⁺ ² P _u	- 108.781 80
Mg	- 199.649 35	Na ₂	- 323.727 55	O ₂ ⁺	- 149.710 37
Al	- 241.930 84	Si ₂	- 577.981 41	P ₂ ⁺	- 681.427 57
Si	- 288.930 28	P ₂	- 681.815 44	S ₂ ⁺	- 795.119 44
P	- 340.815 28	S ₂	- 795.462 81	Cl ₂ ⁺	- 919.010 26
S	- 397.649 53	Cl ₂	- 919.429 84	ClF ⁺	- 558.942 09
Cl	- 459.669 83	NaCl	- 621.682 71	CS ⁺	- 435.291 64
LiH	- 8.027 31	SiO	- 364.206 06	C ⁻	- 37.828 91
BeH	- 15.194 70	CS	- 435.706 58	O ⁻	- 75.037 43
CH	- 38.410 37	SO	- 472.835 03	F	- 99.770 64
CH ₂ (³ B ₁)	- 39.068 04	ClO	- 534.754 63	Si ⁻	- 288.980 72
CH ₂ (¹ A ₁)	- 39.054 77	ClF	- 559.404 24	P ⁻	- 340.837 26
CH ₃	- 39.743 05	CH ₃ Cl	- 499.543 08	S ⁻	- 397.722 68
CH ₄	- 40.407 93	CH ₃ SH	- 438.143 50	Cl ⁻	- 459.803 97
NH	- 55.142 83	HClO	- 535.403 18	CH ⁻	- 38.450 60
NH ₂	- 55.788 70	SO ₂	- 548.031 22	CH ₂ ⁻	- 39.089 96
NH ₃	- 56.452 48	Li ⁺	- 7.235 84	CH ₃ ⁻	- 39.735 78
OH	- 75.647 05	Be ⁺	- 14.276 34	NH ⁻	- 55.154 27
H ₂ O	- 76.332 95	B ⁺	- 24.305 34	NH ₂ ⁻	- 55.814 92
HF	- 100.357 77	C ⁺	- 37.374 67	OH ⁻	- 75.717 76
SiH	- 289.541 71	N ⁺	- 53.985 16	SiH ⁻	- 289.585 41
SiH ₂ (¹ A ₁)	- 290.161 35	O ⁺	- 74.484 62	SiH ₂ ⁻	- 290.196 25
SiH ₂ (³ B ₁)	- 290.124 91	F ⁺	- 98.994 96	SiH ₃ ⁻	- 290.814 35
SiH ₃	- 290.765 70	Na ⁺	- 161.664 29	PH ⁻	- 341.457 07
SiH ₄	- 291.409 63	Mg ⁺	- 199.364 00	PH ₂ ⁻	- 342.085 06
PH	- 341.425 12	Al ⁺	- 241.717 05	SH ⁻	- 398.363 86
PH ₂	- 342.043 17	Si ⁺	- 288.634 79	O ₂ ⁻	- 150.180 82
PH ₃	- 342.669 80	P ⁺	- 340.430 43	NO ⁻	- 129.750 92
SH	- 398.280 52	S ⁺	- 397.276 45	CN ⁻	- 92.727 20
H ₂ S	- 398.922 13	Cl ⁺	- 459.198 52	PO ⁻	- 416.067 24
HCl	- 460.333 34	CH ₄ ⁺	- 39.943 95	PO	- 416.019 06
Li ₂	- 14.910 35	NH ₃ ⁺	- 56.084 98	S ₂ ⁻	- 795.520 01
LiF	- 107.288 29	OH ⁺	- 75.169 23	Cl ₂ ⁻	- 919.524 54
C ₂ H ₂	- 77.186 81	H ₂ O ⁺	- 75.869 84	NH ₄ ⁺	- 56.781 56
C ₂ H ₄	- 78.414 42	HF ⁺	- 99.764 26	H ₂ O ⁺	- 76.587 34
CN	- 92.586 11	SiH ₄ ⁺	- 291.010 06	C ₂ H ₃ ⁺	- 77.431 73
HCN	- 93.282 96	PH ⁺	- 341.052 92	SiH ₅ ⁺	- 291.656 67
CO	- 113.174 79	PH ₂ ⁺	- 341.685 35	PH ₄ ⁺	- 342.965 60
HCO	- 113.697 62	PH ₃ ⁺	- 342.309 03	H ₂ S ⁺	- 399.190 77
				H ₂ Cl ⁺	- 460.545 60

^aCorresponding to MRQDPT2/6-311+G(3df,2p) + ZPVE + HLC.

Table (F.19) MR(QD)-G3/MP2 total energies (in Hartrees).^a

Species	Energy	Species	Energy	Species	Energy
H	- 0.501 57	HCHO	- 114.347 52	SH ⁺	- 397.917 07
Li	- 7.433 75	CH ₃ OH	- 115.547 63	H ₂ S ⁺ (² B ₁)	- 398.557 49
Be	- 14.630 29	N ₂	- 109.406 46	H ₂ S ⁺ (² A ₁)	- 398.469 58
B	- 24.607 50	N ₂ H ₄	- 111.696 52	HCl ⁺	- 459.882 57
C	- 37.788 85	NO	- 129.756 26	C ₂ H ₂ ⁺	- 76.780 46
N	- 54.523 94	O ₂	- 150.176 34	C ₂ H ₄ ⁺	- 78.041 86
O	- 74.990 35	H ₂ O ₂	- 151.391 61	CO ⁺	- 112.675 05
F	- 99.646 28	F ₂	- 199.355 64	N ₂ ⁺ Σ_g^+	- 108.838 23
Na	- 161.847 69	CO ₂	- 188.391 52	N ₂ ⁺ Π_u	- 108.791 15
Mg	- 199.652 93	Na ₂	- 323.731 32	O ₂ ⁺	- 149.722 99
Al	- 241.936 61	Si ₂	- 577.997 43	P ₂ ⁺	- 681.448 23
Si	- 288.938 38	P ₂	- 681.838 50	S ₂ ⁺	- 795.144 95
P	- 340.826 67	S ₂	- 795.490 76	Cl ₂ ⁺	- 919.041 14
S	- 397.664 52	Cl ₂	- 919.463 76	ClF ⁺	- 558.963 13
Cl	- 459.687 89	NaCl	- 621.701 48	CS ⁺	- 435.309 22
LiH	- 8.030 87	SiO	- 364.223 45	C ⁻	- 37.834 09
BeH	- 15.199 75	CS	- 435.726 07	O ⁻	- 75.044 06
CH	- 38.417 79	SO	- 472.856 39	F ⁻	- 99.777 53
CH ₂ (³ B ₁)	- 39.077 14	CIO	- 534.777 79	Si ⁻	- 288.990 39
CH ₂ (¹ A ₁)	- 39.063 76	CIF	- 559.427 57	P ⁻	- 340.852 90
CH ₃	- 39.753 98	CH ₃ Cl	- 499.572 68	S ⁻	- 397.741 17
CH ₄	- 40.420 64	CH ₃ SH	- 438.170 07	Cl ⁻	- 459.823 24
NH	- 55.151 03	HCIO	- 535.428 46	CH ⁻	- 38.461 28
NH ₂	- 55.798 49	SO ₂	- 548.060 19	CH ₂ ⁻	- 39.099 09
NH ₃	- 56.464 16	Li ⁺	- 7.235 84	CH ₃ ⁻	- 39.747 13
OH	- 75.656 03	Be ⁺	- 14.277 90	NH ⁻	- 55.161 93
H ₂ O	- 76.343 74	B ⁺	- 24.308 89	NH ₂ ⁻	- 55.824 90
HF	- 100.366 95	C ⁺	- 37.379 46	OH ⁻	- 75.726 02
SiH	- 289.551 50	N ⁺	- 53.991 14	SiH ⁻	- 289.597 69
SiH ₂ (¹ A ₁)	- 290.173 27	O ⁺	- 74.491 14	SiH ₂ ⁻	- 290.210 76
SiH ₂ (³ B ₁)	- 290.136 63	F ⁺	- 99.003 46	SiH ₃ ⁻	- 290.830 86
SiH ₃	- 290.779 64	Na ⁺	- 161.664 29	PH ⁻	- 341.473 86
SiH ₄	- 291.425 74	Mg ⁺	- 199.365 56	PH ₂ ⁻	- 342.103 30
PH	- 341.438 45	Al ⁺	- 241.720 69	SH ⁻	- 398.382 97
PH ₂	- 342.058 28	Si ⁺	- 288.641 28	O ₂ ⁻	- 150.195 03
PH ₃	- 342.686 47	P ⁺	- 340.441 12	NO ⁻	- 129.763 39
SH	- 398.296 58	S ⁺	- 397.287 42	CN ⁻	- 92.739 55
H ₂ S	- 398.939 89	Cl ⁺	- 459.214 14	PO ⁻	- 416.088 35
HCl	- 460.351 33	CH ₄ ⁺	- 39.954 72	PO	- 416.038 15
Li ₂	- 14.914 03	NH ₃ ⁺	- 56.095 63	S ₂ ⁻	- 795.551 55
LiF	- 107.297 10	OH ⁺	- 75.177 37	Cl ₂ ⁻	- 919.561 47
C ₂ H ₂	- 77.203 16	H ₂ O ⁺	- 75.879 41	NH ₄ ⁺	- 56.794 10
C ₂ H ₄	- 78.433 15	HF ⁺	- 99.772 60	H ₃ O ⁺	- 76.598 54
CN	- 92.597 13	SiH ₄ ⁺	- 291.021 49	C ₂ H ₃ ⁺	- 77.446 45
HCN	- 93.296 44	PH ⁺	- 341.064 07	SiH ₅ ⁺	- 291.672 39
CO	- 113.185 77	PH ₂ ⁺	- 341.698 02	PH ₄ ⁺	- 342.981 67
HCO	- 113.710 36	PH ₃ ⁺	- 342.323 39	H ₃ S ⁺	- 399.207 52
				H ₂ Cl ⁺	- 460.562 83

^aCorresponding to MRQDPT2/G3MP2large + ΔE(SO) + ZPVE + HLC.

ACKNOWLEDGEMENTS

In addition to those whom this work is dedicated, I would like to make several further acknowledgements. While a student at Iowa State University, I have enjoyed kindness, support and guidance from several colleagues, in particular Dr. Rob Bell, Dr. Cheol Ho Choi, Dr. Kurt Glaesemann, Mrs. Kristin Hinders, the future Dr. Heather Netzloff, and Dr. Michael Pak. I thank my Chemistry and Physics students at Mountain-Iron Buhl High School for helping me to leave secondary education with my sanity intact. I cannot overestimate the influence of the Chemistry faculty at the University of Minnesota - Morris, especially Nancy Carpenter and Jim Olson, who helped me to see the order in chemical chaos. In high school and college, Track and Field taught me how to turn fear and anxiety into focus and determination; I should thank my coaches and teammates for their high expectations and unwavering faith in my abilities. Finally, I must of course thank my family, friends, parents and grandparents for setting the example I have tried to live up to. In particular I remember Thomas Alan Freitag, who did so much to set me on the path I now follow.

Pulchra sunt quae videntur,
(Beautiful are the things we see)

Pulchroria quare scientur,
(More beautiful those we understand)

Longe pulcherrima quae ignorantur.
(Much more beautiful those we do not comprehend)

ST. NICOLAUS STEENSEN (STENO)
COPENHAGEN ANATOMICAL THEATER, 1673
BEATIFIED BY POPE JOHN PAUL II, 1988

This work was performed at Ames Laboratory under Contract No. W-7405-Eng-82 with the U.S. Department of Energy. The United States government has assigned the DOE Report number IS-T 2049 to this thesis.

REFERENCES

¹ Schrödinger, E. Ann. Physik. **79**, 361, (1926).

² de Broglie, L., Comptes Rendus, **177**, 507, (1923).

³ Heisenberg, W., Zs. f. Phys., **33**, 879, (1925).

⁴ Born, M. and Jordan, P., Zs. f. Phys., **34**, 858, (1925).

⁵ Dirac, P.A.M., Proc. R. Soc. Lond., **A109**, 642 (1925).

⁶ Szabo, A. and Ostlund, N.S., *Modern Quantum Chemistry*, Dover Publications, 1989.

⁷ Born, M. and Oppenheimer, J.R., Ann. Physik, **84**, 457, (1927).

⁸ Hartree, D.R., Proc. Camb. Phil. Soc., **24**, 89, 111, 426 (1928).

⁹ Born, M., Zs. f. Phys., **37**, 863, (1926).

¹⁰ Togeas, J.B., *Essays on Atoms and Elements*, University of Minnesota, Morris, 1995, p. 108.

¹¹ Pople, J.A. and Beveridge, D.L., *Approximate Molecular Orbital Theory*, McGraw Hill, 1970.

¹² Pauli, W., Zs. f. Phys., **31**, 765, (1925).

¹³ Fock, V., Zs. f. Phys., **61**, 126, (1930).

¹⁴ Heisenberg, W., Zs. f. Phys., **39**, 499, (1926).

¹⁵ Pais, A. *Niels Bohr's times*. Oxford University Press, 1991, p. 297.

¹⁶ Slater, J.C., Phys. Rev., **35**, 509, (1930).

¹⁷ Arfken, G.B. and Weber, H.J., *Mathematical Methods for Physicists*, 4th Ed. Academic Press, 1995.

¹⁸ Jensen, F., *Introduction to Computational Chemistry*, Wiley, 1999.

¹⁹ Bartlett, R.J. and Silver, D.M. Int. J. Quant. Chem. **9**, 183, (1975).

²⁰ Møller, C. and Plesset, M.S. Phys. Rev. **46**, 618, (1934).

²¹ Bartlett, R.J. Ann. Rev. Phys. Chem. **32**, 359, (1981).

²² Glaesemann, K.R., Ph.D. Thesis, Iowa State University, 1998.

²³ Hohenberg, P. and Kohn, W., Phys. Rev., **136**, B864, (1964).

²⁴ Day, P. et. al. J. Chem. Phys. 105, 1968, (1996). Chen, W. and Gordon, M.S. J. Chem. Phys. 105, 11081, (1996).

²⁵ A. J. Stone, *The Theory of Intermolecular Forces*, Oxford University Press, Oxford (1996).

²⁶ See, for example, Reference 1, pp 175-178, and references therein.

²⁷ P. N. Day, J. H. Jensen, M. S. Gordon, S. P. Webb, W. J. Stevens, M. Kraus, D. Garmer, H. Basch, and D. Cohen, *J. Chem. Phys.* **105**, 1968 (1996).

²⁸ J. H. Jensen and M. S. Gordon, *Mol. Phys.* **89**, 1313 (1996); J. H. Jensen and M. S. Gordon, *J. Chem. Phys.* **108**, 4772 (1998).

²⁹ A. J. Stone, *Chem. Phys. Lett.* **83**, 233 (1981).

³⁰ A. D. Buckingham, *Quart. Rev. (London)* **13**, 183 (1959).

³¹ J. N. Murrell and J. J. C. Teixeira-Dias, *Mol. Phys.* **19**, 521 (1970).

³² V. Kairys and J. H. Jensen, *Chem. Phys. Lett.* **315**, 140 (1999).

³³ J. H. Jensen, *J. Chem. Phys.* **104**, 7795 (1996).

³⁴ 1.0 kcal mol⁻¹ = 4.184 kJ mol⁻¹.

³⁵ B. T. Thole, *Chem. Phys.* **59**, 341 (1981).

³⁶ M. Krauss, D. B. Neumann and W. J. Stevens, *Chem. Phys. Lett.* **66**, 29 (1979); A. Koide, *J. Phys.* **B9** 3173, (1976); J. Hepburn, G. Scoles, and R. Penco, *Chem. Phys. Lett.* **36**, 451 (1975); R. Ahlrichs, P. Penco, and G. Scoles, *Chem. Phys.* **19**, 119 (1977).

³⁷ M. W. Schmidt, K. K. Baldridge, J. A. Boatz, S. T. Elbert, M. S. Gordon, J. H. Jensen, S. Koseki, N. Matsunaga, K. A. Nguyen, S. J. Su, T. L. Windus, M. Dupuis, J. A. Montgomery, *J. Comp. Chem.* **14**, 1347 (1993).

³⁸ C. A. Coulson, *Proc. Camb. Phil. Soc.* **38**, 222 (1942).

³⁹ Margenau, H., and Murphy, G.M., *The Mathematics of Physics and Chemistry*, D. Van Nostrand Co., 1949, 1st Ed. p.175.

⁴⁰ A.D. Buckingham and P.W. Fowler, *J. Chem. Phys.*, **79**, 6426 (1983); A.D. Buckingham and P.W. Fowler, *Canad. J. Chem.*, **63**, 2018 (1985).

⁴¹ W. Chen and M. S. Gordon, *J. Chem. Phys.*, **105**, 11081 (1996); P. N. Day and R. Pachter, *J. Chem. Phys.* **107**, 2990 (1997); G. N. Merrill and M. S. Gordon, *J. Phys. Chem.*, **102**, 2650 (1998); C. P. Peterson and M. S. Gordon, *J. Phys. Chem.*, **103**, 4146 (1999).

⁴² Block, F. Hansen, W.W., and Packard, M.E., *Phys. Rev.*, **69**, 127, (1946).

⁴³ Purcell, E.M., Torrey, H.C., and Pound, R.V., *Phys. Rev.*, **69**, 37, (1946).

⁴⁴ Ditchfield, R. *Mol. Phys.*, **27**, 789 (1974).

⁴⁵ See, for example, Helgaker, T, Jaszunski, M, and Ruud, K., *Chem. Rev.*, **99**, 293 (1999) and references therin.

⁴⁶ Mikkelsen, K.V., Jorgensen, P., Ruud, K., Helgaker, T., *J. Chem. Phys.*, **106**, 1170 (1997).

⁴⁷ Cremer, D., Olsson, L., Reichel, F., Kraka, E., *Isr. J. Chem.*, **33**, 369 (1993).

⁴⁸ This presentation of the Hamiltonian is somewhat confusing. Many authors include the prefactor of $1/c$ to the vector potential; see, for example, Dirac's *Principles of Quantum Mechanics*, §67, Eq. (11). It seems that there *should* also be a prefactor of $1/c^2$ before the second term of Eq. (3.3a), as seen in (C.1). I have a strong suspicion that this difficulty goes back to the use of cgs vs. SI systems of units, where the factors of $4\pi\epsilon_0$ and $\mu_0/4\pi$ get thrown around somewhat freely. In atomic units, the latter factor is equal to the speed of light squared.

⁴⁹ London, F., *J. Phys. Radium, Paris*, **8**, 397 (1937).

⁵⁰ Note that the last term of the exact expansion has been dropped as discussed in (C.2).

⁵¹ Dodds, J.L., McWeeny, R., Sadlej, A.J., *Mol. Phys.*, **34**, 1779 (1977).

⁵² Wolinski, K., Hinton, J.F., Pulay, P., *JACS*, **112**, 8251 (1990).

⁵³ Wolinski, K. Private Communication.

⁵⁴ McMurchie, L.E. and Davidson, E.R. *J. Comp. Phys.* **26**, 218 (1978).

⁵⁵ Note that in previous sections, a point in space, particularly a nuclear point, was indicated by R_A . This change has been made to conform with McMurchie and Davidson's original work, and to greatly simplify the notation.

⁵⁶ Boys, S.F, *Proc. Roy. Soc. Ser. A* **200**, 542, (1950).

⁵⁷ Shavitt, "Methods in Computational Physics", vol. 2, p. 7. (1963)

⁵⁸ See, for example, Appendix B of Szabo, A. and Ostlund, N.S., *Modern Quantum Chemistry*, Dover Publications, 1989. For an analytical evaluation of the Fourier transform of a Gaussian, see p. 24 of Math 426: Physical Methods, Fall 1997. To evaluate the Fourier transform of $1/r$ (to within a sign) use Coulson's method of transformation to spheroidal coordinates. The reason for the sign change is unclear at the time of writing.

⁵⁹ Gordon, M.S. and Peterson, C., "The Solvation of Sodium Chloride: An Effective Fragment Study of NaCl(H₂O)_n", *J. Phys. Chem.*, **A103**, 4162 (1999).

⁶⁰ For recent reviews, see, for example, (a) K. K. Irikura and D. J. Frurip, in *Computational Thermochemistry*, ACS Symposium Series 677, edited by K. K. Irikura and D. J. Frurip (American Chemical Society, Washington, DC, 1998), p. 2; (b) M. R. Zachariah and C. F. Melius, in *Computational Thermochemistry*, ACS Symposium Series 677, edited by K. K. Irikura and D. J. Frurip (American Chemical Society, Washington, DC, 1998), p. 162; (c) L. A. Curtiss and K. Raghavachari, in *Computational Thermochemistry*, ACS Symposium Series 677, edited by K. K. Irikura and D. J. Frurip (American Chemical Society, Washington, DC, 1998), p. 176; (d) J. M. L. Martin, in *Computational Thermochemistry*, ACS Symposium Series 677, edited by K. K. Irikura and D. J. Frurip (American Chemical Society, Washington, DC, 1998), p. 212; (e) G. A. Petersson, in *Computational Thermochemistry*, ACS Symposium Series 677, edited by K. K. Irikura and D. J. Frurip (American Chemical Society, Washington, DC, 1998), p. 237; (f) L. A. Curtiss, P. C. Redfern, and D. J. Frurip, in *Reviews in Computational Chemistry*, Vol. 15, edited by K. B. Lipkowitz and D. B. Boyd (Wiley-VCH, New York, 2000), p. 147.

⁶¹ (a) J. A. Pople, M. Head-Gordon, D. J. Fox, K. Raghavachari, and L. A. Curtiss, *J. Chem. Phys.* **90**, 5622 (1989); (b) L. A. Curtiss, C. Jones, G. W. Trucks, K. Raghavachari, and J. A. Pople, *J. Chem. Phys.* **90**, 5622 (1989).

⁶² (a) L. A. Curtiss, K. Raghavachari, G. W. Trucks, and J. A. Pople, *J. Chem. Phys.* **94**, 7221 (1991); (b) L. A. Curtiss, J. E. Carpenter, K. Raghavachari and J. A. Pople, *J. Chem. Phys.* **96**, 9030 (1992); (c) L. A. Curtiss, K. Raghavachari, and J. A. Pople, *J. Chem. Phys.* **98**, 1293 (1993); (d) L. A. Curtiss, K. Raghavachari, and J. A. Pople, *J. Chem. Phys.* **103**, 4192 (1995); (e) B. J. Smith and L. Radom, *J. Phys. Chem.* **99**, 6468 (1995); (f) L. A. Curtiss, P. C. Redfern, B. J. Smith, and L. Radom, *J. Chem. Phys.* **104**, 5148 (1996); (g) L. A. Curtiss, K. Raghavachari, P. C. Redfern, and J. A. Pople, *J. Chem. Phys.* **106**, 1063 (1997); (h) L. A. Curtiss, P. C. Redfern, K. Raghavachari, and J. A. Pople, *J. Chem. Phys.* **109**, 42 (1998).

⁶³ (a) L. A. Curtiss, K. Raghavachari, P. C. Redfern, V. Rassolov and J. A. Pople, *J. Chem. Phys.* **109**, 7764 (1998); (b) L. A. Curtiss, P. C. Redfern, K. Raghavachari, V.

Rassolov and J. A. Pople, *J. Chem. Phys.* **110**, 4703 (1999); (c) L. A. Curtiss, P. C. Redfern, K. Raghavachari, and J. A. Pople, *Chem. Phys. Lett.* **313**, 600 (1999); (d) L. A. Curtiss, P. C. Redfern, K. Raghavachari, P. C. Redfern, A. G. Baboul, and J. A. Pople, *Chem. Phys. Lett.* **314**, 101 (1999); (e) L. A. Curtiss, K. Raghavachari, P. C. Redfern, and J. A. Pople, *J. Chem. Phys.* **112**, 1125 (1999); (f) L. A. Curtiss, K. Raghavachari, P. C. Redfern, and J. A. Pople, *J. Chem. Phys.* **112**, 7374 (2000); (g) L. A. Curtiss, P. C. Redfern, K. Raghavachari, and J. A. Pople, *J. Chem. Phys.* **114**, 108 (2001).

⁶⁴ See, for example, (a) J. W. Ochterski, G. A. Petersson, and J. J. A. Montgomery, *J. Chem. Phys.* **104**, 2598 (1996); (b) J. A. Montgomery, Jr., M. J. Frisch, J. W. Ochterski, and G. A. Petersson, *J. Chem. Phys.* **110**, 2822 (1999).

⁶⁵ See, for example, M.D. Allendorf, C.F. Melius, P. Ho and M.R. Zachariah, *J. Phys. Chem.* **99**, 15285 (1995), and references therein.

⁶⁶ (a) J. M. L. Martin and G. de Oliveira, *J. Chem. Phys.* **111**, 1843 (1999); (b) J. M. L. Martin, *Chem. Phys. Lett.* **310**, 271 (1999).

⁶⁷ See, for example, (a) D. Feller and K. A. Peterson, *J. Chem. Phys.* **108**, 154 (1998); (b) D. Feller and K. A. Peterson, *J. Chem. Phys.* **110**, 8384 (1999); (c) T.H. Dunning, Jr., *J. Phys. Chem. A* **104**, 9062 (2000).

⁶⁸ M. W. Schmidt and M. S. Gordon, *Annu. Rev. Phys. Chem.* **49**, 233 (1998).

⁶⁹ J. A. Pople, M. Head-Gordon, and K. Raghavachari, *J. Chem. Phys.* **87**, 5968 (1987).

⁷⁰ The *Gn* total energies and the G3MP2large basis set can be downloaded via the Internet at <http://chemistry.anl.gov/compmat/comptherm.htm>.

⁷¹ E. M. Siegbahn, J. Almlöf, A. Heiberg and B. O. Roos, *J. Chem. Phys.* **74**, 2384 (1981).

⁷² K. Ruedenberg, M. W. Schmidt, M. M. Gilbert and S. T. Elbert, *Chem. Phys.* **71** 41 (1982).

⁷³ (a) B. O. Roos, P. Linse, E. M. Siegbahn and M. A. R. Blomberg, *Chem. Phys.* **66**, 197 (1982); (b) K. Andersson, P. -A. Malmqvist, B. O. Roos, A. J. Sadlej, K. Wolinsky, *J. Phys. Chem.* **94**, 5483 (1990).

⁷⁴ For the MOLPRO implementation, see: H.-J. Werner, *Mol. Phys.* **89**, 645 (1996).

⁷⁵ (a) H. Nakano, *J. Chem. Phys.* **99**, 7983 (1993); (b) H. Nakano, *Chem. Phys. Lett.* **207**, 372 (1993).

⁷⁶ H. Nakano, K. Hirao and M. S. Gordon, *J. Chem. Phys.* **108**, 5660 (1998).

⁷⁷ M. W. Schmidt, K. K. Baldridge, J. A. Boatz, S. T. Elbert, M. S. Gordon, J. H. Jensen, S. Koseki, N. Matsunaga, K. A. Nguyen, S. Su, T.L. Windus, M. Dupuis, and J. A. Montgomery, Jr., *J. Comput. Chem.* **14**, 1347 (1993).

⁷⁸ For recent studies, see, for example, (a) K. Kowalski and P. Piecuch, *Phys. Rev. A* **61**, 052506 (2000); (b) S. Chattopadhyay, U. S. Mahapatra and D. Mukherjee, *J. Chem. Phys.* **112**, 7939 (2000); (c) V. V. Ivanov and L. Adamowicz, *J. Chem. Phys.* **103**, 8503 (2000), and references therein.

⁷⁹ (a) H.-J. Werner and P.J. Knowles *J. Chem. Phys.* **89** 5803 (1988); (b) P. J. Knowles and H.-J. Werner, *Chem. Phys. Lett.* **145**, 514 (1988).

⁸⁰ This method has been previously referred to as G2(QCI)^{3b} but we use the G2/QCI notation here so as to allow easy generalization to methods such as G2/MP2 and MR-G2/MRCI+Q.

⁸¹ Note that the G3-type procedures defined by Eqs. (9), (11) and (13) should strictly include the designation G3(MP2) rather than G3 because they use the G3MP2large basis set rather than the G3large set. However, the G3 labels are used here for simplicity.

⁸² (a) MOLPRO 96 is a package of ab initio programs written by H.-J. Werner and P. J. Knowles with contributions from J. Almlöf, R. D. Amos, M. J. O. Deegan, S. T. Elbert, C. Hempel, W. Meyer, K. Peterson, R. Pitzer, A. J. Stone, P. R. Taylor and R. Lindh; (b) MOLPRO 98.1 is a package of ab initio programs written by H.-J. Werner and P. J. Knowles, with contributions from J. Almlöf, R. D. Amos, A. Berning, D. L. Cooper, M. J. O. Deegan, A. J. Dobbyn, F. Eckert, S. T. Elbert, C. Hempel, R. Lindh, A. W. Lloyd, W. Meyer, A. Nicklass, K. Peterson, R. Pitzer, A. J. Stone, P. R. Taylor, M. E. Mura, P. Pulay, M. Schütz, H. Stoll, and T. Thorsteinsson.

⁸³ The "SOLVER" function in the Microsoft EXCEL spreadsheet package was used to minimize the mean absolute deviation between the calculated and experimental thermochemical values.

⁸⁴ J. M. L. Martin, *J. Chem. Phys.* **108**, 2791 (1998).

⁸⁵ MR-G2(MP2) does not fit in smoothly and is omitted from the comparison. This arises because of an increased number of iterations required for convergence in the MRCI+Q/6-311G(d,p) calculation. MR-G2(MP2) is not likely in any case to be a widely-used procedure.

⁸⁶ Beckhaus, R., 'Metallocenes,' Ed. Togni, A., and Halterman, R.L., Vol. 1, Ch. 4, Wiley-VCH, 1998.

⁸⁷ A.K. Fischer and G. Wilkinson, Inorg. & Nuc. Chem., **2**, 149 (1956).

⁸⁸ J.D. Dunitz and L.E. Orgel, Nature, **171**, 121 (1953).

⁸⁹ J.D. Dunitz and L.E. Orgel, J. Chem. Phys., **23**, 954 (1955).

⁹⁰ H.H. Jaffé, J. Chem. Phys., **21**, 156 (1953).

⁹¹ W. Moffitt, JACS, **76**, 3386 (1954).

⁹² T.J. Kealy and P.L. Pauson, Nature, **168**, 1039 (1951).

⁹³ A. D. Liehr and C. J. Ballhausen, Acta Chemica Scandinavica, **11**, 207 (1957).

⁹⁴ F.A. Matsen, JACS, **81**, 2023 (1959).

⁹⁵ R.E. Robertson and H. M. McConnell, J. Phys. Chem., **64**, 70 (1960).

⁹⁶ D. R. Scott and R.S. Becker, J. Chem. Phys., **35**, 516 (1961).

⁹⁷ M. Yamazaki, J. Chem. Phys., **24**, 1260 (1956).

⁹⁸ G.W. Watt and L.J. Baye, J. Inorg. Nucl. Chem., **26**, 2099 (1964).

⁹⁹ G.W. Watt, L.J. Baye and F.O. Drummond, JACS, **88**, 1138 (1966).

¹⁰⁰ F. Calderazzo, J.J. Salzmann, and P. Mosimann, Inorg. Chim. Acta., **1**, 65 (1967)

¹⁰¹ J.J. Salzmann and P. Mosimann, Helv. Chim. Acta., **50**, 1831 (1967).

¹⁰² H.H. Brintzinger and L.S. Bartell, JACS, **92**, 1105 (1970).

¹⁰³ J.H. Schachtschneider, R. Prins, and P. Ros, Inorg. Chim. Acta, **1**, 462 (1967).

¹⁰⁴ M.F. Rettig and R.S. Drago, JACS, **91**, 3432 (1969).

¹⁰⁵ H.H. Brintzinger and J.E. Bercaw, JACS, **92**, 6182 (1970).

¹⁰⁶ R.H. Marvich and H.H. Brintzinger, JACS, **93**, 2046 (1971).

¹⁰⁷ F.A. Cotton and G. Wilkinson, "Advanced Inorganic Chemistry", 5th Ed. Wiley-Interscience: New York, 1988.

¹⁰⁸ J. W. Lauher and R. Hoffmann, JACS, **98**, 1729 (1976).

¹⁰⁹ D.W. Clack and K.D. Warren, Inorg. Chim. Acta., **30**, 251 (1978).

¹¹⁰ W.J. Hehre, R. Ditchfield and J.A. Pople, *J. Chem. Phys.* **56**, 2257 (1972); Pople, *J. Chem. Phys.* **62**, 2921 (1975).

¹¹¹ T. H. Dunning, Jr., *J. Chem. Phys.* **55**, 716 (1971); A.D. McClean and G.S. Chandler, *J. Chem. Phys.* **72**, 5639 (1980); A.J.H. Watchers, *J. Chem. Phys.* **52**, 1033 (1970)

¹¹² For the 6-31G** basis: V.A. Rassolov, J.A. Pople, M.A. Ratner, and T.L. Windus, *J. Chem. Phys.* **109**, 1223 (1998).

¹¹³ For the PVTZ basis: V.A. Glezakou, and M.S. Gordon, *J. Phys. Chem. A*, **101**, 8714-8719 (1997).

¹¹⁴ A. D. Becke. *Phys. Rev. A* **38**, 3098 (1988); *J. Chem. Phys.* **98**, 1372, 5648 (1993).

¹¹⁵ M. W. Schmidt, K. K. Baldridge, J. A. Boatz, S. T. Elbert, M. S. Gordon, J. H. Jensen, S. Koseki, N. Matsunaga, K. A. Nguyen, S. J. Su, T. L. Windus, M. Dupuis, J. A. Montgomery, *J. Comp. Chem.* **14**, 1347 (1993).

¹¹⁶ Gaussian 94, Revision E.2, M. J. Frisch, G. W. Trucks, H. B. Schlegel, P. M. W. Gill, B. G. Johnson, M. A. Robb, J. R. Cheeseman, T. Keith, G. A. Petersson, J. A. Montgomery, K. Raghavachari, M. A. Al-Laham, V. G. Zakrzewski, J. V. Ortiz, J. B. Foresman, J. Cioslowski, B. B. Stefanov, A. Nanayakkara, M. Challacombe, C. Y. Peng, P. Y. Ayala, W. Chen, M. W. Wong, J. L. Andres, E. S. Replogle, R. Gomperts, R. L. Martin, D. J. Fox, J. S. Binkley, D. J. Defrees, J. Baker, J. P. Stewart, M. Head-Gordon, C. Gonzalez, and J. A. Pople, Gaussian, Inc., Pittsburgh PA, 1995.

¹¹⁷ C. Hampel, K. Peterson, and H.-J. Werner, *Chem. Phys. Lett.* **190**, 1 (1992)

¹¹⁸ J. D. Watts, J. Gauss and R. J. Bartlett, *J. Chem. Phys.*, **98**, 8718 (1993).

¹¹⁹ W.H. Miller, N.C. Handy, J.E. Adams, *J. Chem. Phys.*, **72**, 99-112 (1980).

¹²⁰ T. Kudo and M.S. Gordon, *J. Chem. Phys.*, **102**, 6805 (1995).

¹²¹ S.P. Webb and M.S. Gordon, *J. Chem. Phys.*, **109**, 919 (1998).

¹²² S.P. Webb and M.S. Gordon, *J. Am. Chem. Soc.*, **120**, 3846 (1998).

¹²³ M.S. Gordon, M.W. Schmidt, G.M. Chaban, K.R. Glaesemann, W.J. Stevens, C. Gonzales, *J. Chem. Phys.*, **110**, 4199 (1999).

¹²⁴ Pais, A. *Inward Bound*. Oxford University Press, 1986

¹²⁵ Zaky, A.A. and Hawley, R. *Fundamentals of Electromagnetic Field Theory*, London, 1974, p. 234ff.

¹²⁶ C. A. Coulson, Proc. Camb. Phil. Soc. **38**, 222 (1942).

¹²⁷ Margenau, H., and Murphy, G.M., *The Mathematics of Physics and Chemistry*, D. Van Nostrand Co., 1949, 1st Ed. p.175.